SYNTHESIS AND CHARACTERIZATION OF HAFNIUM AND MOLYBDENUM BIFUNCTIONAL INITIATORS FOR THE PREPARATION OF TRIBLOCK COPOLYMERS

by

ANDREA JENNIFER GABERT

B.Sc. in Chemistry, Simon Fraser University
(2002)

Submitted to the Department of Chemistry
in Partial Fulfillment of the Requirements
for the Degree of

DOCTOR OF PHILOSOPHY
at the

MASSACHUSETTS INSTITUTE OF TECHNOLOGY
September 2007

Signature of Author _____
Department of Chemistry
May 31, 2007

Certified By _____
Richard R. Schrock
Thesis Supervisor

Accepted By _____
Robert W. Field
Chairman, Departmental Committee on Graduate Students

This doctoral thesis has been examined by a Committee of the Department of Chemistry as follows:

Professor Joseph P. Sadighi _____ Chairman

Professor Richard R. Schrock _____ Thesis Supervisor

Professor Christopher C. Cummins _____

To those who support and love me,
especially my family.

SYNTHESIS AND CHARACTERIZATION OF
HAFNIUM AND MOLYBDENUM BIFUNCTIONAL INITIATORS
FOR THE PREPARATION OF TRIBLOCK COPOLYMERS

by

ANDREA JENNIFER GABERT

Submitted to the Department of Chemistry on May 31, 2007
in Partial Fulfillment of the Requirements
for the Degree of Doctor of Philosophy in Chemistry

ABSTRACT

Chapter 1

Three monofunctional mixed alkyl hafnium complexes containing the $(MesNpy)^{2-}$ ligand ($[(MesitylNCH_2)_2CMe(2\text{-}C_5H_4N)]^{2-}$) were synthesized. (MesNpy)Hf(Neo)R ((**2b**), R = Me; Neo = CH_2CMe_2Ph) and (MesNpy)Hf(CH_2TMS)(R), ((**3b**), R = Me and (**4b**), R = *i*-Bu)) were activated with $\{Ph_3C\}\{B(C_6F_5)_4\}$ and one alkyl group was selectively removed in all cases. The kinetics of activated **4b** were studied and the resulting complex was an initiator for the living polymerization of 1-hexene, with the exception of a slight initiation effect. Five linker molecules were investigated for the preparation of bifunctional hafnium mixed alkyl complexes. One complex synthesized, **disilyl**[(MesNpy)HfMe]$_2$ (**disilyl**$(X)_2$ = X-$CH_2SiMe_2(CH_2)_5SiMe_2CH_2$-X) was activated with $\{Ph_3C\}\{B(C_6F_5)_4\}$ and the methyl groups were successfully removed to form {**disilyl**[(MesNpy)Hf]$_2$}$\{B(C_6F_5)_4\}_2$. This complex was also a living catalyst for the polymerization of α-olefins.

Chapter 2

Addition of *p*-divinylferrocene to Mo(CHCMe$_2$Ph)(NAr)$(OR_{F6})_2$ (OR_{F6} = OCMe$(CF_3)_2$; Ar = 2,6-diisopropylphenyl) produced the bimetallic species [Mo(NAr)$(OR_{F6})_2$(=CHC_5H_4)]$_2$Fe (**6**), which upon treatment with lithium *tert*-butoxide produced the related *tert*-butoxide complex (**7**). X-ray crystallography studies of **6** and **7** showed them to be "*syn/syn*" bimetallic species. In solution, two resonances can be observed in ^{1}H NMR spectra in the alkylidene region for the "*syn/anti*" isomer of **6** and **7**; the total amounts were 4 and 8%, respectively. Bimetallic species **6** and **7** have been shown to initiate competitively at both ends and to produce homopolymers of 2,3-dicarbomethoxynorbornadiene (**DCMNBD**) and methyltetracyclododecene (**MTD**) in a living fashion. MALDI-TOF mass spectra of ferrocene-containing species were obtained and are consistent with the polymerization process being living. Triblock copolymers (poly[(**MTD**)$_{x/2}$(**DCMNBD**)$_y$(**MTD**)$_{x/2}$]) were prepared by adding y equivalents of **DCMNBD** to the bimetallic initiators followed (after consumption of **DCMNBD**) by x equivalents of **MTD**. These triblocks were shown to be of high purity (free of homopolymer and diblock copolymers) and to have relatively low PDIs ($\leq$ 1.2).

Chapter 3

A series of monomers suitable for ring opening metathesis polymerization (ROMP) containing a side chain liquid crystal mesogen were synthesized, where the mesogen was biphenyl-4-carboxylic acid 4-(1-butoxycarbonyl-ethoxy)-phenyl ester (abbreviated as **BPP4**). Two of the monomers have **BPP4** attached to norbornene with a six or ten carbon spacer ((R)-4'-(5-bicyclo[2.2.1]hept-5-en-2-yl-pentyloxy)-**BPP4**, **NB6wBPP4**, and (R)-4'-(10-bicyclo[2.2.1]hept-5-en-2-yl-decyloxy)-**BPP4**, **NB10wBPP4**, respectively), and the third monomer has **BPP4** attached to norbornadiene via a ten carbon spacer ((R)-4'-(10-bicyclo[2.2.1]hepta-2,5-dien-2-yl-decyloxy)-**BPP4**, **NBD10wBPP4**). The monomers were polymerized by ROMP using the bimetallic initiator, $[Mo(NAr)(OR_{F6})_2(=CHC_5H_4)]_2Fe$ (Ar = 2,6-diisopropylphenyl; OR_{F6} = $OCMe(CF_3)_2$). ABA triblock copolymers were also synthesized where the B block is **NBD10wBPP4** or **NBnwBPP4** (n = 6, 10) and the A block is methyltetracyclododecene (**MTD**). All polymerizations are living with isolated yields greater than 90% and PDI values ranging from less than 1.05 to 1.31. The triblock copolymers were found to have glass transition temperatures of the inner block at approximately 20 °C and smectic to isotropic transitions around 150 °C. Small angle X-ray scattering (SAXS) indicated that the triblock copolymers exhibit phase segregation. SAXS data demonstrated that the triblock copolymer containing **NB6wBPP4** forms smectic C* monolayers while the triblock copolymers that contain **NB10wBPP4** and **NBD10wBPP4** form smectic C* bilayers at room temperature. Dynamic mechanical analysis of the triblock copolymers reveals an elastic plateau above the glass transition temperature of the center block, suggesting these systems may be interesting materials for shape-memory elastomers.

Chapter 4

The reaction of $[Mo(NAr)(OR_{F6})_2]_2DVF$ (OR_{F6} = $OCMe(CF_3)_2$; Ar = 2,6-diisopropylphenyl; DVF = divinylferrocene) with lithium pyrrolide (LiPyr) or lithium 2,5-dimethylpyrrolide ($LiMe_2Pyr$) formed the complexes $[Mo(NAr)(Pyr)_2(=CHC_5H_4)]_2Fe\bullet 2Li(Pyr)$ (**8**) and $[Mo(NAr)(Me_2Pyr)_2(=CHC_5H_4)]_2Fe$ (**9**), respectively. X-ray crystallography studies of **8** reveal it to be a dimer of bimetallic complexes while **9** is a monomer in the solid state. The reaction of $[(DME)Mo(NAr)(OR_{F6})_2]_2DVB$ (DVB = divinylbenzene; DME = dimethoxyethane) with $LiMe_2Pyr$ formed $[Mo(NAr)(Me_2Pyr)_2(=CH)]_2(1,4\text{-}C_6H_4)$ (**10**). The reactivities of **8**, **9**, and **10** with various diols were studied. Three compounds, namely, $[Mo(NAr)(\textbf{Biphen})(=CHC_5H_4)]_2Fe$ (**11**, H_2[**Biphen**] = 3,3'-di-*tert*-butyl-5,5',6,6'-tetramethylbiphenyl-2,2'-diol), $[Mo(NAr)(\textbf{Benz}_2\textbf{Bitet})(=CH)]_2(1,4\text{-}C_6H_4)$ (**12**, (R)-H_2[$\textbf{Benz}_2$**Bitet**] = (R)-3,3'-dibenzhydryl-5,5',6,6',7,7',8,8'-octahydro-1,1'-binaphthyl-2,2'-diol) and $[Mo(NAr)(\textbf{MesBitet})(=CH)]_2(1,4\text{-}C_6H_4)$ (**13**, (R)-H_2[**MesBitet**] = (R)-3,3'-dimesityl-5,5',6,6',7,7',8,8'-octahydro-1,1'-binaphthyl-2,2'-diol) were found to be isolable compounds and could be generated cleanly *in situ*. 2,3-Dicarbomethoxynorbornadiene (**DCMNBD**) and 2,3-bis(trifluoromethyl)norbornadiene (**NBDF6**) were polymerized using initiators **11**, **12**, and **13**, both isolated and *in situ* generated. Poly(**DCMNBD**) and poly(**NBDF6**) prepared with **12** and **13** were found to be highly *cis* and highly tactic. Triblock copolymers were also prepared, and the tacticity of the polymer was maintained.

Appendix A

Various monomers suitable for ROMP were synthesized for optimized application in thermoplastic liquid crystal elastomers. Two new inner block monomers, **CBEwBPP4** [4-(1-butoxy-1-oxopropan-2-yloxy)phenyl 4'-(2-(2-(cyclobut-2-enylmethoxy)ethoxy)ethoxy)biphenyl-4-carboxylate] and **ONBwMPOB** [4-methoxyphenyl 4-(4-(7-oxabicyclo[2.2.1]hept-5-en-2-ylmethoxy)butoxy)benzoate] were polymerized and the thermal properties of the polymers were studied. Poly(**CBEwBPP4**) exhibited a glass transition temperature (T_g) of -10 °C but no liquid crystal (LC) transition was observed. Poly(**ONBwMPOB**) exhibited a T_g of 15 °C and a broad LC transition was observed around 40 °C. Three new outer block monomers, *exo*-4-cyclohexyl-4-aza-tricyclo[5.2.1.02,6]dec-8-ene-3,5-dione (**NBwNCy**), [3-(4-fluoro-benzoyl)-bicyclo[2.2.1]hept-5-en-2-yl]-(4-fluoro-phenyl)-methanone, (**NBwCOPh$_F$**), and bicyclo[2.2.1]hept-5-en-2-yl-phenyl-methanone (**NBwCOPh**) were also polymerized and their thermal properties were studied.

Thesis Supervisor: Prof. Richard R. Schrock
Title: Frederick G. Keyes Professor of Chemistry

TABLE OF CONTENTS

LIST OF ABBREVIATIONS

AIBN	2,2′-azobis(2-methylpropionitrile)
Anal.	Analysis
Ar	2,6-diisopropylphenyl
BPP4	biphenyl-4-carboxylic acid 4-(1-butoxycarbonyl-ethoxy)-phenyl ester
br	broad
Calcd	calculated
CBEwBPP4	4-(1-butoxy-1-oxopropan-2-yloxy)phenyl 4'-(2-(2-(cyclobut-2-enylmethoxy)ethoxy)ethoxy)biphenyl-4-carboxylate
Cp	$(C_5H_5)^-$
d	doublet
Da	Dalton
DCC	*N,N′*-dicyclohexylcarbodiimide
DCMNBD	2,3-dicarbomethoxynorbornadiene
DHB	2,5-dihydroxy benzoic acid
dibenzyl$(X)_2$	X-$CH_2(C_6H_4)CH_2$-X
dicyclohexylmethyl$(X)_2$	*trans*-X-$CH_2(C_6H_{10})CH_2$-X
dineophyl$(X)_2$	X-$CH_2CMe_2(C_6H_4)CMe_2CH_2$-X
disilophyl$(X)_2$	X-$CH_2SiMe_2(C_6H_4)SiMe_2CH_2$-X
disilyl$(X)_2$	X-$CH_2SiMe_2(CH_2)_5SiMe_2CH_2$-X
DMA	dynamic mechanical analysis
DMAP	4-(dimethylamino)pyridine
DME	dimethoxyethane
DMSO	dimethylsulfoxide
DSC	differential scanning calorimetry
DT	dithranol
equiv	equivalent(s)
Et	ethyl
ether	diethyl ether
g	gram(s)
GPC	gel permeation chromatography
h	hour(s)
H-**OBPP4**	4-(1-butoxy-1-oxopropan-2-yloxy)phenyl 4′-(2-(2-hydroxyethoxy)ethoxy)biphenyl-4-carboxylate
Hz	Hertz

IAA	*trans*-2-indoleacrylic acid
i-Bu	isobutyl
J	coupling constant in Hertz
k_i	rate constant of initiation
k_p	rate constant of propagation
LC	liquid crystal
LCE	liquid crystal elastomer
m	multiplet(s)
MALDI-TOF MS	matrix assistant laser desorption ionization time-of-flight mass spectrometry
Me	methyl
Me_2Pyr	2,5-$NC_4H_2Me_2$
Mes	mesityl
$(MesNpy)^{2-}$	$[(MesitylNCH_2)_2CMe(2\text{-}C_5H_4N)]^{2-}$
min	minute(s)
M_n	number average molecular weight
MPOB-H	4-hydroxy-benzoic acid 4-methoxy-phenyl ester
MTD	methyltetracyclododecene
NB	norbornene
NB10wBPP4	(R)-4′-(10-bicyclo[2.2.1]hept-5-en-2-yl-decyloxy)-**BPP4**
NB6wBPP4	(R)-4′-(5-bicyclo[2.2.1]hept-5-en-2-yl-pentyloxy)-**BPP4**
NBD	norbornadiene
NBD10wBPP4	(R)-4′-(10-bicyclo[2.2.1]hepta-2,5-dien-2-yl-decyloxy)-**BPP4**
NBDF6	2,3-bis(trifluoromethyl)norbornadiene
NBwCH$_2$Ph$_{F5}$	5-pentafluorophenylmethyl-bicyclo[2.2.1]hept-2-ene
NBwCOPh	bicyclo[2.2.1]hept-5-en-2-yl-phenyl-methanone
NBwCOPh$_F$	[3-(4-fluoro-benzoyl)-bicyclo[2.2.1]hept-5-en-2-yl]-(4-fluoro-phenyl)-methanone,
NBwNCy	*exo*-4-cyclohexyl-4-aza-tricyclo[5.2.1.$0^{2,6}$]dec-8-ene-3,5-dione
NMR	nuclear magnetic resonance
ONBwMPOB	4-methoxyphenyl 4-(4-(7-oxabicyclo[2.2.1]hept-5-en-2-ylmethoxy)butoxy)benzoate
OR_{F0}	*tert*-butoxide
OR_{F6}	hexafluoro-*tert*-butoxide
PDI	polydispersity index
Ph	phenyl

POM	polarized optical microscopy
ppm	parts per million
Pyr	NC_4H_4
q	quartet
rac	racemic
ROMP	ring opening metathesis polymerization
s	singlet
SAXS	small angle X-ray scattering
sept	septet
t	triplet
t-Bu	*tert*-butyl
TBDMS	*tert*-butyldimethylsilyl
TBDPS	*tert*-butyldiphenylsilyl
T_g	glass transition temperature
(R)- or (S)-H_2[**Biphen**]	(R)-or (S)-3,3′-di-*tert*-butyl-5,5′,6,6′-tetramethylbiphenyl-2,2′-diol
(R)-H_2[**Benz$_2$Bitet**]	(R)-3,3′-dibenzhydryl-5,5′,6,6′,7,7′,8,8′-octahydro-1,1′-binaphthyl-2,2′-diol
(R)-H_2[**CF$_3$Binol**]	(R)-3,3′-bis(3,5-bis(trifluoromethyl)phenyl)-1,1′-binaphthyl-2,2′-diol
(R)-H_2[**MesBitet**]	(R)-3,3′-dimesityl-5,5′,6,6′,7,7′,8,8′-octahydro-1,1′-binaphthyl-2,2′-diol
(R)-H_2[**PhBinol**]	(R)-3,3′-diphenyl-1,1′-binaphthyl-2,2′-diol
(R)-H_2[**TRIPBinol**]	(R)-3,3′-bis(2,4,6-triisopropylphenyl)-1,1′-binaphthyl-2,2′-diol
(R)- or (S)-H_2[**Biphen**]	(R)-or (S)-3,3′-di-*tert*-butyl-5,5′,6,6′-tetramethylbiphenyl-2,2′-diol
THF	tetrahydrofuran
TMS	trimethylsilyl
Tos	$CH_3C_6H_4SO_2$
TPE	thermoplastic elastomer
TPLCE	thermoplastic liquid crystal elastomer
δ	chemical shift downfield from tetramethylsilane in ppm

LIST OF COMPOUNDS

CHAPTER 1

1	(MesNPy)$HfCl_2$
2a	(MesNPy)Hf(CH_2CMe_2Ph)Cl
2b	(MesNPy)Hf(CH_2CMe_2Ph)(Me)
2c	{(MesNPy)Hf(CH_2CMe_2Ph)}$^+$
3a	(MesNPy)Hf(CH_2TMS)Cl
3b	(MesNPy)Hf(CH_2TMS)(Me)
3c	{(MesNPy)Hf(CH_2TMS)}$^+$
4a	(MesNPy)Hf(*i*-Bu)Cl
4b	(MesNPy)Hf(CH_2TMS)(*i*-Bu)
4c	{(MesNPy)Hf(CH_2TMS)}$^+$
5a	**disilyl**[(MesNPy)$HfCl]_2$
5b	**disilyl**[(MesNPy)$HfMe]_2$
5c	{**disilyl**[(MesNPy)$Hf]_2$}$^{2+}$

CHAPTER 2

6	[Mo(NAr)(OR_{F6})$_2$(=CHC_5H_4)]$_2$Fe
7	[Mo(NAr)(OR_{F0})$_2$(=CHC_5H_4)]$_2$Fe

CHAPTER 4

8	[Mo(NAr)(Pyr)$_2$(=CHC_5H_4)]$_2$Fe•2Li(Pyr)
9	[Mo(NAr)(Me_2Pyr)$_2$(=CHC_5H_4)]$_2$Fe
10	[Mo(NAr)(Me_2Pyr)$_2$(=CH)]$_2$(1,4-C_6H_4)
11	[Mo(NAr)(**Biphen**)(=CHC_5H_4)]$_2$Fe
12	[Mo(NAr)(**Benz$_2$Bitet**)(=CH)]$_2$(1,4-C_6H_4)
13	[Mo(NAr)(**MesBitet**)(=CH)]$_2$(1,4-C_6H_4)
14	Mo(NAr)(Pyr)$_2$($CHCMe_2Ph$)

APPENDIX A

15	Mo(NAr)(OR_{F6})$_2$($CHCMe_2Ph$)
16	Mo(NAr)(OR_{F0})$_2$($CHCMe_2Ph$)

LIST OF FIGURES

CHAPTER 1

CHAPTER 2

CHAPTER 3

CHAPTER 4

APPENDIX A

LIST OF SCHEMES

CHAPTER 1

CHAPTER 2

CHAPTER 3

CHAPTER 4

APPENDIX A

LIST OF TABLES

CHAPTER 1

CHAPTER 2

CHAPTER 3

CHAPTER 4

APPENDIX A

General Introduction

The quest for new materials has been led in recent years by the discovery of new types of polymers, and in particular, block copolymers.[1] Block copolymers are formed by covalently linking the ends of two or more different polymeric chains. If the blocks are chosen correctly for a block copolymer, microphase separation will occur as opposed to the macrophase separation that occurs when bulk polymers are physically mixed together. This property, as well as the ability to exploit the properties of the individual homopolymers, leads to novel polymeric materials. Diblock (AB) and triblock (ABA or ABC) copolymers are the most studied molecular architectures from an academic point of view while triblock copolymers are the most utilized industrially.[1a] The three general methods for the synthesis of ABA triblock copolymers are (i) sequential monomer addition, (ii) coupling of living AB chains, and (iii) the use of a bifunctional initiator.[1b]

Sequential monomer addition involves the polymerization of monomer A, followed by monomer B, and then followed by monomer A. The disadvantages of this method are (i) the high probability of unsymmetrical A blocks, (ii) the synthesis requires three steps, and (iii) partial termination of the growing chains which leads to the presence of undesirable homo- and diblock co-polymer in the final product. Using this method can make it difficult to obtain identical end groups. In general, the least amount of addition steps possible is desired because there is less probability for contaminants to enter the system.

The coupling of living AB chains method involves connecting two AB chains to form an ABA triblock copolymer. The AB chains are usually formed by sequential monomer addition. Although this technique only requires two addition steps, fractional separation is usually required to separate the ABA triblock copolymer from any unreacted AB starting materials. This method leads to more symmetric A segments as opposed to the simple sequential monomer addition.

The coupling method tends to be more time consuming than the sequential addition method because the coupling reaction generally needs to be run for a significant amount of time.

In view of the difficulties described above, it would be desirable to prepare triblocks via a living method from the "inside out," i.e., through the use of a bifunctional initiator. The central block (B) would then consist primarily of poly(B), with whatever "linker" was employed in the bifunctional initiator located roughly in the middle of the central block. Monomer A can then be added in order to create the outer blocks, which would have the same average chain length. If the polymerization of monomer A and B is living under some set of conditions, then a pure triblock copolymer should be attainable. This process is illustrated in Equation 1.

$$\begin{array}{c} M\text{—linker—}M \\ \downarrow\ 2n(B) \\ M\text{—}(B)_n\text{—linker—}(B)_n\text{—}M \\ \downarrow\ 2m(A) \\ M\text{—}(A)_m\text{—}(B)_n\text{—linker—}(B)_n\text{—}(A)_m\text{-}M \\ \downarrow\ \text{Quench} \\ \text{Endgroup—}(A)_m\text{—}(B)_n\text{—linker—}(B)_n\text{—}(A)_m\text{—Endgroup} \end{array} \qquad (1)$$

Bifunctional initiators allow for the synthesis of fully symmetric triblock copolymers with two sequential monomer additions, as opposed to the monofunctional catalysts that require three additions. In addition, use of a bifunctional initiator should decrease the probability of any AB impurities that are found with sequential addition because of the fewer required addition steps (i.e., reducing the probability of introducing contaminants into the system). Bifunctional initiators may also allow access to ABA triblock copolymers that would otherwise be unattainable. When employing a bifunctional initiator, it is essential that the initiator behaves in

a well-defined manner, or the final product will be a mixture of ABA triblock copolymer and homo- and diblock co-polymer contaminants.

In order for a triblock copolymer to be synthesized using a bifunctional initiator, the system needs to be "living". The generally accepted criteria for a living polymerization system include:[2]

1) Polymerization proceeds to complete monomer consumption.
2) Number average molecular weight (M_n) of the polymer increases linearly as a function of conversion.
3) The M_n can be controlled by stoichiometry.
4) The number of active centers remains constant for the duration of the polymerization (i.e., no chain termination).
5) The polymers display narrow molecular weight distributions described by the ratio of $M_n/M_w \sim 1$.
6) Block copolymers can be prepared by sequential monomer addition.
7) End-functionalized polymers can be synthesized.

For most of the above criteria to hold, the rate of initiation needs to be greater than or equal to the rate of propagation. The benefits of synthesizing polymers with a living system include the ability to control the molecular weight, the end-groups, and the composition (i.e., homo- or block co-polymers). In addition, the polymer will have a low polydispersity index. Various techniques are employed in this research to determine whether the polymerization processes studied are living.

The Schrock group has completed significant research in both Ziegler-Natta polymerization and ring opening metathesis polymerization (ROMP) in previous years.[3] The goal of this thesis was to develop bifunctional initiators (for both Ziegler-Natta and ROMP) for the synthesis of totally symmetric ABA triblock copolymers by joining two catalytic centers

together with a linker molecule. With the synthesis and characterization of various bifunctional initiators, functionalized monomers containing liquid crystal mesogens were polymerized. Both homo- and triblock co-polymers were synthesized with these functionalized monomers, and the polymers were analyzed for their properties.

References

(1) For a general introduction to block copolymers, see: [a)]Hillmyer, M. *Curr. Opin. Solid State Mater. Sci.* **1999**, *4*, 559. [b)] Hadjichristidis, N.; Pispas, S.; Floudas, G. A. *Block Copolymers - Synthetic Strategies, Physical Properties, and Applications*; John Wiley and Sons: New Jersey, USA, 2003.

(2) Coates, G. W.; Hustad, P. D.; Reinarz, S. *Angew. Chemie. Int. Ed.* **2002**, *41*, 2236.

(3) See References in Chapter 1 and 2, respectively.

Chapter 1 - Synthesis of Hafnium Bifunctional Initiators for Ziegler-Natta Polymerization

1.1 Introduction

The polymerization of α-olefins by hafnium and zirconium dialkyl complexes containing diamido-donor ligands was a major focus of research in the Schrock group for many years.[1-29] One of the ligand structures found to support catalysis is a diamido pyridine donor ligand ($[(MesitylNCH_2)_2CMe(2\text{-}C_5H_4N)]^{2-}$, abbreviated as $(MesNpy)^{2-}$) that has enforced facial geometry. Upon activation, dialkyl hafnium and zirconium catalysts containing this ligand were found to be catalysts for the polymerization of α-olefins. The polymerizations were generally well-behaved and were "living" in some cases (the criteria for a "living" polymerization can be found in the General Introduction).

A typical Ziegler-Natta polymerization process involves three steps: activation, initiation and propagation (Scheme 1.1). In the activation step, an activator is added to a dialkyl complex to form the initiator, a monocation coordinated to a weakly bound anion. In the initiation step, one equivalent of α-olefin inserts into the metal-alkyl bond to form the first-insertion product. In the third step, propagation, additional equivalents of the olefin insert into the first-insertion product to form the propagating polymer. Common activators for hafnium and zirconium diamido-donor systems include $\{Ph_3C\}\{B(C_6F_5)_4\}$ and $B(C_6F_5)_3$. An important characteristic of a living polymerization process is that the rate of initiation is greater than or equal to the rate of propagation. In polymerizations involving activated $\{(MesNpy)Hf(R)\}^+$ catalysts, the rate of polymerization of 1-hexene is usually slow enough for the reaction to be monitored by ^1H NMR spectroscopy.

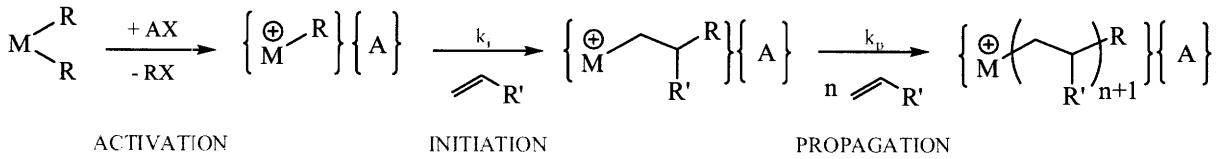

Scheme 1.1 Ziegler-Natta polymerization process.

For the polymerization to proceed, the activated complex {C} must dissociate from the anion {A}. The dissociated cation is then available to react with one equivalent of monomer (M) to produce the propagating species {C-M} (Scheme 1.2).[30] An equation for the rate of polymerization can be derived based upon simple first-order kinetics. The plot of ln[M] versus time is linear, and the slope of the graph is the observed rate constant (k_{obs}). Based on the equations given below, the first-order rate constant for the polymerization (k_p) is simply k_{obs} divided by the catalyst concentration.

$$\{C\text{-}A\} \underset{k_{-1}}{\overset{k_1}{\rightleftharpoons}} \{C\} + \{A\}$$

$$\{C\} + \{M\} \xrightarrow{k_2} \{C\text{-}M\}$$

$$\ln[M] = \ln[M_o] - k_{obs}(t)$$

where M = monomer concentration
M_o = initial monomer concentration
t = time
$k_{obs} = (k_1k_2[\{C_{total}\}])/(k_{-1})[\{A\}]$

Scheme 1.2 First-order kinetic equations.

We wanted to expand the application of these Ziegler-Natta catalysts to the preparation of triblock copolymers. As discussed in the General Introduction, there are many benefits of using a bifunctional initiator instead of a monofunctional initiator for the preparation of triblock copolymers. We hoped to synthesize mixed alkyl bifunctional hafnium species containing the $(MesNpy)H_2$ ligand. This Chapter discusses the investigation of bifunctional hafnium initiators, beginning with the synthesis and study of monofunctional analogs.

1.2 Synthesis and Characterization of Monofunctional Analogs

Before we synthesized bifunctional hafnium compounds, we wanted to establish the basic premise for this project. We needed to determine that when a mixed alkyl compound, $(MesNpy)Hf(R^1)(R^2)$, was activated by a co-catalyst (AX), only one alkyl moiety would be selectively removed to form $\{(MesNpy)Hf(R^1)\}\{A\}$ and R^2X (Equation 1). If this premise did

not hold true, the linker in a bifunctional complex would be cleaved, thereby rendering the initiator useless for the synthesis of triblock copolymers through two addition steps. Therefore, monometallic analogs of the target hafnium species were synthesized that contain alkyl groups representative of some of the proposed linkers.

$$(MesNpy)Hf(R^1)(R^2) + AX \longrightarrow \{(MesNpy)Hf(R^1)\}\{A\} + R^2X \quad (1)$$

The synthesis of $(MesNpy)H_2$ is outlined in Scheme 1.3.[24,31] The ligand can be metallated by reaction with $Hf(NMe_2)_4$ to form $(MesNpy)Hf(NMe_2)_2$ (Scheme 1.4). The dimethylamide groups can be easily exchanged for chloride ions through reaction with TMSCl to form $(MesNpy)HfCl_2$ (**1**).[24] This is the common starting material for all subsequent reactions. The characteristic ^1H NMR chemical shift of the *ortho*-proton of the pyridyl ring is a useful handle when analyzing compounds containing this ligand. For **1**, this resonance is observed at 10.36 ppm.

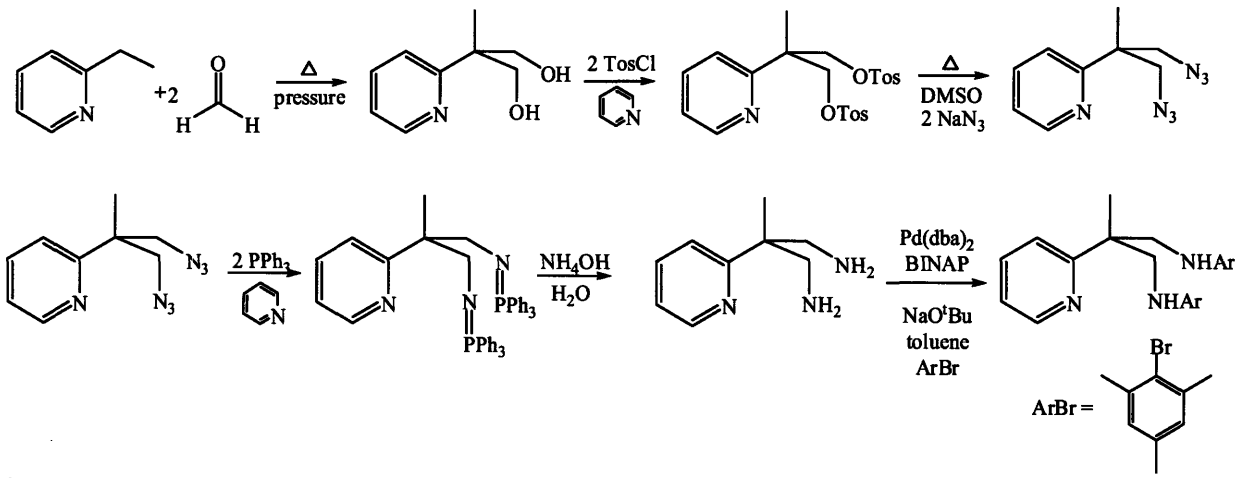

Scheme 1.3 Synthesis of $(MesNpy)H_2$.

$$(MesNpy)H_2 + Hf(NMe_2)_4 \xrightarrow{-\ 2\ HNMe_2} (MesNpy)Hf(NMe_2)_2 \xrightarrow[-\ 2\ TMSNMe_2]{+\ 2\ TMSCl} (MesNpy)HfCl_2\ (\mathbf{1})$$

Scheme 1.4 Synthesis of **1**.

(MesNpy)Hf(Neo)R ((**2b**), R = Me, Neo = CH_2CMe_2Ph) and (MesNpy)Hf(CH_2TMS)(R), ((**3b**), R = Me and (**4b**), R = *i*-Bu)) were the first species investigated. (MesNpy)Hf(Neo)Cl (**2a**), the precursor for the synthesis of **2b,** is synthesized through the dropwise addition of one equivalent of NeoMgCl to **1**. Reaction of one equivalent of MeMgBr with **2a** yields **2b** (Scheme 1.5).

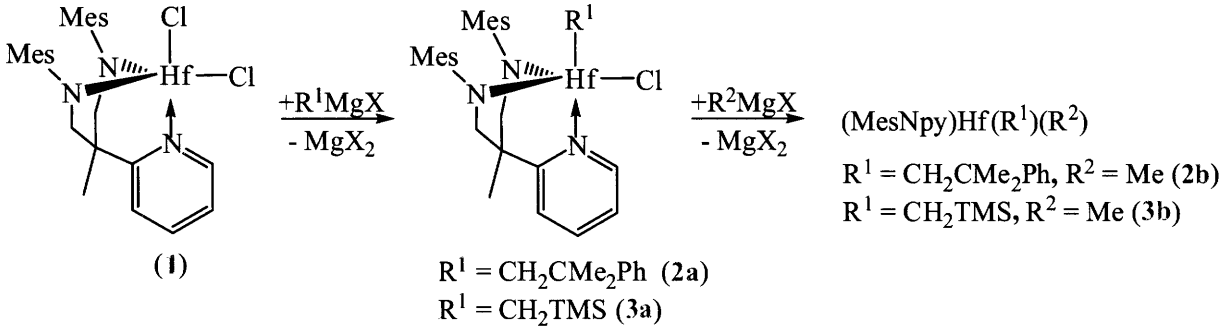

Scheme 1.5 Synthesis of **2a**, **2b**, **3a**, and **3b**.

X-ray quality crystals of **2a** were obtained from a cooled diethyl ether solution. The solid state structure of **2a** contains two chemically equivalent but crystallographically independent molecules (Figure 1.1, Table 1.2). Selected bond lengths and angles are given in Table 1.1. The bond lengths and angles are comparable to those found in related structures; a similar structure was obtained where the alkyl group was isopropyl.[24] In the structure of **2a**, the alkyl group is in the axial position of the trigonal bipyramidal structure. The main difference between the two molecules of the asymmetric unit is the dihedral angle of the neophyl moiety (88° and 168°). ^1H NMR spectroscopy reveals only one *ortho*-pyridyl resonance at 9.66 ppm, indicating that only one isomer is present in solution, as observed in the solid state. Two isomers are possible if the neophyl moiety is in the axial or the equatorial position. Two resonances are observed for the methyl groups of the aryl rings, and the resonances are slightly broad, indicating restricted

rotation about the N-C_{ipso} bond of the mesityl group. The backbone protons are inequivalent on the NMR timescale.

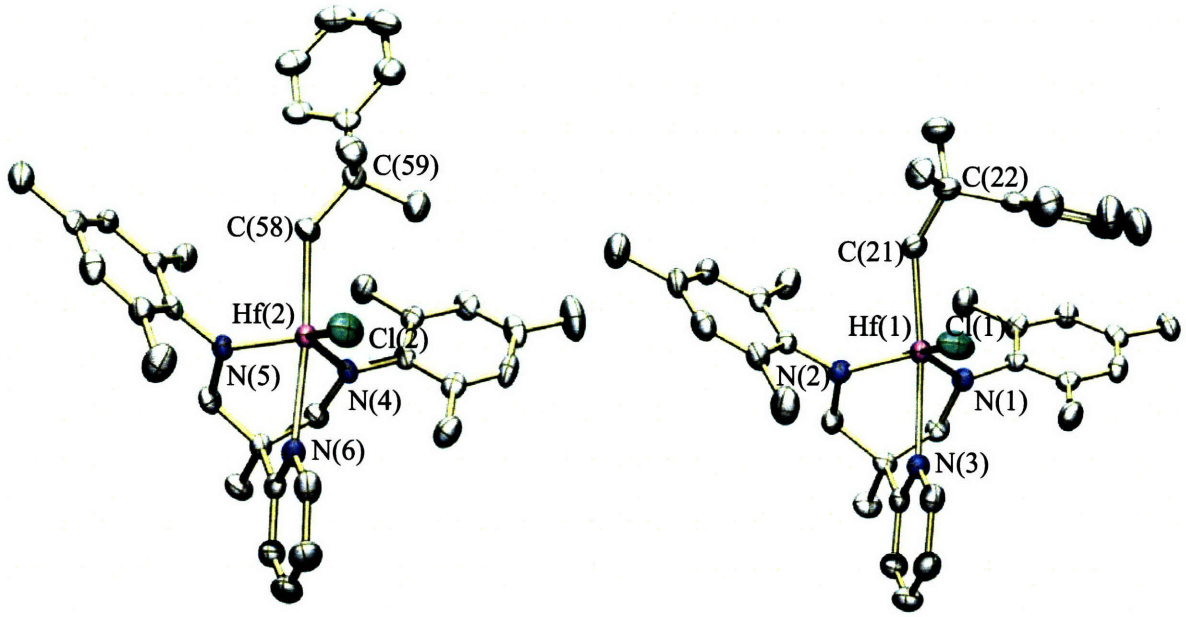

Figure 1.1 Thermal ellipsoid plot of the two crystallographically independent molecules in the unit cell of **2a**. Solvent molecules and hydrogen atoms have been removed for clarity.

Hf(1)-N(1)	2.009(3)	Hf(2)-N(4)	2.003(3)
Hf(1)-N(2)	2.001(3)	Hf(2)-N(5)	2.003(3)
Hf(1)-N(3)	2.427(3)	Hf(2)-N(6)	2.431(4)
Hf(1)-Cl(1)	2.4400(12)	Hf(2)-Cl(2)	2.4497(12)
Hf(1)-C(21)	2.254(4)	Hf(2)-C(58)	2.248(4)
C(21)-Hf(1)-Cl(1)	93.92(12)	C(58)-Hf(2)-Cl(2)	95.24(12)
C(21)-Hf(1)-N(3)	173.33(15)	C(58)-Hf(2)-N(6)	174.00(14)
C(21)-C(22)-C(23)	110.4(4)	C(58)-C(59)-C(60)	113.6(4)

Table 1.1 Selected bonds lengths (Å) and angles (°) for **2a**.

Empirical formula	$C_{39}H_{51}ClHfN_3O_{0.50}$
Formula weight	783.77 g/mol
Compound ID	03061
Temperature	193(2) K
Wavelength	0.71073 Å
Crystal system	Triclinic
Space group	$P\bar{1}$
Unit cell dimensions	a = 9.9535(11) Å b = 16.4513(18) Å c = 23.768(3) Å α= 107.613(2)° β= 94.745(2)° γ = 94.749(2)°
Volume	3673.0(7) $Å^3$
Z	4
Density (calculated)	1.417 Mg/m^3
Absorption coefficient	2.944 mm^{-1}
F(000)	1596
Crystal size	0.27 × 0.19 × 0.17 mm^3
Theta range for data collection	2.32 to 23.30°
Index ranges	-11 <= *h* <= 11 -18 <= *k* <= 17 -17 <= *l* <= 26
Reflections collected	15203
Independent reflections	10447 [*R*(int) = 0.0210]
Completeness to theta = 23.30°	98.6%
Absorption correction	SADABS
Refinement method	Full-matrix least-squares on F^2
Data / restraints / parameters	10447 / 0 / 823
Goodness-of-fit on F^2	1.009
Final R indices [I>2sigma(I)]	R1 = 0.0284, wR2 = 0.0584
R indices (all data)	R1 = 0.0396, wR2 = 0.0619
Largest diff. peak and hole	0.711 and -0.619 $e.Å^{-3}$

Table 1.2 Crystal data and structure refinement for **2a**.

The ^{1}H NMR spectrum of **2b** revealed that both isomers are present in solution in an approximate 2:1 ratio (pyridyl resonances at 8.81 and 8.79 ppm, respectively). An impurity of (MesNpy)HfMe$_2$ is also present as determined by ^{1}H NMR spectroscopy (5%, 8.87 ppm).

3a was synthesized through the addition of TMSCH$_2$MgCl to **1**. By ^{1}H NMR spectroscopy, a small amount of (MesNpy)Hf(CH$_2$TMS)$_2$ and **1** were present in the isolated crude material. These impurities could be removed because of the solubility properties of the three compounds. **1** is insoluble in ether and pentane, **3a** is insoluble in pentane, while (MesNpy)Hf(CH$_2$TMS)$_2$ is soluble in both pentane and ether. The ^{1}H NMR spectrum of **3a** indicates that only one isomer is present in solution (9.68 ppm).

3b was synthesized through the addition of MeMgBr to **3a**. The ^{1}H NMR spectrum suggests that both isomers of **3b** are present in solution (8.97 and 8.89 ppm, 2:1 ratio respectively), as well as small amounts of (MesNpy)HfMe$_2$ and (MesNpy)Hf(CH$_2$TMS)$_2$. When the reaction was stirred for one hour, a greater percentage of the (MesNpy)Hf(CH$_2$TMS)$_2$ and (MesNpy)HfMe)$_2$ formed as compared to a reaction stirred for only 45 minutes. This suggests that the alkyl groups were exchanging in solution. An ^{1}H NMR spectrum of a reaction was stirred for only five minutes revealed that only an impurity of (MesNpy)HfMe$_2$ formed. The absence of (MesNpy)Hf(CH$_2$TMS)$_2$ suggests that the alkyl groups did not exchange during this short reaction time. (MesNpy)HfMe$_2$ can be explained by addition of a small excess of methyl Grignard to **3a**. In isolated **3b** used for subsequent reactions, only an impurity of (MesNpy)HfMe$_2$ (~7%) was present.

It was proposed that alkyl exchange might be slow if the second alkyl group was larger. Therefore, (MesNpy)Hf(CH$_2$TMS)(*i*-Bu) (**4b**) was synthesized via the intermediate (MesNpy)Hf(*i*-Bu)Cl (**4a**) (Scheme 1.6). ^{1}H NMR spectroscopy of **4b** revealed that both the

axial and equatorial isomers (~1:1 ratio) are present in solution as determined by the presence of two equally intense *ortho*-pyridyl resonances (9.05 and 8.92 ppm). **4b** was the only mixed alkyl hafnium compound that was isolated cleanly.

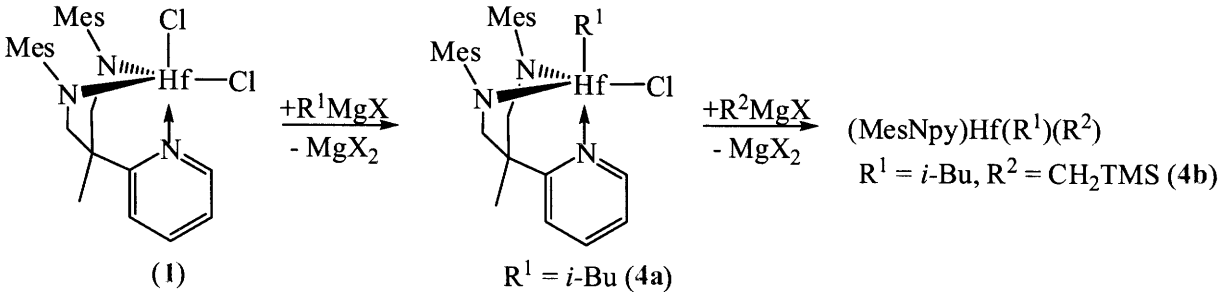

Scheme 1.6 Synthesis of **4a** and **4b**.

The three mixed alkyl hafnium compounds synthesized (**2b**, **3b**, and **4b**) could be used to investigate whether one alkyl moiety could be selectively removed. It should be emphasized that **2a** and **3b** compounds employed in subsequent reactions were approximately 90 – 95% pure as determined by ^{1}H NMR spectroscopy. The impurities present in these compounds were the homo-alkyl species as mentioned above.

1.3 Activation Studies of Monometallic Analogs

The purpose of the activation studies discussed in this section was to determine whether one specific alkyl group could be selectively removed from each of the three mixed alkyl species, **2b**, **3b** and **4b**. If this hypothesis does not hold true, the corresponding bifunctional species would be cleaved and a triblock copolymer would not be synthesized cleanly.

To activate a complex, an activator was added to a stirred solution of the mixed alkyl complex in bromobenzene at -35 °C (e.g. Scheme 1.7). The solution was observed by ^{1}H NMR spectroscopy to confirm activation and to determine the byproduct formed. If the activation was complete and selective, 1-hexene was added to the solution, and in some cases, the

polymerization was followed by ^{1}H NMR spectroscopy. After the polymerization was complete, the polymer was isolated from the reaction mixture and analyzed by gel permeation chromatography (GPC). Unless otherwise stated, all activations and polymerizations were conducted at -35 °C and 0 °C, respectively.

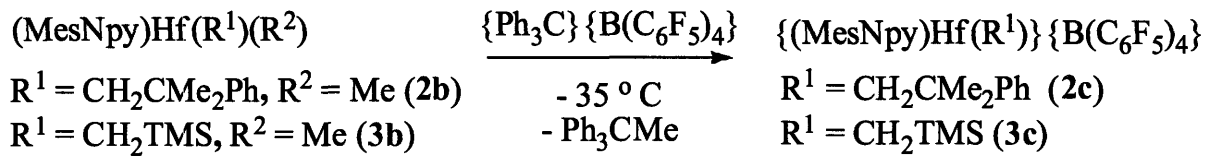

Scheme 1.7 Activation of **2b** or **3b** with $\{Ph_3C\}\{B(C_6F_5)_4\}$.

^{1}H NMR spectroscopy of the mixture of **2b** with $\{Ph_3C\}\{B(C_6F_5)_4\}$ suggested that the methyl ligand was removed selectively to yield $\{(MesNpy)Hf(CH_2CMe_2Ph\}^+$ (**2c**), as determined by the formation of Ph_3CCH_3. **2c** polymerized 160 equivalents of 1-hexene over a twelve-hour period at room temperature. The polymer was isolated and analyzed by GPC. In this Chapter, the number average molecular weights (M_n) obtained by GPC studies can be directly compared with the expected values since the GPC instrument was calibrated using poly(1-hexene) standards. The polydispersity index (PDI) of the polymer isolated was 1.19. The M_n was 4.3×10^4, approximately three times greater than the expected M_n based upon the assumption that the added mixed alkyl species was completely activated. The discrepancy in the molecular weight may be attributed to the impurity of the starting material used for the reaction. While activated $(MesNpy)HfMe_2$ is a known initiator for the polymerization of 1-hexene, the M_n of the polymer formed suggested that its presence alone could not account for the discrepancy. Therefore, $\{(MesNpy)Hf(CH_2CMe_2Ph\}^+$ must be an active catalyst.

Certain experimental criteria should be met by a living system, two of which are that the actual M_n should be equal to the expected M_n and that the polydispersity index should be low. Therefore, the acquired results suggest that **2c** did not function as a living system: possible

reasons for this include interference by the (MesNpy)$HfMe_2$ impurity or incomplete activation and/or deactivation. One possible mode of deactivation includes arene coordination of the neophyl moiety, either inter- or intramolecularly. However, inter- or intramolecular coordination of the aryl moiety of a neophyl-type linker between two hafnium centers would be difficult. Despite the result that this system was not living, a neophyl moiety is an appropriate alkyl group for investigation with bimetallic hafnium systems as the methyl group can be selectively removed from the mixed alkyl species.

Activation of **3b** with $\{Ph_3C\}\{B(C_6F_5)_4\}$ afforded the desired cation, $\{(MesNpy)Hf(CH_2TMS)\}^+$ (**3c**) which polymerized 160 equivalents of 1-hexene over approximately two hours. The actual M_n (2.09×10^4) was slightly larger than the expected M_n (1.32×10^4) and the PDI remained low (1.07), which suggests that the system was more well-behaved than **2c**. Again, the discrepancy of the number average molecular weight of the polymer may be attributed to the impurities present in isolated **3b**.

Kinetic studies were not completed on activated **3b** because significant impurities were present in the isolated material. **4b**, the analogous *i*-Bu complex, was isolated cleanly and so kinetic studies were carried out using this species. When **4b** was activated with $\{Ph_3C\}\{B(C_6F_5)_4\}$ or $B(C_6F_5)_3$, the *i*-Bu moiety was selectively removed (via β-hydride abstraction and formation of isobutene) and the cation, **3c,** was formed. The cation proved to be an initiator for the polymerization of 1-hexene, the disappearance of which was monitored by ^1H NMR spectroscopy. The plot of the natural log of [1-hexene] versus time gave a straight line with the exception of a slight curve at the start (Figure 1.2). This curve is characteristic of a slow initiation process that is competing with chain growth in the early stages of the polymerization. The linearity of the plot suggests that the polymerization was first-order in 1-hexene, and with

simple assumptions, the first-order rate constant (k_p) was calculated. When $\{Ph_3C\}\{B(C_6F_5)_4\}$ is used as a cocatalyst, the calculated k_p values are 0.082 and 0.083 M^{-1} sec^{-1} in two isolated runs and when $B(C_6F_5)_3$ is used, the values are 0.034 and 0.035 M^{-1} sec^{-1}. These values can be compared with those for (MesNpy)Hf(*i*-Bu)$_2$ in which the related k_p values are 0.10 M^{-1} sec^{-1} ($\{Ph_3C\}\{B(C_6F_5)_4\}$ co-catalyst) and 0.048 M^{-1} sec^{-1} ($B(C_6F_5)_3$ co-catalyst).[25] The PDI values for the polymers synthesized are low (average 1.04) and the actual M_n are minimally higher than the expected M_n. These results suggest that activated **4b** consumed 1-hexene in a living fashion, with the exception of a slight initiation effect.

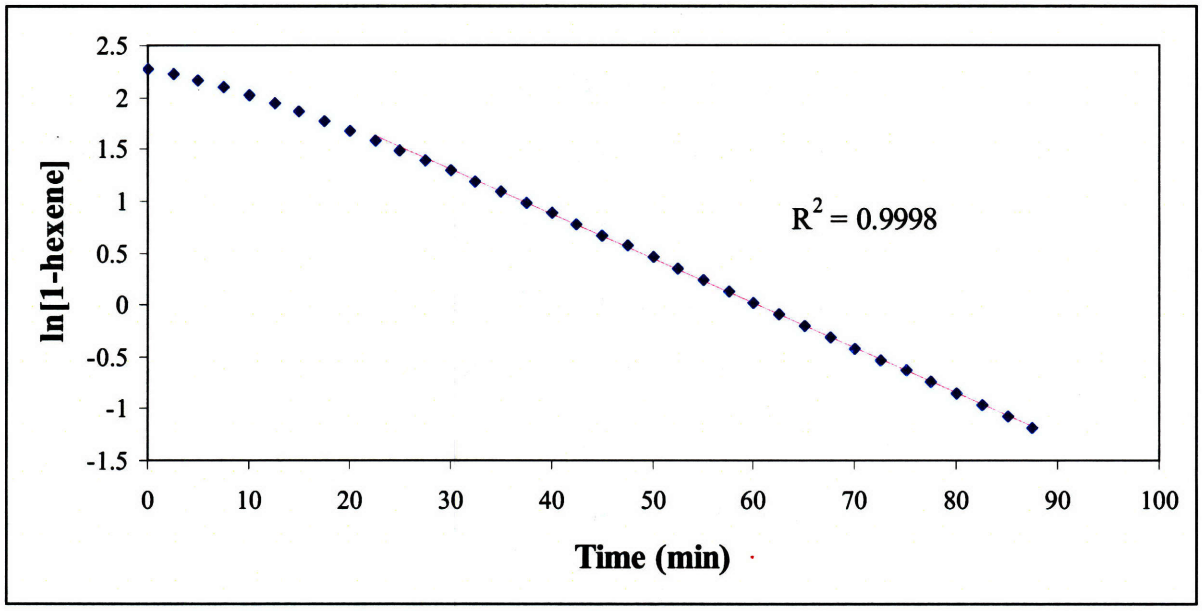

Figure 1.2 Plot of ln[1-hexene] vs. time (min) for the polymerization of 1-hexene catalyzed by **4b** activated with $\{Ph_3C\}\{B(C_6F_5)_4\}$.

1.4 Synthesis and Activation of Bifunctional Hafnium Initiators

Five linkers were investigated for the synthesis of bifunctional hafnium compounds: a) **dineophyl**$(M)_2$ {M-$CH_2CMe_2(C_6H_4)CMe_2CH_2$-M), b) **disilyl**$(M)_2$ (M-$CH_2SiMe_2(CH_2)_5SiMe_2CH_2$-M), c) **disilophyl**$(M)_2$ (M-$CH_2SiMe_2(C_6H_4)SiMe_2CH_2$-M), d)

dicyclohexylmethyl($M)_2$ (*trans*-M-$CH_2(C_6H_{10})CH_2$-M), and e) **dibenzyl**($M)_2$ (M-$CH_2(C_6H_4)CH_2$-M), discussed in this respective order (Figure 1.3).

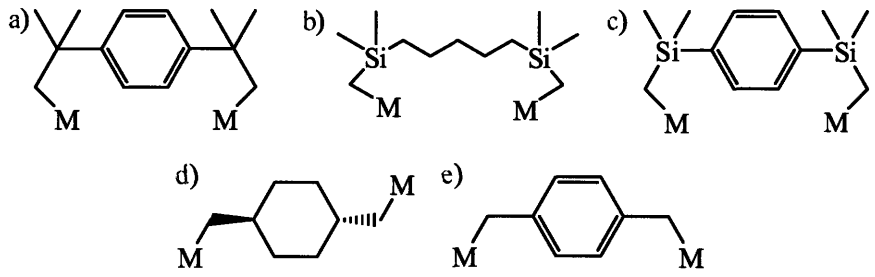

Figure 1.3 Investigated linkers: a) **dineophyl**($M)_2$ b) **disilyl**($M)_2$ c) **disilophyl**($M)_2$ d) **dicyclohexylmethyl**($M)_2$ and e) **dibenzyl**($M)_2$

The first linker to be investigated was **dineophyl**. Although there was a literature preparation available for the synthesis of **dineophyl**$(Cl)_2$, the yield was low (2.6%) and the main product isolated was neophyl chloride (Scheme 1.8).[32] The published method involved the addition of methallyl chloride to five equivalents of benzene over a 24 hour period. This method was improved upon by varying the conditions and by adding three equivalents of methallyl chloride. The reaction is catalyzed by sulfuric acid, but its presence causes an unfavorable reaction as well. When sulfuric acid is added to colorless methallyl chloride the solution immediately turns dark red due to the formation of oligomers/polymers of methallyl chloride. Therefore, the concentration of methallyl chloride has to remain low at all times. Two equivalents of methallyl chloride were added dropwise over two days to a solution of benzene and a catalytic amount of sulfuric acid. A third equivalent of methallyl chloride was added over the third day. The improved yield using this procedure was 7.49 g (5.6%).

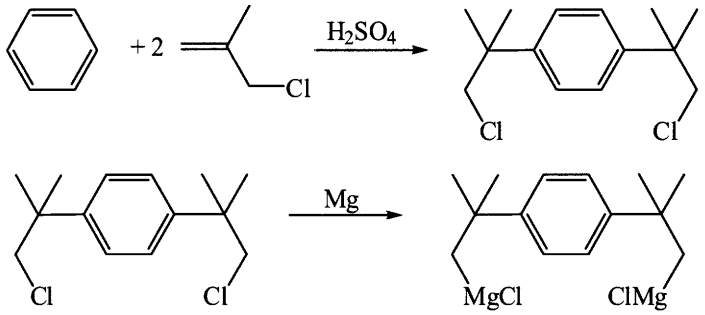

Scheme 1.8 Synthesis of **dineophyl**$(Cl)_2$ and **dineophyl**$(MgCl)_2$

An attempt to synthesize **dineophyl**$(MgCl)_2$ was carried out by the dropwise addition of **dineophyl**$(Cl)_2$ to a suspension of magnesium turnings in tetrahydrofuran. The resulting solution was refluxed for two days, during which time a large amount of white precipitate formed and the solution became light brown. The precipitate, magnesium turnings, and filtrate were isolated individually. The white precipitate reacted with 1,10-phenanthroline to form a purple solution indicating the presence of an alkyl magnesium compound. The purple solution changed color slowly with the addition of 2-propanol. This slow reaction and the insolubility of the white powder suggest that the isolated compound was a polymeric species. Various attempts to identify the white powder were unsuccessful. The reaction of the white powder with **1** yielded unidentifiable products and free ligand. More reactive sources of magnesium such as magnesium anthracene and Rieke magnesium were also used as reagents for the synthesis of **dineophyl**$(MgCl)_2$; all attempts were unsuccessful. To avoid the possibility of a polymeric species, the lithium reagent was targeted; all synthetic attempts were unsuccessful. Therefore, due to the difficulties in isolating a suitable **dineophyl**$(X)_2$ reagent, a new linker, **disilyl**$(X)_2$, was investigated.

The available literature preparation for **disilyl**$(Cl)_2$, involving the reaction of two equivalents of $ClSi(Me_2)CH_2Cl$ to $BrMg(CH_2)_5MgBr$, was followed with slight modifications to allow for ease of isolation (Scheme 1.9).[33,34] **Disilyl**$(Cl)_2$ reacted with two equivalents of

magnesium to form **disilyl**$(MgCl)_2$. With the successful synthesis of the Grignard reagent, the bifunctional hafnium complex could be obtained.

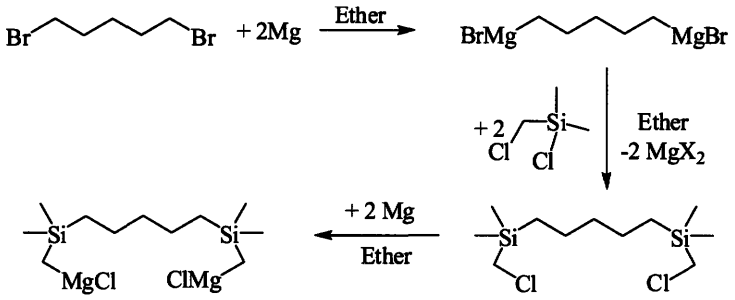

Scheme 1.9 Synthesis of **disilyl**$(Cl)_2$ and **disilyl**$(MgCl)_2$.

The synthesis of a mixed alkyl hafnium bifunctional complex requires two steps (addition of the linker molecule and addition of the second alkyl group). Two synthetic routes could be employed, either via the monometallic, monoalkyl complex (Figure 1.4 – Path A) or via the bimetallic, linked complex (Figure 1.4 – Path B).

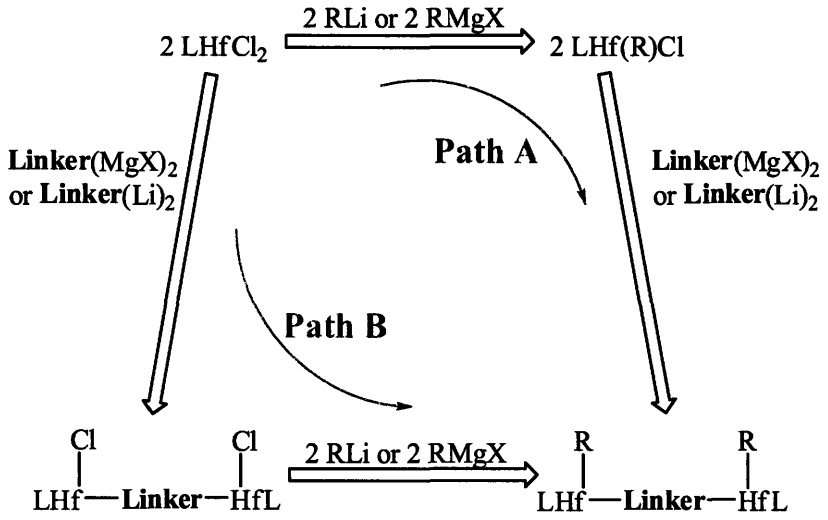

Figure 1.4 Two possible synthetic routes to a bifunctional Hf species (L = [MesNpy])

Path A involves the synthesis of a monometallic, monoalkyl intermediate. When *i*-BuMgBr is used for this synthesis, the intermediate (MesNpy)Hf(*i*-Bu)Cl (**4b**) is readily isolated. However, the second step did not yield a clean product when **disilyl**$(MgCl)_2$ was employed as the

reagent. The crude product isolated contained a significant amount of (MesNpy)Hf(*i*-Bu)$_2$ as determined by ^{1}H NMR spectroscopy. This result indicated that alkyl exchange occurred during the second reaction, most likely formed through transmetallation reactions. Transmetallation reactions may be avoided if the corresponding lithium reagent, **disilyl**(Li)$_2$, is employed instead of the Grignard reagent. Unfortunately, the lithium reagent could not be synthesized. Attempts were also made to synthesize (MesNpy)Hf(Me)Cl, but the reaction did not proceed cleanly when MeLi or MeMgBr was employed as a reagent.

Path B proved to be a more viable route to the desired bimetallic species (Scheme 1.10). Addition of **disilyl**(MgCl)$_2$ to **1** formed the intermediate **disilyl**[(MesNpy)HfCl]$_2$ (**5a**). However, ^{1}H NMR spectroscopy indicated the presence of two bis(alkyl) impurities (~10%). Possible structures for these impurities are given in Figure 1.5. Numerous attempts to remove the bis(alkyl) species were difficult, although clean product was isolated on one occasion from an ether/pentane solution after one month in the freezer.

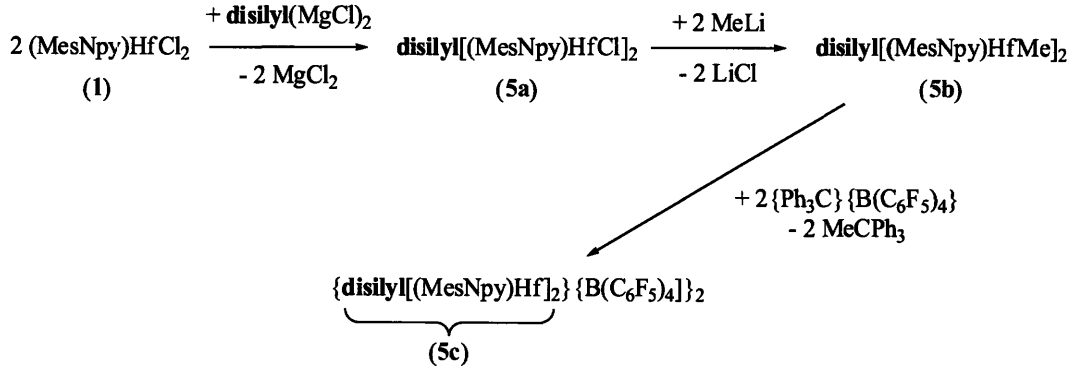

Scheme 1.10 Synthesis of **5a** and **5b**. Activation of **5b** with {Ph_3C}{$B(C_6F_5)_4$}.

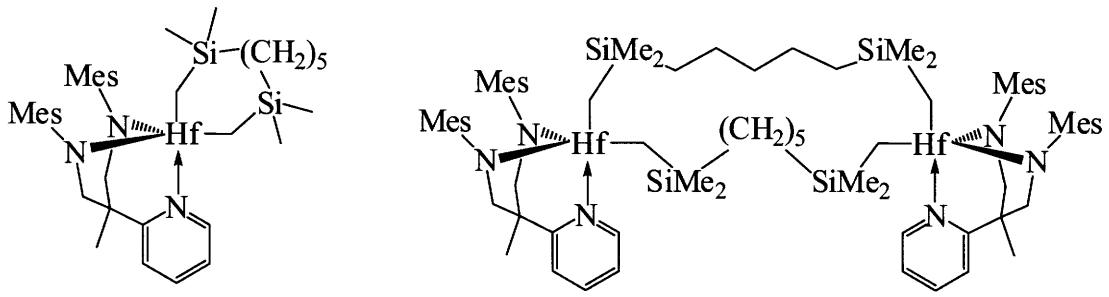

Figure 1.5 Possible bis(alkyl) impurities present in isolated **5a**.

Despite the persisting impurities, the reaction between the the isolated material of **5a** and four different reagents (*i*-BuMgBr, *i*-BuLi, MeMgBr and MeLi) were investigated. When either isobutyl reagent was used, significant alkyl exchange occurred. In the case of *i*-BuMgBr, the large amount of (MesNpy)Hf(*i*-Bu)$_2$ formed was most likely caused by transmetallation reactions. It was hoped that a lithium reagent would produce less dialkyl species because it would limit the possibility of transmetallation reactions that are facilitated by the magnesium reagent. Unfortunately, a large amount of (MesNpy)Hf(*i*-Bu)$_2$ still formed, probably due to the strength of the alkylating reagent. (MesNpy)Hf(*i*-Bu)$_2$ is a known complex for the polymerization of 1-hexene and the presence of such an impurity would have a significant effect on any results gathered.

When MeMgBr was used as an alkylating agent for **5a**, a significant amount of (MesNpy)HfMe$_2$ formed as determined by ^{1}H NMR spectroscopy. The presence of this impurity was again postulated to be caused by transmetallation reactions facilitated by magnesium. When MeLi was employed as the reagent, no (MesNpy)HfMe$_2$ formed, provided the lithium reagent was added very slowly at low temperatures. All three possible isomers of **disilyl**[(MesNpy)HfMe]$_2$ (**5b**) are observed in a 2:1 ratio of the most abundant isomer to the other two isomers combined, as determined by ^{1}H NMR spectroscopy. The structures of the three possible isomers are pictured in Figure 1.6. The linker can occupy both equatorial positions

(Figure 1.6a), both axial positions (Figure 1.6b), or one axial and one equatorial position (Figure 1.6c). It was also determined that the impurity from **5a** was still present. Approximately 85% pure **5b** was isolated and used in numerous kinetic studies; the impurities present were the intermediate **5a** and the bis(alkyl) impurities carried through from the isolation of **5a**.

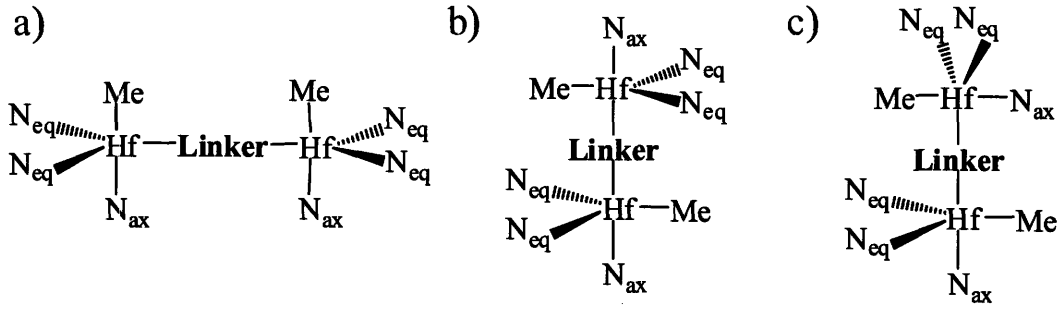

Figure 1.6 Possible isomers of **Linker**[(MesNpy)HfMe]$_2$: a) **Linker** occupying both equatorial positions, b) **Linker** occupying both axial positions, and c) **Linker** occupying one axial and one equatorial position

Activation of isolated **5b** with two equivalents of $\{Ph_3C\}\{B(C_6F_5)_4\}$ forms the desired dication, $\{$**disilyl**[(MesNpy)Hf]$_2\}^{2+}$ (**5c**). 1-Hexene was added to the solution and the polymerization was monitored by ^{1}H NMR spectroscopy. Following the same assumptions used when analyzing the monometallic system data, the average k_p calculated per catalytic center is 0.068 M^{-1} sec^{-1} (over 3 runs) with a standard deviation of 0.006. An initiation period was observed, similar to the monometallic systems. In each case, the PDI values were low (~1.1) and the actual M_n values were slightly higher than the expected M_n values by about the same percentage observed with the monometallic analogs.

5c proved to be a catalyst for the polymerization of 1-octene as well, and the kinetics were analyzed (Figure 1.7). 1-Octene was added to a solution of **5c** after it had polymerized approximately 100 equivalents of 1-hexene. A triblock copolymer should have formed, although this has not been confirmed. The k_p for the polymerization of 1-octene, 0.11 M^{-1} sec^{-1}, is faster than the k_p of 1-hexene, a trend also observed with activated (MesNpy)Hf(*i*-Bu)$_2$.[25] The plot for

the polymerization of 1-octene is straight, which is further evidence that the curve at the beginning the plot for the polymerization of 1-hexene is due to an initiation effect.

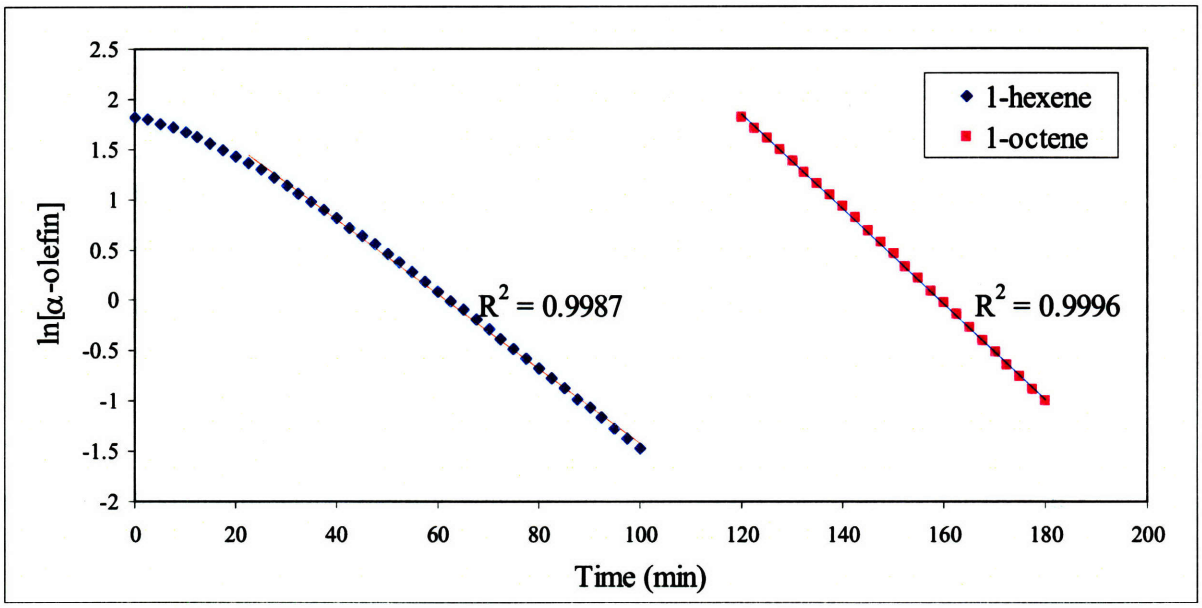

Figure 1.7 Plot of ln[α-olefin] vs. time (min) for the polymerization of 1-hexene and 1-octene catalyzed by **5b** activated with $\{Ph_3C\}\{B(C_6F_5)_4\}$.

The cause of the initiation period was investigated. Control studies were carried out to ensure that incomplete activation was not the cause. A solution of the mixed alkyl species and activator was observed by ^1H NMR spectroscopy. No change was observed in the ^1H NMR spectrum over one hour which suggests that the complex was completely activated by the time the first spectrum was taken (approximately five minutes). In addition, only one major pyridyl resonance was observed, suggesting only one ligand-containing hafnium complex was present in the solution. An interesting relationship was found after addition of the monomer between the pyridyl region resonances and the length of the observed initiation period. During the first twenty minutes, two pyridyl peaks were present in the ^1H NMR spectrum, the growth of one peak corresponding to the disappearance of the other peak (Figure 1.8). At approximately twenty minutes, only one major pyridyl peak was observed. This time corresponds with the end

of the prominent curve observed in the plot of ln[1-hexene] vs. time. This correspondence suggests that the curve in the plot is due to a slow initiation relative to polymerization.

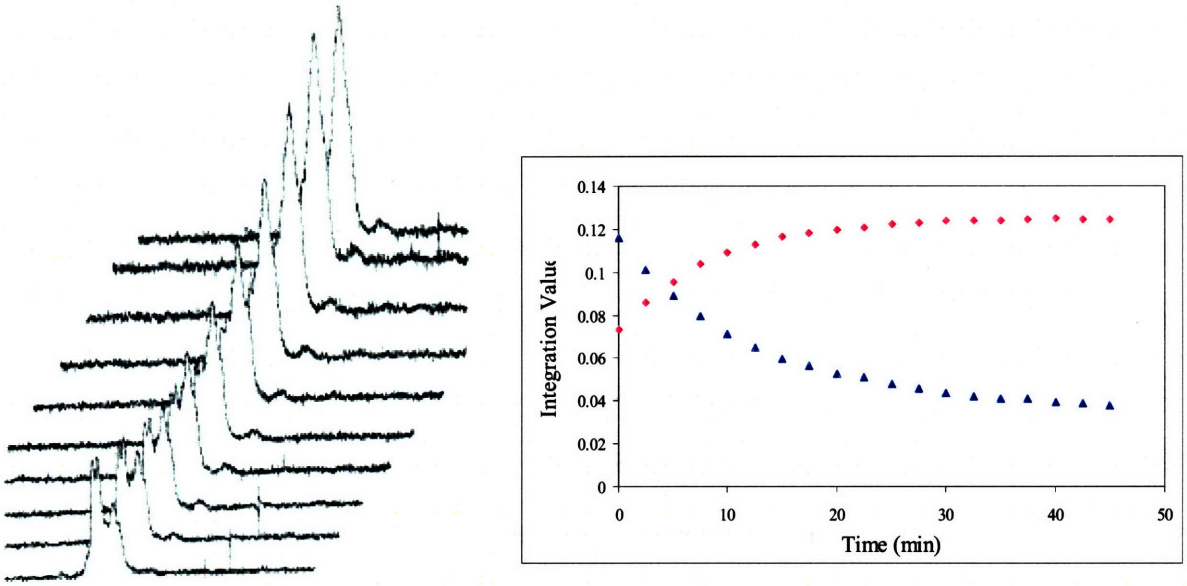

Figure 1.8 Array of ^{1}H NMR spectra of pyridyl region (2.5 minutes per line) (left). Graph of pyridyl peak integration vs. time (right).

Kinetic studies were also completed using $B(C_6F_3)_3$ as the co-catalyst for **5b**. The activation of the mixed alkyl complex does not proceed cleanly, and numerous complexes were observed by ^{1}H NMR spectroscopy. Despite this, kinetic studies were carried out and the k_p value is 0.026 and 0.041 M^{-1} sec^{-1} for two isolated runs. Again, an initiation period was observed during the first twenty minutes. The PDI values of the isolated polymers were much higher (~1.5) and the actual M_n values were approximately three times the expected M_n values. These results, as well as the numerous compounds observed by ^{1}H NMR spectroscopy suggest that **5b** does not act as a living system when activated with $B(C_6F_3)_3$.

The above results demonstrate that **5b** activated with $\{Ph_3C\}\{B(C_6F_5)_4\}$ is an active catalyst for the polymerization of 1-hexene and is relatively well-behaved. Isolation of pure

mixed alkyl species needs to be accomplished as the impurities in solution may be active catalysts and could possibly lead to the synthesis of homopolymer or diblock copolymer as opposed to the desired triblock copolymer. Therefore, three different linkers were investigated: **disilophyl**, **dicyclohexylmethyl**, and **dibenzyl**. We hoped that the more rigid structures of these linkers would aid in recrystallization and purification of the compounds.

The published preparation of **disilophyl**$(Cl)_2$ involved the addition of two equivalents of chloro(chloromethyl)dimethylsilane to the Grignard reagent of 1,4-dibromobenzene in tetrahydrofuran.[35] The publication did not provide a procedure for the synthesis of the di-Grignard reagent and so additional references were consulted. The most cited synthesis of this Grignard reagent uses Rieke Magnesium (Scheme 1.11).[36] Numerous attempts following this method did not yield the desired compound so an alternate synthetic route was employed.[37]

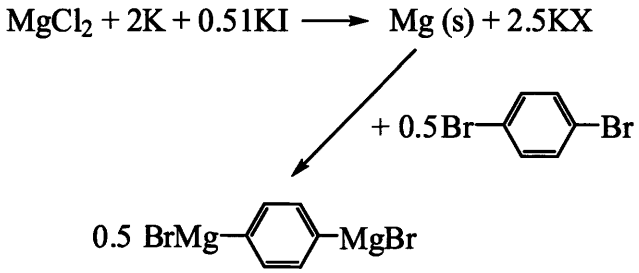

Scheme 1.11 Attempted synthesis of 1,4-$(MgBr)_2(C_6H_4)$.

1,4-Dibromobenzene and magnesium were refluxed in tetrahydrofuran, and one equivalent of dibromoethane was added dropwise over an eight hour period (Scheme 1.12); the slow addition of dibromoethane ensured that the magnesium was constantly activated. Addition of the resulting Grignard reagent to the silane afforded **disilophyl**$(Cl)_2$.

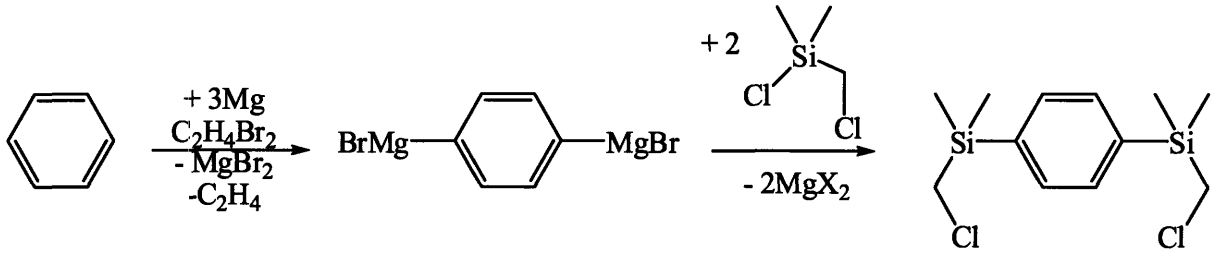

Scheme 1.12 Synthesis of **disilophyl**$(Cl)_2$.

The synthesis of the **disilophyl**$(MgCl)_2$ could proceed with the isolation of the halogen precursor. In the first attempt to synthesize **disilophyl**$(MgCl)_2$, a simple reaction in tetrahydrofuran was carried out. The reaction seemed to proceed readily with refluxing overnight. However, during work-up, the solution was concentrated and a precipitate formed which did not redissolve into tetrahydrofuran or diethyl ether and did not react cleanly with **1**. The Grignard preparation was repeated without concentrating the solution, and a THF solution was isolated with an approximate concentration of 0.075 N.

The reaction between **disilophyl**$(MgCl)_2$ and **1** was investigated in attempts to isolate the desired linked compound, **disilophyl**$[(MesNpy)HfCl]_2$. Various reaction conditions were employed, and moderately pure **disilophyl**$[(MesNpy)HfCl]_2$ was isolated. Attempts to alkylate the isolated material with MeLi or *i*-BuLi yielded multiple products. Therefore, future studies of this linker were abandoned and **dicyclohexylmethyl** was investigated.

The literature preparation of **dicyclohexylmethyl**$(Br)_2$ calls for the addition of **dicyclohexylmethyl**$(OH)_2$ in benzene to a solution of PBr_3 in benzene.[38,39] Attempts to follow this synthetic procedure failed because the alcohol is insoluble in benzene. Therefore, the procedure was modified and PBr_3 was added slowly to a suspension of **dicyclohexylmethyl**$(OH)_2$ in benzene, and the resulting slurry was refluxed for 75 minutes

(Scheme 1.13). After work-up and removal of unreacted alcohol, **dicyclohexylmethyl**$(Br)_2$ was isolated cleanly.

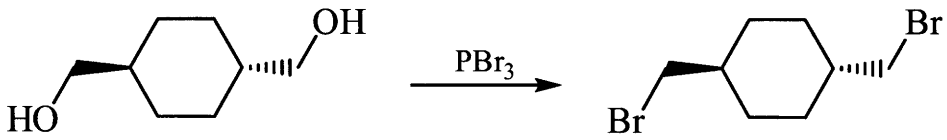

Scheme 1.13 Synthesis of **dicyclohexylmethyl**$(Br)_2$.

Dicyclohexylmethyl$(MgBr)_2$ had been synthesized previously but was used *in situ*.[38] After numerous attempts and modification of the reaction conditions, the Grignard reagent was isolated by recrystallization from a diethyl ether solution. Titration revealed the approximate molecular weight to be 196 g/mole Mg, corresponding to one molecule of diethyl ether per magnesium center.

Dicyclohexylmethyl$(MgBr)_2$ was reacted with **1** and a large amount of halogen exchange occurred; the main product isolated was (MesNpy)$HfBr_2$. To avoid this complication, either (MesNpy)$HfBr_2$ needed to be employed as the starting hafnium material or the dichloride Grignard needed to be synthesized. The latter route was chosen to be investigated.

Dicyclohexylmethyl$(Cl)_2$ is also a known compound, although the synthetic methods are not desirable because of the reagents used.[40,41] PCl_3 was employed in an analogous procedure as described above with PBr_3, but the desired compound was only a minor product. Therefore, a new method was developed and thionyl chloride was added to a solution of the alcohol in pyridine. The reaction was refluxed overnight, and upon work-up, **dicyclohexylmethyl**$(Cl)_2$ was isolated cleanly. Unfortunately, numerous attempts to synthesize the corresponding Grignard reagent, **dicyclohexylmethyl**$(MgCl)_2$, were unsuccessful. Therefore, the last linker to be investigated, **dibenzyl**, became the focus of this research.

Dibenzyl$(Cl)_2$ is commercially available and the corresponding Grignard reagent, **Dibenzyl**$(MgCl)_2$, was readily prepared after condition optimization.[42] After crystallization from a tetrahydrofuran solution, the molecular weight was determined to be 228 g/mol Mg, corresponding to two molecules of tetrahydrofuran per magnesium. This reagent was combined with **1** under varying conditions. All reactions yielded a considerable amount of insoluble, uncharacterized yellow powder. The soluble fraction of the reaction gave multiple products as determined by ^{1}H NMR spectroscopy. **Dibenzyl**[(MesNpy)HfCl]$_2$ was isolated and identified in a small amount once, although the ^{1}H NMR spectrum showed the presence of other products as well.

1.5 Conclusions

Monometallic hafnium mixed alkyl compounds [(MesNpy)Hf(Neo)R] ((**2b**), R = Me, Neo = CH_2CMe_2Ph) and [(MesNpy)Hf(CH_2TMS)(R)], ((**3b**), R = Me and (**4b**), R = *i*-Bu)) were synthesized and characterized. Activation of these species with $\{Ph_3C\}\{B(C_6F_5)_4\}$ or $B(C_6F_5)$ showed that one alkyl group could be selectively removed. Therefore, corresponding bifunctional species were synthesized. Five molecules were considered target linkers, namely **dineophyl**$(M)_2$, **disilyl**$(M)_2$, **disilophyl**$(M)_2$, **dicyclohexylmethyl**$(M)_2$, and **dibenzyl**$(M)_2$. Difficulties were encountered when synthesizing a Grignard or lithium reagent for **dineophyl**. **Disilophyl**$(MgCl)_2$, **dicyclohexylmethyl**$(MgBr)_2$, and **dibenzyl**$(MgCl)_2$ were all successfully synthesized but the reactions with **1** did not yield the desired product. Only the reagent **disilyl**$(MgCl)_2$ yielded the desired product, **disilyl**[(MesNpy)HfCl]$_2$, which could be converted to **disilyl**[(MesNpy)HfMe]$_2$ (**5b**). **5b** was found to act as a living initiator for the polymerization of 1-hexene when activated with $\{Ph_3C\}\{B(C_6F_5)_4\}$. Unfortunately, most of the hafnium compound syntheses were plagued with difficulties of transmetallation reactions and the

contamination of the bifunctional species with monofunctional species. Any monofunctional impurities are detrimental to this project because homo- or diblock co-polymers would form upon activation and therefore, the triblock copolymer would be contaminated. Therefore, due to this underlying problem, this project was abandoned and a new polymerization technique, ring opening metathesis polymerization, became the focus. This research is reported in Chapter 2.

1.6 Experimental Procedures

General Procedures. All manipulations were performed in oven-dried (200 °C) glassware under an atmosphere of nitrogen in a Vacuum Atmospheres glovebox or using standard Schlenk techniques. HPLC-grade solvents were purified by passage through an alumina column and stored over 4 Å Linde-type molecular sieves prior to use. Deuterated solvents were degassed and distilled from CaH_2 or sodium benzophenone ketyl. Commercial reagents were used without further purification. Compound **1**[24] was prepared according to the literature procedure. All Grignard reagents were carefully titrated with 2-propanol in the presence of 1,10-phenanthroline or using the diphenyl ditelluride method[43] prior to use.

NMR spectra were recorded on a Varian INOVA 500 spectrometer. ^{1}H NMR chemical shifts are given in ppm versus residual protons in the deuterated solvents as follows: δ 7.27 $CDCl_3$, δ 7.16 C_6D_6, δ 7.29 C_6D_5Br. X-ray data were collected on a Siemans SMART/CCD diffractometer with λ(MoKα) = 0.71073 Å. GPC analyses were carried out on a system equipped with two Waters Styragel HR 5E columns (300 mm length × 7.8 mm inner diameter) in series. HPLC grade THF was supplied at a flow rate of 1.0 mL/min with a Knauer HPLC pump K501. A Wyatt Technology mini Dawn light-scattering detector coupled with a Knauer differential refractometer was employed. Data analysis was carried out using Astrette 1.2 software (Wyatt technology). PDI values for polymers were obtained using $dn/dc = 0.110$ mL/g.

Synthesis of (MesNpy)Hf(Neo)Cl (2a). A suspension of **1** (0.486 g, 0.749 mmol) in diethyl ether was cooled to -35 °C. NeoMgCl (0.732M in diethyl ether, 1.02 mL, 0.749 mmol) was added to the cooled solution, and the resulting mixture was stirred at room temperature for one hour. During this time the solution changed color slightly and a precipitate formed. 1,4-1,4-Dioxane (0.099 g, 1.12 mmol) was added to the solution and more precipitate formed. The solution was filtered through Celite. The volatile components were removed from the filtrate *in vacuo* to yield a beige powder, which was redissolved in a minimal amount of ether. The solution was filtered and placed in a -35 °C freezer overnight. Colorless crystals formed which were isolated by filtration and dried *in vacuo*; yield 0.138 g (100%); crystal yield 0.050 g (36%): ^{1}H NMR (C_6D_6) δ 9.63 (d, 1H, py-*o*-CH), some aryl peaks omitted here, 6.91 (d, 2H, C*H*), 6.73 (s, 2H, C*H*), 4.19 (d, 2H, CH_2), 2.77 (d, 2H, CH_2), 2.59 (s, 6H, *o*-CH_3), 2.14 (s, 6H, *p*-CH_3), 1.86 (s, 6H, *o*-CH_3), 1.36 (s, 6H, $CH_2C(CH_3)_2Ph$), 1.35 (s, 2H, CH_2CMe_2Ph), 0.95 (s, 3H, CH_3).

Synthesis of (MesNpy)Hf(Neo)(Me) (2b). A solution of **2a** (0.100 g, 0.134 mmol) in diethyl ether was cooled to -35 °C. MeMgBr (3.44 M in diethyl ether, 0.039 mL, 0.134 mmol) was added to the cooled solution, and the resulting mixture was stirred at room temperature for one hour. 1,4-Dioxane (17 mg, 0.201 mmol) was then added to the solution and a white precipitate formed. The solution was filtered through Celite. The volatile components were removed from the filtrate *in vacuo* to yield a beige powder. The powder was redissolved in a minimal amount of pentane, and the solution was filtered. The volatile components were again removed from the filtrate *in vacuo*: ^{1}H NMR (C_6D_6, A and B denote the two isomers, A:B ≅ 2:1) δ 8.81 (d, 1H, py-*o*-CH, A), 8.79 (d, 1H, py-*o*-CH, B), some aryl peaks omitted here, 4.16 (d, 2H, CH_2, A), 4.11 (d, 2H, CH_2, B), 2.86 (d, 2H, CH_2, B), 2.83 (d, 2H, CH_2, A), 2.21 (s, 6H, *p*-CH_3, A and B), 2.2 (broadened into baseline, 12H, *o*-CH_3, A and B), 1.60 (s, 6H,

$CH_2C(CH_3)_2Ph$, B), 1.38 (s, 6H, $CH_2C(CH_3)_2Ph$, A), 1.33 (s, 3H, CH_3, A), 1.24 (s, 3H, CH_3, B), 0.93 (s, 2H, CH_2CMe_2Ph, A), 0.92 (s, 2H, CH_2CMe_2Ph, B), 0.17 (s, 3H, Hf-CH_3, B), 0.14 (s, 3H, Hf-CH_3, A). Also present in the isolated solid was (MesNpy)$HfMe_2$ (8.87, ~5%)

Synthesis of (MesNpy)Hf(CH_2TMS)Cl (3a). A suspension of **1** (0.600 g, 0.925 mmol) in diethyl ether was cooled to -35 °C. $TMSCH_2MgCl$ (0.72M in diethyl ether, 1.21 mL, 0.878 mmol) was added to the cooled solution, and the resulting mixture was stirred at room temperature for one hour. During this time the solution became mostly clear. 1,4-Dioxane (0.122 g, 1.39 mmol) was added to the solution and a precipitate formed. The solution was filtered through Celite. The volatile components were removed from the filtrate *in vacuo* to yield a reddish powder. The solid was washed with a small amount of pentane to remove any (MesNpy)$Hf(CH_2TMS)_2$ formed. The remaining powder was then dissolved in a minimal amount of diethyl ether, and the solution was filtered and placed in a -35 °C freezer overnight. Light pink crystals formed which were isolated by filtration and dried *in vacuo*; yield 0.39 g (61%): ^{1}H NMR (C_6D_6) δ 9.65 (d, 1H, py-*o*-CH), 6.99 (dt, H, py-C*H*), 6.94 (s, 2H, C*H*), 6.74 (s, 2H, C*H*), 6.72 (t, H, py-C*H*), 4.60 (m, H, py-C*H*), 4.16 (d, 2H, CH_2), 2.79 (d, 2H, CH_2), 2.70 (s, 6H, *o*-CH_3), 2.13 (s, 6H, *p*-CH_3), 1.86 (s, 6H, *o*-CH_3), 0.90 (s, 3H, CH_3), 0.48 (s, 2H, $CH_2Si(CH_3)_3$), 0.09 (d, 9H, $CH_2Si(CH_3)_3$).

Synthesis of (MesNpy)Hf(CH_2TMS)(Me) (3b). A solution of **3a** (0.096 g, 0.137 mmol) in diethyl ether was cooled to -35 °C. MeMgBr (3.75 M in diethyl ether, 0.039 mL, 0.130 mmol) was added to the cooled solution and a white precipitate formed immediately. The solution was stirred at room temperature for an allotted time (60, 45 or 5 minutes). 1,4-Dioxane (17 mg, 0.201 mmol) was added to the solution and additional white precipitate formed. The solution was filtered through Celite. The volatile components were removed from the filtrate *in*

vacuo to yield a beige powder. The powder was redissolved in a minimal amount of pentane, and the solution was filtered and placed in a -35 °C freezer. A solid formed which was isolated by filtration and dried *in vacuo*; yield 0.111 g (83%): ^{1}H NMR (C_6D_5Br, A and B denote the two isomers, A:B ≅ 2:1) δ 8.98 (d, 1H, py-*o*-C*H*, B), 8.93 (d, 1H, py-*o*-C*H*, A), 7.48 (t, 2H, py-C*H*, B), 7.46 (t, 2H, py-C*H*, A), 7.17 (d, 2H, py-C*H*, B), 7.14 (d, 2H, py-C*H*, A), 7.01 (t, 2H, py-C*H*, B), 6.97 (t, 2H, py-C*H*, A), 6.82 (s, 4H, C*H*, A and B), 4.11 (d, 2H, CH_2, A and B), 2.84 (d, 2H, CH_2, B), 2.82 (d, 2H, CH_2, A), 2.63 (broadened into baseline, 6H, *o*-CH_3, A and B), 2.15 (s, 6H, *p*-CH_3, A and B), 1.76 (broadened into baseline, 6H , *o*-CH_3, A and B), 1.20 (s, 3H, CH_3, B), 1.19 (s, 3H, CH_3, A), 0.21 (s, 2H, CH_2Si(CH$_3$)$_3$, A), 0.10 (s, 2H, CH_2Si(CH$_3$)$_3$, B), 0.09 (s, 3H, Hf-CH_3, A), 0.07 (s, 3H, Hf-CH_3, B), -0.15 (s, 9H, CH$_2$Si(CH_3)$_3$, A and B). From py-*o*-C*H* resonances, also present when the reaction was stirred for one hour was (ratio w.r.t A), (MesNpy)Hf(CH$_2$TMS)Cl (0.16), (MesNpy)Hf(CH$_2$TMS)$_2$ (0.16), (MesNpy)HfMe$_2$ (0.16). In the reaction that stirred for 5 minutes only (MesNpy)HfMe$_2$ (0.22) was present.

Synthesis of *i*-BuLi. A Fischer Porter bottle was charged with *i*-BuBr (12.6 g, 0.0919 mol) in heptane (20 mL). The bottle was removed from the glovebox and was purged with argon. High sodium, granular lithium (2.6 g, 0.367 mol) was then added quickly to the cooled solution (0 °C) under a constant flow of argon. The bottle was then sealed with the Fischer Porter top, and the solution was slowly warmed to room temperature at which time a white precipitate began to form. The solution was stirred overnight at 60 °C. In the glovebox, the solution was filtered through Celite, was concentrated and placed in -35 °C freezer overnight. A solid formed which was isolated by filtration and dried *in vacuo*; crude yield 5.8 g (100%): ^{1}H NMR (C_6D_6) δ 1.64 (m, 1H, C*H*), 1.11 (d, 1H, CH(CH_3)$_2$), -0.79 (s, 2H, CH_2).

Synthesis of (MesNpy)Hf(*i*-Bu)Cl (4a). A suspension of **1** (0.500 g, 0.770 mmol) in diethyl ether was cooled to -35 °C. *i*-BuMgCl (2.8 M in diethyl ether, 0.261 μL, 0.732 mmol) was added to the cooled solution, and the resulting mixture was stirred at room temperature for fifteen minutes. During this time the solution changed color slightly. 1,4-Dioxane (98 μL, 1.16 mmol) was added to the solution and a precipitate formed. The solution was filtered through Celite. The volatile components were removed from the filtrate *in vacuo* to yield a white powder. The powder was washed with a minimal amount of diethyl ether to remove any (MesNpy)Hf(*i*-Bu)$_2$ product. The powder was redissolved in a minimal amount of benzene and the solution was filtered. The volatile components were removed from the filtrate *in vacuo*. The remaining powder was dissolved in a minimal amount of toluene, and the solution was diluted with pentane and placed in a -35 °C freezer overnight. A solid formed which was isolated by filtration and dried *in vacuo*; yield 0.20 g (41%): ^{1}H NMR (C_6D_6) δ 9.70 (d, 1H, py-*o*-CH), some aryl peaks omitted here, 4.20 (d, 2H, CH_2), 2.80 (d, 2H, CH_2), 2.70 (s, 6H, *o*-CH_3), 2.66 (m, 1H, $CH_2CH(CH_3)_2$), 2.15 (s, 6H, *p*-CH_3), 1.90 (s, 6H, *o*-CH_3), 1.00 (d, 2H, $CH_2CH(CH_3)_2$), 0.92 (s, 3H, CH_3), 0.90 (s, 6H, $CH_2CH(CH_3)_2$); Anal. Calcd for $C_{31}H_{42}ClHfN_3$: C, 55.52; H, 6.31; N, 6.27; Cl, 5.29. Found: C, 55.38; H, 6.26; N, 6.22; Cl, 5.53.

Synthesis of (MesNpy)Hf(CH_2TMS)(*i*-Bu) (4b). A solution of **4a** (0.060 g, 0.0895 mmol) in toluene was cooled to -35 °C. TMSCH_2Li (0.91 M in diethyl ether, 93 μL, 0.0849 mmol) was added to the cooled solution, and the reaction mixture was stirred for fifteen minutes. The solution was filtered through Celite and the volatile components were removed from the filtrate *in vacuo*. The resulting white solid was dissolved in ether and the solution was placed in a -35 °C freezer overnight. Unreacted **4a** precipitated from the solution and was isolated by filtration and dried *in vacuo*. The volatiles components were removed from the filtrate *in vacuo*.

The solid isolated was washed with pentane and dried *in vacuo*: ^{1}H NMR (C_6D_5Br, 273 K, two isomers present in approximately a 1:1 mixture, both peaks are reported) δ 9.04 and 8.93 (d, 1H, py-*o*-C*H*), 7.06 and 7.04 (t, 2H, py-C*H*), 6.90 (s, 4H, C*H*), 6.79 and 6.78 (d, 2H, py-C*H*), 6.69 and 6.62 (t, 2H, py-C*H*), 4.10 and 4.07 (d, 2H, CH_2), 2.82 (d, 2H, CH_2), 2.52 and 2.33 (m, 1H, $CH_2CH(CH_3)_2$), 2.4 (broadened into baseline, 6H, *o*-CH_3), 2.17 and 2.15 (s, 6H, *p*-CH_3), 1.9 (broadened into baseline, 6H, *o*-CH_3), 0.92 and 0.89 (m, 6H, $CH_2CH(CH_3)_2$), 0.33 and 0.09 (s, 9H, $CH_2Si(CH_3)_3$), 0.32 and 0.19 (s, 2H, $CH_2Si(CH_3)$), δ 0.83 and 0.08 (d, 2H, $CH_2CH(CH_3)_2$); Anal. Calcd for $C_{35}H_{53}HfN_3Si$: C, 58.19; H, 7.40; N, 5.82. Found: C, 58.26; H, 7.35; N, 5.80.

Activation of 2b with {Ph_3C}{$B(C_6F_5)_4$}. Solutions of **2b** (7.3 mg, 0.0101 mmol) and {Ph_3C}{$B(C_6F_5)_4$} (9.6 mg, 0.0105 mmol), each in C_6D_5Br (0.500 mL) were prepared and cooled to -35 °C. The solutions were mixed while still cold and the resulting orange solution was transferred to an NMR tube and kept at 0 °C. The following NMR data correspond to {(MesNpy)Hf(Neo)}{$B(C_6F_5)_4$}: ^{1}H NMR (C_6D_5Br, 273 K), δ 8.26 (d, 1H, py-*o*-CH), aryl peaks omitted here, 4.07 (d, 2H, CH_2), 2.79 (d, 2H, CH_2), 2.19 (s, 6H, *p*-CH_3), 2.18 (bs, 6H, *o*-CH_3), 1.50 (s, 6H, *o*-CH_3), 1.17 (s, 3H, CH_3), 1.11 (s, 2H, CH_2CMe_2Ph), 0.94 (s, 6H, $CH_2C(CH_3)_2Ph$).

Reaction of activated 2b with 1-hexene. The NMR sample was prepared by adding 1-hexene (0.200 mL, 1.6 mmol) to the sample above.

Activation of 3b with {Ph_3C}{$B(C_6F_5)_4$}. Solutions of **3b** (7.0 mg, 0.0102 mmol) and {Ph_3C}{$B(C_6F_5)_4$} (9.5 mg, 0.0102 mmol) in C_6D_5Br (0.500 mL and 0.300 mL respectively) were prepared and cooled to -35 °C. The solutions were mixed while still cold and the resulting orange solution was transferred to an NMR tube and kept at 0 °C. The following NMR data correspond to {(MesNpy)Hf(CH_2TMS)}{$B(C_6F_5)_4$}: ^{1}H NMR (C_6D_5Br, 273 K) 8.59 (d, 1H, py-*o*-C*H*), some aryl peaks omitted here, 6.81 (s, 4H, C*H*), 4.24 (d, 2H, CH_2), 2.98 (d, 2H, CH_2),

2.17 (s, 6H, *p*-CH_3), 1.70 (broadened into baseline, 12H, *o*-CH_3), 0.14 (s, 2H, CH_2Si(CH$_3$)$_3$), -0.31 (s, 9H, CH$_2$Si(CH_3)$_3$).

Reaction of activated 3b with 1-hexene. The NMR sample was prepared by adding 1-hexene (0.200 mL, 1.6 mmol) to the sample above.

Activation of 4b with {Ph$_3$C}{B(C$_6$F$_5$)$_4$}. Solutions of **4b** (7.2 mg, 0.00996 mmol) and {Ph$_3$C}{B(C$_6$F$_5$)$_4$} (9.2 mg, 0.00996 mmol) in C$_6$D$_5$Br (0.400 mL each) were prepared and cooled to -35 °C. The solutions were mixed while still cold and the resulting orange solution was transferred to an NMR tube and kept at 0 °C. The following NMR data correspond to {(MesNpy)Hf(CH$_2$TMS)}{B(C$_6$F$_5$)$_4$}: ^{1}H NMR (C$_6$D$_5$Br, 273 K) δ 8.55 (d, 1H, py-*o*-C*H*), some aryl peaks omitted here, 6.81 (s, 4H, C*H*), 4.25 (d, 2H, CH_2), 3.00 (d, 2H, CH_2), 2.18 (s, 6H, *p*-CH_3), 1.70 (broadened into baseline, 12H, *o*-CH_3), 1.30 (s, 3H, CH_3), 0.14 (s, 2H, CH_2Si(CH$_3$)$_3$), -0.31 (s, 9H, CH$_2$Si(CH_3)$_3$). Also observed in the NMR spectrum is CH$_2$CMe$_2$ (4.71 and 1.62) and Ph$_3$CH (5.45).

Activation of 4b with B(C$_6$F$_5$)$_3$. Solutions of **4b** (7.4 mg, 0.0102 mmol) and B(C$_6$F$_5$)$_3$ (5.2 mg, 0.0102 mmol) in C$_6$D$_5$Br (0.400 mL each) were prepared and cooled to -30 °C. The solutions were mixed while still cold and the resulting orange solution was transferred to an NMR tube and kept at 0 °C. The following NMR data correspond to {(MesNpy)Hf(CH$_2$TMS)}{MeB(C$_6$F$_5$)$_3$}: ^{1}H NMR (C$_6$D$_5$Br, 273 K) δ 8.66 (d, 1H, py-*o*-C*H*), some aryl peaks omitted here, 6.81 (s, 4H, C*H*), 4.21 (d, 2H, CH_2), 3.00 (d, 2H, CH_2), 2.16 (s, 6H, *p*-CH_3), 1.70 (broadened into baseline, 12H, *o*-CH_3), 1.30 (s, 3H, CH_3), 0.18 (s, 2H, CH_2Si(CH$_3$)$_3$), -0.36 (s, 9H, CH$_2$Si(CH_3)$_3$). Also observed in the NMR spectrum is CH$_2$CMe$_2$ (4.71 and 1.62).

Reaction of activated 4b with 1-hexene: kinetic studies. The NMR sample was prepared by adding 1-hexene (0.190 mL, 1.52 mmol) to the samples above. An internal standard, CH_2Ph_2 (4.5 M, 10 μL) was added to the solution as well.

Synthesis of dineophyl(Cl)$_2$. Methallyl chloride (100 mL, 1.01 mol) was added dropwise over two days to a rapidly stirred solution of benzene (39.6 mL, 0.506 mol) and H_2SO_4 (2.69 mL, 0.0506 mol). On the third day, another equivalent of methallyl chloride (50 mL, 0.505 mol) was added dropwise to the brown solution. Ether (30 mL) was added to the resulting browny-purple liquid. The solution was extracted with water (4 × 200 mL) to removed sulfuric acid. The volatile components were removed from the organic layer *in vacuo*. The residue was distilled under reduced pressure and a colorless oil (mainly neophyl chloride) was removed. Ethanol was added to the residual oil and the solution was cooled in a dry ice/acetone bath. A large amount of light brown precipitate quickly formed which was isolated by filtration (the precipitate dissolves rapidly upon warming of the solution). The solid was recrystallized from hot ethanol or heptane that was cooled in a salt bath. The recrystallization was repeated numerous times to produce fine beige needle crystals; yield 7.49 g (5.6%): ^{1}H NMR (C_6D_6) δ 7.09 (s, 4H, C*H*), 3.31 (s, 4H, CH_2), 1.20 (s, 12H, CH_3); HRMS Calcd for $C_{14}H_{20}Cl_2$ [M + H$^+$]: 258.0937. Found: 258.0935.

Synthesis of dineophyl(MgCl)$_2$. A three-necked flask was charged with crushed magnesium turnings (0.75 g, 0.0309 mol) in tetrahydrofuran (20 mL). The flask openings were equipped with a condenser, stopper, and addition funnel charged with a solution of **dineophyl**(Cl)$_2$ (1.0 g, 3.85 mmol) in tetrahydrofuran (20 mL). The **dineophyl**(Cl)$_2$ solution was added dropwise and the reaction mixture was refluxed (95 °C) for two days. During this time the solution became yellow in color and a significant amount of white precipitate formed. The solid

was isolated by filtration and dried *in vacuo*. The magnesium turnings were manually separated from the white powder; yield of Mg 0.565 g; yield of white powder 0.691g. The white powder isolated was used in further reactions without further purification.

Synthesis of $BrMg(CH_2)_5MgBr$.[34] A three-necked flask was charged with crushed magnesium turnings (8.48 g, 0.349 mol) in diethyl ether (200 mL). The flask openings were equipped with a condenser, stopper, and addition funnel charged with a solution of 1,5-dibromopentane (40.2 g, 0.175 mmol) in diethyl ether (40 mL). The dibromopentane solution was added dropwise to the stirred magnesium turnings and the reaction mixture refluxed and stirred for three hours. The solution became light yellow and contained a significant amount of white precipitate. The solution was cooled and used immediately without further purification. The Grignard reagent settles out as a dark oil at the bottom of a cloudy white solution.

Synthesis of disilyl$(Cl)_2$.[33] A three-necked flask was charged with chloro(chloromethyl)dimethyl silane (49.9 g, 0.349 mol) in diethyl ether (300 mL). The flask openings were equipped with a condenser, stopper, and cannula attached to the flask with the above solution of $BrMg(CH_2)_5MgBr$. The Grignard solution was added slowly via the cannula. The solution was refluxed for four hours, and slowly cooled to room temperature and stirred overnight. The solution was quickly filtered through Celite (avoiding as much air/water contact as possible) and the volatile components were removed from the filtrate *in vacuo*. This process removes any excess chloro(chloromethyl)dimethyl silane which reacts violently with water to form a siloxane which is difficult to remove from the product. Diethyl ether was added to the flask and the solution was cooled to 0°C. The solution was quenched by addition of NH_4Cl solution. The aqueous layer was extracted three times with diethyl ether. The diethyl ether fractions were collected and washed with distilled water three times. The volatile components

were removed *in vacuo* from the organic layers to yield a light yellow oil. A careful distillation was then carried out as any siloxane that formed distills at almost the exact same temperature as the desired product. Therefore, after collecting the first couple milliliters, the collection flask was switched to isolate clean product. The desired fraction was isolated when the heating oil was at 140 °C and the head temperature was 77 °C; yield 14.0 g (18%): ^{1}H NMR (C_6D_6) δ 2.79 (s, 4H, ClC*H*$_2$), 1.35 (m, 6H, $CH_2(CH_2)_3CH_2$), 0.63 (m, 4H, C*H*$_2$(CH$_2$)$_3$CH$_2$), 0.11 (s, 12H, Si(C*H*$_3$)$_2$).

Synthesis of disilyl(MgCl)$_2$. A three-necked flask was charged with crushed magnesium turnings (0.507 g, 0.0210 mol) and diethyl ether (10 mL). The flask openings were equipped with a condenser, stopper, and addition funnel charged with a solution of **disilyl**(Cl)$_2$ (1.5 g, 5.26 mmol) in diethyl ether (5 mL). The magnesium was activated with a crystal of I_2. The dichloride solution was added dropwise to the activated magnesium which had been cooled to 10 °C. The solution was slowly heated. At 30 °C, the reaction became vigorous and slight heating was added to maintain reflux overnight. The gray solution was brought into the glovebox, filtered and concentrated slightly. The Grignard reagent concentration of the resulting yellow filtrate was determined using the Ph_2Te_2 titration method: ^{1}H NMR (C_6D_6) δ 1.78 (m, 6H, $CH_2(CH_2)_3CH_2$), 0.90 (m, 4H, C*H*$_2$(CH$_2$)$_3$CH$_2$), 0.39 (s, 12H, Si(C*H*$_3$)$_3$), -1.12 (s, 4H, ClMgC*H*$_2$).

Attempted Synthesis of disilyl(Li)$_2$. A Fischer Porter bottle was charged with **disilyl**(Cl)$_2$ (1.5 g, 0.00525 mol) in heptane (10 mL). The bottle was removed from the glovebox and purged with argon. High sodium, granular lithium (> 0.29 g, 0.042 mol) was added quickly to the cooled solution (0 °C) under a constant flow of argon. The bottle was sealed with the Fischer Porter top and the solution was slowly warmed to room temperature. The solution was

stirred at 130 °C for four days at which time it was gray in color. In the glovebox, the solution was filtered through Celite. The resulting yellow solution was concentrated and placed in the freezer to crystallize out the desired material. ^{1}H NMR spectroscopy showed that some lithium reagent had formed (δ -1.86), but no clean material was isolated.

Synthesis of disilyl[(MesNpy)HfCl]$_2$ (5a). A suspension of **1** (2.175 g, 3.35 mmol) in diethyl ether was cooled to -35 °C. **Disilyl**$(MgCl)_2$ (1.22 M in diethyl ether, 2.61 mL, 3.18 mmol) was added to the cooled solution and the resulting mixture was stirred at room temperature for thirty minutes during which time a precipitate formed. 1,4-Dioxane (483 μL, 5.02 mmol) was added to the solution and additional precipitate formed. The solution was filtered through Celite. The volatile components were removed from the filtrate *in vacuo* to yield a yellow powder. The powder was redissolved in a minimal amount of diethyl ether and the solution was filtered. The volatile components were removed from the filtrate *in vacuo*. Various attempts were made to recystallize the desired compound in a variety of fashions to remove the dialkyl impurities. The powder was extremely soluble in diethyl ether and insoluble in pentane. A diethyl ether/pentane solution yielded crystals after a month in the freezer; powder yield 2.3 g (100%): ^{1}H NMR (C_6D_6) δ 9.70 (d, 1H, py-*o*-CH), some aryl peaks omitted here, 4.18 (d, 2H, CH_2), 2.80 (d, 2H, CH_2), 2.73 (s, 6H, *o*-CH_3), 2.17 (s, 6H, *p*-CH_3), 1.87 (s, 6H, *o*-CH_3), 1.35 (m, 3H, $CH_2(CH_2)_3CH_2$), 0.91 (s, 3H, CH_3), 0.50 (m, 2H, $CH_2(CH_2)_3CH_2$), 0.46 (s, 2H, CH_2SiMe_2), 0.10 (s, 6H, $Si(CH_3)_2$); Anal. Calcd for $C_{65}H_{92}Cl_2Hf_2N_6Si_2$: C, 54.16; H, 6.43; N, 5.83; Cl, 4.92. Found: C, 54.05; H, 6.37; N, 5.78; Cl, 4.83. In the material used in subsequent reactions, also present were two dialkyl impurities (see Figure 1.5, ~10%).

Synthesis of disilyl[(MesNpy)HfMe]$_2$ (5b). A solution of **5a** (0.130 g, 0.0928 mmol) in diethyl ether was cooled to -35 °C. MeLi (1.83 M in diethyl ether, 94 μL, 0.172 mmol) was

added to the cooled solution dropwise. Upon addition of a drop, the solution became yellow, and then the color dissipated. After all the lithium reagent was added, the solution was yellow with a white precipitate. The solution was filtered through Celite. The volatile components were removed from the filtrate *in vacuo* to yield a yellow powder. The powder was redissolved in a minimal amount of diethyl ether, and the solution was filtered and placed in a -35 °C freezer overnight. A solid formed which was isolated by filtration and dried *in vacuo*. In a similar preparation when MeMgBr was used, a large amount of (MesNpy)$HfMe_2$ was present as determined by ^{1}H NMR spectroscopy: ^{1}H NMR (C_6D_6, 3 isomers present in unequal amounts, 2:1 ratio of 1 isomer to 2 other isomers, peaks that could be identified are reported) δ 9.04 and 9.02 and 8.92 (d, 1H, py-*o*-CH), 4.13 (d, 2H, CH_2), 2.88 and 2.84 (d, 2H, CH_2), 2.29 (broadened into baseline s, 12H, *o*-CH_3), 2.20 and 2.19 (s, 6H, *p*-CH_3), 1.37 (m, 3H, $CH_2(CH_2)_3CH_2$), 0.93 (br s, 3H, CH_3), 0.06 and 0.05 and 0.03 (s, 6H, $Si(CH_3)_2$). From py-*o*-C*H* resonance, also present when the reaction was stirred for one hour is (ratio w.r.t the most abundant isomer), (MesNpy)$HfMe_2$ (0.20), (MesNpy)HfX_2 (where X is some silyl species) (0.22), **5a** (0.24).

Activation of 5b with $\{Ph_3C\}\{B(C_6F_5)_4\}$. Solutions of **5b** (8.2 mg, 0.00585 mmol) and $\{Ph_3C\}\{B(C_6F_5)_4\}$ (10.7 mg, 0.0117 mmol) in C_6D_5Br (0.400 mL each) were prepared and cooled to -35 °C. The solutions were mixed while still cold and the resulting orange solution was transferred to an NMR tube and kept at 0 °C. The following NMR data correspond to $\{$**disilyl**[(MesNpy)Hf]$_2\}\{B(C_6F_5)_4\}_2$: ^{1}H NMR (C_6D_5Br, 273 K), δ 8.70 (d, 1H, py-*o*-CH), some aryl peaks omitted here, 4.29 (d, 2H, CH_2), 3.08 (d, 2H, CH_2), 2.25 (s, 6H, *p*-CH_3), 1.36 (s, 3H, CH_3), 0.93 (m, 3H, $CH_2(CH_2)_3CH_2$), 0.30 (s, 2H, CH_2SiMe_2), 0.21 (s, 6H, $Si(CH_3)_2$), δ 0.09 (m, 2H, $CH_2(CH_2)_3CH_2$).

Activation of 5b with $B(C_6F_5)_3$. Solutions of **5b** (10.2 mg, 0.00728 mmol) and $B(C_6F_5)_3$ (7.5 mg, 0.0102 mmol) in C_6D_5Br (0.400 mL each) were prepared and cooled to -35 °C. The solutions were mixed while still cold and the resulting orange solution was transferred to an NMR tube and kept at 0 °C.

Reaction of activated 5b with 1-hexene: kinetic studies. The NMR sample was prepared by adding 1-hexene (0.190 mL, 1.52 mmol) to the samples above. An internal standard, CH_2Ph_2 (4.5 M, 10 μL), was added to the solution as well.

Reaction of activated 5b with 1-hexene: bulk polymerization. Solutions of **5b** (10.2 mg, 0.00742 mmol) and $\{Ph_3C\}\{B(C_6F_5)_4\}$ (13.4 mg, 0.00145 mmol) in C_6D_5Br (0.500 mL each) were prepared and cooled to -35 °C. The solutions were mixed while still cold and were added to a cooled solution of 1-hexene (0.460 mL, 3.64 mmol) and bromobenzene (0.540 mL). The reaction mixture was stirred at 0 °C for seven hours, the polymerization was quenched with methanol, and the volatile components were removed from the reaction mixture *in vacuo*. The residue was redissolved in pentane, and the solution was passed through silica and the volatile components were *in vacuo*.

Disilyl[(MesNpy)Hf(*i*-Bu)]$_2$ synthesized via 4a. A solution of **4a** (0.200 g, 0.298 mmol) in diethyl ether was cooled to -35 °C. **Disilyl**$(MgCl)_2$ (0.44 M in diethyl ether, 0.644 mL, 0.283 mmol) was added dropwise to the cooled solution. The solution was stirred for one minute. 1,4-Dioxane was added (38 μL, 0.447 mmol) and a white precipitate formed. The volatile components were removed *in vacuo*, the resulting powder was redissolved in pentane, and the solution was filtered. Diethyl ether was added to the reaction flask and the remainder of the precipitate dissolved and was filtered through Celite as well. The diethyl ether solution and

pentane solution were both dried *in vacuo*. The isolated fractions were not pure by ^{1}H NMR spectroscopy as significant (MesNpy)Hf(*i*-Bu)$_2$ was present.

Disilyl[(MesNpy)Hf(*i*-Bu)]$_2$ synthesized via 5a. A solution of **5a** (0.240 g, 0.166 mmol) in toluene was cooled to -35 °C. *i*-BuLi (20 mg, 0.316 mmol) was added dropwise to the cooled solution. After five minutes of stirring, the solution was filtered through Celite and the volatile components were removed from the filtrate *in vacuo* to yield a yellow powder. The powder was redissolved in a minimal amount of diethyl ether and the solution was filtered. ^{1}H NMR spectroscopy indicated that a large amount of (MesNpy)Hf(*i*-Bu)$_2$ had formed.

Synthesis of BrMg(C$_6$H$_4$)MgBr.[37] A three-necked flask was charged with magnesium (4.3 g, 176 mmol) and BrC$_6$H$_4$Br (10 g, 42 mmol) and 100 mL of diethyl ether. The flask openings were equipped with a condenser, septa and an addition funnel charged with dibromoethane (7.3 mL, 85 mmol). The solution was refluxed and the dibromoethane was added dropwise over approximately eight hours. The solution was refluxed for twenty hours. A dark oil formed which settled out when the stirring was stopped. The reaction mixture was used without further purification.

Synthesis of disilophyl(Cl)$_2$.[35] The above prepared Grignard reagent (BrMgC$_6$H$_4$MgBr) was added dropwise over one hour to a solution of chloro(chloromethyl)dimethylsilane (15.9 g, 85 mmol) in THF. The solution was heated to 40 °C overnight. The volatile components were removed *in vacuo* (this removes any excess chloro(chloromethyl)dimethylsilane which would form siloxanes when the reaction was quenched with water). The reaction was quenched with saturated NH$_4$Cl solution. An extraction was carried out with diethyl ether, and the volatile components were removed *in vacuo* from the combined organic layers. The resulting powder was recrystallized from a hexane solution in a dry ice/acetone bath. White crystals were isolated

by filtration and dried *in vacuo*; yield 4.0 g (33%): ^{1}H NMR (C_6D_6) δ 7.39 (s, 2H, C*H*), 2.66 (s, 2H, CH_2Cl), 0.25 (s, 6H, Si(CH_3)$_2$).

Synthesis of disilophyl(MgCl)$_2$. A three-necked flask was charged with crushed magnesium turnings (0.34 g, 0.14 mol) in tetrahydrofuran (25 mL). The flask openings were equipped with a condenser, stopper, and addition funnel charged with a solution of **disilophyl**(Cl)$_2$ (0.5 g, 0.0017 mol) in tetrahydrofuran (10 mL). The magnesium was activated with a crystal of I_2. The dichloride solution was added dropwise to the magnesium suspension and the reaction mixture was refluxed overnight. The solution was transferred to a Schlenk flask and brought into the glovebox. The yellow solution was filtered through Celite and triturated with both Ph_2Te_2 and isopropanol/1,10 phenanthroline (approximated molarity = 0.075 N): ^{1}H NMR (C_6D_6) δ 7.95 (s, 2H, C*H*), 0.68 (s, 6H, Si(CH_3)$_2$), -0.95 (s, 2H, CH_2MgCl).

Synthesis of disilophyl[(MesNpy)HfCl]$_2$. A solution of **1** (0.75 g, 1.2 mmol) in tetrahydrofuran was cooled to -35 °C. **Disilophyl**(MgCl)$_2$ (~0.075 M in tetrahydrofuran, 11.6 mL, 0.87 mmol) was added to the cooled solution and the resulting mixture was stirred at room temperature for fifteen minutes. 1,4-Dioxane was added and the volatile components were removed *in vacuo* to yield a beige powder. The powder was redissolved in diethyl ether and the solution was filtered through Celite. The volatile components were removed from the filtrate *in vacuo*. Attempts were made to recystallize the desired compound in a variety of fashions to remove any impurities. A powder formed from a diethyl ether solution and the powder was isolated by filtration and dried *in vacuo*: ^{1}H NMR (C_6D_6) δ 9.68 (d, 1H, py-*o*-CH), 7.59 (s, 2H, $Si_2C_6H_4$), some aryl peaks are omitted here, 4.15 (d, 2H, CH_2), 2.81 (d, 2H, CH_2), 2.67 (s, 6H, *o*-CH_3), 2.17 (s, 6H, *p*-CH_3), 1.85 (s, 6H, *o*-CH_3), 0.89 (s, 3H, CH_3), 0.68 (s, 2H, CH_2SiMe$_2$), 0.31 (s, 6H, Si(CH_3)$_2$).

Synthesis of dicyclohexylmethyl(Br)$_2$.[38,39] PBr_3 (37.7 g, 0.14 moles) was added dropwise over a two hour period to a suspension of *trans*-1,4-bis(hydroxymethyl)cyclohexane (**dicyclohexylmethyl**(OH)$_2$, 20 g, 0.14 moles) in benzene (100 mL). The solution was heated to 70 °C for 75 minutes during which time the solid alcohol dissolved and the solution became yellow in color. The reaction was quenched by pouring over ice (200 g). The benzene was removed *in vacuo* and the aqueous layer was extracted with CH_2Cl_2 (3 × 100 mL). The organic layers were combined and washed with saturated $NaHCO_3$ (3 × 50mL) and deionized water (3 × 50 mL). The organic layer was dried over Mg_2SO_4 and the volatile components were removed from the solution *in vacuo*. The resulting solid was recrystallized from a solution of MeOH and diethyl ether at -78 °C. A small amount of **dicyclohexylmethyl**(OH)$_2$ was present so the crystals were dissolved in hexanes and the solution was passed through a silica plug. The solution was dried again over Mg_2SO_4 and the volatile components were removed *in vacuo*; yield 5.9 g (16%): ^{1}H NMR (C_6D_6) δ 2.78 (d, 4H, C*H*$_2$Br), 1.48 (m, 4H, C*H*$_2$), 1.07 (br s, 2H, C*H*), 0.56 (m, 4H, C*H*$_2$).

Synthesis of dicyclohexylmethyl(MgBr)$_2$. A three-necked flask was charged with crushed magnesium turnings (0.15 g, 6.2 mmol) in diethyl ether (25 mL). The flask openings were equipped with a condenser, stopper, and addition funnel charged with a solution of **dicyclohexylmethyl**(Br)$_2$ (0.7 g, 2.6 mmol) in diethyl ether (10 mL). The magnesium was activated with a crystal of I_2. The dibromide solution was added dropwise to the magnesium suspension and the reaction mixture was refluxed for 1.5 hours. The solution was transferred to a Schlenk flask and brought into the glovebox. Overnight, crystals formed from the room temperature solution. The crystals were isolated by filtration and dried *in vacuo*. The solid was titrated with isopropanol and the molecular weight was approximated 196 g/Mg center which

corresponds to one molecule of diethyl ether per magnesium; yield of crystals 0.8 g; ^{1}H NMR (C_6D_6) δ 1.48 (m, 4H, C*H*$_2$), 1.07 (br s, 2H, C*H*), 0.56 (m, 4H, C*H*$_2$), 0.32 (d, 4H, C*H*$_2$MgBr).

Synthesis of dicyclohexylmethyl(Cl)$_2$.[40,41] $SOCl_2$ (15.3 mL, 0.21 moles) was added dropwise to a solution of **dicyclohexylmethyl**(OH)$_2$ (10 g, 0.07 moles) in pyridine (11.3 mL, 0.14 moles). After approximately 5 mL had been added, crystals began to form. The solution was heated to 60 °C and the remaining $SOCl_2$ was added dropwise. The solution was refluxed overnight at which time it was brown with precipitate. The volatile components were removed *in vacuo* and water was added to the cooled flask. The aqueous layer was extracted with methylene chloride. The volatile components were removed from the organic layer *in vacuo* and a yellow oil remained. Hexane was added to the oil and the solution was passed through a silica plug to remove any residual **dicyclohexylmethyl**(OH)$_2$. The resulting solution was concentrated slightly and cooled in a dry ice/acetone bath. A solid formed which was isolated by quick filtration. The solid became an oil once it returned to room temperature. Hexane was added to the yellow oil, and the solution was dried over Mg_2SO_4. The volatile components were removed *in vacuo* to afford a yellow oil; yield 5.8 g (46%): ^{1}H NMR (C_6D_6) δ 2.93 (d, 4H, C*H*$_2$Br), 1.51 (m, 4H, C*H*$_2$), 1.12 (br s, 2H, C*H*), 0.60 (m, 4H, C*H*$_2$).

Synthesis of dibenzyl(MgCl)$_2$.[42] A three-necked flask was charged with crushed magnesium turnings (1.8 g, 74 mmol) in tetrahydrofuran (30 mL). The flask openings were equipped with a condenser, stopper, and addition funnel charged with a dibromoethane (0.86 mL, 10 mmol). Dibromoethane was added dropwise over thirty minutes to activate the magnesium and the solution was stirred overnight. The addition funnel was charged with $ClCH_2(C_6H_4)CH_2Cl$ (4.4 g, 25 mol) in tetrahydrofuran (230 mL) which was added dropwise over approximately three hours. The solution was stirred overnight at which time almost all the

magnesium had reacted. The solution was transferred to a Schlenk flask, brought into the glovebox and filtered through Celite. After concentrating the solution to approximately 130 mL, crystals formed which were isolated by filtration and dried *in vacuo*; yield 4.3 g. The crystals were titrated with isopropanol and the molecular weight was approximately 228 g/mole Mg which corresponds to two molecules of tetrahydrofuran per magnesium center: ^{1}H NMR (C_6D_6) δ 7.07 (s, 4H, C*H*), 1.78 (s, 4H, CH_2).

1.7 References

(1) Warren, T. H.; Schrock, R. R.; Davis, W. M. *Organometallics* **1996**, *15*, 562.

(2) Baumann, R.; Davis, W. M.; Schrock, R. R. *J. Am. Chem. Soc.* **1997**, *119*, 3830.

(3) Warren, T. H.; Schrock, R. R.; Davis, W. M. *Organometallics* **1998**, *17*, 308.

(4) Schrock, R. R.; Schattenmann, F.; Aizenberg, M.; Davis, W. M. *J. Chem. Soc., Chem. Commun.* **1998**, 199.

(5) Schattenmann, F.; Schrock, R. R.; Davis, W. M. *Organometallics* **1998**, *17*, 989.

(6) Baumann, R.; Schrock, R. R. *J. Organometal. Chem.* **1998**, *557*, 69.

(7) Aizenberg, M.; Turculet, L.; Davis, W. M.; Schattenmann, F.; Schrock, R. R. *Organometallics* **1998**, *17*, 4795.

(8) Graf, D. D.; Davis, W. M.; Schrock, R. R. *Organometallics* **1998**, *17*, 5820.

(9) Schrock, R. R.; Seidel, S. W.; Schrodi, Y.; Davis, W. M. *Organometallics* **1999**, *18*, 428.

(10) Graf, D. G.; Schrock, R. R.; Davis, W. M.; Stumpf, R. *Organometallics* **1999**, *18*, 843.

(11) Liang, L.-C.; Schrock, R. R.; Davis, W. M. *J. Am. Chem. Soc.* **1999**, *121*, 5797.

(12) Flores, M. A.; Manzoni, M.; Baumann, R.; Davis, W. M.; Schrock, R. R. *Organometallics* **1999**, *18*, 3220.

(13) Schrock, R. R.; Baumann, R.; Reid, S. M.; Goodman, J. T.; Stumpf, R.; Davis, W. M. *Organometallics* **1999**, *18*, 3649.

(14) Baumann, R.; Stumpf, R.; Davis, W. M.; Liang, L.-C.; Schrock, R. R. *J. Am. Chem. Soc.* **1999**, *121*, 7822.

(15) Schrock, R. R.; Liang, L.-C.; Baumann, R.; Davis, W. M. *J. Organomet. Chem.* **1999**, *591*, 163.

(16) Liang, L.-C.; Schrock, R. R.; Davis, W. M. *Organometallics* **2000**, *19*, 2526.

(17) Mehrkhodavandi, P.; Bonitatebus, P. J., Jr.; Schrock, R. R. *J. Am. Chem. Soc.* **2000**, *122*, 7841.

(18) Schrock, R. R.; Casado, A. L.; Goodman, J. T.; Liang, L.-C.; Bonitatebus, P. J., Jr., Davis, W. M. *Organometallics* **2000**, *19*, 5325.

(19) Schrock, R. R.; Bonitatebus, P. J., Jr.; Schrodi, Y. *Organometallics* **2001**, *20*, 1056.

(20) Greco, G. E.; Schrock, R. R. *Inorg. Chem.* **2001**, *40*, 3850.

(21) Schrodi, Y.; Schrock, R. R.; Bonitatebus, P. J. Jr. *Organometallics* **2001**, *20*, 3560.

(22) Mehrkhodavandi, P.; Schrock, R. R. *J. Am. Chem. Soc.* **2001**, *123*, 10746.

(23) Goodman, J. T.; Schrock, R. R. *Organometallics* **2001**, *20*, 5205.

(24) Mehrkhodavandi, P.; Schrock, R. R.; Bonitatebus, P. J. Jr. *Organometallics* **2002**, *21*, 5785.

(25) Mehrkhodavandi, P.; Schrock, R. R.; Pryor, L. L. *Organometallics* **2003**, *22*, 4569.

(26) Schrock, R. R.; Adamchuk, J.; Ruhland, K.; Lopez, L. P. H. *Organometallics* **2003**, *22*, 5079.

(27) Tonzetich, Z. J.; Lu, C. C.; Schrock, R. R.; Hock, A. S.; Bonitatebus, P. J., Jr. *Organometallics* **2004**, *23*, 4362.

(28) Schrock, R. R.; Adamchuk, J.; Ruhland, K.; Lopez, L. P. H. *Organometallics* **2005**, *24*, 857.

(29) Tonzetich, Z. J.; Schrock, R. R.; Hock, A. S.; Müller, P. *Organometallics* **2005**, *24*, 3335.

(30) Mehrkhodavandi, P. *Living α-olefin polymerization by cationic zirconium and hafnium complexes containing chelating diamidopyridine ligands*, Ph.D. Thesis, Massachusetts Institute of Technology, Cambridge, **2002**.

(31) Gade, L. H.; Mountford, P. *Coord. Chem. Rev.* **2001**, *216*, 65.

(32) Smith, W. T.; Sellas, J. T., *Org. Syn.* **1963**, *4*, 702.

(33) Tacke, R.; Niedner, R.; Frohnecke, J.; Ernst, L.; Sheldrick, W. S. *Liebigs. Ann. Chem.* **1980**, 1859.

(34) Nutzel, K.; Gilman, H.; Wright, G. F. *Methoden der Organischen Chemie* **1973**, *VIII*, 101.

(35) Dakternieks, D.; Duthie, A.; Zobel, B. *Organometallics* **2002**, *21*, 647.

(36) Rieke, R. D.; Bales, S. E. *J. Am. Chem. Soc.* **1974**, *96*, 1775.

(37) Dakternieks, D.; Duthie, A.; Zobel, B. *Organometallics* **2002**, *21*, 647.

(38) Kuck, D.; Tholmann, D.; Grutzmacher, H.-F. *J. Chem. Soc., Perkin Trans.* **1990**, *2*, 251.

(39) Swepston, P. N.; Lin, S.-T.; Hawkins, A.; Humphrey, S.; Siegel, S.; Cordes, A. W. *J. Org. Chem.* **1981**, *46*, 3754.

(40) Richter, R.; Tucker, B. *J. Org. Chem.* **1983**, *48*, 2625.

(41) Solladie, G.; Zimmermann, R.; Bartsch, R.; Walborsky, H. M. *Synthesis* **1985**, *6-7*, 662.

(42) Leung, W.-P.; Raston, C. L.; Skelton, B. W.; White, A. H. *J. Chem. Soc., Dalton Trans.* **1984**, 1801.

(43) Aso, Y.; Yamashita, H.; Otasubo, T.; Ogura, F. *J. Org. Chem.* **1989**, *54*, 5627.

Chapter 2 - Molybdenum Bifunctional Initiators for ROMP: Characterization and Living Polymerization

A portion of this work has appeared in print: *Synthesis of High Oxidation State Bimetallic Alkylidene Complexes for Controlled ROMP Synthesis of Triblock Copolymers,* Schrock, R. R.; Gabert, A. J.; Singh, R.; Hock, A. S., *Organometallics* **2005**, *24*, 5058.

2.1 Introduction

Complexes of the type $Mo(NAr)(OR')_2(CHR)$ are metathesis catalysts that have been well studied and developed by the Schrock Group.[1] Ring opening metathesis polymerization (ROMP) is one application of these type of catalysts when the substrate is a strained cyclic olefin, such as norbornene and norbornadiene.[1] The alkylidene in the starting molybdenum complex reacts with the strained olefin to form a metallocyclobutane, which then undergoes cycloreversion to form a new alkylidene in which the substituent is the propagating polymer (Scheme 2.1).

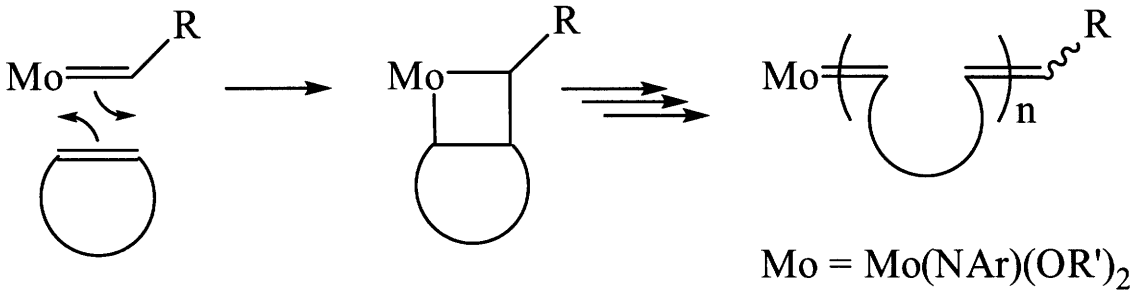

Scheme 2.1 Ring opening metathesis polymerization.

ROMP is a useful method for the preparation of norbornene- and norbornadiene-based polymers. Polymerizations by molybdenum alkylidene initiators have been found to be "living" under specified conditions. The criteria of a "living" polymerization can be found in the General Introduction. A second advantage of employing molybdenum alkylidene catalysts for ROMP is the polymers can be terminated in a Wittig-like fashion using aldehydes such as benzaldehyde or ferrocenecarboxaldehyde.[2,3,4,5] Therefore, functionalized endgroups can be installed to the polymers, which is useful for endgroup analysis.

We were interested in preparing bifunctional ROMP initiators for the preparation of ABA triblock copolymers. By linking two monofunctional ROMP initiators we are able to take advantage of the living characteristics of molybdenum initiators, as well as installing endgroups

easily. The General Introduction also discussed the benefits of using a bifunctional initiator as opposed to a monofunctional initiator to prepare ABA triblock copolymers. There were a limited number of bifunctional ROMP initiators mentioned in the literature previous to these studies.

In 1993, we reported the synthesis of bifunctional initiators of the type: $[(R_{F6}O)_2(ArN)Mo{=}CHCH_2CH(OMe)]_2(1,4\text{-}C_6H_4)$ (where OR_{F6} = $OCMe(CF_3)_2$; Ar = 2,6-diisopropylphenyl), $(DME)(R_{F6}O)_2(ArN)Mo(CH)_6Mo(NAr)(R_{F6}O)_2(DME)$ (DME = 1,4-dimethoxyethane), $(quin)(t\text{-}BuO)_2(ArN)Mo(CH)_6Mo(NAr)(O\text{-}t\text{-}Bu)_2(quin)$ (where quin is quinuclidine), and $[Mo(NAr)(OR_{F6})_2(=CH)]_2(1,4\text{-}C_6H_4)\bullet 2DME$.[6] Although these initiators were used to prepare homopolymers of **DCMNBD** (2,3-dicarbomethoxynorbornadiene), no triblock copolymers were reported. There are also examples of titanocyclobutene compounds[7] and Ru bifunctional catalysts[8] that were employed for ROMP. Since the research reported in this chapter was published, there have been additional reports of bi- and tri-functional Mo and Ru initiators for the preparation of homo- and triblock co-polymers of 1,6-heptadiynes and/or norbornene-based monomers.[9,10]

This Chapter reports the synthesis and investigation of bifunctional molybdenum initiators linked by divinylferrocene.[11] Two initiators were synthesized, namely, $[Mo(NAr)(OR_{F6})_2(=CHC_5H_4)]_2Fe$ (**6**) and $[Mo(NAr)(OR_{F0})_2(=CHC_5H_4)]_2Fe$ (**7**, OR_{F0} = $OCMe_3$). These initiators were fully characterized by NMR spectroscopy and by X-ray crystallography. The initiators were then employed for the synthesis of homo- and triblock co-polymers of **DCMNBD** and methyltetracyclododecene (**MTD**). The polymers were fully characterized by MALDI-TOF MS and gel permeation chromatography (GPC). End group analysis of a **DCMNBD** oligomer is also reported.

2.2 Synthesis of Bifunctional Initiators Linked by Divinylferrocene

The synthesis of divinylferrocene is a three-step procedure starting with ferrocene (Scheme 2.2). Diacetylferrocene is synthesized by Friedel-Crafts acylation of ferrocene with $AlCl_3$ and acetyl chloride.[12] Diacetylferrocene is hydrolyzed with lithium aluminum hydride to form 1,1′-bis(α-hydroxyethyl)ferrocene.[13,14] The third step in the synthesis of divinylferrocene is the dehydration of 1,1′-bis(α-hydroxyethyl)ferrocene by refluxing the precursor with alumina in toluene to form divinylferrocene.[15,16] Divinylferrocene reacts with residual water not trapped immediately by the alumina to form an impurity, 1,1'-(oxydiethylidene)ferrocene (25%). This impurity was present in the divinylferrocene used in all further reactions. This impurity does not interfere with the metallation step and can be successfully removed in the subsequent step.

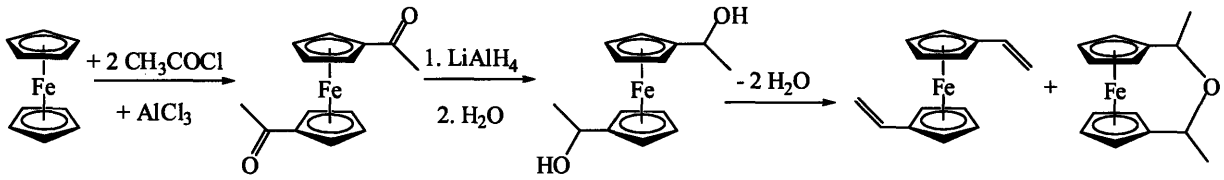

Scheme 2.2 Synthesis of divinylferrocene.

One half equivalent of divinylferrocene was added rapidly to a solution of Mo(NAr)(OR_{F6})$_2$($CHCMe_2Ph$) in toluene (Scheme 2.3). The solution immediately turned red and upon cooling the solution to -35 °C, burgundy crystals of the bimetallic species, [Mo(NAr)(OR_{F6})$_2$(=CHC_5H_4)]$_2$Fe (**6**), were isolated. The related *tert*-butoxide complex, [Mo(NAr)(OR_{F0})$_2$(=CHC_5H_4)]$_2$Fe (OR_{F0} = $OCMe_3$, **7**) could not be synthesized from direct reaction of Mo(NAr)(OR_{F0})$_2$($CHCMe_2Ph$) and divinylferrocene as the reaction was very slow and did not proceed to completion. Therefore, 7 was synthesized by the addition of four equivalents of $LiOR_{F0}$ to **6**.

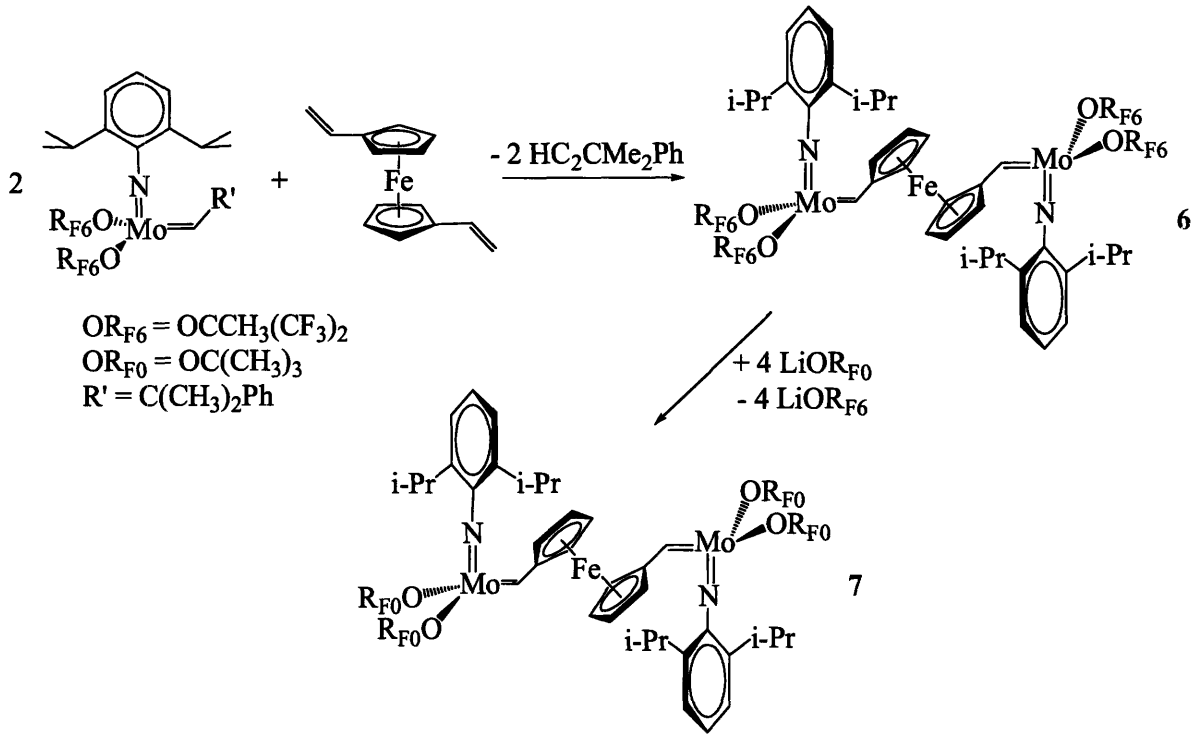

Scheme 2.3 Synthesis of **6** and **7**.

Crystals suitable for X-ray studies of both **6** and **7** were isolated and the thermal ellipsoid plots are shown in Figure 2.1 (Table 2.1). One molecule of benzene and one molecule of toluene are present in the unit cell of **6** and **7**, respectively. Selected bond lengths and angles are found in Table 2.2. All bond lengths and angles are comparable to those found in monometallic four-coordinate structures in this class.[17,18] In both complexes, the alkylidene is oriented *syn* with respect to the imido group. To our knowledge,[19] these are the only high oxidation state Mo or W ferrocenyl alkylidene complexes to be structurally characterized, although Mo(NAr)(O-*t*-Bu)$_2$[CHC$_5$H$_4$FeCp][5] has been reported and *anti*-Re[CHC$_5$H$_4$FeCp](C-*t*-Bu)[OCMe(CF$_3$)$_2$]$_2$[20] has been structurally characterized.

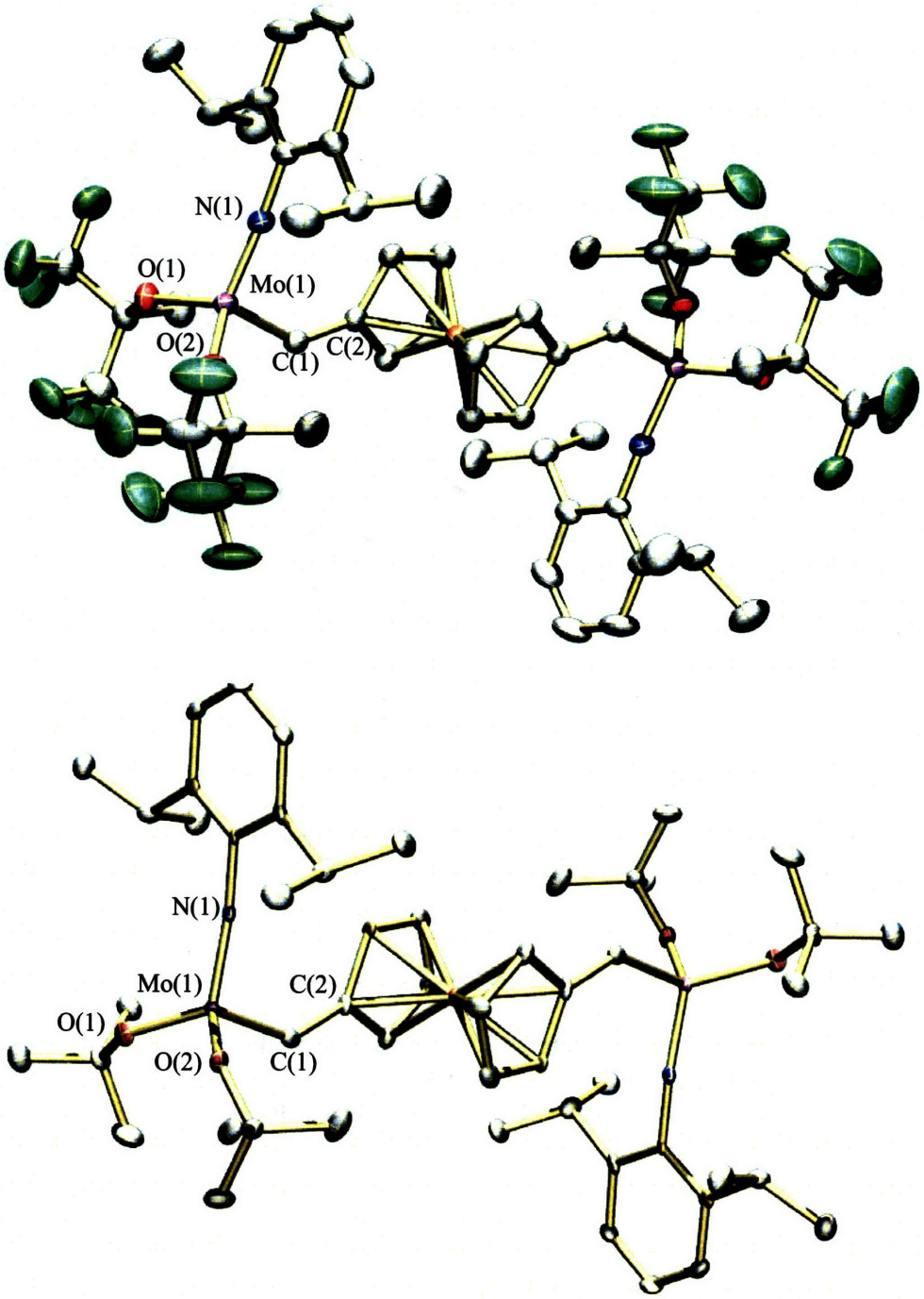

Figure 2.1 Thermal ellipsoid drawings of **6** (top) and **7** (bottom). Hydrogen atoms are omitted for clarity.

Compound	**6**	**7**
Empirical formula	$C_{58}H_{62}F_{24}FeMo_2N_2O_4$	$C_{59}H_{88}FeMo_2N_2O_4$
Formula weight	1554.83	1137.04
Compound ID	04136	04151
Temperature	194(2) K	373(2) K
Crystal system	Triclinic	Monoclinic
Space group	$P\bar{1}$	$C/2c$
Unit cell dimensions	a = 10.6901(11) Å b = 11.1070(12) Å c = 15.2513(17) Å α = 101.756(2)° β = 103.821(2)° γ = 106.968(2)°	a = 26.209(5) Å b = 10.958(2) Å c = 20.732(4) Å α = 90° β = 101.62(3)° γ = 90°
Volume	1607.3(3) $Å^3$	5832(2) $Å^3$
Z	1	4
Density (calculated)	1.606 Mg/m^3	1.295 Mg/m^3
Absorption coefficient	0.722 mm^{-1}	0.713 mm^{-1}
F(000)	782	2392
Crystal size	0.22 × 0.17 × 0.06 mm^3	0.08 × 0.08 × 0.05 mm^3
Theta range for data collection	2.01 to 28.33°	1.59 to 25.03°
Index ranges	-14 <= *h* <= 14 -14 <= *k* <= 14 -18 <= *l* <= 20	-31 <= *h* <= 31 -12 <= *k* <= 13 -24 <= *l* <= 24
Reflections collected	27210	32410
Independent reflections	7977 [*R*(int) = 0.0264]	5110 [*R*(int) = 0.0891]
Completeness to theta = 26.37°	99.4%	99.4%
Absorption correction	Empirical	-
Max. and min. transmission	-	0.9652 and 0.9452
Data / restraints / parameters	7977 / 0 / 416	5110 / 0 / 310
Goodness-of-fit on F^2	1.024	1.320
Final R indices [I > 2sigma(I)]	R1 = 0.0297 wR2 = 0.0757	R1 = 0.0826 wR2 = 0.1624
R indices (all data)	R1 = 0.0342 wR2 = 0.0787	R1 = 0.0923 wR2 = 0.1659
Largest diff. peak and hole	0.536 and -0.298 $e.Å^{-3}$	1.296 and -1.931 $e.Å^{-3}$

Table 2.1 Crystal data and structure refinement for **6** and **7**.

Compound **6**		Compound **7**	
Mo(1)-N(1)	1.7241(15)	Mo(1)-N(1)	1.734(5)
Mo(1)-C(1)	1.9098(18)	Mo(1)-C(1)	1.912(7)
Mo(1)-O(1)	1.9309(12)	Mo(1)-O(1)	1.889(5)
Mo(1)-O(2)	1.9342(13)	Mo(1)-O(2)	1.892(5)
N(1)-Mo(1)-C(1)	98.79(7)	N(1)-Mo(1)-C(1)	99.3(3)
C(7)-N(1)-Mo(1)	174.37(13)	C(15)-N(1)-Mo(1)	166.2(5)
C(2)-C(1)-Mo(1)	139.06(13)	C(2)-C(1)-Mo(1)	137.8(5)

Table 2.2 Selected bond lengths (Å) and angles (°) for **6** and **7**.

^{1}H and ^{13}C NMR spectra of **6** and **7** are consistent with the structure found in the solid state; largely one alkylidene H_{α} resonance is found at 11.84 (for **7**) and 12.53 ppm (for **6**) with J_{CH} values of 127 and 129 Hz, respectively (as determined by ^{13}C NMR spectroscopy). The J_{CH} coupling constants are characteristic of a *syn* orientation of the alkylidene with respect to the imido group. However, in each case, two reproducible additional resonances are present in equal amounts. In **7** these are found at 12.31 (J_{CH} = 154 Hz, 4% of total area) and 11.97 ppm (J_{CH} = 125 Hz, 4% of total area) (Table 2.3). (The coupling constants were determined through a proton NMR spectrum of a concentrated solution). These data suggest that these resonances can be ascribed to an isomer in which one of the alkylidenes (with the alkylidene resonance at 12.31 ppm and J_{CH} = 154 Hz) has the *anti* orientation; the position of the other resonance (11.97 ppm and J_{CH} = 125 Hz) is characteristic of a *syn* alkylidene. Therefore the sample of **7** consists of 92% *syn/syn* and 8% *syn/anti* isomers. Similar resonances are found for **6** at 13.03 (*anti*) and 12.64 ppm (*syn*) for the *syn/anti* isomer (2% each of total). The lower solubility of **6** compared to **7** and the smaller amount of the *syn/anti* isomer prevented confirmation of this assignment through measurement of the J_{CH} values. No resonances are found for an *anti/anti* isomer in

either case. The relatively low amounts of the *syn/anti* isomers of **6** and **7** that are found suggest that the amount of *anti/anti* isomer in each case would probably be much less than 1%.

To confirm that all the alkylidene resonances observed for **6** and **7** were indeed bimetallic complexes, the corresponding monosubstituted analog of **6** was synthesized and analyzed by ^{1}H NMR spectroscopy. One equivalent of divinylferrocene was added to $Mo(NAr)(OR_{F6})_2(CHCMe_2Ph)$ to form a compound of the type, $[Mo(NAr)(OR_{F6})_2(=CHC_5H_4\text{-}Fe\text{-}C_5H_4CH=CH_2)]$ and the ^{1}H NMR spectrum was recorded after twenty minutes. Alkylidene resonances are observed for the starting material and **6** as well as two addition resonances observed at 13.10 (6.7% of total area) and 12.68 ppm (25.8% of total area). We ascribe these additional resonances to the *anti* and *syn* isomers, respectively, of $[Mo(NAr)(OR_{F6})_2(=CHC_5H_4\text{-}Fe\text{-}C_5H_4CH=CH_2)]$.

	Initiator	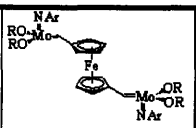	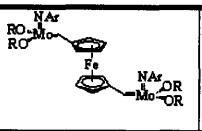		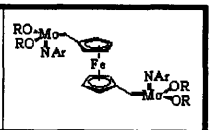
Isomer Configuration		Anti/Anti	Anti/Syn		Syn/Syn
^{1}H NMR shift (ppm)	6	Not observed	13.03	12.64	12.53
	7	-	12.31	11.97	11.84
Percentage (%)	6	-	2	2	96
	7	-	4	4	92
J_{CH} (Hz)	6	-	-	-	129
	7	-	154*	125*	127

Table 2.3 ^{1}H NMR spectroscopy data for **6** and **7**.

2.3 Initiation Studies

For a polymerization process with a bifunctional initiator to be living, it is important to establish that both ends initiate quickly with a given monomer. It is also required that the rate of initiation is greater than or equal to the rate of propagation. To examine whether these

requirements are met by **6** and **7**, aliquots of **DCMNBD** were added to solutions of the bifunctional initiator. Table 2.4 gives the percent of **6** initiated per added equivalent of **DCMNBD** per molybdenum center. The addition of a total of eight equivalents of **DCMNBD** to **6** (4 equiv per Mo) in C_6D_6 led to the disappearance of the initial alkylidene resonances and appearance of broadened alkylidene resonances at 12.69 (~15%) and 12.10 ppm (~85%) as judged by the ^{1}H NMR spectra. These resonances match those observed for the initiation of the related divinylbenzene-linked species, $[(THF)Mo(NAr)(OR_{F6})_2(=CH)]_2(1,4\text{-}C_6H_4)$.[11] The resonance at 12.69 ppm is proposed to be that for the *anti* isomer of the propagating polymer chain while the resonance at 12.10 ppm is proposed to be the *syn* isomer. The addition of four aliquots of **DCMNBD** to **7** (2 equiv per Mo) in C_6D_6 revealed that the initial alkylidene protons are replaced by two doublet alkylidene proton patterns at 11.71 and 11.66 ppm (2.5:1). The pattern observed in the alkylidene region of the ^{1}H NMR spectrum is the same as that obtained using the monometallic initiator, $Mo(NAr)(CHCMe_2Ph)(O\text{-}t\text{-}Bu)_2$ and the related divinylbenzene-linked initiator, $[(THF)Mo(NAr)(OR_{F0})_2(=CH)]_2(1,4\text{-}C_6H_4)$,[11] as should be the case. Since the *trans* content of poly(**DCMNBD**) is approximately the same in the polymers synthesized, we believe that the two alkylidene resonances can be ascribed to polymer chains in which the alkylidene at the chain end contains a *trans* or a *cis* double bond between the last and next to last monomer unit. The alkylidene itself is likely to be the average of rapidly equilibrating *anti* and *syn* isomers.[21] These data indicate that initiation appears to be facile for both the *tert*-butoxide and hexafluoro-*tert*-butoxide complex and only 4-8 equivalents of **DCMNBD** are needed in order to initiate polymerization at both metal sites of **6** and **7**.

Number of equivalents **DCMNBD** added per molecule	1	2	3	5	8
Percent **6** Initiated	50%	74%	80%	94%	100%

Table 2.4 Percent of **6** initiated per equivalent of **DCMNBD** added per molecule.

2.4 Polymerization Studies using 6 and 7

Homopolymers and ABA triblock copolymers were prepared using initiators **6** and **7** in toluene (Scheme 2.4). A typical polymerization reaction involved the addition of a monomer solution to the initiator in solution, followed by continued stirring at room temperature for one hour. To prepare triblock copolymers, a second monomer solution was added to the reaction (after the first monomer had been completely polymerized) and the mixture stirred for another hour. Ultimately, all reactions were quenched with excess benzaldehyde and the polymers were precipitated by the addition of methanol.

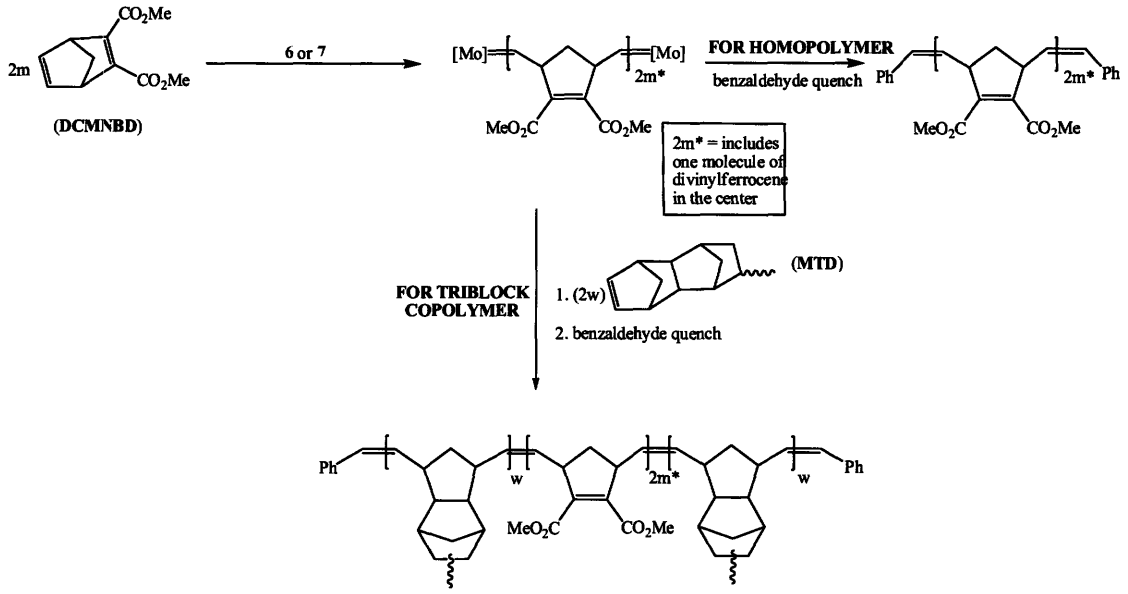

Scheme 2.4 Example of preparation of poly(**MTD**)$_w$(**DCMNBD**)$_{2m*}$(**MTD**)$_w$ and poly(**DCMNBD**)$_{2m*}$ prepared using **6** or 7 as the initiator and quenched with benzaldehyde.

Homopolymers of **DCMNBD** and **MTD** prepared using **6** or **7** as initiators in toluene showed low polydispersity indexes (PDIs) (< 1.10), as determined by GPC (calibrated using polystyrene standards) (Table 2.5). The experimental M_n values cannot be compared directly with the expected M_n values as the GPC system was calibrated using polystyrene standards. GPC traces of poly(**DCMNBD**) samples prepared with **7** as the initiator showed a high molecular weight shoulder, but were unimodal when **6** was employed. ABA Triblock copolymers were also prepared in toluene using the bifunctional initiators **6** or **7** and showed narrow PDI values (Table 2.6).

Monomer	Initiator	Equivalents	PDI
DCMNBD	**6**	50	< 1.05
		100	< 1.05
		150	< 1.05
	7	50	< 1.05
		100	1.05
		150	1.07
MTD	**6**	50	1.09
		100	1.10
	7	50	< 1.05
		100	< 1.05

Table 2.5 GPC data for poly(**DCMNBD**) and poly(**MTD**) homopolymers prepared using **6** or **7** as the initiator.

Initiator	Triblock Copolymer	PDI
6	$(\mathbf{MTD})_{15}(\mathbf{DCMNBD})_{20}(\mathbf{MTD})_{15}$	1.19
	$(\mathbf{MTD})_{15}(\mathbf{DCMNBD})_{24}(\mathbf{MTD})_{15}$	1.13
	$(\mathbf{MTD})_{21}(\mathbf{DCMNBD})_{32}(\mathbf{MTD})_{21}$	1.30
	$(\mathbf{MTD})_{24}(\mathbf{DCMNBD})_{31}(\mathbf{MTD})_{24}$	1.13
	$(\mathbf{MTD})_{25}(\mathbf{DCMNBD})_{50}(\mathbf{MTD})_{25}$	< 1.05
	$(\mathbf{MTD})_{25}(\mathbf{DCMNBD})_{100}(\mathbf{MTD})_{25}$	< 1.05
	$(\mathbf{MTD})_{47}(\mathbf{DCMNBD})_{103}(\mathbf{MTD})_{47}$	1.11
	$(\mathbf{DCMNBD})_{16}(\mathbf{MTD})_{34}(\mathbf{DCMNBD})_{16}$	1.27
	$(\mathbf{DCMNBD})_{14}(\text{norbornene})_{47}(\mathbf{DCMNBD})_{14}$	1.19
7	$(\mathbf{MTD})_{25}(\mathbf{DCMNBD})_{50}(\mathbf{MTD})_{25}$	1.09
	$(\mathbf{MTD})_{25}(\mathbf{DCMNBD})_{100}(\mathbf{MTD})_{25}$	1.08

Table 2.6 GPC data for triblock copolymers prepared using **6** or **7** as the initiator.

Several samples of poly$(\mathbf{DCMNBD})_x$ that were prepared using **6** as the initiator were characterized by MALDI-TOF mass spectroscopy. MALDI-TOF mass spectrometry is considered a "soft" technique as the energy of the laser is spent volatilizing the matrix instead of degrading the polymer.[22] To prepare a MALDI sample, a matrix and sample are cocrystallized on the MALDI target. In some cases, dopants may be added as well. The matrix is excited by high intensity, short duration laser pulses. The absorbed energy results in vaporization and ionization of the analyte in a very dense MALDI plume. The ions that are generated at this point in time and space enter a vacuum where they are accelerated by a strong electric field and are separated in time and finally impact onto the detector. An analyzer measures the time-of-flight (TOF) taken for particular ions to hit the detector and these results are related by a mass-to-charge ratio (*m*/z).

One or more ferrocene molecules in the ROMP polymers were required for us to analyze the polymers by MALDI-TOF MS (vide infra). Therefore, the polymers analyzed were either

prepared using the divinylferrocene-linked initiator (which incorporates one ferrocene moiety in the center of each polymer chain), and/or through quenching of the polymerization with ferrocenecarboxaldehyde (which incorporates two ferrocene moieties, one at both ends of each polymer chain). The cause for the dependence on ferrocene is unknown and likely complicated. It has been found that ferrocene containing molecules formed analyte molecular radical cations instead of the commonly observed proton-transfer reactions between analyte and matrix or cation adduction.[23] The three matrices that were investigated for MALDI included 2,5-dihydroxy benzoic acid (DHB), dithranol (DT), and *trans*-3-indoleacrylic acid (IAA) (Figure 2.2). Dopants included Na^+ (source = NaI), K^+ (source = KCl), or Ag^+ (source = silver trifluoroacetate). After several sample preparations and optimization of conditions, DT was found to be the most appropriate matrix for the ROMP polymers of this type. The results are presented in Table 2.7.

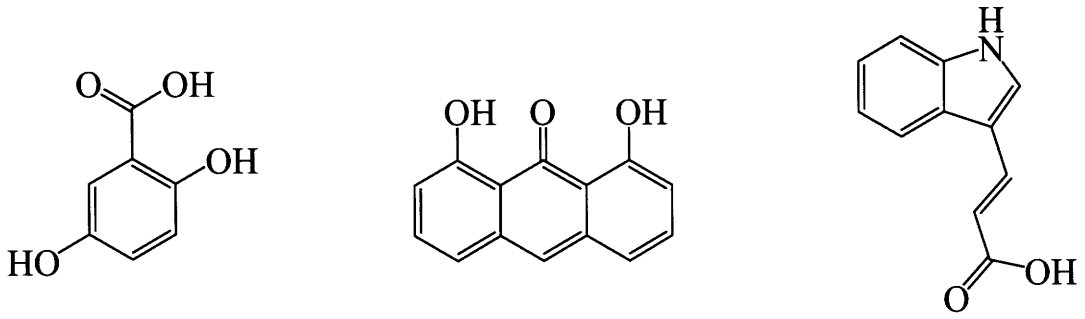

Figure 2.2 Matrixes investigated for MALDI-TOF analysis of poly(**DCMNBD**): 2,5-dihydroxy benzoic acid (DHB, left), dithranol (DT, center), and *trans*-3-indoleacrylic acid (IAA, right).

Equivalents of **DCMNBD**	Expected M_n ($\times 10^4$)	Actual M_n ($\times 10^4$)	PDI
49	1.06	1.02	< 1.05
		1.05	< 1.05
102	2.16	2.22	< 1.05
		2.25	< 1.05

Table 2.7 MALDI-TOF MS data acquired for poly(**DCMNBD**) synthesized using **6** as the initiator.

A typical MALDI spectrum of poly(**DCMNBD**)$_x$ synthesized using **6** is shown in Figure 2.3. Two distributions are present, one centered at the expected mass, the other at approximately half the expected mass. The resolution is not sufficient to know if the half molecular weight species contain iron or not. Two possible explanations for the half molecular weight chains are either (i) a significant amount of monometallic initiator was present in the catalyst, or (ii) some polymer chains are fragmented under the MALDI conditions employed. The first seems unlikely since (i) no monometallic initiator can be observed in the proton NMR spectrum of the catalyst employed, (ii) if a significant amount of monometallic catalyst was present, the experimental molecular weight should be larger than that expected and observed for a living system, and (iii) the size of the half-mass peak varies depending on the MALDI conditions employed, and in some cases, it was not present. In all four samples the distance between peaks corresponds approximately to the mass of the monomer (**DCMNBD** = 208.21); the M_n values are approximately that expected for a living polymerization ($210.06 + n \times 208.21 + 2 \times 90.12$, where n = the number of monomers added), and the PDI values (calculated from the MALDI spectrum) are analogous to that obtained by ordinary GPC methods (Table 2.5).

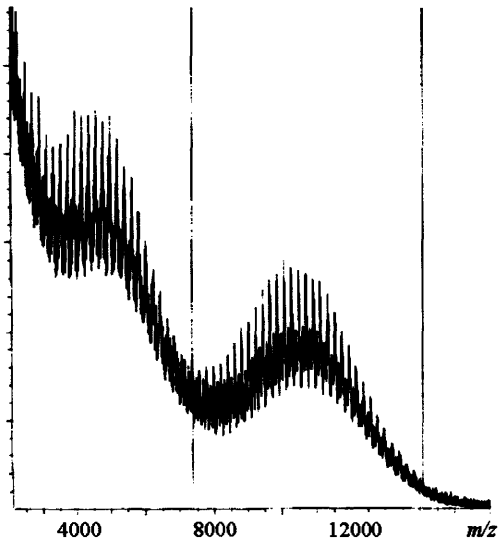

Figure 2.3 MALDI-TOF spectrum of poly(**DCMNBD**)$_{50}$/(CHPh)$_2$ synthesized using **6** as the initiator and quenched with benzaldehyde. (Matrix used = DT; doped with Ag^+; $M_n = 1.02 \times 10^4$; PDI = 1.02).

Similar studies were carried out on poly(**DCMNBD**)$_{30}$ that was prepared using [(THF)Mo(NAr)(OR$_{F0}$)$_2$(=CH)]$_2$(1,4-C$_6$H$_4$) as an initiator.[24] As mentioned previously, one or more ferrocene moieties within each polymer chain was required to see a significant signal in the MALDI spectrum. Therefore, analysis of the polymer synthesized with [(THF)Mo(NAr)(OR$_{F0}$)$_2$(=CH)]$_2$(1,4-C$_6$H$_4$) as an initiator (the polymer would not contain a ferrocene moiety in the center of each chain) and quenched using with excess benzaldehyde, gave only extremely weak signals in the MALDI spectrum. However, when the polymer was quenched with excess ferrocenecarboxaldehyde, significant signals are observed in the MALDI spectrum. The MALDI spectrum of the polymer shows a single distribution ($M_n = 6.8 \times 10^3$) with the molecular weight centered around the expected molecular weight (6.7×10^3) as shown in Figure 2.4. The distance between peaks corresponds approximately to the mass of the monomer (**DCMNBD** = 208.21), and the PDI is 1.08. It is important to note that no half-

molecular weight chains were observed for this polymer, which further suggests that the half molecular weight chains in the polymers synthesized using **6** as the initiator can be ascribed to fragmentation under the MALDI conditions employed.

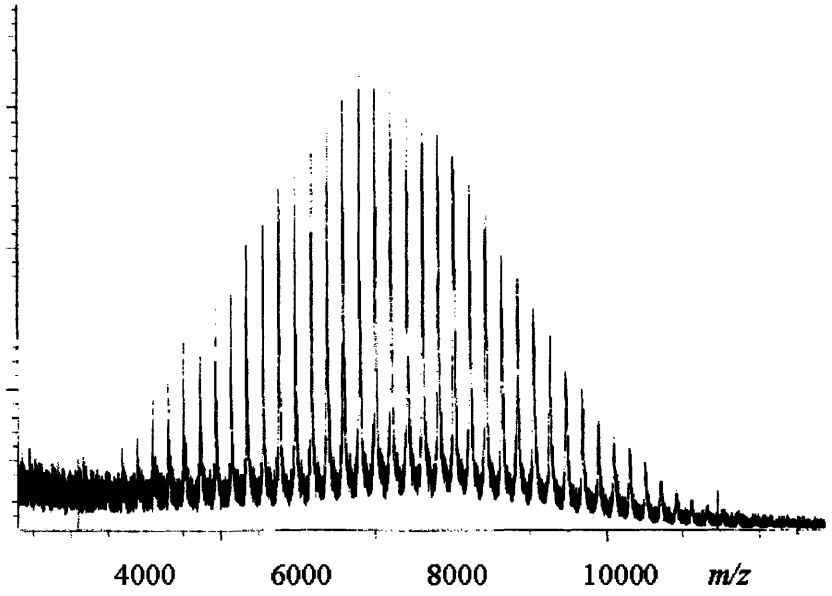

Figure 2.4 MALDI-TOF spectrum of poly(**DCMNBD**)$_{30}$/[$(CHC_5H_4)FeCp]_2$ synthesized using [(THF)Mo(NAr)$(OR_{F0})_2$(=CH)]$_2$(1,4-C_6H_4) as the initiator and quenched with ferrocenecarboxaldehyde. (Matrix used = DT; doped with Na^+; $M_n = 6.8 \times 10^3$; PDI = 1.08).

MALDI-TOF MS was attempted on some homopolymers of **MTD** synthesized using **6**. Unfortunately, although peaks were observed in the spectra which were separated by approximately 174 *m/z* (the molecular weight of **MTD**), the lower molecular weight polymers were observed with much higher sensitivities as opposed to the higher molecular weight polymers. This observance is commonly observed for polymers and is related to mass discrimination effects and to decreasing detector response at higher masses.[25] Therefore, the M_n of the **MTD** polymers as well as the PDI value could not be determined by MALDI. MALDI was also attempted on a poly(**MTD**)(**DCMNBD**)(**MTD**) triblock copolymers. Unfortunately,

similar results were observed as those obtained for the **MTD** homopolymers; the M_n was skewed from the expected M_n, and the PDI value, although low, may be incorrect (Figure 2.5).

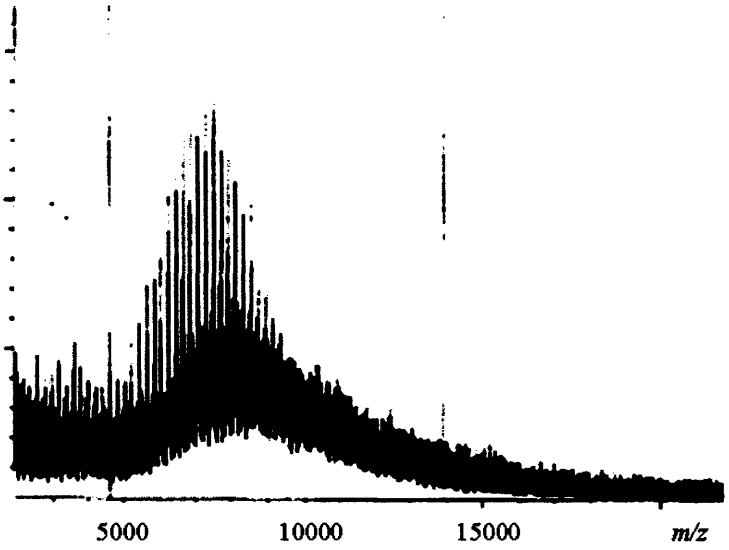

Figure 2.5 MALDI-TOF MS of poly(**MTD**)$_{15}$(**DCMNBD**)$_{24}$(**MTD**)$_{15}$ prepared using **6** as the initiator. PDI = 1.07; $M_n = 8.4 \times 10^3$; Expected $M_n = 1.02 \times 10^4$.

To confirm further that both ends of the bifunctional initiator were activated, end-group analysis was performed on an oligomer. An oligomer of **DCMNBD** (12 mer average) was prepared by adding 12 equivalents of **DCMNBD** to a solution of **6** in toluene. After one hour, the solution was divided into two portions. One portion was quenched with benzaldehyde to yield poly(**DCMNBD**)$_{12}$/(CHPh)$_2$ and the other portion with ferrocenecarboxaldehyde to yield poly(**DCMNBD**)$_{12}$/[(CHC$_5$H$_4$)FeCp]$_2$ (where CHPh and (CHC$_5$H$_4$)FeCp are the benzylidene and ferrocenylmethylene endgroups, respectively) (Figure 2.6). Each oligomer was analyzed by MALDI-TOF MS.

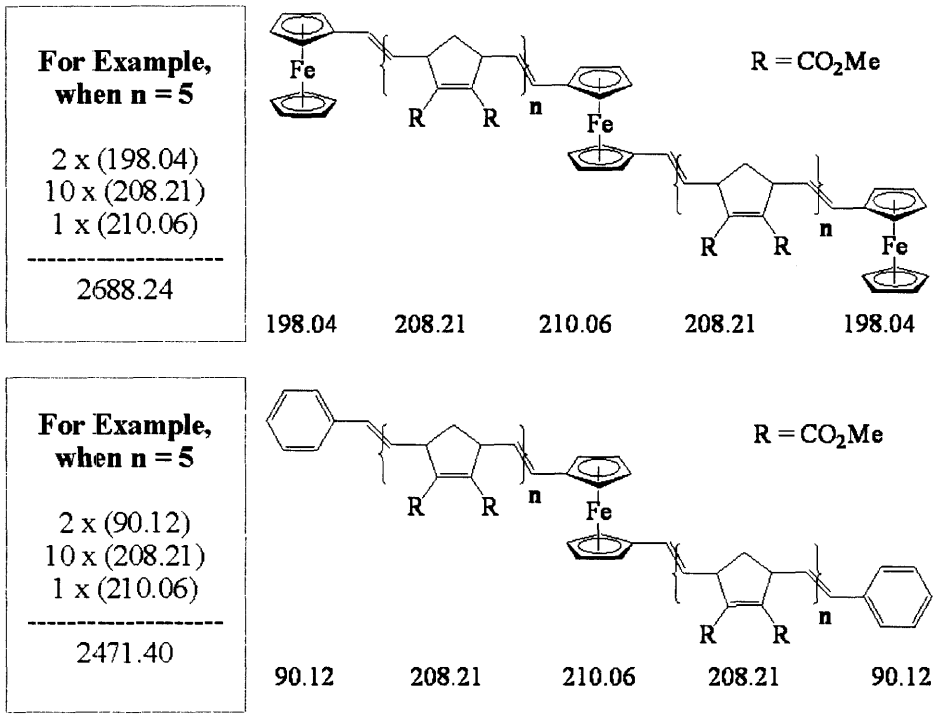

Figure 2.6 Expected molecular weight values for **DCMNBD** oligomers synthesized using **6** and then capped with ferrocenecarboxaldehyde (top) or benzaldehyde (bottom).

A spectrum of the poly(**DCMNBD**)$_{12}$/(CHPh)$_2$ sample (doped with Na^+ and Ag^+) is shown in Figure 2.7 (The H^+ doped peak is also present, as in any MALDI spectrum). The difference between any two peaks is approximately 208.21 Da, which is the molecular weight of one monomer unit. An expansion of the [Fe($C_5H_4CH)_2$](**DCMNBD**)$_{10}$(CHPh)$_2$ peak is shown in Figure 2.8. The expected distributions are shown in the Figure underneath the respective peak, and match closely those expected for the H^+, Na^+, and Ag^+ doped oligomer. MALDI spectra of poly(**DCMNBD**)$_{12}$/[(CHC_5H_4)FeCp]$_2$ are analogous to those of poly(**DCMNBD**)$_{12}$/(CHPh)$_2$. The expanded region of the [Fe($C_5H_4CH)_2$](**DCMNBD**)$_{10}$[(CHC_5H_4)FeCp]$_2$ peak (Figure 2.9) matches closely with that of the benzaldehyde capped polymer with the difference corresponding to twice the difference in the molecular weight of the end groups (benzylidene versus ferrocenylmethylene). The expected and found molecular weights differ by no more than 1 Da

and the isotopic distributions closely match for both $[Fe(C_5H_4CH)_2]$(**DCMNBD**)$_{10}(CHPh)_2$ and $[Fe(C_5H_4CH)_2]$(**DCMNBD**)$_{10}[(CHC_5H_4)FeCp]_2$. Only the expected peaks are observed in the MALDI spectrum, not even the fragmented chains noted above. These data suggest that polymerization of **DCMNBD** by **6** as the initiator is a living process under the conditions employed, and that the polymer chain ends are still active after the polymerization is complete. Since NMR studies discussed in the previous section suggest that both ends of the bifunctional initiator react with **DCMNBD** to yield the expected new alkylidenes, these polymerizations must proceed in a living fashion from the initiator in both directions with the number of monomers incorporated being statistical, and on average, equal in number on each side of the central linking unit, $Fe(C_5H_4CH)_2$.

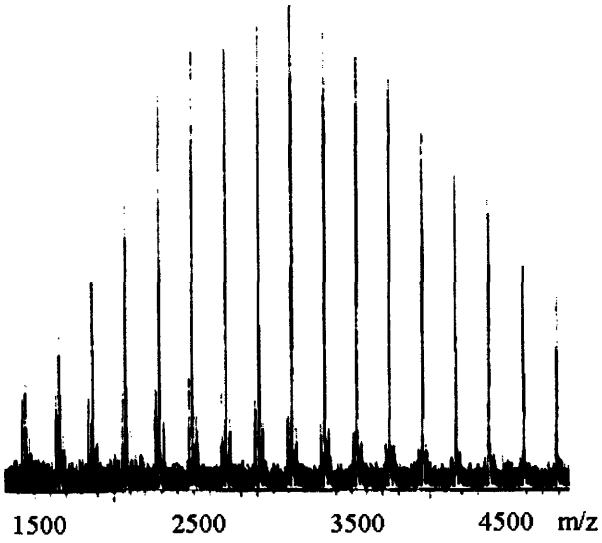

Figure 2.7 Spectrum of Ag^+ and Na^+ doped oligomer of **DCMNBD** synthesized using **6** as the initiator and capped with benzaldehyde (poly(**DCMNBD**)$_{12}$/$(CHPh)_2$). The most intense peak is the Na^+ doped macromolecules (Matrix = DT).

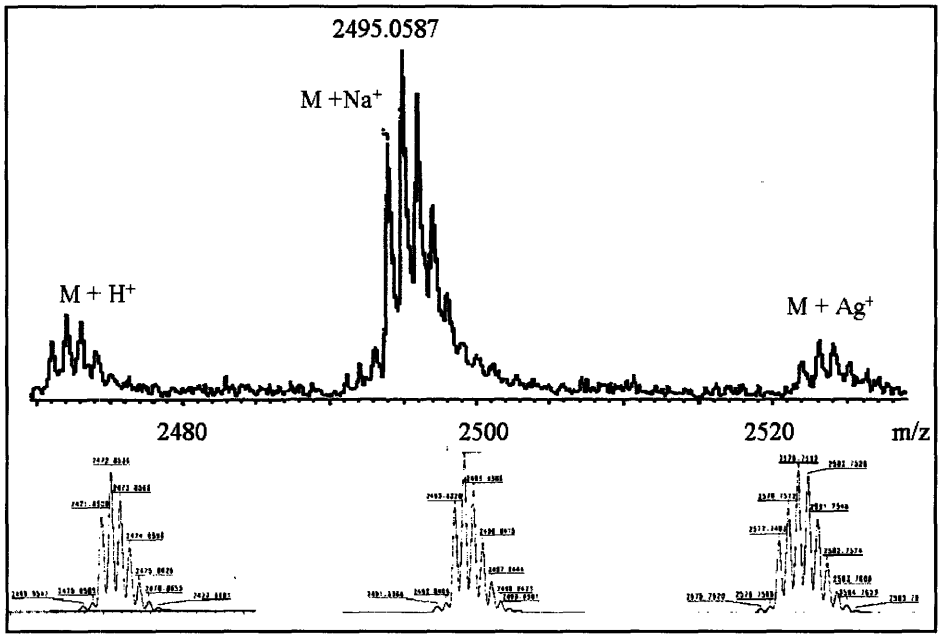

Figure 2.8 Expanded peak for $[Fe(C_5H_4CH)_2][\mathbf{DCNMBD}]_{10}(CHPh)_2$. The three peaks correspond to H^+, Na^+ and Ag^+ adducts respectively. The expected isotopic distributions are shown underneath the respective peaks.

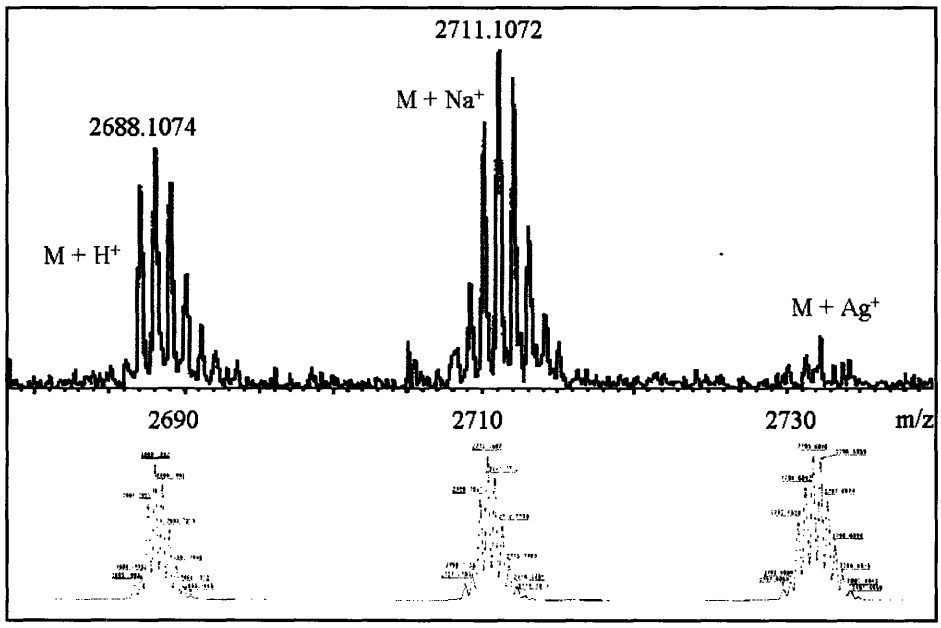

Figure 2.9 Expanded peak for $[Fe(C_5H_4CH)_2](\mathbf{DCMNBD})_{10}[(CHC_5H_4)FeCp]_2$. The three peaks correspond to H^+, Na^+ and Ag^+ adducts respectively. The expected isotopic distributions are shown underneath the respective peaks.

2.5 Conclusions

Two bifunctional initiators for ROMP were reported and shown to be "living" initiators for the ROMP of various norbornene- and norbornadiene-based monomers. Triblock copolymers were also synthesized using these initiators. The polymers were characterized by gel permeation chromatography and MALDI-TOF MS. Through GPC, the polymers were shown to have unimodal distributions and low PDI values. By MALDI-TOF MS, the polymers were determined to have M_n values that match the expected M_n values. MALDI-TOF MS was also used for endgroup analysis, and the results gave proof that both molybdenum centers are initiated and can be capped with a chosen endgroup.

2.6 Experimental Procedures

General Procedures. All manipulations were performed in oven-dried (200 °C) glassware under an atmosphere of nitrogen in a Vacuum Atmospheres glovebox or using standard Schlenk techniques. HPLC-grade solvents were purified by passage through an alumina column and stored over 4 Å Linde-type molecular sieves prior to use. Deuterated solvents were degassed and distilled from CaH_2 or sodium benzophenone ketyl. Commercial reagents were used without further purification unless stated otherwise. Methyltetracyclododecene (**MTD**) and norbornene were dried over CaH_2 and vacuum distilled. Benzaldehyde was vacuum distilled and stored over molecular sieves. $Mo(NAr)(OR_{F6})_2(CHCMe_2Ph)$,[26] and 4,5-dicarbomethoxynorbonadiene[27] (**DCMNBD**) were synthesized according to published procedures.

NMR spectra were recorded on a Varian INOVA 500 spectrometer. ^1H NMR chemical shifts are given in ppm versus residual protons in the deuterated solvents as follows: δ 7.27 $CDCl_3$, δ 7.16 C_6D_6, δ 5.32 CD_2Cl_2, and δ 2.09 $CD_3C_6D_5$. MALDI-TOF mass spectra were

recorded on a Bruker Omni-Flex MALDI-TOF and data were analyzed using Xtof Software Version 5.1.5 by Bruker Daltonics, Inc. Matrix solutions were prepared as 10 mg/mL solutions in THF. Samples were prepared as 0.1 to 1 mg/mL solutions in THF and the matrix:sample ratio was 10:1. Dopant concentration when applicable was approximately 0.1 mg/mL. GPC analyses were carried out on a system equipped with two Waters Styragel HR 5E columns (300 mm length × 7.8 mm inner diameter) in series. HPLC grade THF was supplied at a flow rate of 1.0 mL/min with a Knauer HPLC pump K501. A Wyatt Technology mini Dawn light-scattering detector coupled with a Knauer differential refractometer was employed. Data analysis was carried out using Astrette 1.2 software (Wyatt technology).

Synthesis of $\{(CH_3CO)C_5H_4\}_2Fe$.[12] A solution of CH_3COCl (24.1 mL, 0.34 mol) in methylene chloride (150 mL) was added dropwise under a flow of nitrogen to a suspension of $AlCl_3$ (45 g, 0.34 mol) in methylene chloride (200 mL). The solution became dark black during the addition. A solution of ferrocene (25.3 g, 0.14 mol) in methylene chloride was added dropwise over two hours. The solution was stirred overnight and was poured onto ice (500 g). The organic phase was washed with water three times, washed with saturated $NaHCO_3$ solution until the phase was neutral, the organic layers were dried over Mg_2SO_4, and the volatile components were removed to give a crude brick red powder (31 g, 84%). Crystallization from cold methanol yielded pure $\{(CH_3CO)C_5H_4\}_2Fe$: ^1H NMR (C_6D_6) δ 2.03 (s, 3H, C*H*$_3$), 3.91 (d, 2H, C*H*), 4.45 (d, 2H, C*H*).

Synthesis of $\{(CH_3CHOH)C_5H_4\}_2Fe$.[13,14] Solid $\{(CH_3CO)C_5H_4\}_2Fe$ (3 g, 11.1 mmol) was added slowly to an ice cooled solution of $LiAlH_4$ (300 mg, 7.9 mmol) in tetrahydrofuran (25 mL) under a flow of nitrogen. The solution was stirred overnight at which time ethyl acetate (2.5 mL) was added. The solution was cooled again and a mixture of water (1.73 mL), ethanol and

diethyl ether was added dropwise. The solution was filtered through Celite and rinsed through with diethyl ether. The volatile components of the filtrate were removed *in vacuo* and the resulting solid was recrystallized from hexanes in a dry ice/acetone bath. Multiple batches of crystal were isolated; yield 1.68 g (55%): ^{1}H NMR ($CDCl_3$) δ 1.40 (t, 3H, C*H*$_3$), 4.00 (m, 2H, C*H*), 4.25 (d, 1H, C*H*OH), 5.33 (m, 2H, C*H*).

Synthesis of {(CH$_2$CH)C$_5$H$_4$}$_2$Fe, Route A.[16] A mixture of {(CH$_3$CHOH)C$_5$H$_4$}$_2$Fe (1.68 g, 6.1 mmol) and activated neutral alumina (10.1 g) was placed in a sublimation apparatus. The apparatus was heated under vacuum to 155 °C for twenty hours during which time red crystals grew on the cold finger. The apparatus was cooled and pumped into the glovebox overnight. When the apparatus was brought into the glovebox no solid was on the cold finger and a red oil was now present. It was determined the divinylferrocene had react with the water that had absorbed into the alumina and formed {Fe(C$_5$H$_4$)CMe}$_2$O, the decomposition product. Therefore, route B was investigated.

Synthesis of {C$_5$H$_4$(CH$_2$=CH)}$_2$Fe, Route B.[15] (This synthesis is a modification of that reported in the literature). A mixture of {(CH$_3$CHOH)C$_5$H$_4$}$_2$Fe (5 g, 0.18 mol) and activated neutral alumina (50 g) in toluene (50 mL) was refluxed for two hours. The solution was transferred into a Schlenk flask via a cannula and brought into the glovebox. The solution was then filtered through Celite, and the volatile components of the filtrate were then removed *in vacuo*. According to ^{1}H NMR spectra, the compound was approximately 75% product and 25% ({Fe(C$_5$H$_4$)CMe}$_2$O). This mixture was used in further reactions since the presence of {Fe(C$_5$H$_4$)CMe}$_2$O provided no complications, and the amount of {C$_5$H$_4$(CH$_2$=CH)}$_2$Fe actually present in the mixture was known: ^{1}H NMR (C_6D_6) δ 6.32 (m, 1H, C*H*CH$_2$), 5.29 (m, 1H, CHC*H*$_2$), 5.04 (m, 1H, CHC*H*$_2$), 4.06 (m, 4H, C*H*).

[Mo(NAr)(OR_{F6})$_2$(=CHC_5H_4)]$_2$Fe (6). The isolated divinylferrocene from above (0.27 g, 0.96 mmol) was added all at once to a yellow toluene solution (10 mL) of Mo(NAr)(OR_{F6})$_2$($CHCMe_2Ph$) (1.2 g, 1.6 mmol) with stirring at ambient temperature. After one hour, the solution was stored at -30 °C to afford dark red crystals; yield 1.2 g (83% yield): ^{1}H NMR (C_6D_6) δ 13.03 (s, 1H, MoC*H*R, *syn/anti* isomer, 2%), 12.64 (s, 1H, MoC*H*R, *syn/anti* isomer, 2%), 12.53 (s, 2H, MoC*H*R, *syn/syn* isomer, 96%). The following peaks are reported for the major isomer only: 6.99 (s, 6H, C*H*), 4.00 (m, 16H, C_5H_4), 3.47 (s, 4H, C*H*(CH_3)$_2$), 1.34 (s, 12H, CC*H*$_3$(CF_3)$_2$), 1.14 (d, 24H, CH(C*H*$_3$)$_2$); ^{13}C NMR (C_6D_6, alkylidene region only) δ 269.10 (d, J_{CH} = 129 Hz, Mo*C*HR); Anal. Calcd for $C_{54}H_{62}F_{24}Mo_2N_2O_4Fe$: C, 43.04; H, 4.15; N, 1.86. Found: C, 42.88; H, 4.07; N, 1.81.

[Mo(NAr)(OR_{F0})$_2$(=CHC_5H_4)]$_2$Fe (7). Lithium *tert*-butoxide (200 mg, 2.5 mmol) was added all at once to a toluene solution (75 mL) of **6** (0.6 g, 0.40 mmol) with stirring at ambient temperature. The solution was stirred for five hours at which time the volatile components were removed. Pentane was added to the resulting solid and the solution was filtered through Celite. The filtrate was concentrated and placed in the freezer overnight during which time crystals formed; yield 0.4 g (65%): ^{1}H NMR (C_6D_6) δ 12.31 (s, 1H, MoC*H*R, *syn/anti* isomer, 4%), 11.97 (s, 1H, MoC*H*R, *syn/anti* isomer, 4%), 11.84 (s, 2H, MoC*H*R, *syn/syn* isomer, 92%). The following peaks are reported for the major isomer only: 7.09 (br s, 6H, C*H*), 4.25 (m, 4H, C_5H_4), 4.17 (m, 4H, C_5H_4), 3.99 (s, 4H, C*H*(CH_3)$_2$), 1.37 (s, 36H, C(C*H*$_3$)$_3$), 1.28 (d, 24H, CH(C*H*$_3$)$_2$). The following data is reported for the alkylidene region only: ^{1}H NMR ($C_6D_5CD_3$) δ 12.24 (s, 1H, MoC*H*R, J_{CH} = 154 Hz, *syn/anti* isomer, 4%), 11.90 (s, 1H, J_{CH} = 125 Hz, MoC*H*R, *syn/anti* isomer, 4%), 11.77 (s, 1H, J_{CH} = 130 Hz, MoC*H*R, *syn/syn* isomer, 92%); ^{13}C NMR (C_6D_6,

alkylidene region only) δ 247.05 (d, J_{CH} = 127 Hz, Mo*C*H*R*); Anal. Calcd for $C_{54}H_{86}Mo_2N_2O_4Fe$: C, 60.33; H, 8.06; N, 2.61. Found: C, 60.15; H, 7.88; N, 2.54.

Observation of monometallic ferrocenylidene. Divinylferrocene from above (5.4 mg, 0.015 mmol) and Mo(NAr)(OR_{F6})$_2$(CHCMe$_2$Ph) (18.2 mg, 0.0234 mmol) were each dissolved in 0.5 mL of benzene and the solutions were rapidly mixed and placed in an NMR tube. By ^{1}H NMR, the various products were observed twenty minutes after mixing. Only the alkylidene region peaks are reported: ^{1}H NMR (C_6D_6) δ 13.10 (s, 1H, Mo*C*H, 6.7%, monometallic species), 13.02 (s, 1H, Mo*C*H, 6.2%, *syn/anti* isomer of **6**), 12.68 (s, 1H, Mo*C*H, 25.8%, monometallic species), 12.64 (s, 1H, Mo*C*H, 6.7%, *syn/anti* isomer of **6**), 12.52 (s, 1H, Mo*C*H, 42.8%, *syn/syn* isomer of **6**), 12.14 (s, 1H, Mo*C*H, 11.8%, unreacted starting material).

General procedure for the preparation of homopolymers. To the catalyst solution in toluene, a solution of the monomer in toluene was added in one portion and the solution was stirred at room temperature for 45 minutes to one hour. The polymerization was quenched with benzaldehyde and stirred for another 45 minutes to one hour. The polymer was precipitated out of methanol, filtered and dried *in vacuo*.

General procedure for the preparation of triblock copolymers. The first monomer (inside block) in toluene was added in one portion to the catalyst solution in toluene and the solution was stirred at room temperature for one hour. Then a solution of the second monomer (outside block) in toluene was added in one portion and the reaction stirred for another hour. Benzaldehyde was added and the solution was stirred for 45 minutes to one hour. The polymer was precipitated by addition of methanol, filtered and dried under vacuum.

Example of polymerization of MTD with 6. A solution of **MTD** (63.9 mg, 54 equiv) in 3 mL of toluene was added rapidly to a solution of **6** (10.3 mg, 0.0069 mmol) in 10 mL of

toluene. The solution was stirred for 45 minutes. Two drops benzaldehyde was added to quench the reaction and the solution was allowed to stir for an additional 45 minutes. 100 mL of methanol was added to the solution and it was stirred overnight. The solid that precipitated was isolated by filtration, dried *in vacuo*, and used in further studies.

Example of polymerization of MTD and DCMNBD with 6. A solution of **DCMNBD** (91 mg, 52 equiv) in 3 mL of toluene was added rapidly to a solution of **6** (12.7 mg, 0.0084 mmol) in 10 mL of toluene. The solution was stirred for 45 minutes. A solution of **MTD** (98.7 mg, 54 equiv) in 3 mL toluene was added rapidly and the solution was stirred for another 45 minutes. Two drops benzaldehyde were added to quench the reaction and the solution was allowed to stir for an additional 45 minutes. 100 mL of methanol was added to the solution and it was stirred overnight. The solid that precipitated was isolated by filtration, dried *in vacuo*, and used in further studies.

Synthesis of DCMNBD oligomer using 6, quenched with both benzaldehyde and ferrocenecarboxaldehyde. A solution of **DCMNBD** (208.2 mg, 12 equiv) in 10 mL of toluene was added rapidly to a solution of **6** (181 mg, 0.0069 mmol) in 75 mL of toluene. The solution was stirred for 45 minutes and was then split into two approximately equal portions. Two drops of benzaldehyde were added to one portion and a spatula tip of ferrocenecarboxaldehyde was added to the other portion to quench the reaction, and the solutions were stirred for an additional 45 minutes. 50 mL of methanol was added to each solution and the volatile components were removed *in vacuo*. 10 mL of tetrahydrofuran was added to each solution and they were rinsed through a silica plug with additional tetrahydrofuran. The volatile components were again removed *in vacuo* to yield two powders that were used in further studies.

X-Ray Crystallographic Studies. Crystals were coated in Paratone-N oil in an inert

atmosphere and examined under a microscope. A suitable crystal was placed on the end of a glass fiber or in a glass loop and frozen in an inert gas stream. Data were collected on a Siemens Platform three-circle diffractometer equipped with a CCD or Bruker Apex-CCD detector at low temperature. Mo Kα radiation (λ = 0.71073 Å) was used. Integration was performed using the SAINT package and corrected for absorption effects with SADABS, unless otherwise noted. The initial solutions were obtained using direct methods, unless otherwise noted, and refined against F^2 on all data using full-matrix least squares using the SHELXTL package.[24] All non-hydrogen atoms were refined anisotropically and hydrogen atoms were refined using a riding model. The isotropic displacement parameters of all hydrogen atoms were fixed to 1.2 times the *U* value of the atoms they are linked to, except for methyl groups which were fixed at 1.5. Details of the data and refinement statistics are listed in Table 1 for all structures.

Compound **6** was crystallized at room temperature from a benzene solution and contains one ordered benzene of solvation. All hydrogen atoms except H1 were placed in calculated positions and refined using a riding model. H1 was located in the difference map and refined satisfactorily. Compound **7** was obtained from a saturated toluene solution at –30 °C; one equivalent of ordered toluene was found in the crystal. During data collection the sample degraded substantially due to ice formation. Enough data were collected prior to icing to determine the structure. However, the resulting R factors are somewhat higher and the redundancy is somewhat lower than a typical data collection. The data were corrected for absorption effects using psi-scans in XPREP.

2.7 References

(1) Schrock, R. R., *Acc. Chem. Res.* **1990,** 23, 158-165 and references therein.

(2) Schrock, R. R.; Hoveyda, A. H. *Angew. Chem. Int. Ed.* **2003**, *42*, 4592.

(3) Schrock, R. R. *Acc. Chem. Res.* **1990**, *23*, 158.

(4) Albagli, D.; Bazan, G.; Schrock, R. R.; Wrighton, M. S. *J. Phys. Chem.* **1993**, *97*, 10211.

(5) Albagli, D.; Bazan, G. C.; Wrighton, M. S.; Schrock, R. R. *J. Am. Chem. Soc.* **1992**, *114*, 4150.

(6) Fox, H. H.; Lee, J.-K.; Park, L. Y.; Schrock, R. R. *Organometallics* **1993**, *12*, 759.

(7) Risse, W.; Wheeler, D. R.; Cannizzo, L. F.; Grubbs, R. H. *Macromolecules* **1989**, *22*, 3205.

(8) Weck, M.; Schwab, P.; Grubbs, R. H. *Macromolecules* **1996**, *29*, 1789.

(9) Mayershofer, M. G.; Nuyken, O.; Buchmeiser, M. R. *Macromolecules* **2006**, *39*, 2452.

(10) Mayershofer, M. G.; Nuyken, O.; Buchmeiser, M. R. *Macromolecules* **2006**, *39*, 3484.

(11) Schrock, R. R.; Gabert, A. J.; Singh, R.; Hock, A. S., *Organometallics* **2005**, 24, 5058.

(12) Vogel, M.; Rausch, M.; Rosenberg, H. *J. Org. Chem.* **1957**, *22*, 1016

(13) Carrol, M. A.; White, A. J. P.; Widdowson, D. A.; Williams, D. J. *J. Chem. Soc., Perkin Trans. 1* **2000**, *1*, 1551.

(14) Graham, P. J.; Lindsey, R. V.; Parshall, G. W.; Peterson, M. L.; Whitman, G. M. *J. Am. Chem. Soc.* **1957**, *79*, 3416.

(15) Gamble, A. S.; Patton, J. T.; Boncella, J. M. *Makromol. Chem., Rapid Commun,* **1993**, *13*, 109.

(16) Rausch, M. D.; Siegel, A. *J. Organomet. Chem.* **1968**, *11*, 317.

(17) Schrock, R. R. *Chem. Rev.* **2002**, *102*, 145.

(18) Feldman, J.; Schrock, R. R. *Prog. Inorg. Chem.* **1991**, *39*, 1.

(19) SciFinder 2006, Chemical Structure Search M=CH-(η^5-C_5R_4)Fe(η^5-C_5R_5) where M = W or Mo.

(20) Toreki, R.; Vaughan, G. A.; Schrock, R. R.; Davis, W. M. *J. Am. Chem. Soc.* **1993**, *115*, 127.

(21) Oskam, J. H.; Schrock, R. R. *J. Am. Chem. Soc.* **1993**, *115*, 11831.

(22) For a general introduction to MALDI-TOF MS see: Montaudo, G. Samperi, F.; Montaudo, M. S. *Prog. Polym. Sci.* **2006**, *31*, 277 and Pasch, H; Schrepp, W. *MALDI-TOF mass spectrometry of synthetic polymers*. Springer: New York, **2003**.

(23) McCarley, T. D.; McCarley, R. L.; Limbach, P. A. *Anal. Chem.* **1998**, *70*, 4376.

(24) These polymers were synthesized by Rojendra Singh.

(25) Adamus, G.; Rizzarelli, P.; Montaudo, M. S.; Kowalczuk, M.; Montaudo, G. *Rap. Commun. Mass. Spec.* **2006**, *20*, 804.

(26) Schrock, R. R.; Murdzek, J. S.; Bazan, G. C.; Robbins, J.; DiMare, M.; O'Regan, M. *J. Am. Chem. Soc.* **1990**, *112*, 3875.

(27) Tabor, D. C.; White, F. H.; Collier, L. W.; Evans, S. A. *J. Org. Chem.* **1983**, *48*, 1638.

Chapter 3 - Synthesis and Characterization of ABA Triblock Copolymers Containing Smectic C* Liquid Crystal Side Chains

A portion of this work has appeared in print: *Synthesis and Characterization of ABA Triblock Copolymers Containing Smectic C* Liquid Crystal Side Chains via Ring-Opening Metathesis Polymerization Using a Bimetallic Molybdenum Initiator*, Gabert, A. J.; Verploegen, E.; Hammond, P. T.; Schrock, R. R., *Macromolecules* **2006**, *39*, 3993.

3.1 Introduction

Living polymerization systems allow for the synthesis of polymers with well-defined structures and controlled chemical compositions.[1,2,3,4,5] In addition, living techniques can be employed for the synthesis of block copolymers. With appropriate conditions and choice of block materials, block copolymers can self-assemble into various morphologies with nanometer-sized domains.[6] ABA triblock copolymers which exhibit microphase separation can act as thermoplastic elastomers (TPEs) when the outer block is amorphous and has a high glass transition temperature (T_g) and the inner block is flexible and has a low T_g.[7] An ABA triblock copolymer is preferred for TPE applications as opposed to AB diblock copolymers because the A blocks are linked to the B blocks through covalent bonds at the domain boundaries, essentially providing "physical crosslinks" between the two different A blocks.[8]

Further application of TPEs can be realized when the central block is functionalized by liquid crystal (LC) mesogens, forming novel block copolymers termed thermoplastic liquid crystal elastomers (TPLCEs).[9,10,11] TPLCEs combine the properties of TPEs and liquid crystal elastomers (LCEs). The phase segregation of the triblock copolymers confine the liquid crystals in restricted geometries. LCEs are of interest because they possess electro-mechanical and electro-optical properties while TPEs are elastomers that can be processed and reshaped. This processing feature is not available in conventional LCEs, which are formed through chemical crosslinking of homopolymers containing liquid crystal mesogens.[12,13,14,15] In addition, the combination of TPE and LCE properties has been found to stabilize some liquid crystal phases. The block copolymer interface of TPLCEs, also known as the inter-material dividing surface (IMDS) allows for the alignment of the liquid crystal mesogens, unlike LCEs which require surface techniques for alignment. Mesogens which exhibit the chiral smectic C* phase in LCEs

and TPLCEs are of particular interest because this phase has been found to exhibit ferroelectric and piezoelectric properties.

Figure 3.1 shows the liquid crystal phases of interest for this Chapter (For a general overview, please see References 16, 17, 18, and 19). The liquid crystals are in an isotropic phase when there is no order to the system. The nematic phase generally precedes the isotropic phase; the transition (nematic to isotropic) is termed the liquid crystal clearing point. In a nematic phase, the mesogens have directional order with respect to a director, but have no long range positional order. In a smectic A phase, the mesogens again have directional order with respect to a director, but long range dimensional order is now present and the mesogens are arranged in layers. A smectic C phase maintains the same dimensional order as a smectic A phase (layers), but the mesogens are oriented at an angle with respect to a director. The "star" in a smectic C* phase is present when the mesogens contain a chiral center.

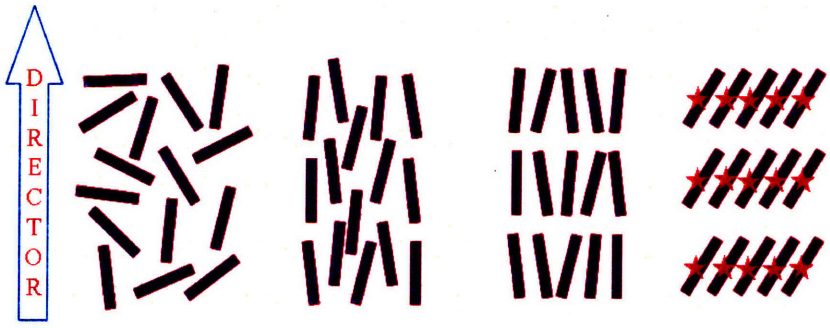

Figure 3.1 Relevant liquid crystal phases for this Chapter (left to right): isotropic, nematic, smectic A, and smectic C*.

Smectic C* phases are of interest because of the unique properties that they have been found to exhibit.[11,13,20,21,22,23,24,25,26,27,28,29] A consequence of the chiralty in the smectic C* phase is that each layer is oriented at an angle with respect to the layer before it.[17] Therefore, a helical type structure forms (Figure 3.2). Each layer has a net polarization associated with it because of the tilt of the LCs with respect to the director. If we consider one rotation of the helix (one

pitch), the net polarization is zero. However, if we can unwind the pitch, by confining the mesogens in a restricted geometry, there will be an overall net polarization. The IMDS of triblock copolymers provides confinement within small gaps and has been found to unwind the pitch of a smectic C* phase.[30]

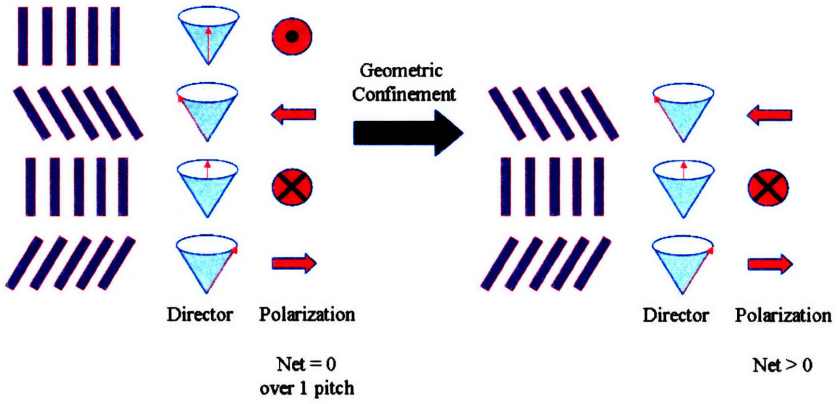

Figure 3.2 The helical type structure that forms from a smectic C* LC phase and the polarization associated with each layer (left). The result when the helix is unwound (right).

The properties that are associated with smectic C* LC phases are ferroelectricity and piezoelectricity. Ferroelectricity is the spontaneous net polarization that remains in the absence of an electric field. Essentially, if an electric field is applied to a geometrically confined smectic C* phase, the dipoles of all layers will align. If the electric field is removed, the net polarization will remain – hence, the material is ferroelectric. Ferroelectric materials can be exploited as bistable switches.[19] Opposite electric fields can be applied to the material and the net polarization will switch directions (Figure 3.3).

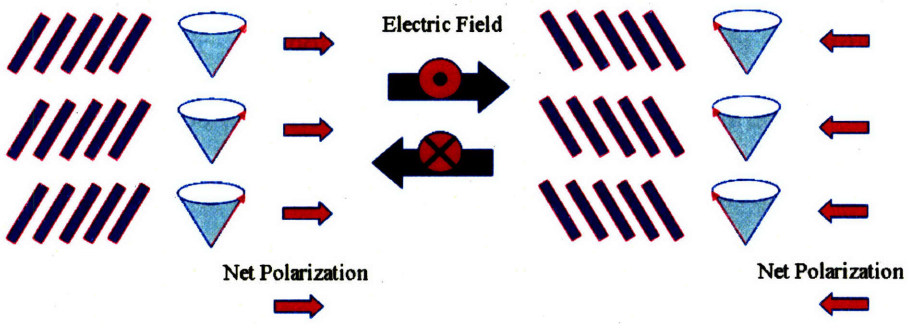

Figure 3.3 Bistable switching of a geometrically confined smectic C* phase.

The second property that can be exploited with geometrically confined smectic C* materials is piezoelectricity. When a piezoelectric material is placed in an electric field, the material will exhibit strain. Essentially, each layer of liquid crystals will tilt to align with the electric field. The total change of height of each layer is the difference between the original layer height (h_o) and the tilted layer height (h). This value, Δh (h_o-h) multiplied by the total number of layers (N), will give the total strain exhibited by the material (Figure 3.4).[31]

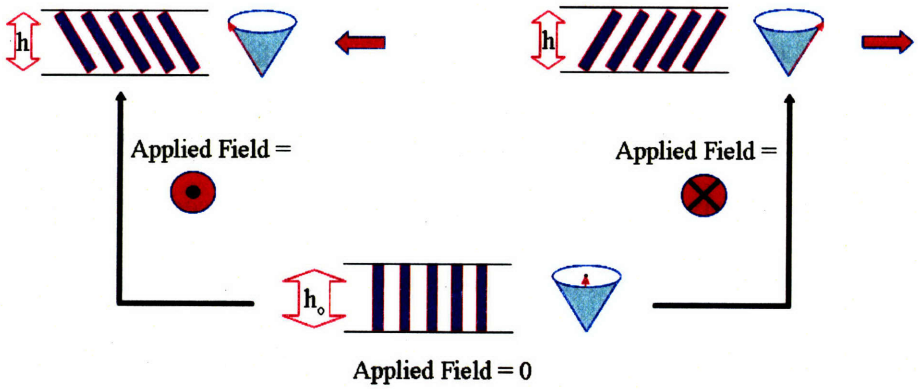

Figure 3.4 A piezoelectric liquid crystalline material. When an external electric field is applied, the mesogens tilt to align with the field. The change in total height of the material is (h_o-h) × N (where N is the total number of layers).

One living polymerization method that can be employed for the synthesis of well-defined triblock copolymers is ring opening metathesis polymerization (ROMP).[5] Although many monomers containing liquid crystal mesogens have been synthesized for ROMP,[32,33,34,35,36] no

work has been completed with smectic C* mesogens (for reviews, see References 37, 38, and 39). In addition, although ABA triblock copolymers have been synthesized via ROMP,[40,41,42,43,44] there are no examples in which the central block is functionalized by liquid crystal mesogens. Therefore, there has been no examination of the potential for triblock copolymers synthesized via ROMP to function as TPLCEs.

To take advantage of the properties inherent to smectic C* LC mesogens, we needed to synthesize triblock copolymers in which the central block is functionalized by liquid crystal mesogens. The goal of this research project was to synthesize triblock copolymers which exhibit phase segregation and contain smectic C* liquid crystal mesogens in the central block. Through examination of the thermal and mechanical properties of the synthesized polymers, we are able to explore the possibility of triblock copolymers synthesized by ROMP to function as TPLCEs.

In Chapter 2 we discussed the synthesis of a series of bifunctional molybdenum initiators which are active for living ROMP.[44] These initiators allow for the controlled synthesis of well-defined triblock copolymers. We have expanded the use of these initiators for the synthesis of ABA triblock copolymers where the A block is composed of high T_g amorphous methyltetracyclododecene (**MTD**) and the central block is functionalized by the smectic C* liquid crystal mesogens, **BPP4** (Figure 3.5).[45] This chapter reports the synthesis of triblock copolymers containing **BPP4** and the thermal and mechanical characterization of these polymers.

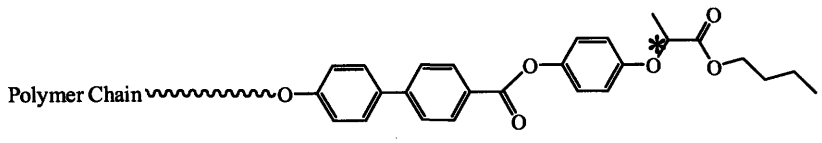

Figure 3.5 BPP4 mesogen.

3.2 Synthesis of BPP4 Containing Monomers

When synthesizing polymers containing liquid crystal mesogen, four aspects of the monomer can be altered: the polymer backbone, the nature of the LC attachment, the spacer, and the mesogens (Figure 3.6). We first chose to investigate norbornene and norbornadiene monomers for the backbone structure as they are the common monomers for ROMP. The attachment of the spacer to the polymer backbone may or may not be present, and is generally chosen based upon synthetic methodology. The spacer is generally an alkyl or ether chain, and we first chose to examine two different length alkyl chains. The liquid crystal mesogens chosen, **BPP4**, has been found to exhibit a smectic C* phase in other systems. The systems containing this mesogens are typically synthesized by attaching the mesogens to a polymers (e.g. siloxane) backbone. [45,46,47,48,49,50,51,52] Using this method of syntheses and depending on the reaction conditions, the percent substitution and pattern of mesogens attachment is varied. Therefore, an addition benefit to the bifunctional ROMP method is that the mesogens are attached to the monomer before synthesis of the polymer so the percentage and pattern of attachment is known and constant.

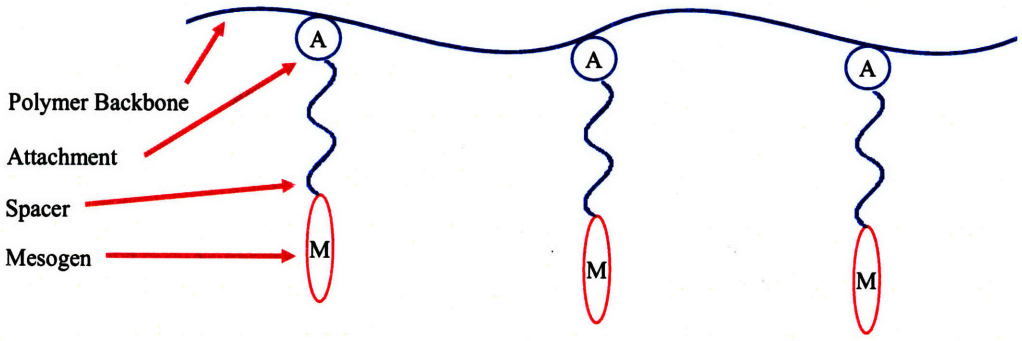

Figure 3.6 Schematic of a polymer containing LC mesogens.

For the purpose of these studies, three monomers were synthesized and investigated. One set of monomers consist of the LC mesogen attached to norbornene by a six or ten carbon spacer (**NB6wBPP4** or **NB10wBPP4**, respectively). These two monomers allow us to compare the effects of an increase in the length of the carbon spacer in the triblock copolymers synthesized. The third monomer contains the LC mesogens attached to norbornadiene with a ten carbon spacer (**NBD10wBPP4**). This monomer can be compared with **NB10wBPP4** to examine the effects of a more rigid backbone.

The liquid crystal of interest, **BPP4**, has been investigated previously for siloxane-based polymers. The typical synthetic route for this monomer is shown in Scheme 3.1. The mesogen was functionalized by a vinyl group which can be used for direct attachment to the siloxane-based polymer. This synthetic protocol needed to be modified to form a suitable monomer for ROMP which was functionalized by a norbornene or norbornadiene group. The typical route to a functionalized monomer for ROMP is to react HO-spacer-LC and the acid chloride of norbornadiene to form norbornadiene-COO-spacer-LC (Scheme 3.2). If a similar synthetic route is to be employed (as for the siloxane-based polymers) to a liquid crystal containing monomer for ROMP, the vinyl moiety of the mesogens (vinyl-spacer-**OBPP4**) in Scheme 3.1 needs to be replaced with a hydroxyl group to form HO-spacer-**BPP4**. The most direct route to this molecule would be hydrolyzation of the vinyl moiety. This was attempted using BH_3 as a reagent; the result of this was cleavage of the ester groups of the liquid crystal mesogen. A second option that was employed was ozonolysis; this reaction did not yield promising results.

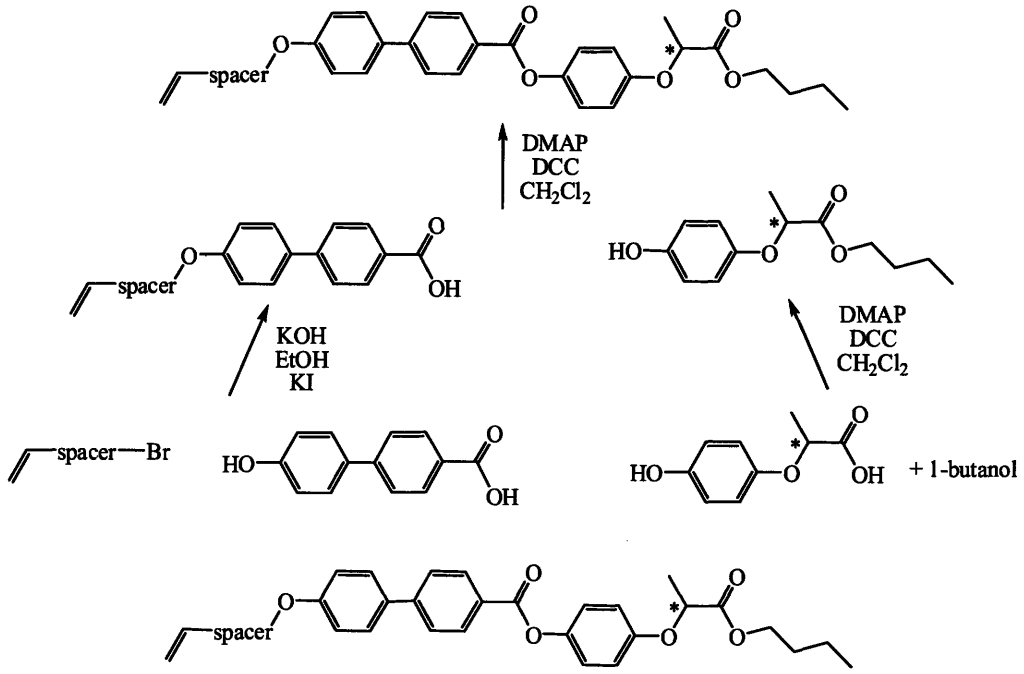

Scheme 3.1 Literature preparation of **BPP4** mesogen for attachment to siloxane-based polymers.

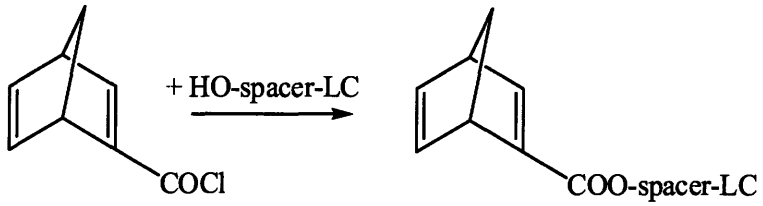

Scheme 3.2 Typical route for the synthesis of norbornadiene monomers containing a liquid crystal mesogen.

Another possible synthetic route to HO-spacer-**BPP4** is to replace vinyl-spacer-Br in the original synthetic scheme with a PGO-spacer-Br (where PG is a protecting group, Scheme 3.3). This was first attempted by using a silyl protected alcohol (*t*-$BuMe_2Si$-, TBDMS or *t*-$BuPh_2Si$-, TBDPS) (Scheme 3.4). For example, a protected alkyl chain was synthesized through reaction of 11-bromoundecan-1-ol with *tert*-butylchlorodimethylsilane. The product of this reaction, 11-bromoundecyloxy)(*tert*-butyl)dimethylsilane, was then reacted with 4′-hydroxy-4-biphenylcarboxylic acid to potentially form TBDMS-$(CH_2)_{11}$-O**BPP4**. Unfortunately, upon work-up of this reaction, the silyl group was cleaved. A stronger protecting group, benzyl, was

also used following the same synthetic procedure. Upon work-up of this reaction, it was determined that the protecting group had been cleaved to afford benzyl alcohol and the vinyl counterpart of the targeted molecule. Therefore, a new synthetic scheme had to be devised which deviated from the general synthetic procedure first introduced in Scheme 3.1.

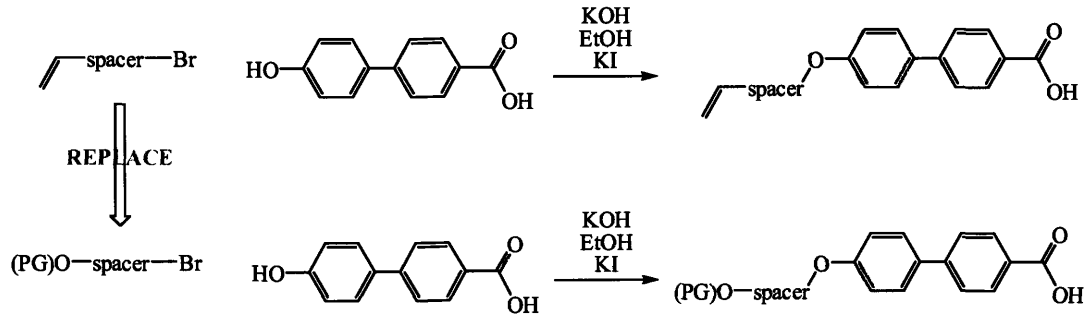

Scheme 3.3 Synthetic methodology alteration for the synthesis of **BPP4** containing monomer (PG = protecting group)

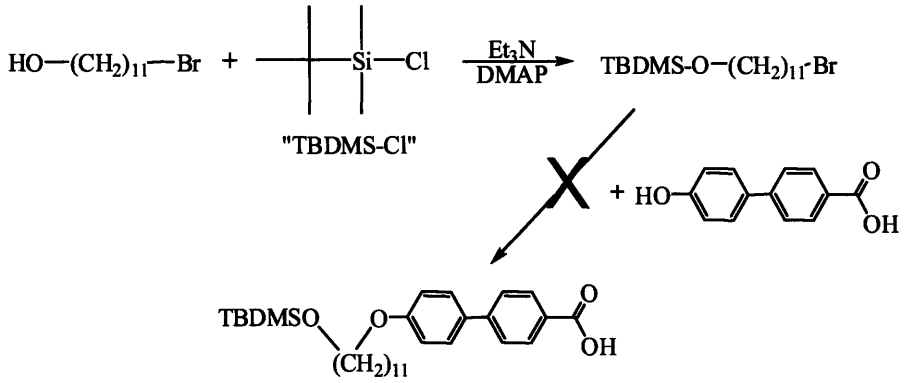

Scheme 3.4 Attempted synthesis of silyl protected alcohol linked to **BPP4**.

The modified synthetic route to the three target monomers is shown in Scheme 3.5. The halogen functionalized norbornenes required for the **NBnwBPP4** monomers (n = 6 or 10) were synthesized according to Scheme 3.6 through reaction of the corresponding bromo-functionalized compound through copper-catalyzed Grignard coupling with bromomethylnorbornene. The respective halogen functionalized norbornadiene required for **NBD10wBPP4** was synthesized according to Scheme 3.7 by deprotonation of norbornadiene

with Schlosser's base followed by reaction with 1,10-dibromodecane. These bromide functionalized compounds were reacted with 4'-hydroxy-4-biphenylcarboxylic acid to form one half of the corresponding monomers, **NB6**, **NB10**, and **NBD10**. Further coupling with (+)-2-(4-hydroxyphenoxy)propionic acid yielded the desired monomers **NB6wBPP4**, **NB10wBPP4** and **NBD10wBPP4**, respectively. For **NB6wBPP4** and **NB10wBPP4**, the ratio of *endo*:*exo* isomers was 80:20.

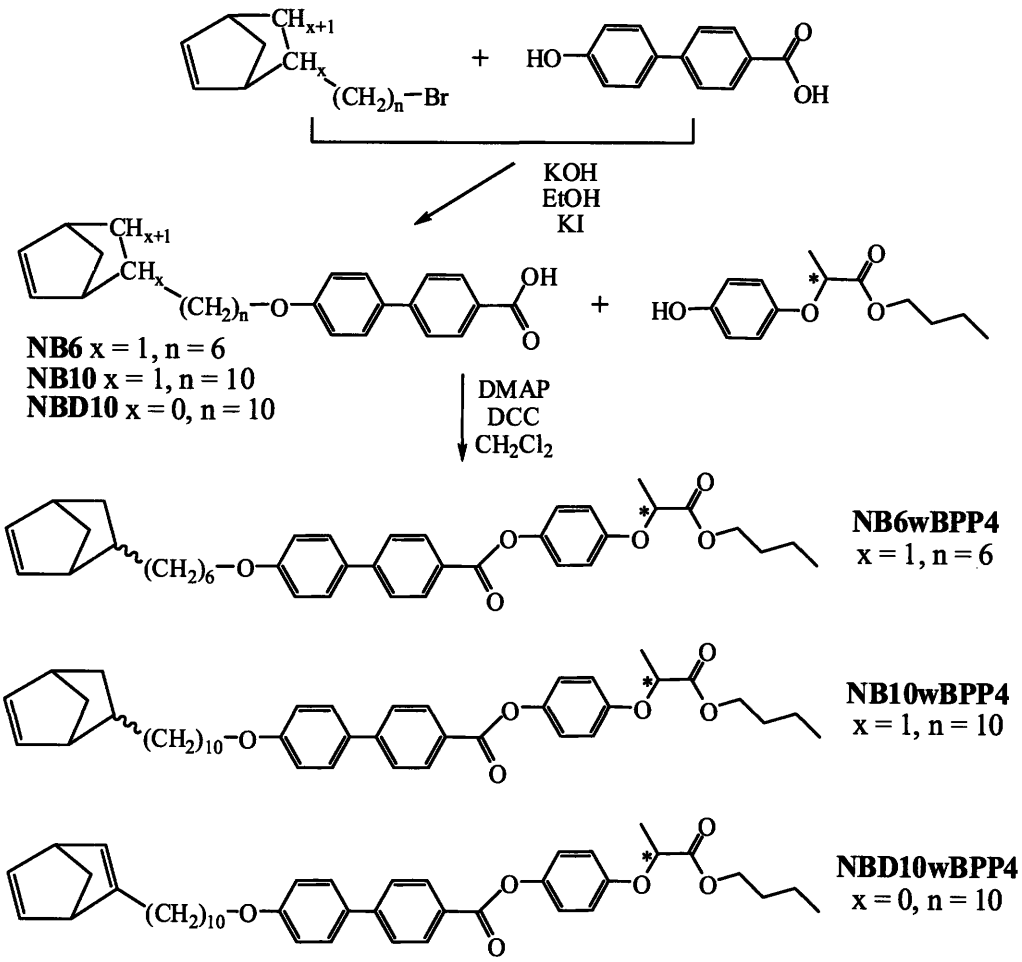

Scheme 3.5 Synthesis of **NBnwBPP4** (n = 6, 10) and **NBD10wBPP4**.

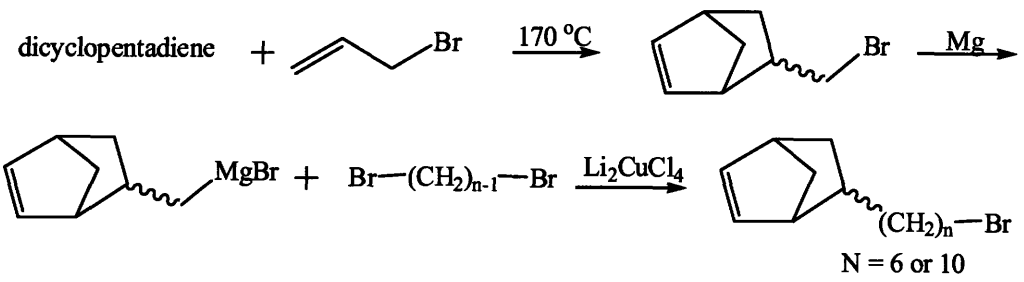

Scheme 3.6 Synthesis of 10-bromo-decanorbornene or 6-bromo-hexylnorbornene.

Scheme 3.7 Synthesis of 10-bromo-decanorbornadiene.

3.3 Polymerization of Monomers

Monomers **NBnwBPP4** (n = 6 or 10) and **NBD10wBPP4** were quantitatively polymerized in toluene using the bifunctional ROMP initiator, $[Mo(NAr)(OR_{F6})_2(=CHC_5H_4)]_2Fe$ (**6**), (Scheme 3.8). The molecular weight of the polymers was controlled by varying the ratio of monomer to initiator ([M]/[I]). For the synthesis of the triblock copolymers, the desired amount of methyltetracyclododecene (**MTD**) was added to the stirring mixture after time had elapsed. For all polymerizations, benzaldehyde was added to the solution to quench the reaction. In all cases, the polymers were purified by precipitation from methanol.

A series of homopolymers of **NB6wBPP4** were synthesized to prove that the liquid crystal containing monomers could be polymerized in a living fashion using the initiator **6**. Recall that in Chapter 2, **6** was shown to polymerize norbornene- and norbornadiene-based monomers in a living fashion. However, the M_n values obtained from gel permeation chromatography (GPC) data could not be compared directly with the expected values as the GPC instrument is calibrated using polystyrene standards. Therefore, we synthesized a series of

homopolymers (50-, 100-, 150-, 200-, and 300-mers). The graph of the M_n values as a function of [M]/[I] should be linear if the polymerization is living. The isolated yields of the polymers were all greater than 90%. As shown in Figure 3.7, a linear relationship is obtained by plotting the number-average molecular weight values (M_n vs. polystyrene) of poly(**NB6wBPP4**) as a function of ([M]/[I]). The results are summarized in Table 3.1. Note that all PDI values were less than 1.18. The linear relationship observed and the low PDI values are consistent with the living polymerization of **NB6wBPP4** under the conditions employed.

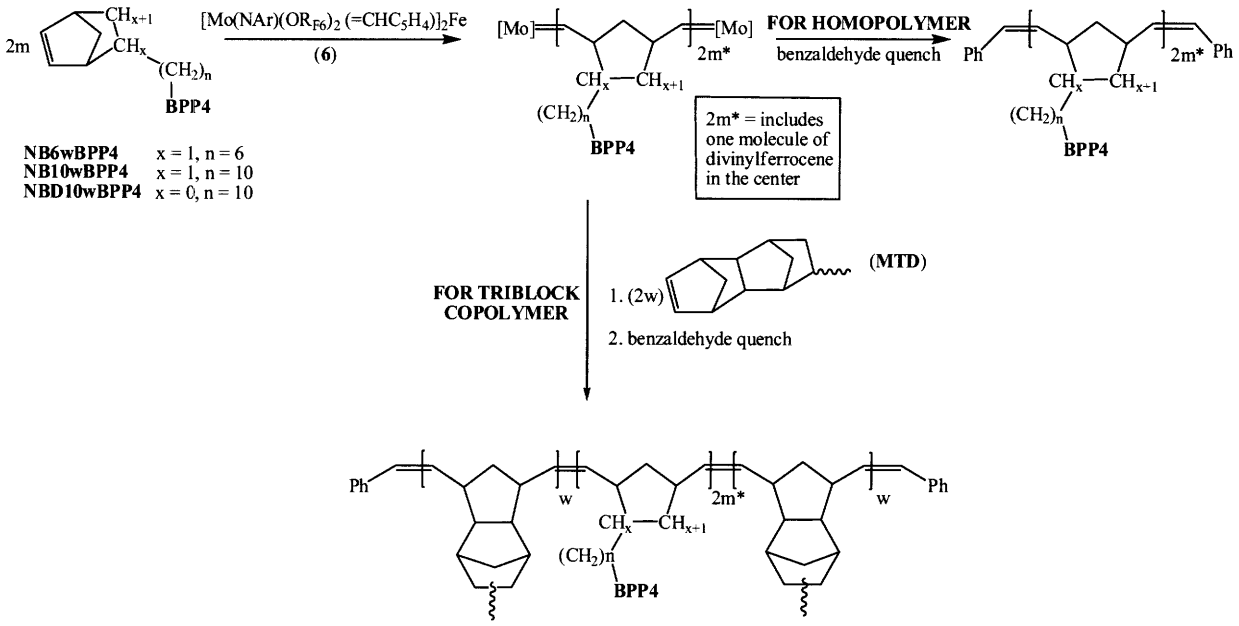

Scheme 3.8 Synthesis of homo- and triblock co-polymers of **BPP4** containing monomers.

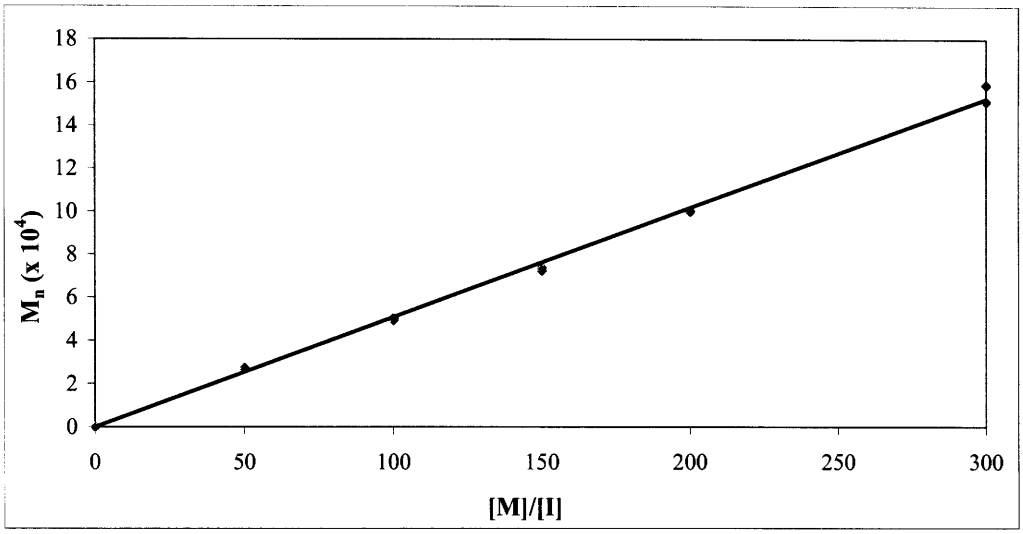

Figure 3.7 Graph of [M]/[I] vs. M_n for homopolymers of poly(**NB6wBPP4**).

Equivalents ([M])	Expected M_n (× 10^4)	Actual M_n (× 10^4)[a]	PDI
50	3.1	2.7, 2.7	1.18, 1.18
100	6.1	4.9, 5.0	1.10, 1.11
150	9.2	7.2, 7.4	1.09, 1.11
200	12.2	10.0, 10.0	1.12, 1.13
300	18.3	15.1, 15.9	1.15, 1.15

Table 3.1 Summary of GPC data for poly(**NB6wBPP4**) homopolymers. [a]M_n value versus polystyrene standards. Samples run in dichloromethane.

A short oligomer, (**NB6wBPP4**)$_{15}$ was synthesized for analysis by MALDI-TOF MS. It was hoped that direct molecular weight values could be obtained as previously observed in Chapter 2 for the analysis of poly(**DCMNBD**). Although peaks were observed in the MALDI spectrum of the oligomer (Figure 3.8), it was found that the higher molecular weight oligomers gave poor signals as compared to the lower molecular weight oligomers. The peaks observed are separated by a difference which correlates to the approximate molecular weight of the monomer (610.78 g/mol).

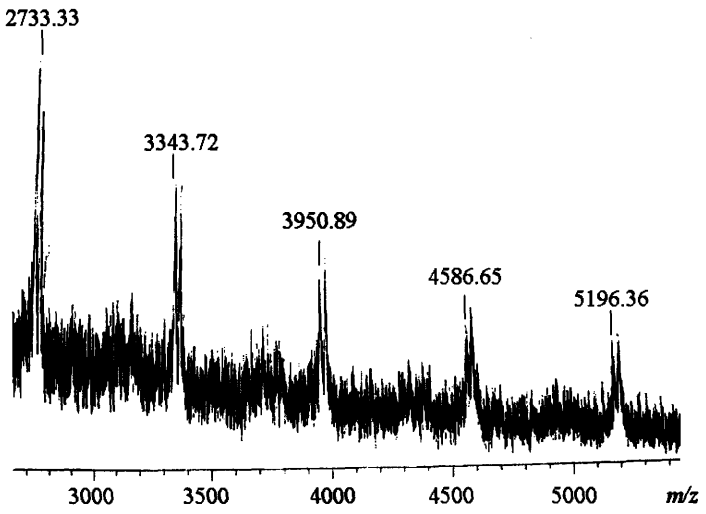

Figure 3.8 MALDI-TOF MS of poly(**NB6wBPP4**)$_{15}$. The double peaks are due to H^+ and Na^+ doping.

Homopolymers (100-mers) of the other two other monomers were prepared (**NB10wBPP4** and **NBD10wBPP4**). Triblock copolymers of all monomers were also synthesized where methyltetracyclododecene (**MTD**) was the outer hard block (50 equivalents per side) and the inner block was the liquid crystal functionalized monomers (200 equivalents). The results of these polymerizations are summarized in Table 3.2 and the GPC traces of the polymers are shown in Figure 3.10. The polydispersities (PDI) are less than 1.13 for the homopolymers and 1.31 for the triblock copolymers; isolated yields were all greater than 90%.

The polymers were also analyzed by ^{1}H NMR spectroscopy. The resonances in the olefinic range were quite broad, indicating a lack of stereoregularity of the main chain. The ^{1}H NMR spectra of the triblock copolymers were virtual superpositions of the homopolymers as shown in Figure 3.9. The ratio of the integration of the resonances in the olefinic region was used to approximate the ratio of LC functionalized monomer to **MTD** (**MTD**:LC monomer = 100:200 = 0.5). These values are given in Table 3.2 and are close to the expected value. The

low PDI values, correct ratio of monomers, and quantitative yields are consistent with a living system.

Polymer	Mn ($\times 10^4$)[a]	PDI	Yield	Expected A:B[b]	Actual A:B[c]
(NB6wBPP4)$_{100}$	6.95	1.07	95	-	-
(MTD)$_{50}$**(NB6wBPP4)**$_{200}$**(MTD)**$_{50}$	18.0	1.22	95	0.5	0.48
(NB10wBPP4)$_{100}$	6.88	1.13	90	-	-
(MTD)$_{50}$**(NB10wBPP4)**$_{200}$**(MTD)**$_{50}$	11.7	1.31	92	0.5	0.50
(NBD10wBPP4)$_{100}$	7.8	> 1.05	96	-	-
(MTD)$_{50}$**(NBD10wBPP4)**$_{200}$**(MTD)**$_{50}$	14.9	1.05	94	0.5	0.48

Table 3.2 Summary of polymerization data for homo- and triblock co-polymers.
[a] M_n value versus polystyrene standards. Samples run in dichloromethane.
[b] Ratio of monomer B vs. monomer A according to added [M]/[I] ratios.
[c] Ratio of monomer B vs. monomer A according to ^{1}H NMR spectroscopy.

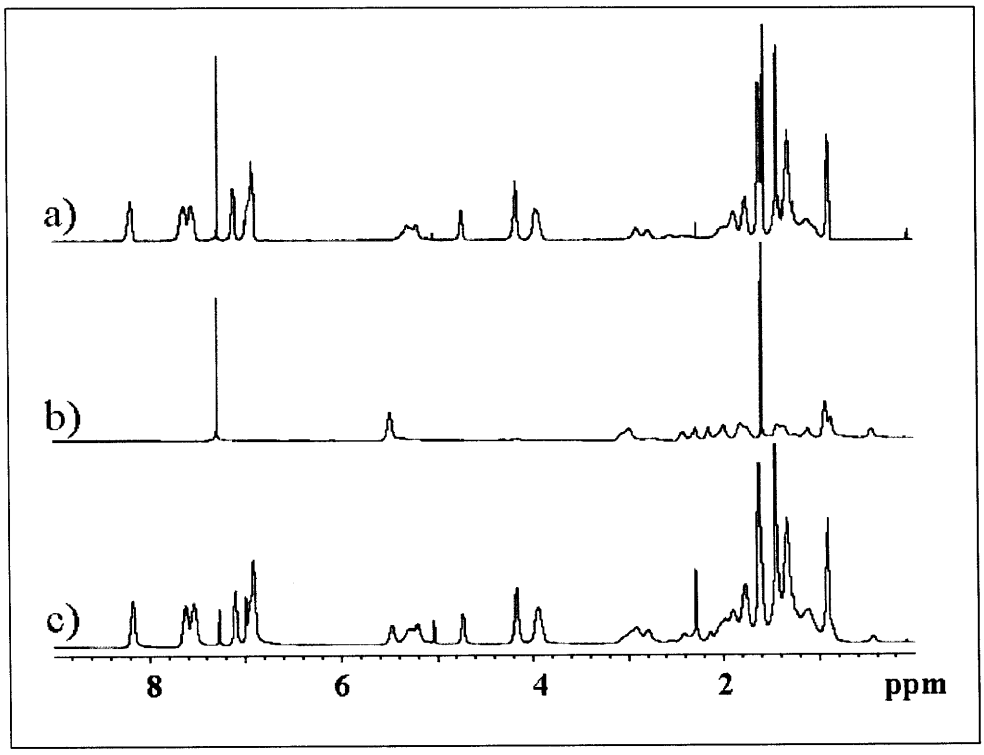

Figure 3.9 ^{1}H NMR spectra of a) poly(**NB6wBPP4**)$_{100}$, b) poly(**MTD**)$_{100}$ c) poly(**MTD**)$_{50}$(**NB6wBPP4**)$_{200}$(**MTD**)$_{50}$

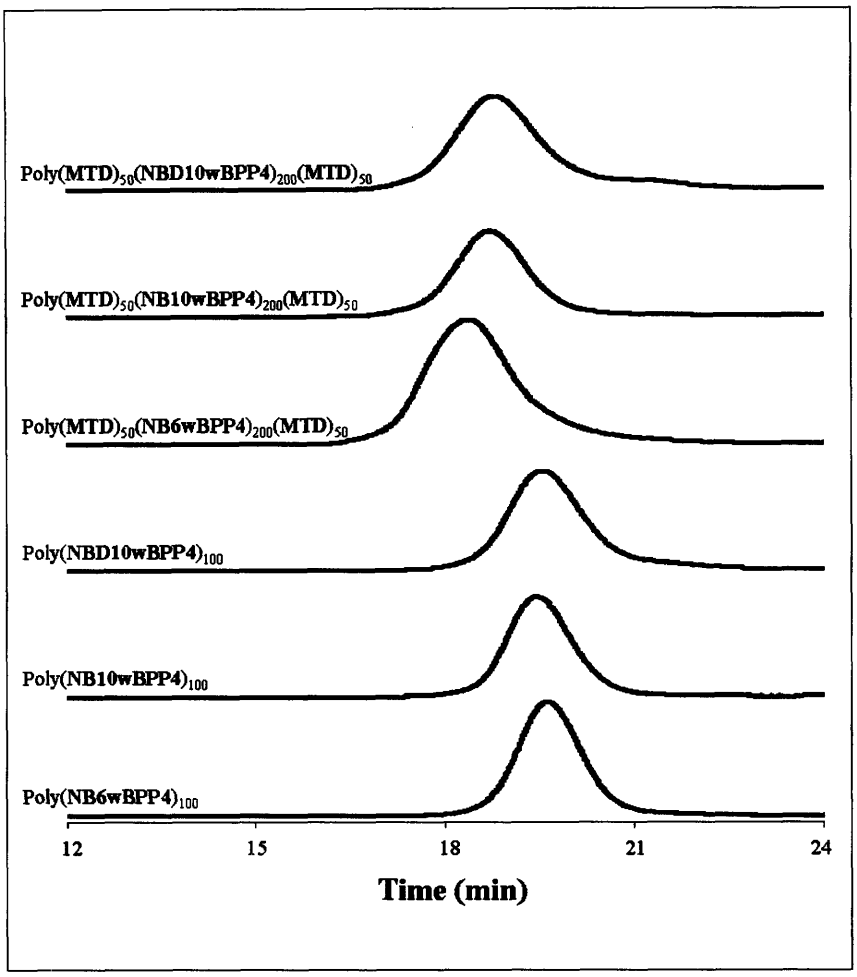

Figure 3.10 GPC traces of homo- and triblock co-polymers.

3.4 Thermal Characterization of Polymers

The homo- and triblock co-polymers were analyzed by differential scanning calorimetry (DSC) to determine the T_g values of the central blocks with the attached mesogens. The T_g of a polymer is the temperature at which it goes from being more rigid to more rubbery. Above the inner block T_g, the triblock copolymer will function as a elastomer. Above the T_g of the outer block, the polymer will lose its morphology. If the two blocks are phase segregated, two distinct transitions should be observed for the two blocks of the polymer. All transition values are reported in Table 3.3 and DSC traces of the second heating and first cooling cycles of the

triblock copolymers are shown in Figure 3.11. There was no notable difference observed when comparing the three monomers with increased length of the carbon spacer (**NB6wBPP4** versus **NB10wBPP4**) or with increased rigidity of the backbone structure (**NB10wBPP4** versus **NBD10wBPP4**). The T_g of the inner blocks of the respective triblock copolymers corresponded to the T_g of the LC homopolymers at approximately 20 °C, suggesting that the blocks are well phase segregated. However, the T_g of the **MTD** blocks was not observed in any of the three triblock copolymers. One explanation for this may be the inherently weak thermal signal obtained for the glass transition of poly(**MTD**). In DSC scans of poly(**MTD**) we observed only a weak transition around 210 °C. In the triblock copolymers, the weight percentage of **MTD** may be too small for its glass transition to be observed. A second possible explanation is that there may be some phase mixing in the continuous phase of the system.

DSC analysis was also employed to investigated the LC phase transitions. Phase transitions in the liquid crystalline sections of the monomers, homopolymers, and triblock copolymers are reported in Table 3.3. For the monomers, the transitions observed at low temperatures indicate the crystallization of the monomers, which behave as classical low molar mass liquid crystals. The smectic to isotropic transitions occur in these monomers at approximately 85 °C.

Side chain crystallization is not observed in the homopolymers over the temperature range of the DSC scans; as is observed with the majority of LC polymers, the material exists as a glass at temperatures below the T_g and transition directly into the LC phase at the T_g. The smectic to isotropic transitions are observed at higher temperatures and are broader as compared to the monomer. In general, it is expected that certain LC phases are stabilized when mesogens

are attached to polymer backbones, and this trend has been reported in other systems.[11,22,29] The smectic to isotropic transitions are elevated near 150 °C for all three homopolymers.

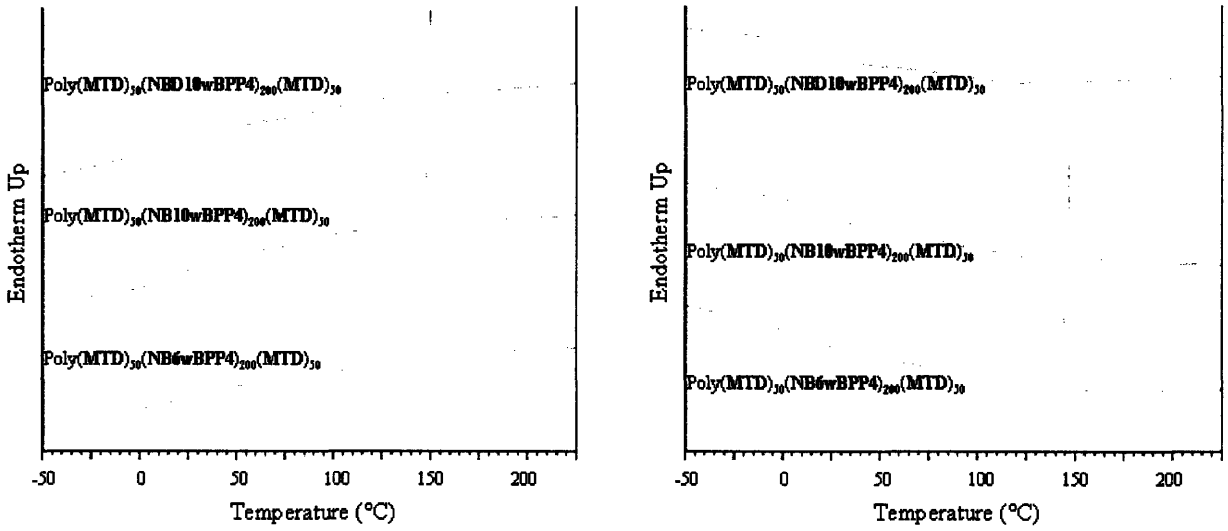

Figure 3.11 Second heating (left) and first cooling (right) DSC curves of **(MTD)**$_{50}$(LC)$_{200}$**(MTD)**$_{50}$ triblocks.

In DSC scans of the triblock copolymers, there are slight increases in the final smectic to isotropic phase transitions by a few degrees for the triblock copolymers containing **NB6wBPP4** and **NBD10wBPP4**. This suggests that the presence of the **MTD** block interface stabilizes the liquid crystalline phases. However, there is a slight decrease in the final smectic to isotropic phase transition for the triblock copolymer containing **NB10wBPP4**, suggesting a destabilization of the liquid crystalline phases. When analyzing the DSC scans for all three triblock copolymers, two transitions occur near the LC clearing point. In the triblock copolymer containing **NB6wBPP4**, however, the temperatures of the two transitions are so close that the peaks merge into one broad transition. The first of the two transitions is likely to be a smectic C* to A transition, whereas the second transition is the clearing point. This is confirmed by small angle X-ray scattering (SAXS) analysis (vida infra).

NBD10wBPP4		
	Heating	Cooling
Monomer	K 56 S_1 81 I	I 79 S_1 19 K
Homopolymer	G_{LC} 20 S_C* 138-149 S_A 150 I	I 148 S_A 147-138 S_C* 20 G_{LC}
Triblock Copolymer	G_{LC} 20 S_C* 140-151 S_A 152 I	I 148 S_A 147-133 S_C* 20 G_{LC}
NB10wBPP4		
Monomer	K 68 S_1 88 I	I 86 S_1 42-33 K
Homopolymer	G_{LC} 20 S_C* 138 S_A 161 I	I 158 S_A 128 S_C* 20 G_{LC}
Triblock Copolymer	G_{LC} 20 S_C* 134-149 S_A 150 I	I 146 S_A145-133 S_C* 20 G_{LC}
NB6wBPP4		
Monomer	K 65 S_1 86 I	I 85 S_1 18 K
Homopolymer	G_{LC} 20 S_C* S_A 118-144 I	I 131 S_A 125 S_C* 20 G_{LC}
Triblock Copolymer	G_{LC} 20 S_C* S_A 128-158 I	I 155-120 S_A S_C* 20 G_{LC}

Table 3.3 Summary of thermal data (°C) for monomers, homo- and triblock co-polymers. K = crystallization, G_{LC} = glass transition temperature, S_C* = smectic C*, S_A = smectic A, I = isotropic.

Further confirmation of the liquid crystal clearing points for the monomers, homopolymers, and triblock copolymers was established by polarized optical microscopy (POM). Birefringence for all samples was observed for the smectic liquid crystal phases, which disappeared as the temperature of the sample was increased above the liquid crystal clearing points. The POM data were in good agreement with the DSC data. Figure 3.12 shows the POM images of poly(**NB6wBPP4**)$_{100}$ and poly(**MTD**)$_{50}$(**NB6wBPP4**)$_{200}$(**MTD**)$_{50}$ before the liquid clearing point temperature is reached.

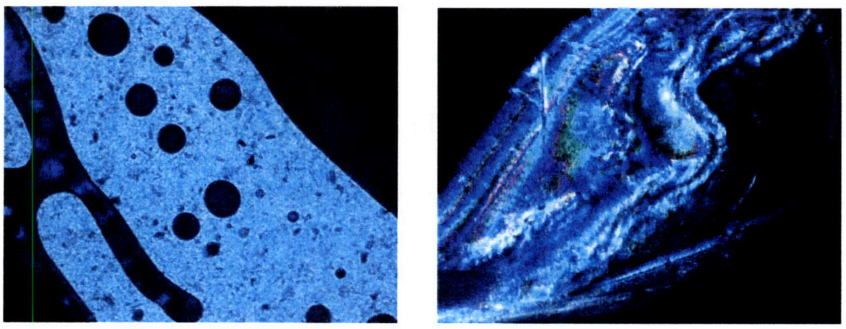

Figure 3.12 POM of poly(**NB6wBPP4**)$_{100}$ (left) and poly(**MTD**)$_{50}$(**NB6wBPP4**)$_{200}$(**MTD**)$_{50}$ (right) before the liquid crystal clearing point.

SAXS studies[53] were performed on the triblock copolymers in order to investigate the morphology of the block copolymers and the liquid crystalline mesophases. All three samples exhibited a scattering peak on the order of 30 – 40 nm, which indicates phase segregation (Figure 3.13). However, higher order peaks are not observed, which suggests that there is no long range order. The high T_g of the **MTD** blocks could provide kinetic limitations for achieving well ordered systems. The triblock copolymer with the **NB6wBPP4** block has a first order scattering peak at 2.9 nm, indicating the presence of smectic monolayers. Considering the calculated molecular length of the mesogen unit attached to the backbone (3.5 nm),[54] it is concluded that the triblock copolymer containing **NB6wBPP4** forms a smectic C* phase with a mesogen tilt angle of approximately 34 ° related to the layer normal. Figure 3.14 illustrates how this angle is calculated.

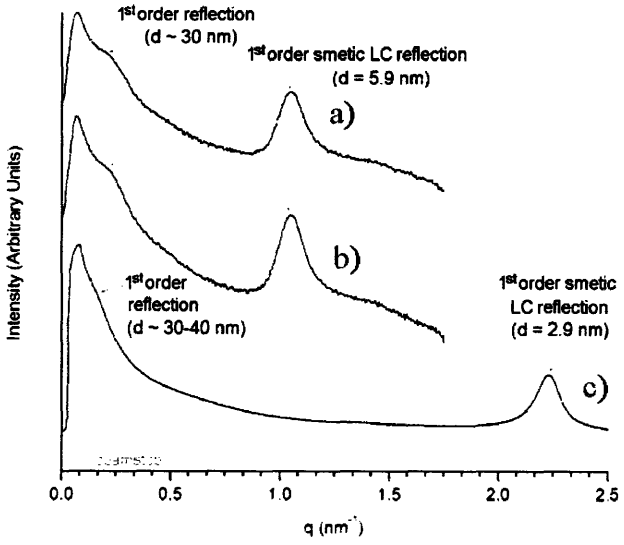

Figure 3.13 SAXS of a) **(MTD)$_{50}$(NBD10wBPP4)$_{200}$(MTD)$_{50}$**
b) **(MTD)$_{50}$(NB10wBPP4)$_{200}$(MTD)$_{50}$** and c) **(MTD)$_{50}$(NB6wBPP4)$_{200}$(MTD)$_{50}$**

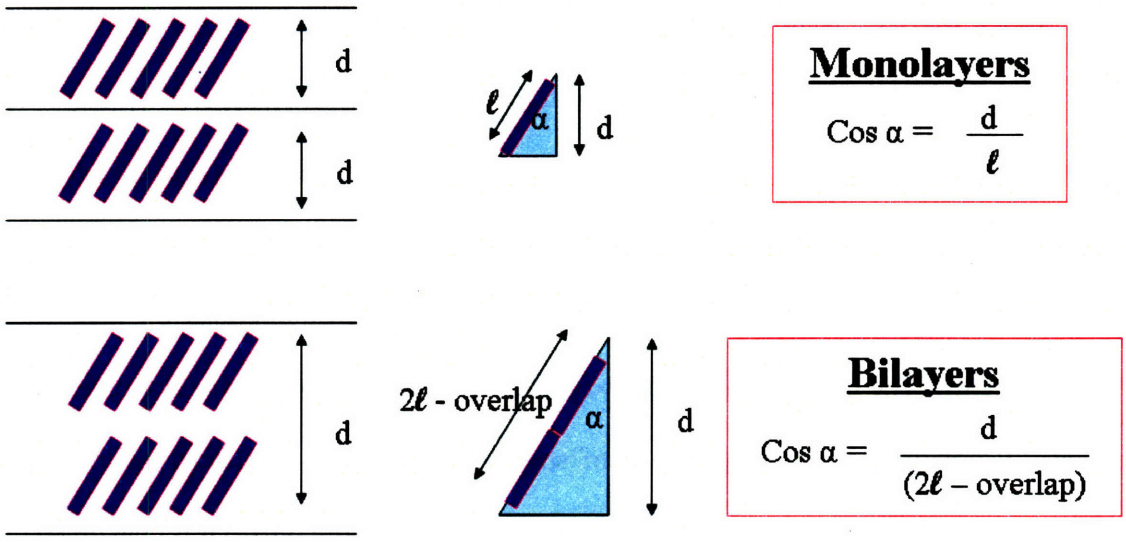

Figure 3.14 Illustration of how the tilt angle for smectic C* monolayers (top) and bilayers (bottom) is calculated.

At room temperature, the triblock copolymers containing **NB10wBPP4** and **NBD10wBPP4** have first order scattering peaks at 5.9 nm, suggesting the presence of smectic C* bilayers. However, when the former was heated to 100 °C, a scattering peak at 3.8 nm was observed, which indicated that a phase transition has occurred from smectic C* bilayers to monolayers. Across a broad range of intermediate temperatures, scattering for both layer spacings are observed indicating that the two phases coexist. The tilt angles for the smectic C* phases are calculated to be ~42° and ~18°, for the bilayer and the monolayer, respectively, by using a calculated molecular length of 4.0 nm.[54] The bilayer angle calculation was completed based on assumption that there was no intercalation of the mesogens. Therefore, the given calculated tilt angle may be greater than the actual value (if intercalation is actually occurring). A similar bilayer to monolayer transition was observed for the triblock copolymer containing the **NBD10wBPP4** mesogen. It is not surprising that the transition from bilayers to monolayers was not observed by DSC and POM for these two triblock copolymers as the transition occurs over a wide temperature range with the two phases coexisting. In addition, the textures of liquid

crystalline polymers in POM had very small domain sizes, inhibiting the ability to observe smectic to smectic transitions. The SAXS data affirms that the two transitions observed by DSC near the LC clearing point are smectic C* to smectic A transitions followed by smectic A to isotropic transitions.

The mechanical properties of the triblock copolymers were investigated by dynamic mechanical analysis (DMA).[53] DMA analysis confirmed the T_g of the LC polymer center block and also revealed the presence of an elastic plateau above the T_g of the LC center block in all of the triblock copolymers. The triblocks containing **NB6wBPP4** displayed an elastic plateau (Figure 3.15-B) above the T_g (Figure 3.15-A) of the LC center block until the onset of the smectic to isotropic transition, where the sample failed. However, in the triblock containing **NB10wBPP4** the elastic plateau is interrupted by a transition near 70 °C (Figure 3.15-C), which is attributed to the smectic C* bilayer to monolayer transition. A similar DMA profile was also observed for the **NBD10wBPP4** containing triblock copolymer, also confirming the bilayer to monolayer transition.

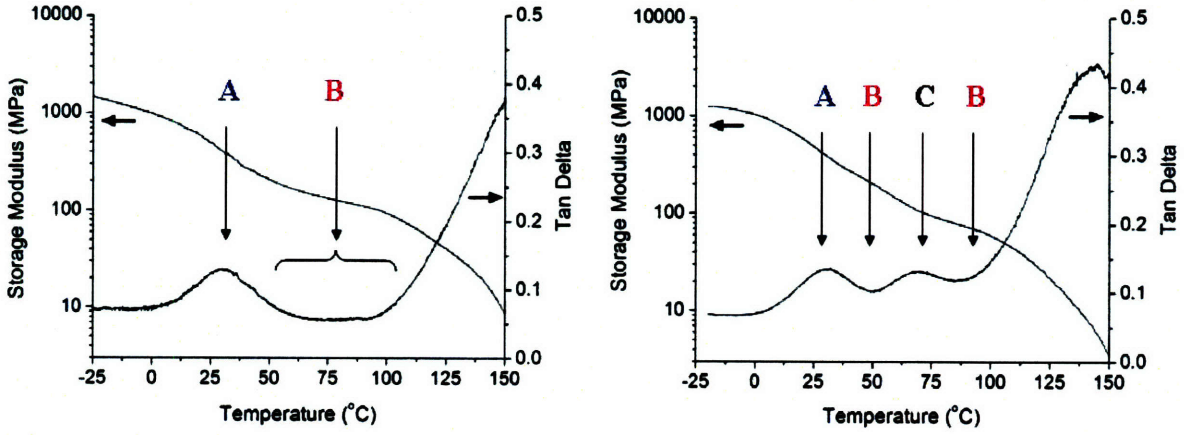

Figure 3.15 DMA of **(MTD)$_{50}$(NB6wBPP4)$_{200}$(MTD)$_{50}$** (left) and **(MTD)$_{50}$(NB10wBPP4)$_{200}$(MTD)$_{50}$** (right). A = T_g, B = elastic plateau, C = bilayer to monolayer transition.

The elastomeric nature of the system is revealed by the presence of the elastic plateau in the DMA profiles and indicates that these materials show potential for use as TPLCE actuators or other smart materials. In future studies, we will focus on systems with a lower T_g for both the inner and outer blocks. The T_g of the outer blocks will be optimized to ease the processability of the polymer as well as allow the system to achieve long-range ordering, while still providing enough rigidity to act as physical crosslinks. The lower T_g of the inner block will enable the system to act as an elastomer at room temperature. Some of the modified monomers synthesized with these desired optimizations in mind are discussed in Appendix A.

3.5 Conclusions

Liquid crystal functionalized monomers, **NB6wBPP4**, **NB10wBPP4** and **NBDw10BPP4**, were synthesized and then polymerized by ROMP in a living manner using the bimetallic molybdenum initiator, $[Mo(NAr)(OR_{F6})_2(=CHC_5H_4)]_2Fe$. A series of triblock copolymers were synthesized, where the outer block was **MTD**. The liquid crystalline polymer inner blocks exhibited T_g values around 20 °C, and the smectic to isotropic transitions were observed around 150 °C. SAXS studies showed that the triblock copolymers containing **NB6wBPP4** form smectic C* monolayers, while those containing **NB10wBPP4** and **NBD10wBPP4** form smectic C* bilayers at room temperature. For the latter two triblock copolymers, a transition was observed at elevated temperatures and two phases were observed: smectic C* bilayers and monolayers. In addition, phase segregation was observed for the triblock copolymer systems, as indicated by the SAXS studies and correspondence of the T_g of the inner blocks to the homopolymer transitions. DMA analysis showed that the triblock copolymers exhibit elastic plateaus. The results of the studies of the triblock copolymers give evidence that with optimization, ABA triblock copolymers synthesized via ROMP have the potential to act as

TPLCEs, actuators or shape-memory materials at elevated or at room temperature. Future studies will focus on developing systems that exhibit T_g values of the central block below operating temperatures (i.e., below room temperature) and increasing phase separation and long range order by altering the composition of the outer block.

3.6 Experimental Procedures

General Procedures. All manipulations were performed in oven-dried (200 °C) glassware under an atmosphere of nitrogen in a Vacuum Atmospheres glovebox or using standard Schlenk techniques. HPLC-grade solvents were purified by passage through an alumina column and stored over 4 Å Linde-type molecular sieves prior to use. Deuterated solvents were degassed and distilled from CaH_2 or sodium benzophenone ketyl. Commercial reagents were used without further purification unless stated otherwise. Norbornene, 1,10-dibromodecane, 1,9-dibromononane, and 1,5-dibromopentane were dried over activated sieves and distilled. Norbornylmethylene bromide[55] and $[Mo(NAr)(OR_{F6})_2(=CHC_5H_4)]_2Fe$ (**6**)[44] were prepared according to literature.

NMR spectra were recorded on a Varian INOVA 500 spectrometer. ^1H NMR chemical shifts are given in ppm versus residual protons in the deuterated solvents as follows: δ 7.27 $CDCl_3$, δ 7.16 C_6D_6, δ 2.5 $(CD_3)_2SO$, δ 2.09 $(CD_3C_6D_5)$. For calculation of polymer compositions the relaxation time, D1, was set to fifteen sec. Some GPC analyses (solvent = methylene chloride, 1 mL/min) were carried out on a system equipped with two Jordi-Gel DVB mixed bed columns (250 mm length × 10 mm inner diameter) in series. A Wyatt Technology mini Dawn light-scattering detector coupled with a Knauer differential refractometer was employed. Other GPC analyses (solvent = tetrahydrofuran, 1mL/min) were carried out using a Waters GPC system equipped with 1 Styragel HT3 column (500 - 30,000 MW range), 1

Styragel HT4 column (5,000 - 600,000 MW range), 1 Styragel HT5 column (50,000 - 4×10^6 MW range), a refractive index detector, and a UV detector (254 nm) was used for molecular weight measurement relative to polystyrene standards. All polymer samples were cast from a concentrated (~10 wt%) toluene solution onto a Teflon coated sheet, then air-dried for ~24 h. A TA Instruments Q1000 was used for Differential Scanning Calorimetry (DSC), the heating and cooling rate was 5 °C min^{-1} in all cases. The optical micrographs were taking using a Zeiss Axioskop2 polarized light microscope with a Zeiss AxioCam HRc digital camera. The samples were heated using a Linkam THMS 600 hot stage at a rate of 5 °C min^{-1}. A TA instruments Q800 was used for Dynamic Mechanical Analysis (DMA). The heating rate was 3 °C min^{-1} and oscillations of amplitude of 25 μm were applied to films in 0.02 MPa of tension at a frequency of 1 Hz. SAXS data were collected with a Siemens 2-D small angle X-ray scattering detector. The X-rays were Cu Kα radiation with a wavelength 0.1542 nm, set at 40 kV and 0.66 mA. Silver behenate was used to calibrate the sample to detector distance with a first order scattering vector of q of 1.076 nm^{-1} (with $q = 4\pi \sin\theta/\lambda$ where 2θ is the scattering angle and λ is the wavelength).

Synthesis of 5-(6-bromo-hexyl)-bicyclo[2.2.1]hept-2-ene. This procedure was adapted from the literature.[56] Magnesium turnings (3.10 g, 0.128 moles) in 100 mL of THF were placed in a three-neck flask equipped with a condenser, nitrogen inlet, and addition funnel containing norbornylmethylene bromide (20 g, 0.106 mol). The norbornene was slowly added to the magnesium over an hour period and the solution was refluxed and stirred overnight. The solution was cooled and transferred via a cannula into an addition funnel that was attached to a Schlenk flask charged with Li_2CuCl_4 (0.1 M in THF, 11 mL) and 1,5-dibromopentane (30 g, 0.130 mol). The reaction mixture was cooled to approximately -20 °C and the solution of the Grignard reagent was added slowly over two hours. The reaction was slowly warmed to room

temperature overnight. Diethyl ether (100 mL) was added to the solution and it was washed with saturated NH_4Cl solution. The aqueous layer was extracted with ether, the organic layers were combined and then washed with brine. The volatile components were removed *in vacuo* and the residue was distilled under reduced pressure; yield of crude oil 10.96 g (41%). This fraction was purified by column chromatography on silica gel using hexanes ($R_f = 0.53$). A total of 6 g (22%) of clean product (colorless oil) was isolated from this first column. A second column was run on the remaining residues; yield 3.86 g (14%; *endo*:*exo* = 80:20): ^{1}H NMR ($CDCl_3$) (all peaks reported are for the *endo* isomer unless otherwise stated) δ 6.10 (1H, m, $HCCH_{endo}$), 6.08 (1H, m, $HCCH_{exo}$), 6.02 (1H, m, $HCCH_{exo}$), 5.91 (1H, m, $HCCH_{endo}$), 3.42 (2H, m, $(CH_2)_5CH_2Br$), 2.78 (1H, s, $CHCHCHCH_{2exo}$), 2.75 (1H, s, $CHCHCHCH_{2endo}$), 2.50 (1H, s, 1H, s, $CHCHCHCH_{2exo}$), 1.97 (1H, m, $(CH_2)_6CH$), 1.8 - 1.1 (12H, m), 0.49 (1H, m, $(CH_2)_5CHCHH$); ^{13}C NMR ($CDCl_3$) δ 137.07, 132.53, 49.73, 45.55, 42.68, 38.87, 34.85, 34.21, 33.02, 32.58, 29.20, 28.63, 28.38.

Synthesis of 5-(10-deca-hexyl)-bicyclo[2.2.1]hept-2-ene. Prepared in a similar manner as described for 5-(6-bromo-hexyl)-bicyclo[2.2.1]hept-2-ene. A total of 6.2 g (37%) of clean product (colorless oil) was isolated from the column; *endo*:*exo* = 80:20: ^{1}H NMR ($CDCl_3$) (all peaks reported are for the *endo* isomer unless otherwise stated) δ 6.10 (1H, m, $HCCH_{endo}$), 6.08 (1H, m, $HCCH_{exo}$), 6.02 (1H, m, $HCCH_{exo}$), 5.91 (1H, m, $HCCH_{endo}$), 3.42 (2H, m, $(CH_2)_5CH_2Br$), 2.78 (1H, s, $CHCHCHCH_{2exo}$), 2.75 (1H, s, $CHCHCHCH_{2endo}$), 2.74 (1H, s, $CHCHCHCH_{2endo}$), 2.50 (1H, s, 1H, s, $CHCHCHCH_{2exo}$), 1.97 (1H, m, $(CH_2)_6CH$), 1.8 - 1.1 (21H, m), 0.48 (1H, m, $(CH_2)_5CHCHH$); ^{13}C NMR ($CDCl_3$) δ 137.04, 132.65, 49.75, 45.59, 42.71, 38.94, 35.01, 34.31, 33.05, 32.63, 30.10, 29.84, 29.75, 29.65, 28.99, 28.67, 28.39.

Synthesis of 2-(10-bromo-decyl)-bicyclo[2.2.1]hepta-2,5-diene. This procedure was adapted from the literature.[57] A three-neck flask equipped with a nitrogen inlet was charged with

potassium *tert*-butoxide (3.9 g, 0.035 mol) and norbornadiene (5 mL, 0.046 mol) in THF (100 mL). The solution was cooled to -78 °C and *n*-butyl lithium (13.6 mL, 2.5 M, 0.035 mol) was added dropwise over one hour, while keeping the temperature below -65 °C. The solution was stirred at -65 °C for thirty minutes and then at -40 °C for thirty minutes. It was then cooled to -78 °C and transferred via a cannula over one hour to a second flask charged with 1,10-dibromodecane (13 mL, 0.058 mol) in THF (100 mL) which was cooled to -65 °C. After the addition was complete, the reaction was stirred at -40 °C for two hours and then at 0 °C for two hours. At this time, the reaction was quenched with saturated NH_4Cl (50 mL) and H_2O (50 mL). The reaction was extracted with ether (3 × 200 mL). The organic layers were combined and washed with water and brine. The organic layer was dried over Mg_2SO_4 and the volatile components were removed by rotovap. The residue was distilled under reduced pressure. The first fraction that was distilled was mostly 1,10-dibromodecane. The second fraction (oil: 200 °C, head: 130 °C, pressure: 300 mTorr) was clean 2-(10-bromo-decyl)-bicyclo[2.2.1]hepta-2,5-diene; yield 2.8 g (26%): ^{1}H NMR ($CDCl_3$) δ 6.76 (2H, m, *H*CC*H*), 6.12 (1H, m, C*H*), 3.50 (1H, s, CHCHC*H*CH_2), 3.42 (2H, t, C*H*$_2$Br), 3.28 (1H, s, CHCHC*H*CH_2), 2.18 (2H, m, CHCC*H*$_2$), 1.96 (2H, s, C*H*$_2$-norbornadiene), 1.86 (2H, m, C*H*$_2$$CH_2O$), 1.41 - 1.25 (14H, m, CH_2(C*H*$_2$)$_7$$CH_2CH_2O$); ^{13}C NMR ($CDCl_3$) δ 159.24, 144.01, 142.59, 133.27, 73.63, 53.66, 50.17, 34.27, 33.01, 31.71, 29.65, 29.62, 29.60, 29.53, 28.94, 28.36, 27.39; HRMS (ESI) Calcd for $C_{17}H_{27}Br$ [M]: 310.1291. Found: 310.1296.

Synthesis of NB6. A three-neck flask equipped with a condenser was charged with KOH (1.5 g), ethanol (195 mL), water (9.7 mL), a few crystals of KI, and 4'-hydroxy-biphenyl-4-carboxylic acid (2.5 g, 0.012 mol). The solution was heated to reflux and 5-(6-bromo-hexyl)-bicyclo[2.2.1]hept-2-ene (6 g, 0.023 mol) was added. The solution was refluxed overnight at

which time a solution of 10% KOH in 70% ethanol was added. The solution became yellow in color and was refluxed for an additional three hours. The compound was cooled to room temperature at which time a dilute solution of HCl was added in order to hydrolyze the secondary ester product. The solid formed was collected and washed with ethanol and water. The white product was insoluble in most organics; yield 4.2 g (92%). The powder was triturated with pentane and dried *in vacuo* overnight. The compound isolated was then further reacted to yield **NB6wBPP4**, therefore confirming the identity of the product.

Synthesis of NB10. Prepared in a similar manner as described for **NB6**; yield 3.4 g (79%): ^{1}H NMR (all peaks reported are for the major isomer (*endo*:*exo* = 80:20) unless otherwise stated) δ 12.92 (1H, s, COO*H*), 7.97 (2H, d, aromatic C*H*), 7.54 (2H, d, aromatic C*H*), 7.67 (2H, d, aromatic C*H*), 7.03 (2H, d, aromatic C*H*), 6.11 (1H, m, *H*CCH$_{endo}$), 6.08 (1H, m, *H*CCH$_{exo}$), 6.02 (1H, m, *H*CCH$_{exo}$), 5.91 (1H, m, HCC*H*$_{endo}$), 4.01 (2H, m, (CH$_2$)$_9$C*H*$_2$O), 2.72 (1H, s, CHCHC*H*CH$_{2exo}$ and $_{endo}$), 1.93, 1.79, (both 1H, m), 1.73, 1.41 (both 2H, m), 1.31 – 10.98 (17 H, m), δ 0.41 (1H, m, C*H*HCH(CH$_2$)$_{10}$); Due to the poor solubility of this compound, ^{13}C NMR data were not collected; HRMS (ESI) Calcd for $C_{30}H_{38}O_3$ [M+]: 446.2815. Found: 446.2819.

Synthesis of NBD10. Prepared in a similar manner as described for **NB6**; yield 1.8 g (84%): ^{1}H NMR (CD$_3$)$_2$SO) δ 12.92 (1H, s, COO*H*), 7.98 (2H, d, aromatic C*H*), 7.78 (2H, d, aromatic C*H*), 7.67 (2H, d, aromatic C*H*), 7.03 (2H, d, aromatic C*H*), 6.73 (2H, m, *H*CC*H*), 6.10 (1H, m, C*H*), 4.00 (2H, t, OC*H*$_2$), 3.45 (1H, s, CHCHC*H*CH$_2$), 3.26 (1H, s, CHCHC*H*CH$_2$), 2.13 (2H, m), 1.86 (2H, m), 1.72 (2H, m), 1.41 - 1.25 (14H, m); Due to the poor solubility of this compound, ^{13}C NMR data were not collected; HRMS (ESI$^-$) Calcd for $C_{30}H_{36}O_3$ [M-H]: 443.2581. Found: 443.2582.

Synthesis of NB6wBPP4. To a round bottom flask was added **NB6** (3.7 g, 9.5 mmol), dimethylaminopyridine (0.12 g, 0.95 mmol), (+)-2-(4-hydroxyphenoxy)propionic acid (2.25 g, 9.5 mmol) and dry methylene chloride (100 mL) under a nitrogen atmosphere. The solution was cooled to 0 °C and dicyclohexylcarbodiimide (4.9 g, 23.7 mmol) in methylene chloride was added and the reaction was stirred overnight and slowly warmed to room temperature. The reaction solution was filtered and the volatile components were removed *in vacuo*. The compound was purified by column chromatography on silica gel using 1:9 ethyl acetate:hexanes. The appropriate fraction (R_f = 0.42) was dried over Mg_2SO_4 and the volatile components were removed *in vacuo* to afford a white powder; yield 3.0 g (52%): ^{1}H NMR (C_6D_6) (all peaks reported are for the major isomer (*endo*:*exo* = 80:20) unless otherwise stated) δ 8.31 (2H, d, aromatic C*H*) , 7.45 (2H, d, aromatic C*H*), 7.37 (2H, d, aromatic C*H*), 7.05 (2H, d, aromatic C*H*), 6.91 (2H, d, aromatic C*H*), 6.86 (2H, d, aromatic C*H*), 6.11 (1H, m, *H*CCH$_{endo}$), 6.04 (1H, m, *H*CCH$_{exo}$), 5.95 (1H, m, HCC*H*$_{endo}$), 4.52 (1H, q, C*H*CH$_3$), 3.93 (2H, m, $(CH_2)_5CH_2O$), 3.71 (3H, m, $OCH_2CH_2CH_2CH_3$), 2.73 (1H, s, CHCHC*H*CH$_{2exo}$ and $_{endo}$), 2.69 (1H, s, CHCHC*H*CH$_{2endo}$), 2.48 (1H, s, CHCHC*H*CH$_{2exo}$), 1.93, 1.78, 1.52, (all 1H, m), 1.68 (2H, m), 1.45 (3H, d, CHC*H*$_3$), 1.41 - 1.00 (13 H, m), 0.73 (t, 3H, $CH_3(CH_2)_3O$), 0.54 (1H, m, C*H*HCH$(CH_2)_5$); ^{13}C NMR (C_6D_6, major isomer only) δ 172.08, 165.46, 160.43, 156.33, 154.06, 146.40, 146.08, 137.55, 132.97, 131.40, 129.1, 128.68, 127.25, 123.47, 116.35, 115.58, 73.68, 68.41, 65.17, 50.32, 46.20, 43.32, 39.51, 35.50, 33.15, 31.10, 30.41, 30.01, 29.38, 26.80, 19.52, 18.97, 14.03; HRMS (ESI) Calcd for $C_{39}H_{46}O_6$ [M+Na]: 633.3186. Found: 633.3164.

Synthesis of NB10wBPP4. Prepared in a similar manner as described for **NB6wBPP4**; yield 1.9 g (43%): ^{1}H NMR [$CDCl_3$, all peaks reported are for the major isomer (*endo*:*exo* = 80:20) unless otherwise stated] δ 8.22 (2H, d, aromatic C*H*), 7.69 (2H, d, aromatic C*H*), 7.60

(2H, d, aromatic C*H*), 7.14 (2H, d, aromatic C*H*), 7.01 (2H, d, aromatic C*H*), 6.93 (2H, d, aromatic C*H*), 6.11 (1H, m, *H*CCH$_{endo}$), 6.08 (1H, m, *H*CCH$_{exo}$), 6.01 (1H, m, *H*CCH$_{exo}$), 5.91 (1H, m, HCC*H*$_{endo}$), 4.75 (1H, q, C*H*CH$_3$), 4.18 (2H, m, (CH$_2$)$_9$C*H*$_2$O), 4.03 (3H, m, OC*H*$_2$CH$_2$CH$_2$CH$_3$), 2.76 (1H, s, CHCHC*H*CH$_{2exo}$ and $_{endo}$), 2.74 (1H, s, CHCHC*H*CH$_{2exo}$), 2.51 (1H, s, CHCHC*H*CH$_{2endo}$), 2.0 - 1.5 (129 H, m), 0.92 (t, 3H, CH$_3$(CH$_2$)$_3$O), 0.49 (1H, m, C*H*HCH(CH$_2$)$_5$); ^{13}C NMR (C$_6$D$_6$, major isomer only) δ 172.06, 165.45, 160.41, 156.32, 146.41, 146.07, 137.51, 132.97, 132.70, 131.38, 129.12, 127.25, 123.45, 116.34, 115.56, 73.38, 68.39, 65.16, 50.31, 46.22, 43.32, 39.59, 39.55, 35.63, 33.16, 31.09, 30.77, 30.51, 30.43, 30.40, 30.18, 29.99, 29.52, 26.80, 19.50, 18.95, 14.01; HRMS (ESI) Calcd for C$_{43}$H$_{54}$O$_6$ [M+Na]: 689.3813. Found: 689.3834.

Synthesis of NBD10wBPP4. Prepared in a similar manner as described for **NB6wBPP4**; yield 1.0 g (44%): ^{1}H NMR (CDCl$_3$) δ 8.22 (2H, d, aromatic C*H*), 7.69 (2H, d, aromatic C*H*), 7.60 (2H, d, aromatic C*H*), 7.14 (2H, d, aromatic C*H*), 7.02 (2H, d, aromatic C*H*), 6.93 (2H, d, aromatic C*H*), 6.76 (2H, m, *H*CC*H*), 6.12 (1H, s, CC*H*), 4.75 (1H, q, CH$_3$C*H*), 4.18 (2H, m, OC*H*$_2$CH$_2$CH$_2$CH$_3$), 3.56 (2H, m OC*H*$_2$(CH$_2$)$_9$), 3.50 (1H, m, CHCHC*H*CH$_2$), 3.28 (1H, m, CHCHC*H*CH$_2$), 2.18, 1.96 (both 2H, m), 1.64 (3H, d, C*H*$_3$CH), 1.63 - 1.2 (18 H, m), 0.92 (3H, t, C*H*$_3$CH$_2$CH$_2$CH$_2$O); ^{13}C NMR (CDCl$_3$) δ 172.35, 165.48, 159.71, 159.22, 155.46, 146.06, 145.28, 143.98, 142.56, 133.26, 132.09, 130.83, 128.53, 127.64, 126.71, 122.75, 116.02, 115.12, 73.61, 73.33, 68.28, 65.33, 53.65, 50.15, 31.70, 30.68, 29.72, 29.70, 29.64, 29.55, 29.54, 29.41, 27.39, 26.21, 19.14, 18.80, 13.81; HRMS (ESI) Calcd for C$_{43}$H$_{52}$O$_6$ [M+Na]: 687.3656. Found: 687.3664.

Example of Homopolymerization: Synthesis of poly(NB6wBPP4)$_{100}$. **6** (5.0 mg, 0.0033 mmol) and **NB6wBPP4** (203 mg, 0.33 mmol, 100 equiv) were weighed into separate

vials and toluene was added to each. The monomer solution was added to the catalyst and stirred rapidly for one hour. At this time, two drops of benzaldehyde were added and the solution was stirred for another hour. The solution was brought out of the box, added to methanol (100 mL) and allowed to sit overnight. The solution was filtered through a pad of Celite on which the precipitate collected. The precipitate was then washed through with tetrahydrofuran and the volatile components were removed to yield poly(**NB6wBPP4**)$_{100}$; yield 169 mg (83%).

Example of Triblock Copolymerization: Synthesis of poly(MTD)$_{50}$(NB6wBPP4)$_{200}$(MTD)$_{50}$. **6** (4.5 mg, 0.00299 mmol) and **NB6wBPP4** (365 mg, 0.598 mmol, 200 equiv) were weighed into separate vials and toluene was added to each. The monomer solution was added to the catalyst and rapidly stirred for one hour. A solution of **MTD** (52 mg, 0.299 mmol, 100 equiv) in toluene was added and the solution stirred for another hour. At this time, a couple drops of benzaldehyde were added and the solution was stirred for another hour. The solution was brought out of the box, added to methanol (100 mL) and allowed to sit overnight. The solution was filtered through a pad of Celite on which the precipitate collected. The precipitate was washed through with tetrahydrofuran and the volatile components were removed to yield poly(**MTD**)$_{50}$(**NB6wBPP4**)$_{200}$(**MTD**)$_{50}$; yield 462 mg (109%). The greater than 100% yield is ascribed to the presence of residual solvent in the polymer.

3.7 References

(1) Grubbs, R. H.; Tumas, W. *Science* **1989**, *243*, 907.

(2) Odian, G. *Principles of Polymerization*. Wiley: New York, **1981**.

(3) Rempp, R.; Merrill, E. W. *Polymer Synthesis*. Huthig and Wepf: New York, **1986**.

(4) Webster, O. W. *Science* **1991**, *251*, 887.

(5) Schrock, R. R. *Acc. Chem. Res.* **1990**, *23*, 158.

(6) Bates, F. S.; Fredrickson, G. H. *Ann. Rev. Phys. Chem.* **1990**, *41*, 525.

(7) Noshay, A.; McGrath, J. E. *Block Copolymers*. Academic Press: New York, **1977**.

(8) Young, R. J.; Lovell, P. A. *Introduction to Polymers 2nd Edition*. CRC Press: Boca Raton, **1991**.

(9) Nair, B. R.; Osbourne, M. A. R.; Hammond, P. T. *Macromolecules* **1998**, *31*, 8749.

(10) Moment, A.; Miranda, R.; Hammond, P. T. *Macromol. Rapid Comm.* **1998**, *19*, (11), 573.

(11) Moment, A.; Hammond, P. T. *Polymer* **2001**, *42*, 6945.

(12) Hiraoka, K.; Stein, P.; Finkelmann, H. *Macromol. Chem. and Phys.* **2004**, *205*, 48.

(13) Lehmann, W.; Hartmann, L.; Kremer, F.; Stein, P.; Finkelmann, H.; Kruth, H.; Diele, S. *J. Appl. Phys.* **1999**, *86*, 1647.

(14) Lehmann, W.; Skupin, H.; Tolksdorf, C.; Gebhard, E.; Zentel, R.; Kruger, P.; Losche, M.; Kremer, F. *Nature* **2001**, *410*, 447.

(15) Naciri, J.; Srinivasan, A.; Jeon, H.; Nikolov, N.; Keller, P.; Ratna, B. R. *Macromolecules* **2003**, *36*, 8499.

(16) Wang, X.-J.; Zhou, Q.-F. *Liquid Crystalline Polymers*. World Scientific Publishing Co.: Singapore, **2004**.

(17) Singh, S. *Liquid Crystals: Fundamentals*. World Scientific Publishing Co.: Singapore, **2002**.

(18) Lagerwall, S. T. *Ferroelectric and Antiferroelectric Liquid Crystals*. Wileg-VCH: Weienheim, **1999**.

(19) Donald, A.; Windle, A.; Hanna, S. *Liquid Crystalline Polymers*. Cambridge University Press: Cambridge, **2006**.

(20) Anthamatten, M.; Zheng, W. Y.; Hammond, P. T. *Macromolecules* **1999**, *32*, 4838.

(21) Fischer, H.; Poser, S.; Arnold, M.; Frank, W. *Macromolecules* **1994**, *27*, 7133.

(22) Hamley, I. W.; Castelletto, V.; Lu, Z. B.; Imrie, C. T.; Itoh, T.; Al-Hussein, M. *Macromolecules* **2004**, *37*, 4798.

(23) Hamley, I. W.; Davidson, P.; Gleeson, A. J. *Polymer* **1999**, *40*, 3599.

(24) Hiraoka, K.; Uematsu, Y.; Stein, P.; Finkelmann, H. *Macromol. Chem. Phys.* **2002**, *203*, 2205.

(25) Osuji, C.; Zhang, Y. M.; Mao, G. P.; Ober, C. K.; Thomas, E. L. *Macromolecules* **1999**, *32*, 7703.

(26) Poser, S.; Fischer, H.; Arnold, M. *J. Poly. Sci. Part A* **1996**, *34*, 1733.

(27) Sentenac, D.; Demirel, A. L.; Lub, J.; de Jeu, W. H. *Macromolecules* **1999**, *32*, 3235.

(28) Yamada, M.; Itoh, T.; Hirao, A.; Nakahama, S.; Watanabe, J. *High Perform. Poly.* **1998**, *10*, 131.

(29) Zheng, W. Y.; Albalak, R. J.; Hammond, P. T. *Macromolecules* **1998**, *31*, 2686.

(30) Clark, N. A.; Lagerwall, S. T. *Appl. Phys. Let.* **1980**, *36*, 899.

(31) Lehmann, W.; Skupin, H.; Tolksdorf, C.; Gebhard, E.; Zentel, R.; Krüger, P.; Lösche, M.; Kremer, F. *Nature* **2001**, *410*, 447.

(32) Pugh, C.; Schrock, R. R. *Macromolecules* **1992**, *25*, 6593.

(33) Komiya, Z.; Pugh, C.; Schrock, R. R. *Macromolecules* **1992**, *25*, 3609.

(34) Komiya, Z.; Pugh, C.; Schrock, R. R. *Macromolecules* **1992**, *25*, 6586.

(35) Komiya, Z.; Schrock, R. R. *Macromolecules* **1993**, *26*, 1387.

(36) Komiya, Z.; Schrock, R. R. *Macromolecules* **1993**, *26*, 1393.

(37) Ungerank, M.; Winkler, B.; Stelzer, F., Side Chain Liquid Crystalline Polymers via ROMP. In *Metathesis Polymerization of Olefins and Polymerization of Alkynes*, Imamoglu, Y., Ed. Kluwer Academic Publishers: The Netherlands, **1998**; pp 225-241.

(38) Trimmel, G.; Riegler, S.; Fuchs, G.; Slugovic, C.; Stelzer, F. *Liquid Crystalline Polymers by Metathesis Polymerization*. Springer: The Netherlands, **2005**, *176*, p 43-88.

(39) Pugh, C.; Kiste, A. L. *Prog. Poly. Sci.* **1997**, *22*, 601.

(40) Mayershofer, M. G.; Nuyken, O.; Buchmeiser, M. R. *Macromolecules* **2006**, *39*, 2452.

(41) Risse, W.; Wheeler, D. R.; Cannizzo, L. F.; Grubbs, R. H. *Macromolecules* **1989**, *22*, 3205.

(42) Weck, M.; Schwab, P.; Grubbs, R. H. *Macromolecules* **1996**, *29*, 1789.

(43) Wu, Z.; Grubbs, R. H. *Macromolecules* **1994**, *27*, 6700.

(44) Schrock, R. R.; Gabert, A. J.; Singh, R.; Hock, A. S. *Organometallics* **2005**, *24*, 5058.

(45) Svensson, M.; Helgee, B.; Skarp, K.; Andersson, G. *J. Mat. Chem.* **1998**, *8*, 353.

(46) Verploegen, E.; McAfee, L. C.; Tian, L.; Verploegen, D.; Hammond, P. T. *Macromolecules* **2007**, *40*, 777.

(47) Helgee, B.; Hjertberg, T.; Skarp, K.; Andersson, G.; Gouda, F. *Liq. Cryst.* **1995**, *18*, 871.

(48) Panarina, O. E.; Panarin, Yu. P.; Antonelli, F.; Vij, J. K.; Reihmann, M.; Galli, G. *J. Mat. Chem.* **2006**, *16*, 842.

(49) Geer, R. E.; Naciri, J.; Ratna, B. R.; Shashidhar, R. *Appl. Phys. Let.* **1996**, *69*, 1405.

(50) Scherowsky, B.; Fichna, U.; Wolff, D. *Liq. Crys.* **1995**, *19*, 621

(51) Sharp, K.; Uto, S.; Myojin, K.; Moritake, H.; Ozaki, M.; Helgee, B.; Yoshino, K. *Japanese J. App. Phys. 1*, **1995**, *34*, 5433.

(52) Naciri, J.; Ratna, B. R.; Baral-Tosh, S.; Keller, P.; Shashidhar, R. *Macromolecules* **1995**, *28*, 5274.

(53) SAXS and DMA analysis was performed by Eric Verploegen.

(54) The molecular lengths were calculated from minimized models of the molecules using Accelrys Materials Studio Molecular Modelling Software.

(55) Dolman, S. J.; Hultzsch, K. C.; Pezet, F.; Teng, X.; Hoveyda, A. H.; Schrock, R. R. *J. Am. Chem. Soc.* **2004**, *126*, 10945.

(56) Stubbs, L., P.; Weck, M. *Chem. Eur. J.* **2003**, *9*, 992.

(57) Yip, C.; Handerson, S.; Tranmer, G., K.; Tam, W. *J. Org. Chem.* **2001**, *66*, 276.

Chapter 4 - Pyrrolide Precursors to Bifunctional Molybdenum Initiators Containing Chiral Diolates

4.1 Introduction

Chapter 2 discussed various bifunctional initiators for the preparation of triblock copolymers by ring opening metathesis polymerization (ROMP).[1] These complexes, namely $[Mo(NAr)(OR)_2(=CHC_5H_4)]_2Fe$ (where Ar = 2,6-diisopropylphenyl; OR = $OCMe_3$ or $OCMe(CF_3)_2$) were found to be living initiators for the preparation of ABA triblock copolymers using various norbornene- and norbornadiene-based monomers. We also recently reported the synthesis of the analogous compounds, $[Mo(NAr)(OR)_2(=CH)]_2(1,4\text{-}C_6H_4)\bullet 2X$ (X = DME or THF), linked by divinylbenzene instead of divinylferrocene. Chapter 3 discussed the preparation of ABA triblock copolymers using the divinylferrocene-linked complexes, where the inner blocks of the triblock copolymers were functionalized by liquid crystal mesogens.[2]

These polymers were synthesized to explore their bulk properties. We wanted to determine whether polymers synthesized by ROMP could function as thermoplastic liquid crystal elastomers (TPLCEs) and ultimately, as room temperature TPLCE actuators or as field-activated shape memory polymers.[2] In order to explore the potential application of such functionalized polymers further, it is important that we control the bulk properties of the polymers. These properties depend to a significant degree on the tacticity of the polymer (e.g., the glass transition temperature).[3,4,5]

The ROMP of various strained cyclic olefins by molybdenum imido alkylidene initiators containing chiral diolates has previously been explored by our group.[4,6,7,8] An advantage of using a molybdenum initiator that contains a chiral ligand for ROMP is the possibility of enantiomorphic site control – "mistakes" made in the polymer synthesis will be corrected instead of propagated.[8] The ratio of *cis*-to-*trans* double bonds in a polymer synthesized using molybdenum ROMP initiators is dependent on the relative reactivity and conversion of the *syn*

and *anti* isomers of the initiator in solution during the polymerization process.[6,8] It is suggested that the tacticity of the polymer depends on the approach of the olefin to the initiator.[8] If the monomer continually approaches the same CNO face of the initiator in each step, an isotactic polymer will form. On the other hand, if the monomer approaches alternating CNO faces sequentially, a syndiotactic polymer will form. Molybdenum initiators that contain chiral diolates have been used for the synthesis of 2,3-dicarbomethoxynorbornadiene (**DCMNBD**) and 2,3-bis(trifluoromethyl)norbornadiene (**NBDF6**) polymers.[4,6,7,8] One molybdenum initiator that contains the chiral biphenolate, 3,3′,5,5′-tetra-*tert*-butyl-1,1′-biphenyl-2,2′-diolate, yielded highly *cis*, isotactic poly(**NBDF6**).[6]

We desired to expand upon the application of the previously developed bifunctional initiators used for the synthesis of ABA triblock copolymers. By replacing the alkoxides groups with various chiral diolates to form complexes of the type $[Mo(NAr)(DIOLATE)(=CHC_5H_4)]_2Fe$ and $[Mo(NAr)(DIOLATE)(=CH)]_2(1,4\text{-}C_6H_4)$ (where DIOLATE = chiral diolate), we hoped to control the microstructure of the polymers synthesized. We were also interested in developing a general route for the preparation of bifunctional initiators. We recently reported bispyrrolide complexes of the type $Mo(NAr)(Pyr)_2(CHCMe_2R)$ (where Pyr = NC_4H_4).[9,10] Pyrrolide precursors are appealing for the *in situ* generation of initiators. The precursors react rapidly with various alcohols and diols to yield two equivalents of pyrrole and the active catalyst of the general type, $Mo(NAr)(OR)_2(CHCMe_2R)$. We planned to take a similar approach to bifunctional molybdenum initiators containing chiral diolates. Therefore, potential catalysts could be prepared and screened quickly. We report here the synthesis of three pyrrolide complexes of the type $[Mo(NAr)(X)_2]_2$(linker) (where X = pyrrolide or 2,5-dimethylpyrrolide, linker = divinylbenzene or divinylferrocene) and the reaction of these complexes with various chiral

diols. We also report the use of these initiators (isolated and prepared *in situ*) for the preparation of homo- and triblock co-polymers of **DCMNBD** and **NBDF6**.

4.2 Synthesis and Characterization of Pyrrolide Metal Complexes

The first complex to be investigated was $[Mo(NAr)(Pyr)_2(=CHC_5H_4)]_2Fe$ (where Pyr = NC_4H_4), the pyrrolide complex of the divinylferrocene-linked initiator. Four equivalents of lithium pyrrolide were added to a cooled solution of $[Mo(NAr)(OR_{F6})_2(=CHC_5H_4)]_2Fe$ (OR_{F6} = $OCMe(CF_3)_2$) in dichloromethane. Initially, the reaction was performed on a small scale and only one alkylidene peak was observed in the ^1H NMR spectrum (C_6D_6) at 14.01 ppm. When this reaction was repeated on a preparative scale, three major alkylidene resonances (14.10, 14.01 and 13.72 ppm) and two minor alkylidene resonances (14.49 and 14.17 ppm) were observed in the ^1H NMR spectrum. Assuming that contamination may have occurred in this second reaction to yield multiple products, the large scale reaction was repeated. The isolated product from the third reaction revealed two major resonances (14.10 and 13.7 ppm) and two minor resonances (14.49 and 14.17 ppm) in the ^1H NMR spectrum (Figure 4.1). Therefore, the material isolated from the second synthetic attempt appeared to be a combination of the products observed in the first and third synthetic attempts. We propose that all the products must have a related chemical structure because when 4 – 10 equivalents of H_2[**Biphen**] (H_2[**Biphen**] = 3,3′-di-*tert*-butyl-5,5',6,6'-tetramethylbiphenyl-2,2'-diol) were added to the above reaction mixtures, identical ^1H NMR spectra were observed. We postulate that two different "ate" complexes were forming; the product with one major alkylidene peak in the ^1H NMR spectrum (14.01 ppm) has one extra equivalent of lithium pyrrolide per molybdenum atom (a "double ate" compound), and the product with two major alkylidene resonances in the ^1H NMR spectra (14.10 and 13.72 ppm) has one extra equivalent of lithium pyrrolide per molecule (an "ate" compound). The structure

of the "ate" complex likely has the extra equivalent of lithium pyrrolide bound to only one molybdenum atom, which would explain the two major alkylidene resonances observed in the ^{1}H NMR.

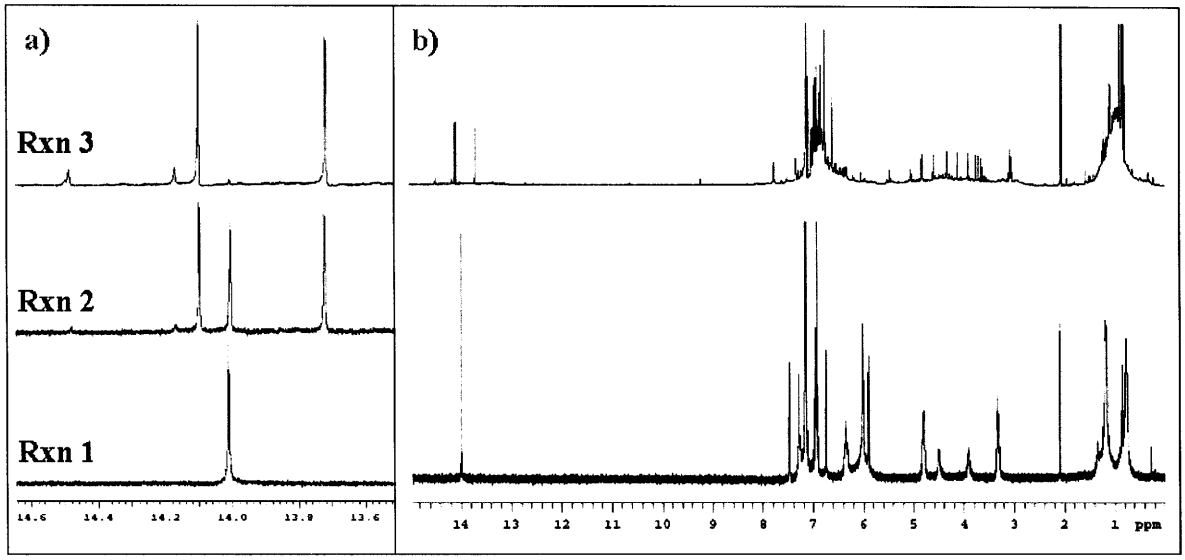

Figure 4.1 a) ^{1}H NMR of the alkylidene region of three separate reaction mixtures of $[Mo(NAr)(OR_{F6})_2(=CHC_5H_4)]_2Fe$ and LiPyr; b) Corresponding full ^{1}H NMR spectra.

The "double ate" complex with one extra equivalent of lithium pyrrolide per molybdenum, $[Mo(NAr)(Pyr)_2(=CHC_5H_4)]_2Fe\bullet 2Li(Pyr)$ (**8**), was cleanly synthesized when six equivalents of lithium pyrrolide were added to a cooled solution of $[Mo(NAr)(OR_{F6})_2(=CHC_5H_4)]_2Fe$ in toluene (Equation 1). The complex was isolated as bright red crystals and a single alkylidene resonance at 14.01 ppm was observed in the ^{1}H NMR spectrum. X-ray quality crystals of **8** were grown from a hot benzene solution that slowly returned to room temperature.

$$\{Mo(NAr)(OR_{F6})_2(=CHC_5H_4)\}_2Fe \xrightarrow[-\,4\ LiOR_{F6}]{6\ LiPyr} \underset{\mathbf{8}}{\{Mo(NAr)(Pyr)_2(=CHC_5H_4)\}_2Fe\bullet 2LiPyr} \qquad (1)$$

The unit cell of **8** is a dimer of the bimetallic compound and contains four molybdenum atoms, four lithium atoms and two iron atoms (Figure 4.2, Table 4.2). A representative drawing of the metal atom core is shown in Figure 4.3. From the two-dimensional view shown, the lithium atoms form the corners of a square and the four molybdenum atoms are located on the four edges of the square. The iron atoms are located in the center of the square, and the molybdenum atoms associated with each ferrocene-linker are on opposite edges of the square. Each lithium atom is coordinated in a variety of fashions to three pyrrolide ligands, two of which are coordinated to one molybdenum atom, and a third pyrrolide ligand which is coordinated to a second molybdenum atom. The alkylidene ligand adopts a *syn* conformation with respect to the imido group, and the Mo-N_{Ar}-C_{ipso} angle is 164.74°. Relevant bond lengths and angles can be found in Table 4.1. The bond lengths and angles are comparable to other crystallographically characterized divinylferrocene-linked complexes of this nature.[1] There are 9.5 crystallographically independent benzene rings within the asymmetric unit. The second half of the half-benzene ring is generated by a crystallographic inversion center. The geometry around the molybdenum center is approximated to be between trigonal bipyramidal and square pyramidal. The cyclopentadiene rings of ferrocene are almost eclipsed. It is also interesting to note that the two substituents on the cyclopentadiene rings are related by a torsion angle of approximately 55°, as opposed to the *ca.* 180° observed in other divinylferrocene-linked structures.[1] We attribute this disparity to the crystal packing of the complex and to the formation of a dimer of bimetallic complexes in the solid state. A related compound, {Mo(NAr)$(Pyr)_2$$(CHCMe_2Ph)$}, was also found to be a dimer in the solid state.[9]

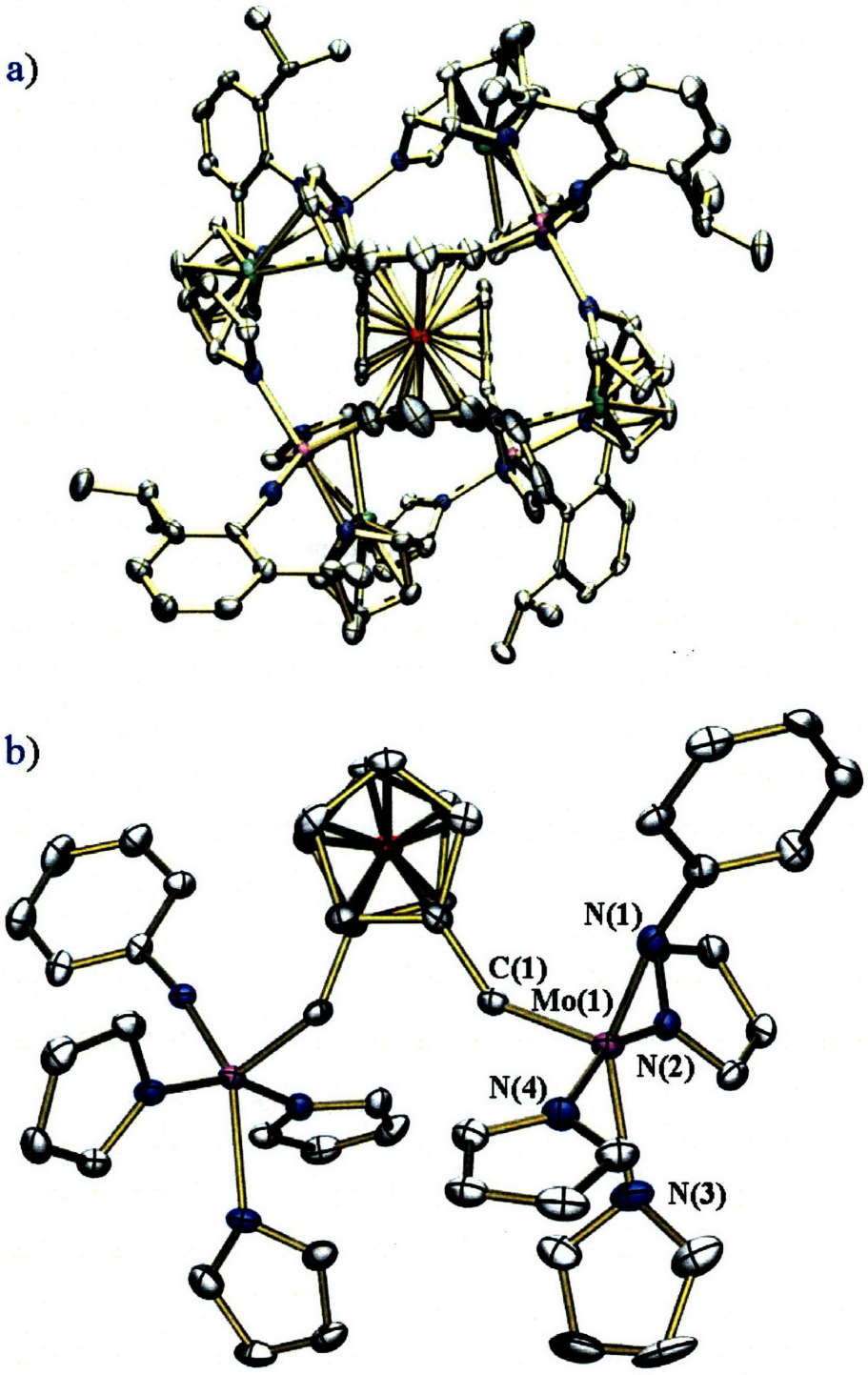

Figure 4.2 Thermal ellipsoid drawing of **8**: a) Full asymmetric unit cell; b) One molecule within the unit cell. Solvent molecules, and hydrogen atoms have been removed for clarity. Isopropyl groups and lithium atoms have also been removed in (b).

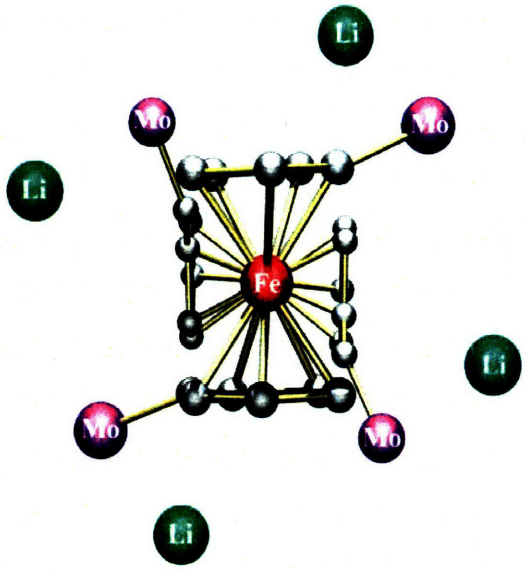

Figure 4.3 Representative drawing of the metal core in the solid state structure of **8**.

Selected Bond Lengths (Å) and Angles (°)	Compound **8**	Compound **9**
Mo(1)-C(1)	1.885(4)	1.9523(17)
Mo(1)- N(1)	1.721(3)	1.7455(17)
Mo(1)- N(2)	2.129(3)	2.0915(14)
Mo(1)- N(3)	2.158(3)	2.4352(15)
Mo(1)- N(4)	2.162(3)	n/a
Mo(1)-C(1)-C(2)	141.3(3)	136.21(13)
Mo(1)-N(1)-C(11)	164.8(3)	178.77(13)

Table 4.1 Selected bond lengths (Å) and angles (°) for **8** and **9**.

Compound	**8**	**9**
Empirical formula	$C_{177}H_{193}Fe_2Li_4Mo_4N_{16}$	$C_{64}H_{86}FeMo_2N_6O$
Formula weight	3067.69	1203.12
Compound ID	07025	07035
Temperature	100(2) K	100(2) K
Wavelength	0.71073 Å	0.71073 Å
Crystal system	Triclinic	Monoclinic
Space group	$P\bar{1}$	P2(1)/n
Unit cell dimensions	a = 14.8816(18) Å b = 15.647(2) Å c = 34.236(4) Å α = 101.630(2)° β = 96.790(2)° γ = 93.384(2)°	a = 10.1779(13) Å b = 28.119(4) Å c = 11.5174(15) Å α = 90° β = 114.802(2)° γ = 90°
Volume	7725.4(17) $Å^3$	2992.1(7) $Å^3$
Z	2	2
Density (calculated)	1.319 Mg/m^3	1.335 Mg/m^3
Absorption coefficient	0.556 mm^{-1}	0.697 mm^{-1}
F(000)	3198	1260
Crystal size	0.10 × 0.06 × 0.04 mm^3	0.15 × 0.10 × 0.04 mm^3
Theta range for data collection	1.58 to 24.71°	1.45 to 29.57°
Index ranges	-17 <= *h* <= 17 -18 <= *k* <= 18 -39 <= *l* <= 40	-14 <= *h* <= 14 -39 <= *k* <= 39 -15 <= *l* <= 15
Reflections collected	95875	57968
Independent reflections	26348 [*R*(int) = 0.1108]	8375 [*R*(int) = 0.0632]
Completeness to theta = 29.57°	99.9%	100.0%
Absorption correction	Semi-empirical from equivalents	Semi-empirical from equivalents
Max. and min. transmission	0.9781 and 0.9465	0.9726 and 0.9026
Data / restraints / parameters	26348 / 9334 / 2133	8375 / 35 / 369
Goodness-of-fit on F^2	1.005	1.028
Final R indices [I>2sigma(I)]	R1 = 0.0517, wR2 = 0.1028	R1 = 0.0292, wR2 = 0.0663
R indices (all data)	R1 = 0.1075, wR2 = 0.1244	R1 = 0.0406, wR2 = 0.0718
Largest diff. peak and hole	1.101 and -0.649 $e.Å^{-3}$	0.560 and -0.562 $e.Å^{-3}$

Table 4.2 Crystal data and structure refinement for **8** and **9**.

The ^{1}H NMR spectrum of **8** at room temperature depicts broad signals associated with the pyrrolide protons. The J_{CH} value for the alkylidene proton is 124 Hz, indicating that in solution, the alkylidene is oriented *syn* to the imido ligand as observed in the solid state. Variable temperature ^{1}H NMR spectroscopic studies ($C_6D_5CD_3$) were also completed for **1**; the spectra are shown in Figure 4.1. Only one alkylidene peak is observed in the temperature interval between -80 °C and 60 °C. The isopropyl groups are rotating freely at elevated temperature as evidenced by only one resonance is observed for the methine (3.26 ppm) and methyl groups (0.92 ppm). At -40 °C, the methine resonances broaden into the baseline. At -80 °C, all four methyl groups (1.46 – 0.55 ppm) and two methine (3.85 and 2.81 ppm) protons are inequivalent indicating locked rotation on the NMR timescale. The part of the spectrum exhibiting the ferrocene resonances undergoes an unusual transition. At low temperature, four resonances are observed (4.93, 4.58, 4.44 and 3.79 ppm). Two of the cyclopentadiene resonances are sharp for the entire temperature range, but the resonances merge into one peak at elevated temperatures due to chemical shift changes. The other two cyclopentadiene resonances are sharp and separated at low temperatures, broaden into the baseline around room temperature, and coalesce into one peak at elevated temperatures. The pyrrolide resonances (7.69 – 5.82 ppm) are sharp and resolved at low temperatures and broaden at high temperatures.

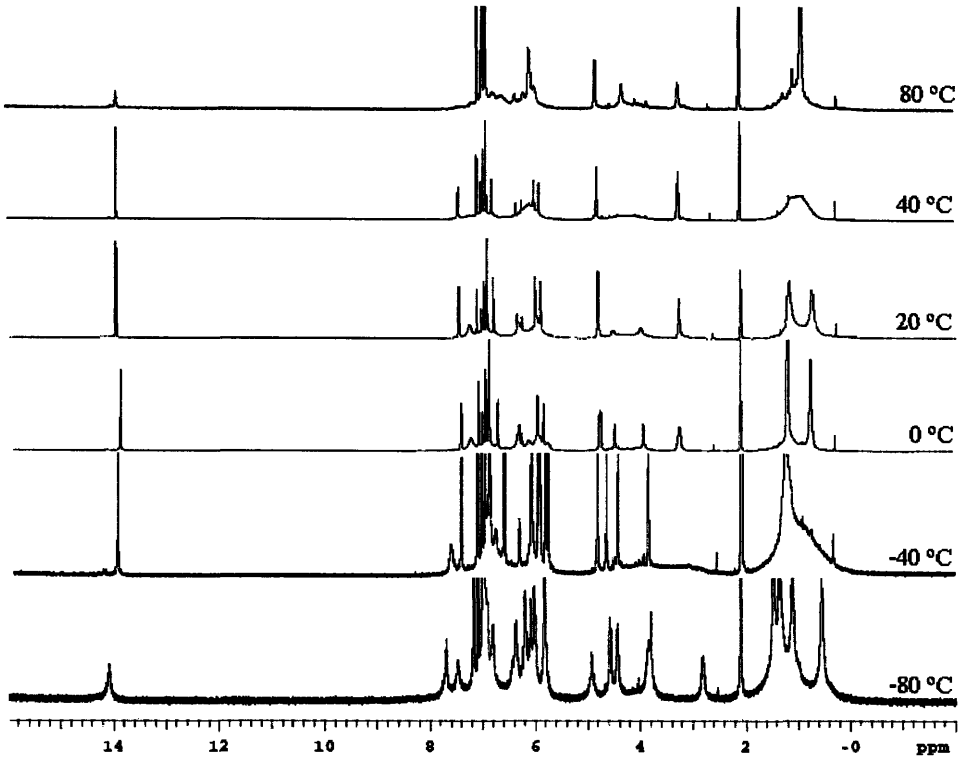

Figure 4.4 Variable temperature ^{1}H NMR spectra of **8**.

We were also interested in synthesizing bimetallic complexes which contain 2,5-dimethylpyrrolide ligands. In recent investigations, such complexes were found to undergo alcoholysis cleanly in many cases.[10] Lithium 2,5-dimethylpyrrolide was added to a cooled solution of $[Mo(NAr)(OR_{F6})_2(=CHC_5H_4)]_2Fe$ in dichloromethane. Four equivalents of lithium 2,5-dimethylpyrrolide are required to form the clean product, $[Mo(NAr)(Me_2Pyr)_2(=CHC_5H_4)]_2Fe$ (**9**, where Me_2Pyr = 2,5-dimethylpyrrolide) (Equation 2). If the reaction mixture is cooled to -35 °C, the lithium hexafluoro-*tert*-butoxide byproduct crystallizes from the solution and is removed from the product by filtration.

$$\{Mo(NAr)(OR_{F6})_2(=CHC_5H_4)\}_2Fe \xrightarrow[-\,4\ LiOR_{F6}]{4\ LiMe_2Pyr} \underset{\mathbf{9}}{\{Mo(NAr)(Me_2Pyr)_2(=CHC_5H_4)\}_2Fe} \qquad (2)$$

X-ray quality crystals of **9** were grown from a cooled diethyl ether solution and the solid state structure is shown in Figure 4.5. The bond lengths and angles are comparable to other crystallographically characterized divinylferrocene-linked complexes of this nature.[1] Relevant bond lengths and angles can be found in Table 4.1. The Mo-N_{Ar}-C_{ipso} bond angle is almost linear at 178.76°, and there is one molecule of diethyl ether in the unit cell. The geometry of the molybdenum center is a piano stool. One of the 2,5-dimethylpyrrolide ligands is η^5 while and the other is η^1. The alkylidene is oriented *syn* with respect to the imido ligand. In this structure, the substituents on the cyclopentadiene rings are related by a torsion angle of 180°. It is interesting to note that **9** is a monomer in the solid state. Another complex containing 2,5-dimethylpyrrolide, {W(NAr)($CHCMe_2Ph$)(Me_2Pyr)$_2$} was also found to be a monomer in the solid state with one η^5 and one η^1 pyrrolide.[11]

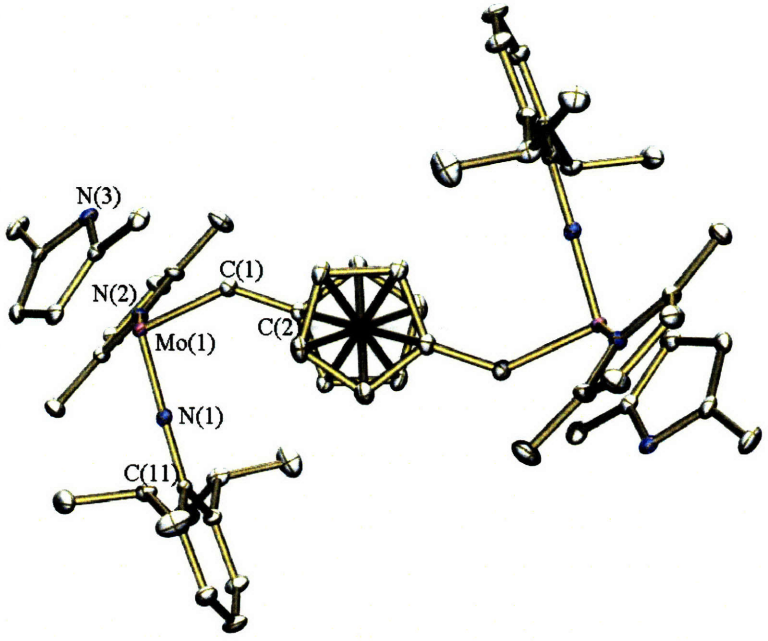

Figure 4.5 Thermal ellipsoid drawing of **9**. Solvent molecules and hydrogen atoms have been removed for clarity.

The alkylidene resonance for compound **9** is at 13.1 ppm in the ^{1}H NMR spectrum (C_6D_6) with J_{CH} of 136 Hz which is approximately half-way between typical *syn* and *anti* coupling constants. Variable temperature ^{1}H NMR studies ($C_6D_5CD_3$) reveal free rotation of the imido aryl groups and rapid interconversion of the η^1- and η^5-bound pyrrolides at high temperature (60 °C) (Figure 4.6). At room temperature, the pyrrolide resonances and the methine and methyl resonances of the arylimido groups are broadened into the baseline. At -30 °C, the spectrum begins to sharpen, and two alkylidene resonances are observed in a 1:0.7 ratio (at 13.01 and 12.94 ppm, respectively). We ascribe these two resonances to the *meso* and the *rac* dimeric forms (as a consequence of chirality at Mo) of the two possible isomers when the interconversion of the η^1- and η^5-bound pyrrolides on the molybdenum is slowed on the NMR timescale. At -60 °C, there are eight ferrocene resonances and four methine resonances.

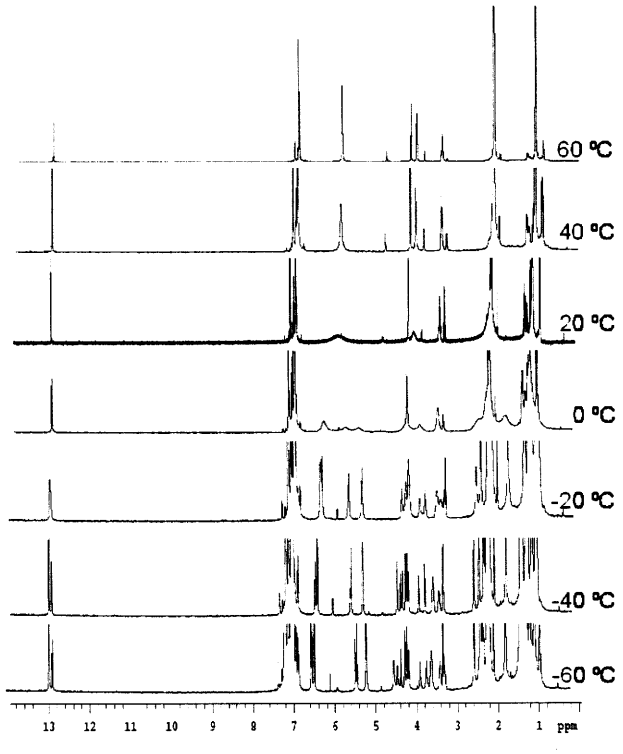

Figure 4.6 Variable temperature ^{1}H NMR spectra of **9**.

Synthesis of the compounds analogous to **8** and **9** linked by divinylbenzene instead of divinylferrocene were also attempted. Various approaches to synthesize $[Mo(NAr)(Pyr)_2(CH)]_2(1,4\text{-}C_6H_4)$, the unsubstituted pyrrolide compound linked by divinylbenzene, were unsuccessful. The addition of four or six equivalents of lithium pyrrolide to $[Mo(NAr)(OR_{F6})_2(CH)]_2(1,4\text{-}C_6H_4)\bullet 2DME$ in different solvents (e.g., toluene, THF, dichloromethane, DME) yielded multiple uncharacterizable compounds.

Reaction of four equivalents of lithium 2,5-dimethylpyrrolide with $[Mo(NAr)(OR_{F6})_2(=CH)]_2(1,4\text{-}C_6H_4)\bullet 2DME$ in cold DME produced $[Mo(NAr)(Me_2Pyr)_2(=CH)]_2(1,4\text{-}C_6H_4)$ (**10**) in good yield (Equation 3). The alkylidene resonance is observed at 13.5 ppm in the ^1H NMR spectrum with J_{CH} of 134 Hz, again, a value between what is typically observed for *syn* and *anti* alkylidenes. Variable temperature ^1H NMR spectroscopic studies reveal behavior similar to the analogous divinylferrocene-linked initiator, **9**. Free rotation of the arylimido group and interconversion of the pyrrolide ligands is observed above room temperature (to 50 °C). At low temperature (-30 °C to -70 °C), two diastereomers are observed in a ratio of approximately 1:0.6.

$$\{Mo(NAr)(OR_{F6})_2(=CH)\}_2(1,4\text{-}C_6H_4)\bullet 2DME \xrightarrow[-\,4\ LiOR_{F6}\ -\,2\ DME]{4\ LiMe_2Pyr} \underset{\mathbf{10}}{\{Mo(NAr)(Me_2Pyr)_2(=CH)\}_2(1,4\text{-}C_6H_4)} \qquad (3)$$

The fact that upon treatment with lithium pyrrolide, the divinylferrocene-linked compound preferentially forms an "ate" complex and the divinylbenzene-linked compound forms no stable complex suggests that the nature of the alkylidene ligand plays an important role in the stability of these molecules. The nature of the alkylidene ligand also plays an important role in the reactivity of the compounds, as will be revealed in the following section which discusses the reactivity of **8**, **9**, and **10** with various diols.

4.3 Reactivity of Bifunctional Molybdenum Pyrrolide Complexes with Enantiomerically Pure Diols

When synthesizing polymers using initiators containing chiral diolates, racemic diolates can be used with little consequence to the bulk properties of the polymers (provided the monomer itself is not chiral).[8] However, when synthesizing a bifunctional initiator containing a chiral diolate, it is important to use enantiomerically pure ligands in order to minimize the number of possible metal complex isomers formed. The complexity that arises when using a racemic diol will be discussed in detail later in this text. All syntheses reported in these studies were completed using enantiomerically pure ligands unless otherwise stated.

Six enantiomerically pure diols were investigated, namely, (R)- and (S)-H_2[**Biphen**],[9,12,13,14,15,16,17,18,19,20,21] (R)-H_2[**TRIPBinol**] ((R)-3,3′-bis(2,4,6-triisopropylphenyl)-1,1′-binaphthyl-2,2′-diol),[12,22,23] (R)-H_2[**PhBinol**] ((R)-3,3′-diphenyl-1,1′-binaphthyl-2,2′-diol),[8,23,24] (R)-H_2[**CF_3Binol**] ((R)-3,3′-bis(3,5-bis(trifluoromethyl)phenyl)-1,1′-binaphthyl-2,2′-diol),[10] (R)-H_2[**$Benz_2$Bitet**] ((R)-3,3′-dibenzhydryl-5,5′,6,6′,7,7′,8,8′-octahydro-1,1′-binaphthyl-2,2′-diol),[16,23,25] and (R)-H_2[**MesBitet**] ((R)-3,3′-dimesityl-5,5′,6,6′,7,7′,8,8′-octahydro-1,1′-binaphthyl-2,2′-diol)[16] (Figure 4.7). These diols were chosen because of the diversity of their steric demand and because their use with molybdenum-based metathesis initiators was previously explored. The reaction of these six ligands with **8**, **9**, and **10** is summarized in Table 4.3 and will be discussed in detail, organized with respect to the diolates.

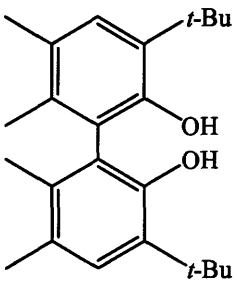

(R)- and (S)-H_2[**Biphen**]

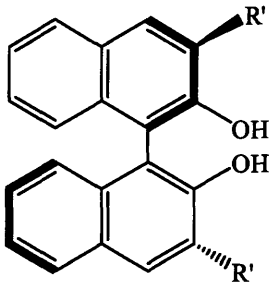

(R)-H_2[**TRIPBinap**], R' = 2,4,6-triisopropylphenyl
(R)-H_2[**PhBinap**], R' = Ph
(R)-H_2[**CF_3Binap**], R' = 3,5-bis(trifluoromethyl)phenyl

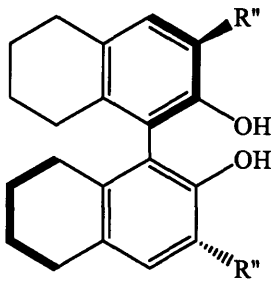

(R)-H_2[**$Benz_2$Bitet**], R" = $CHPh_2$
(R)-H_2[**Mes_2Bitet**], R" = 2,4,6-trimethylphenyl

Figure 4.7 Chiral diols selected to be screened: (R)- and (S)-H_2[**Biphen**], (R)-H_2[**TRIPBinol**], (R)-H_2[**PhBinol**], (R)-H_2[**CF_3Binol**], (R)-H_2[**$Benz_2$Bitet**] and (R)-H_2[**MesBitet**].

Metal Complex → **Ligand ↓**	Compound **8**	Compound **9**	Compound **10**
H_2[**Biphen**]	Three equiv required for clean reaction. Product isolated.	No reaction.	Reaction only in the presence of $LiOR_{F6}$.
H_2[**TRIPBinol**]	Multiple alkylidene peaks.	No reaction.	94% of starting material consumed after 16 hours at 60 °C
H_2[**PhBinol**]	Multiple alkylidene peaks.	Multiple alkylidene peaks.	Clean reaction on small scale. Multiple alkylidene peaks on large scale.
H_2[**CF_3Binol**]	Multiple alkylidene peaks.	Multiple alkylidene peaks.	Multiple alkylidene peaks.
H_2[**$Benz_2$Bitet**]	Incomplete reaction with 2 equiv to form complex of the type [Mo(NAr)(Pyr){Li[**$Benz_2$Bitet**]}$(=CHC_5H_4)]_2Fe$.	Multiple alkylidene peaks.	Clean reaction. Product isolated.
H_2[**MesBitet**]	Clean reaction on small scale. Multiple alkylidene peaks on large scale.	40% of starting material consumed after 12 hours at room temperature.	Clean reaction. Product isolated.

Table 4.3 Summary of reactions of **8**, **9**, and **10** with diols.

H_2[**Biphen**] is a highly sterically demanding ligand due to the presence of the *tert*-butyl group in the 3 and 3′ positions. Three equivalents of H_2[**Biphen**] are required for a clean reaction with **8** to form [Mo(NAr)(**Biphen**)(=CHC_5H_4)]$_2$Fe (**11**) (Equation 4). The third equivalent of H_2[**Biphen**] reacts with the two equivalents of lithium pyrrolide in the "double ate" complex to form Li_2[**Biphen**] and two equivalents of pyrrole.

$$\{Mo(NAr)(Pyr)_2(=CHC_5H_4)\}_2Fe \cdot 2LiPyr \xrightarrow[\text{- 6 PyrH}\\ \text{- } Li_2[\textbf{Biphen}]]{+\ 3\ H_2[\textbf{Biphen}]} \underset{\textbf{11}}{\{Mo(NAr)(\textbf{Biphen})(=CHC_5H_4)\}_2Fe} \qquad (4)$$

^{1}H NMR spectroscopy of **11** reveals four resonances in the alkylidene region at 12.71 ppm (70%, J_{CH} = 152 Hz), 12.55 ppm (14%, J_{CH} = 152 Hz), 11.31 ppm (14%, J_{CH} = 125 Hz) and 11.13 ppm (2%, J_{CH} = 125 Hz). We assign these four alkylidene resonances to the *anti/anti* isomer, the *anti* peak of the *anti/syn* isomer, the *syn* peak of the *anti/syn* isomer, and the *syn/syn* isomer, respectively. All four alkylidene resonances are observed in the ^{13}C NMR spectra (265.23, 264.87, 260.47, 260.05 ppm). As mentioned above, it was important to use enantiomerically pure diols when synthesizing bifunctional compounds. When an enantiomerically pure diol is used in the synthesis of the bifunctional compounds, only one isomer is possible; either (R,R) or (S,S) depending one which diol is used. These two compounds should have identical NMR spectra as the two complexes are enantiomers. To demonstrate this, a solution containing equal amounts of (R,R)-**11** and (S,S)-**11** (synthesized through reaction of **8** with (R)- or (S)-H_2[**Biphen**], respectively) was studied by ^{1}H NMR spectroscopy. The only resonances in the alkylidene region are the four peaks mentioned above (12.71, 12.55, 11.31 and 11.13 ppm). If the synthesis is repeated with (rac)-H_2[**Biphen**], three potential isomers are possible namely, (R,R)-**11**, (S,S)-**11** and (S,R)-**11**. Two sets of peaks should be observed in the alkylidene region of the ^{1}H NMR spectrum: one set associated with the

enantiomers and one set associated with (S,R)-**11**. The alkylidene region of the spectrum ((rac)-**11**) has eight resonances (Figure 4.8), the four previously observed for (R,R)-**11** and (S,S)-**11** and four additional resonances for (S,R)-**11** (12.62, 12.50, 11.37 and 11.25 ppm). Only one alkylidene peak is observed for each of the *anti/anti* (12.62) and *syn/syn* (11.25) rotamers of (S,R)-**11** as the alkylidene protons are related by an inversion center. The added complexity of the spectrum associated with the racemic diol demonstrates why it is important to use enantiomerically pure diols when synthesizing bifunctional compounds.

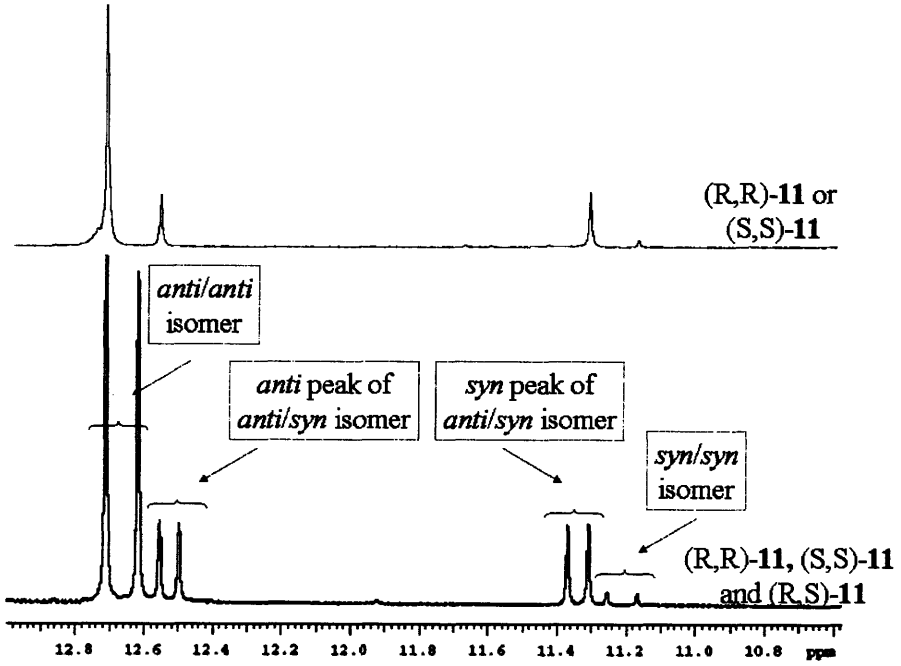

Figure 4.8 Alkylidene region of ^{1}H NMR spectra for (R,R)-**11** or (S,S)-**11** (top) and (R,R)-**11**, (S,S)-**11** and (S,R)-**11** (bottom).

Variable temperature ^{1}H NMR studies of (S,S)-**11** yield no significant changes in the spectra from -60 °C to 60 °C, except for the typical locked rotation of the isopropyl resonances on the NMR timescale at low temperatures and rapid rotation observed at high temperatures. X-ray quality crystals of **11** have remained elusive due to its high solubility in most organic solvents. Attempted crystallization conditions include mixing equal amounts of (R,R)-**11** and

(S,S)-**11** to form a racemic mixture since enantiomerically pure compounds are sometimes difficult to crystallize.

Compound **9** shows no reaction with H_2[**Biphen**], even when the reaction mixture is heated to 60 °C for 16 hours. Interestingly, **10**, the divinylbenzene-linked complex analogous to **9**, reacts with H_2[**Biphen**] to form [Mo(NAr)(**Biphen**)(=CH)]$_2$(1,4-C_6H_4), but only in the presence of lithium hexafluoro-*tert*-butoxide. The dependence of the reaction of **10** with H_2[**Biphen**] on the presence of $LiOR_{F6}$ was discovered when compound **10** was generated *in situ* and then immediately reacted with H_2[**Biphen**] (Equation 5). The reaction mixture therefore contained two equivalents of DME and four equivalents of lithium hexafluoro-*tert*-butoxide per equivalent of **10** formed. When the synthesis was repeated with H_2[**Biphen**] and isolated **10** (i.e., lithium hexafluoro-*tert*-butoxide and DME was not present), no reaction occurred (Equation 6). The cause for the dependence on $LiOR_{F6}$ for the formation of [Mo(NAr)(**Biphen**)(=CH)]$_2$(1,4-C_6H_4) to proceed is unknown.

$$\{Mo(NAr)(OR_{F6})_2(=CH)\}_2(1,4\text{-}C_6H_4)\bullet 2DME \xrightarrow[\text{- 4 Me}_2\text{PyrH}\\ \text{- 2 DME}]{\text{- 4 LiOR}_{F6}} \{Mo(NAr)(\textbf{Biphen})(=CH)\}_2(1,4\text{-}C_6H_4) \quad (5)$$

1) 4 $LiMe_2Pyr$
2) H_2(**Biphen**)

$$\{Mo(NAr)(Me_2Pyr)_2(=CH)\}_2(1,4\text{-}C_6H_4) \xrightarrow{+ 2\ H_2[\textbf{Biphen}]} \text{No Reaction} \quad (6)$$

10

The ^{1}H NMR spectrum (C_6D_6) of [Mo(NAr)(**Biphen**)(=CH)]$_2$(1,4-C_6H_4) revealed four resonances in the alkylidene region at 12.88 (5%), 12,74 (20%, J_{CH} = 149 Hz), 11.22 (20%), and 11.06 ppm (55%, J_{CH} = 127 Hz). We tentatively assign these four alkylidene resonances to the *anti/anti* isomer, the *anti* peak of the *anti/syn* isomer, the *syn* peak of the *anti/syn* isomer, and the *syn/syn* isomer respectively. The ^{1}H NMR data in the alkylidene region for compound **11** and [Mo(NAr)(**Biphen**)(=CH)]$_2$(1,4-C_6H_4) are similar since four alkylidene resonances are observed

in both cases. However, the *anti/anti* isomer is the major isomer present for **11** and the major isomer present for [Mo(NAr)(**Biphen**)(=CH)]$_2$(1,4-C_6H_4) is the *syn/syn* isomer.

The reaction between H_2[**TRIPBinol**] and **8** gives multiple products in a small scale reaction as indicated by the number of alkylidene resonances in the ^{1}H NMR spectrum. Approximately twenty resonances appear in the ^{1}H NMR spectrum between 14 and 9 ppm, and free pyrrole is liberated. The resonances occurring around 9 ppm suggest the imido group has been protonated to form an amido complex. Heating the reaction to 60 °C for twelve hours did not change the ^{1}H NMR spectrum. The presence of multiple peaks in the alkylidene region for this and subsequent reactions could be attributed to numerous factors. As demonstrated above, the spectra are complex for bifunctional initiators because of the large number of possible isomers. The spectra may also be additionally complicated if solvent or other adducts form or if there is incomplete coordination of the diol. Pyrrole has been observed to tautomerize and form pyrrolenine adducts with monofunctional analogs similar to those being studied in this chapter.[26]

There is no reaction observed between **9** and H_2[**TRIPBinol**] even upon heating the sample at 60 °C for 16 hours. Most of the starting material (**10**, 94%) is consumed in the reaction of **10** and H_2[**TRIPBinol**] to form [Mo(NAr)(**TRIPBinol**)(=CH)]$_2$(1,4-C_6H_4) upon heating the sample at 60 °C for 16 hours. Free 2,5-dimethylpyrrole is observed in the ^{1}H NMR spectrum and three new resonances are observed in the alkylidene region at 13.44 ppm (19%, *anti* peak of the *anti/syn* isomer), 10.95 ppm (19%, *syn* peak of the *anti/syn* isomer) and 10.85 ppm (62%, *syn/syn* isomer). However, since this reaction required heat to proceed, it was not investigated further as *in situ* catalysts could not be generated quickly at room temperature.

It was speculated that the size of the substituent on the H_2[**TRIPBinol**] diol might be the cause for the poor reactivity with the pyrrolide complexes. Therefore, a similar ligand with a

smaller substituent on the 3 and 3′ positions, phenyl, was investigated. Unfortunately, the reaction between **8** and H_2[**PhBinol**] yields a similar result as seen in the reaction between H_2[**TRIPBinol**] and **8**. Multiple alkylidene resonances are present in the ^{1}H NMR spectrum between 14 and 11 ppm, and free pyrrole is observed. No resonances are present which would indicate the protonation of the imido nitrogen. A similar result is observed in the reaction between **9** and H_2[**PhBinol**]. Multiple resonances in the alkylidene region and free 2,5-dimethylpyrrole are observed. A small scale reaction between **10** and H_2[**PhBinol**] indicated that this reaction proceeded cleanly as only one major peak at 11.2 ppm is present in the alkylidene region of the ^{1}H NMR spectrum. Unfortunately, numerous attempts to synthesize this compound on a large scale yielded uncharacterizable products. It is possible that the phenyl substituents in the 3 and 3′ positions of the binol ligand do not provide enough steric protection for this complex to be stable.

Another binol ligand with smaller substituents in the 3 and 3′ positions as compared to H_2[**TRIPBinol**] is H_2[**CF_3Binol**], which has 3,5-bis(trifluoromethyl)phenyl substituents on the 3 and 3′ position of the binol backbone. The reactions of **8**, **9**, or **10** with H_2[**CF_3Binol**] yield similar results as are observed in the reaction with H_2[**PhBinol**]. In all cases, multiple resonances are present in the alkylidene region, and free pyrrole, in the case of **8**, or free 2,5-dimethylpyrrolide, in the case of **9** and **10** is liberated. Therefore, this diol was also abandoned due to poor reactivity with the molybdenum pyrrolide complexes.

A small scale reaction between **8** and two equivalents of H_2[**$Benz_2$Bitet**] gave what appeared to be a clean compound by ^{1}H NMR spectroscopy. One major peak is observed in the alkylidene region at 13.37 ppm along with free pyrrole. However, when this reaction was repeated on a larger scale with three equivalents of H_2[**$Benz_2$Bitet**] (an extra equivalent was

added to react with the two equivalents of lithium pyrrolide), the ^{1}H NMR spectrum of the reaction mixture contained numerous resonances in the alkylidene region of the ^{1}H NMR between 13.37 and 10.8 ppm. It is plausible that in the reaction with only two equivalents of diol, a complex of the type [Mo(NAr)(Pyr){Li[**Benz$_2$Bitet**]}(=CHC$_5$H$_4$)]$_2$Fe forms along with two equivalents of pyrrole. It is likely that one equivalent of pyrrolide is still bound to the complex, but this cannot be confirmed because the typical area of resonance for coordinated pyrrolide in the ^{1}H NMR spectrum is obscured by the numerous aryl resonances. The formation of this type of complex (i.e., still an "ate" complex) would explain why the alkylidene peak was shifted downfield compared to what would be expected for [Mo(NAr)[**Benz$_2$Bitet**](=CHC$_5$H$_4$)]$_2$Fe (in the range of 10.5 – 11.5 ppm). The reaction between only two equivalents of H$_2$[**Benz$_2$Bitet**] and **8** was then repeated on a larger scale and the same ^{1}H NMR spectrum was observed as in the first synthesis. The alkylidene proton is observed at 13.37 ppm (86%, *syn/syn* isomer) with two minor resonances at 13.90 ppm and 13.29 ppm (7% each, the *anti* and *syn* resonances of the *anti/syn* isomer, respectively).

The reaction between **9** and H$_2$[**Benz$_2$Bitet**] gave results similar to what was observed with the other diolates and compound **9**. Numerous resonances are present in the ^{1}H NMR spectrum between 10 and 15 ppm along with resonances for free 2,5-dimethylpyrrole.

The reaction between **10** and two equivalents of H$_2$[**Benz$_2$Bitet**] in toluene to form [Mo(NAr)(**Benz$_2$Bitet**)(=CH)]$_2$(1,4-C$_6$H$_4$) (**12**) proceeds cleanly. The product can be isolated and recrystallized in moderate yield as a brown powder. The alkylidene proton in the ^{1}H NMR spectrum is observed at 11.25 ppm and has a J_{CH} value of 125 Hz, consistent with an alkylidene oriented *syn* with respect to the imido group.

Two equivalents of H_2[**MesBitet**] reacts with **8** to give a compound with an alkylidene signal at 10.95 ppm in the ^{1}H NMR spectrum. Unfortunately, multiple attempts to repeat this result on a larger scale have been unsuccessful; multiple peaks are observed in the alkylidene region of the ^{1}H NMR spectra. The reaction between two equivalents H_2[**MesBitet**] and **9** is not facile; only approximately 40% of the starting material had reacted after 12 hours to give new alkylidene resonances around 11 ppm in the ^{1}H NMR spectrum. Therefore, this combination of molybdenum pyrrolide complex and diol was not investigated further.

Two equivalents of H_2[**MesBitet**] react cleanly with **10** to yield [Mo(NAr)(**MesBitet**)(=CH)]$_2$(1,4-C_6H_4) (**13**) in moderate yield. A new alkylidene peak is observed in the ^{1}H NMR spectrum at 11.23 ppm with an associated J_{CH} value of 125 Hz, which is indicative of a *syn* orientation of the alkylidene with respect to the imido group.

The reactivity of compound **8**, **9**, and **10** can be summarized as follows. Compound **8** forms a clean complex when reacted with H_2[**Biphen**] and the product (**11**) can be isolated. When **8** is treated with all other diols, the reactions are either incomplete (H_2[**Benz$_2$Bitet**]), or multiple new alkylidene resonances are observed in the ^{1}H NMR spectra (H_2[**PhBinol**], H_2[**TRIPBinol**], H_2[**CF$_3$Binol**], H_2[**MesBitet**]).

Compound **9** either does not react with the various diolates (H_2[**Biphen**], H_2[**TRIPBinol**]) or there are multiple new resonances in the alkylidene region of the ^{1}H NMR spectra (H_2[**PhBinol**], H_2[**CF$_3$Binol**], H_2[**Benz$_2$Bitet**]), H_2[**MesBitet**]).

The reactions between compound **10** with the examined diols are the most 'well-behaved' of the three molybdenum pyrrolide complexes. Compound **10** reacts cleanly with H_2[**Benz$_2$Bitet**] and H_2[**MesBitet**] to yield isolable complexes, **12** and **13**, respectively. It should be noted that reaction between **10** and H_2[**Biphen**] requires the presence of lithium hexafluoro-

tert-butoxide, the reaction with H_2[**TRIPBinol**] requires heat to proceed, and the reaction with H_2[**CF_3Binol**] or H_2[**PhBinol**] gives multiple inseparable products.

We speculate that compound **8** behaves erratically upon the addition of a diol due to the presence of the two equivalents of lithium pyrrolide per bimetallic molecule. We can compare **9** and **10** directly because they are identical except for the alkylidene substituent. Therefore, the divinylferrocene-linked complex, **9**, seems to react more slowly as compared to the divinylbenzene-linked complex, **10**. After the reactivity of compound **8**, **9**, and **10** with respect to the diols was determined, the polymerization ability of the compounds could be investigated.

4.4 Polymerization of 2,3-Dicarbomethoxynorbornadiene (DCMNBD) and 2,3-Bis(trifluoromethyl)norbornadiene (NBDF6) with *In Situ* Generated and Isolated Bifunctional Initiators Containing Chiral Diolates

Two monomers were chosen to be polymerized, namely, **DCMNBD** and **NBDF6**. These monomers were chosen because polymerization studies with monofunctional molybdenum imido alkylidene initiators containing chiral diolates are known.[6,7,8] The *cis*-to-*trans* ratio as well as the percent tacticity of the polymers can be determined by examining the ^{13}C NMR spectra.[27] Three initiators were investigated, namely, **11**, **12**, and **13**. These initiators were chosen because they can be isolated as well as cleanly generated *in situ*. The two monomers were polymerized with these three initiators, using both the prepared *in situ* and the isolated complexes.

The synthesis of the polymers prepared with the isolated initiators is straightforward. To a stirred solution of either **11**, **12**, or **13** in toluene, a solution of either **DCMNBD** of **NBDF6** was added in one portion. To prepare the corresponding *in situ* initiators, 2.2 equivalents of H_2[**Biphen**], H_2[**$Benz_2$Bitet**] or H_2[**MesBitet**] were added to a solution of **8** or **10** (for the latter two diols), respectively. The diol and pyrrolide complex were stirred at room temperature for

fifteen minutes, at which time a solution of either **DCMNBD** or **NBDF6** (approximately 100 equivalents) was added. All of the polymerization reactions were stirred at room temperature for four hours, at which time the polymerization was quenched with excess benzaldehyde (see Experimental Procedures section for details). Poly(**DCMNBD**) was precipitated from methanol while poly(**NBDF6**) was precipitated from pentane.

The *cis*-to-*trans* ratio and the percent tacticity of the polymers were determined by ^{13}C NMR spectroscopy; the values are given in Table 4.4. Polymers prepared using initiator **11** show a varied ratio of *cis*-to-*trans* double bonds, and the tacticity observed is moderate. The fact that multiple isomers are observed in the ^{1}H NMR spectrum of **11** (recall 70% *anti/anti*, 28% *anti/syn*, and 2% *syn/syn*) may explain the observation of both *cis* and *trans* double bonds in the polymer since the *syn* and *anti* isomers play a major role in the determining whether polymers prepared from norbornene or norbornadienes contain *cis* or *trans* double bonds.[6,8] It is interesting to note that the poly(**NBDF6**) prepared with either the *in situ* generated or the isolated initiator **11** gives identical results. Poly(**DCMNBD**) prepared with **11** gives different results depending on whether the initiator is isolated or prepared *in situ*. In both cases however, the tacticity is lower than desired. The lower tacticity of poly(**DCMNBD**) prepared with initiator **11** is likely the reason that these were the only polymers that were soluble in THF, and therefore the only polymers that we had the ability to analyze by gel permeation chromatography (GPC). The GPC scans of poly(**DCMNBD**) prepared with the *in situ* generated and isolated initiator **11** gave M_n values of 1.3×10^4 and 1.8×10^4 (vs. polystyrene standards) and PDI values of 1.22 and 1.25, respectively.

The polymers prepared using initiator **12**, either isolated or prepared *in situ*, gave identical results for both poly(**DCBNBD**) and poly(**NBDF6**). The polymers contain 100% *cis* double bonds and are greater than 95% tactic.

Similar results were observed for polymers prepared using either isolated or *in situ* prepared initiator **13**. Poly(**NBDF6**) prepared with isolated or *in situ* generated **13** gave similar results and the polymers contained contain approximately 80% *cis* double bonds, and are all highly tactic. Different results were observed in the preparation of poly(**DCMNBD**) depending on the method of catalyst preparation. The isolated initiator gave similar result as compared to poly(**NBDF6**) while the *in situ* generated catalyst gave all *cis*, highly tactic poly(**DCMNBD**).

Ligand	Metal Complex	Isolated or *In Situ*	Monomer	*Trans*:*Cis*	% Tacticity	Isolated Yield
H_2[**Biphen**]	**8**	Isolated (**11**)	**NBDF6**	84:16	79%	> 95%
		In Situ	**NBDF6**	83:17	79%	> 95%
		Isolated (**11**)	**DCMNBD**	42:58	45%	90%
		In Situ	**DCMNBD**	29:71	65%	75%
	14	*In Situ*	**DCMNBD**	n/a[a]	n/a[a]	> 95%
H_2[**Benz$_2$Bitet**]	**10**	Isolated (**12**)	**NBDF6**	0:100	> 95%	> 95%
		In Situ	**NBDF6**	0:100	> 95%	> 95%
		Isolated (**12**)	**DCMNBD**	0:100	> 95%	> 95%
		In Situ	**DCMNBD**	0:100	> 95%	> 95%
	14	*In Situ*	**DCMNBD**	0:100	> 95%	> 95%
H_2[**MesBitet**]	**10**	Isolated (**13**)	**NBDF6**	16:84	74%	84%
		In Situ	**NBDF6**	16:84	74%	> 95%
		Isolated (**13**)	**DCMNBD**	14:86	82%	> 95%
		In Situ	**DCMNBD**	0:100	> 95%	> 95%
	14	*In Situ*	**DCMNBD**	0:100	> 95%	> 95%

Table 4.4 Polymer data for polymerization of **DCMNBD** and **NBDF6** prepared using various initiators which were isolated or generated *in situ*. [a]The lack of stereoregularity of this polymer made it impossible to determine these values.

We also wanted to show that monofunctional and bifunctional initiators containing certain diols gave similar polymerization results. To demonstrate this, monofunctional initiators were synthesized *in situ* from Mo(NAr)(Pyr)$_2$(CHCMe$_2$Ph) (**14**) and H$_2$[**Biphen**], H$_2$[**Benz$_2$Bitet**] or H$_2$[**MesBitet**]. The initiators were stirred at room temperature for fifteen minutes before the addition of 100 equivalents of **DCMNBD**. The polymerizations were quenched with benzaldehyde and the polymers were precipitated from methanol. The results of the polymerization are given in Table 4.4. As shown by these results, the microstructure of the polymers synthesized is identical for the bifunctional and monofunctional initiators prepared *in situ* containing [**Benz$_2$Bitet**]$^{2-}$ or [**MesBitet**]$^{2-}$. The initiator containing [**Biphen**]$^{2-}$ gave a different result depending on the method of preparation; the difference may be attributed to the presence of the extra two equivalents of lithium pyrrolide in the bifunctional initiator prepared *in situ*.

Triblock copolymers of the type poly(**DCMNBD**)$_{50}$(**NBDF6**)$_{100}$(**DCMNBD**)$_{50}$ and poly(**NBDF6**)$_{50}$(**DCMNBD**)$_{100}$(**NBDF6**)$_{50}$ were prepared using *in situ* generated **12**. Initiator **12** was chosen for the synthesis of these polymers because it was found to give highly tactic and highly *cis* homopolymers of both poly(**DCBNBD**) and poly(**NBDF6**). The two triblock copolymers were synthesized to show that the tacticity of the polymer structure can be controlled in a triblock copolymers. Unfortunately, these polymers were insoluble in all common organic NMR solvents (CD_2Cl_2, $CDCl_3$, d_8-THF, d_8-toluene, d_6-acetone, d_6-DMSO) and therefore, the polymers could not be analyzed by ^{1}H and ^{13}C NMR spectroscopy. The low solubility of these polymers is likely due to highly tactic microstructures.

Triblock copolymers of the type poly(**DCMNBD**)$_{33}$(**MTD**)$_{56}$(**DCMNBD**)$_{33}$ (**MTD** = methyltetracyclododecene) and poly(**MTD**)$_{33}$(**DCMNBD**)$_{56}$(**MTD**)$_{33}$ were prepared using *in situ*

generated **12**. These polymers were soluble in $CDCl_3$ and could be analyzed by ^1H and ^{13}C NMR spectroscopy. Due to the overlapping of the **MTD** and **DCMNBD** peaks, the tacticity and the *cis*-to-*trans* ratio could not be determined quantitatively, but the ^{13}C spectra could be analyzed qualitatively. ^{13}C NMR spectra of poly(**DCMNBD**)$_{100}$, poly(**MTD**)$_{100}$ and poly(**DCMNBD**)$_{33}$(**MTD**)$_{56}$(**DCMNBD**)$_{33}$ are shown in Figure 4.9. The spectrum for poly(**MTD**)$_{33}$(**DCMNBD**)$_{56}$(**MTD**)$_{33}$ is not shown but is identical to that shown for poly(**DCMNBD**)$_{33}$(**MTD**)$_{56}$(**DCMNBD**)$_{33}$. The NMR spectra show that the peaks associated with poly(**DCMNBD**) (marked with X's in Figure 4.9) are sharp in the spectra of the triblock copolymer. This suggests that the **DCMNBD** block is highly tactic and highly *cis*, as observed in the homopolymer.

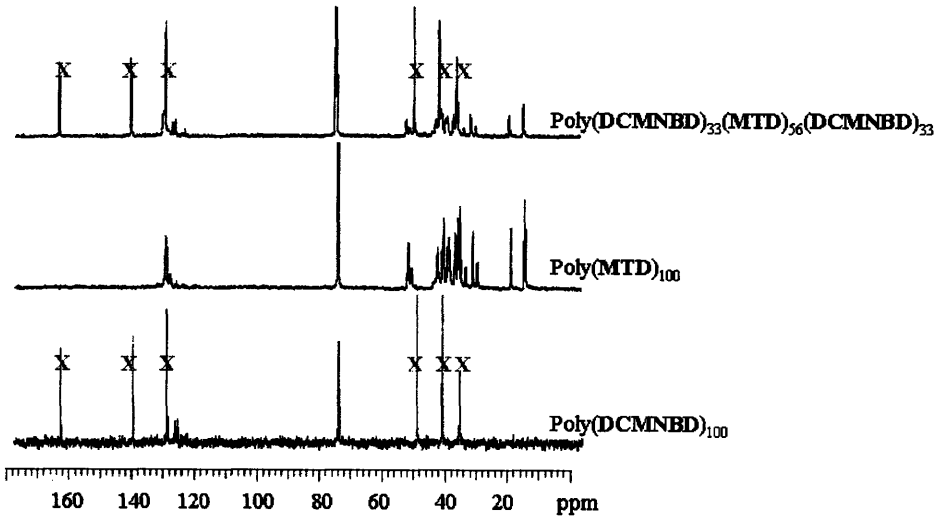

Figure 4.9 ^{13}C NMR spectra for polymers synthesized using *in situ* generated **12**. Poly(**DCMNBD**)$_{100}$ (bottom), poly(**MTD**)$_{100}$ (middle), and poly(**DCMNBD**)$_{33}$(**MTD**)$_{56}$(**DCMNBD**)$_{33}$ (top).

4.5 Bis(alkoxide) Bis(2,5-dimethylpyrrolide) Bifunctional Complexes

Recently, it was discovered that monoalkyl, mono(2,5-dimethylpyrrolide) molybdenum imido alkylidene complexes can be synthesized by alcoholysis of the corresponding bis(2,5-

dimethylpyrrolide) complexes.[28] These monoalkyl, mono(2,5-dimethylpyrrolide) complexes have given rise to reactivities with olefin substrates that have not been previously seen for molybdenum metathesis catalysts. We wanted to briefly explore this type of chemistry with the bifunctional (2,5-dimethylpyrrolide) complexes, **9** and **10**. Eight alcohols (Figure 4.10 A-H) were investigated for the synthesis of bifunctional monopyrrolide, monoalkoxide molybdenum imido alkylidene initiators. The synthetic route for the synthesis of these complexes is outlined in Scheme 4.1. Two equivalents of alcohol were added to a stirred solution of **9** or **10**. The results of these reactions are tabulated in Table 4.5.

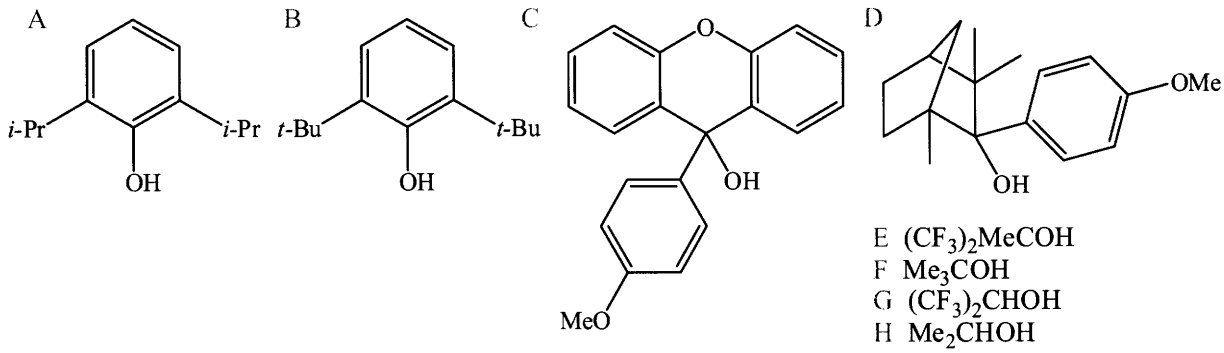

Figure 4.10 Alcohols screened for the synthesis $\{Mo(NAr)(Me_2Pyr)(OR)\}_2$linker complexes.

$$\underset{\textbf{(9)}}{\{Mo(NAr)(Me_2Pyr)_2(=CHC_5H_4)\}_2Fe} \xrightarrow[-\,2\ Me_2PyrH]{+\,2\ ROH} \{Mo(NAr)(Me_2Pyr)(OR)(=CHC_5H_4)\}_2Fe$$

$$\underset{\textbf{(10)}}{\{Mo(NAr)(Me_2Pyr)_2(=CH)\}_2(1,4\text{-}C_6H_4)} \xrightarrow[-\,2\ Me_2PyrH]{+\,2\ ROH} \{Mo(NAr)(OR)(Me_2Pyr)(=CH)\}_2(1,4\text{-}C_6H_4)$$

Scheme 4.1 Synthetic route to $\{Mo(NAr)(Me_2Pyr)(OR)\}_2$linker.

Metal Complex	9	10
Alcohol A	A mixture of starting material, mono- and di-substituted products is observed.	A mixture of starting material, mono- and di-substituted products is observed.
Alcohol B	No reaction.	No reaction.
Alcohol C	No reaction.	No reaction.
Alcohol D	1 major and 1 minor alkylidene peak.	The materials reacted but no alkylidene resonances were observed in ^{1}H NMR spectrum.
Alcohol E	A mixture of starting material, mono- and di-substituted products is observed.	A mixture of starting material, mono- and di-substituted products is observed.
Alcohol F	No reaction.	No reaction.
Alcohol G	A mixture of starting material, mono- and di-substituted products is observed.	A mixture of starting material, mono- and di-substituted products is observed.
Alcohol H	A mixture of starting material, mono- and di-substituted products is observed.	A mixture of starting material, mono- and di-substituted products is observed.

Table 4.5 Summary of the results for the reactions between **9** and **10** and the selected alcohols. The alcohols employed are pictured in Figure 4.10.

Alcohol A was chosen to be investigated first as this alcohol was studied with the monofunctional catalyst and was found to react cleanly with Mo(NAr)(Me_2Pyr)$_2$(CHCMe_2Ph) to form Mo(NAr)(Me_2Pyr)(2,6-*i*PrC_6H_3O)(CHCMe_2Ph); the protonation of the second pyrrolide ligand is slower as compared to the first. When two equivalents of alcohol A are added to a solution of either **9** or **10**, a mixture of starting material, mono-substituted and di-substituted products was observed by ^{1}H NMR spectroscopy. The chemical shift of the di-substituted complexes (for both the DVF- and DVB-linked species) was confirmed by addition of two more equivalents of alcohol A, upon which only one resonance became prominent in the alkylidene region of the respective ^{1}H NMR spectra.

Alcohols B, C, and D were investigated because they are bulkier than alcohol A and may only allow one equivalent to bind to each molybdenum center. No reaction occurred between alcohol B or C and **9** or **10**. Alcohol D reacts with **10** to give an unknown product; no alkylidene peaks were observed in the ^{1}H NMR spectrum. One major and one minor resonance (~11 ppm for both) were observed in the alkylidene region of the ^{1}H NMR spectrum for the reaction between **9** and alcohol D.

We also wanted to investigate alcohols which were smaller in size and more commonly found in molybdenum metathesis compounds. When two equivalents of alcohol E, G or H were added to a solution of either **9** or **10**, mixtures of starting material, mono-substituted and di-substituted products are observed by ^{1}H NMR spectroscopy. Alcohol F showed no reaction when mixed with **10** or **9**; this is probably because the pK_a of 2,5-dimethylpyrrole is similar to that for *tert*-butanol.

We were unable to cleanly synthesize a bifunctional monopyrrolide, monoalkoxide molybdenum imido alkylidene using alcohols A-H. It is probable that such a complex could be isolated if an alcohol with the ideal steric and pK_a requirements is found.

4.6 Conclusions

A series of pyrrolide bifunctional molybdenum complexes linked by either divinylferrocene or divinylbenzene were prepared. The reactivities of the prepared complexes, $[Mo(NAr)(X)_2]_2$(linker) (where X = pyrrolide or 2,5-dimethylpyrrolide, linker = divinylbenzene or divinylferrocene) with various diols were determined. Six diols were screened with the three pyrrolide complexes, **8**, **9**, and **10**, and three new bifunctional initiators were prepared and isolated, namely, **11**, **12**, and **13**. Complexes **11**, **12**, and **13** were used for the polymerization of

DCMNBD and **NBDF6**, and the percent tacticity and *cis*:*trans* ratios of the polymers were determined.

We have demonstrated that initiators can be prepared *in situ* and used for the preparation of block copolymers. However, the method to prepare bifunctional initiators by addition of a chiral diol to a pyrrolide precursors cannot be viewed as a general route. It is important to first screen the diol and the pyrrolide precursor to determine whether the reaction is facile, complete, and/or well-behaved. The initiators that formed completely and cleanly can be used for the preparation of tactic triblock copolymers.

4.7 Experimental Procedures

General Procedures. All manipulations were performed in oven-dried (200 °C) glassware under an atmosphere of nitrogen in a Vacuum Atmospheres glovebox or using standard Schlenk techniques. HPLC-grade solvents were purified by passage through an alumina column and stored over 4 Å Linde-type molecular sieves prior to use. Deuterated solvents were degassed and distilled from CaH_2 or sodium benzophenone ketyl. Commercial reagents were used without further purification unless stated otherwise. $\{Mo(NAr)(OR_{F6})_2[=CHC_5H_4]\}_2Fe$,[1] $[Mo(NAr)(OR_{F6})_2(=CH)]_2(1,4\text{-}C_6H_4)\bullet 2DME$,[1] $Mo(NAr)(Pyr)_2(CHCMe_2Ph)$ (**14**),[9] (R)- and (S)-H_2[**Biphen**],[18] (R)-H_2[**TRIPBinol**],[29] (R)-H_2[**PhBinol**],[8] (R)-H_2[**CF_3Binol**],[10] (R)-H_2[**$Benz_2$Bitet**],[16] and (R)-H_2[**MesBitet**][16] were prepared according to literature procedures.

NMR spectra were recorded on a Varian INOVA 500 spectrometer. ^1H NMR chemical shifts are given in ppm versus residual protons in the deuterated solvents as follows: δ 7.27 ppm ($CDCl_3$), δ 7.16 ppm (C_6D_6), δ 2.09 ppm ($C_6D_5CD_3$), δ 2.05 ($(CD_3)_2CO$). GPC analyses (solvent = tetrahydrofuran, 1 mL/min) were carried out using a Waters GPC system equipped with 1 Styragel HT3 column (500 - 30,000 MW range), 1 Styragel HT4 column (5,000 - 600,000 MW

range), 1 Styragel HT5 column (50,000 – 4 × 10^6 MW range), a refractive index detector, and a UV detector (254 nm) was used for molecular weight measurement relative to polystyrene standards.

Synthesis of [Mo(NAr)(Pyr)$_2$(=CHC$_5$H$_4$)]$_2$Fe•2Li(Pyr) (8). Solid Li(NC$_4$H$_4$) (0.51 g, 6.9 mmol) was added to a -30 °C solution of [Mo(NAr)(OR$_{F6}$)$_2$(=CHC$_5$H$_4$)]$_2$Fe (1.7 g, 1.2 mmol) in CH_2Cl_2 (10 mL). The solution was stirred at room temperature for two hours during which time a bright red precipitate formed. The precipitate was isolated by filtration and dried *in vacuo*; yield 1.3 g (97%): ^{1}H NMR (C_6D_6) δ 14.01 (s, 1H, MoC*H*R, J_{CH} = 124 Hz), 7.49 (m, 1H, py-C*H*), 7.31 (m, 2H, py-C*H*), 7.12 (m, 3H, Ar-C*H*), 6.76 (br s, 1H, py-C*H*), 6.37 (br s, 2H, py-C*H*), 6.03 (br s, 4H, py-C*H*), 5.92 (br s, 2H, py-C*H*), 4.82 (br s, 2H, FeC$_4$*H*$_5$), 4.52 (br s, 1H, FeC$_4$*H*$_5$), 3.94 (br s, 1H, FeC$_4$*H*$_5$), 3.48 (sept, 2H, C*H*(CH$_3$)$_2$), 1.91 (br s, 6H, CH(C*H*$_3$)$_2$), 0.79 (br s, 6H, CH(C*H*$_3$)$_2$); ^{13}C NMR ($C_6D_5CD_3$) δ 283.07, 151.73. 126.89, 109.11, 108.81, 106.45, 94.45, 73.63, 71.78, 70.27, 30.72, 28.42, 23.19, 22.31; There were no resonances in the ^{19}F NMR spectrum. Anal. Calcd for $C_{60}H_{68}FeLi_2Mo_2N_8$: C, 61.97; H, 5.89; N, 9.64. Found: C, 48.42, 49,20, 57.83; H, 5.53, 5.66, 5.61; N, 5.58, 4.42, 9.17.

Synthesis of [Mo(NAr)(Me$_2$Pyr)$_2$(=CHC$_5$H$_4$)]$_2$Fe (9). Solid Li(NC$_4$H$_2$Me$_2$) (0.14 g, 1.4 mmol) was added to a -30 °C solution of [Mo(NAr)(OR$_{F6}$)$_2$(=CHC$_5$H$_4$)]$_2$Fe (0.50 g, 0.34 mmol) in CH_2Cl_2 (10 mL). The reaction mixture was stirred at room temperature for two hours then placed in a -35 °C freezer for twelve hours. The precipitate of LiOR$_{F6}$ formed was quickly removed by filtration. The volatile components of the red filtrate were removed *in vacuo*. The resulting solid was redissolved in ether (5 mL), and the solution was placed in a -35 °C freezer. The burgundy crystals that formed were isolated via filtration and dried *in vacuo*; yield 0.25 g (65%): ^{1}H NMR (C_6D_6) δ 13.1 (s, 1H, MoC*H*R, J_{CH} = 136 Hz), 7.00 (m, 3H, Ar-C*H*), 5.98 (br

s, 2H, $NC_4H_2(CH_3)_2$), 4.17 (br s, 2H, FeC_4H_5), 3.84 (br s, 2H, FeC_4H_5), 3.39 (sept, 2H, $CH(CH_3)_2$), 2.08 (br s, 12H, $NC_4H_2(CH_3)_2$), 1.04 (br s, 6H, $CH(CH_3)_2$); Due to the poor solubility of this compound, ^{13}C NMR data were not collected; There were no resonances in the ^{19}F NMR spectrum. Anal. Calcd for $C_{60}H_{76}FeMo_2N_6$: C, 63.83; H, 6.79; N, 7.44. Found: C, 56.42, 50.89, 52.15; H, 5.93, 5.44, 4.91; N, 8.30, 3.85, 4.88.

Synthesis of [Mo(NAr)(Me$_2$Pyr)$_2$(CH)]$_2$(C$_6$H$_4$) (10). Solid $Li(NC_4H_2Me_2)$ (0.16 g, 1.6 mmol) was added to a -30 °C solution of $[Mo(NAr)(OR_{F6})_2(=CH)]_2(1,4\text{-}C_6H_4)\bullet 2DME$ (0.59 g, 0.39 mmol) in DME (10 mL). The solution was stirred at room temperature for one hour and the volatile components were removed *in vacuo*. The solid was triturated with diethyl ether multiple times until a bright orange powder was obtained. The compounds changes color upon exposure to heat or during prolonged periods at room temperature. The powder was isolated by filtration and dried *in vacuo*; yield 0.40 g (88%): ^1H NMR (C_6D_6) δ 13.51 (s, 1H, MoC*H*R, J_{CH} = 134 Hz), 7.12 (m, 3H, Ar-C*H*), 7.00 (m, 2H, Ar-C*H*), 5.96 (br s, 4H, $NC_4H_2(CH_3)_2$), 3.44 (sept, 2H, $CH(CH_3)_2$), 2.11 (br s, 12H, $NC_4H_2(CH_3)_2$), 0.96 (br s, 6H, $CH(CH_3)_2$); ^{13}C NMR ($C_6D_5CD_3$) δ 291.99, 157.72, 148.03, 123.99, 106.99, 28.23, 24.06, 21.75, 18.53; There were no resonances in the ^{19}F NMR spectrum; Anal. Calcd for $C_{56}H_{72}Mo_2N_6$: C, 65.87; H, 7.11; N, 8.23. Found: C, 26.42, 61.20; H, 1.91, 6.58; N 0.82, 6.75.

Synthesis of [Mo(NAr)(Biphen)(=CHC$_5$H$_4$)]$_2$Fe (11). 2.9 equivalents of (R)- or (S)-H_2[**Biphen**] (441 mg, 1.25 mmol) were added to a stirred solution of **8** (500 mg, 0.43 mmol) in toluene (5 mL). The solution was stirred at room temperature for three hours and the volatile components were removed *in vacuo*. The remaining solid was dissolved in pentane and passed through a glass filter tip pipette to remove the byproduct in the reaction (LiPyr). The volatile components were again removed *in vacuo*, the solid redissolved in pentane (2 mL), and the

solution was placed in a -35 °C freezer overnight. A burgundy solid formed which was isolated by filtration and dried *in vacuo*; yield 400mg (65%): ^{1}H NMR (C_6D_6) δ 12.71 ppm (s, MoC*H*R, 70%, *anti/anti* isomer, J_{CH} = 152 Hz), 12.55 ppm (s, MoC*H*R, *anti* peak of *anti/syn* isomer, 14%, J_{CH} = 152 Hz), 11.31 ppm (s, MoC*H*R, 14%, *syn* peak of *anti/syn* isomer, J_{CH} = 125 Hz) and 11.13 ppm (s, MoC*H*R, 2%, *syn/syn* isomer, J_{CH} = 125 Hz). The following resonances are reported for the major isomer only: δ 7.32, 7.29, 7.16, 7.09 (m, 5H, Ar-C*H*), 4.60 (s, 1H, FeC$_4$*H*$_5$), 4.56 (s, 1H, FeC$_4$*H*$_5$), 3.95 (s, 1H, FeC$_4$*H*$_5$), 3.87 (s, 1H, FeC$_4$*H*$_5$), 3.82 (sept, 2H, C*H*(CH$_3$)$_2$), 2.26 (s, 3H, Me-**Biphen**), 2.20 (s, 3H, Me-**Biphen**), 1.87 (s, 3H, Me-**Biphen**), 1.77 (s, 3H, Me-**Biphen**), 1.63 (s, 9H, *t*-Bu-**Biphen**), 1.52 (s, 9H, *t*-Bu-**Biphen**), 1.36 (d, 6H, CH(C*H*$_3$)$_2$), 1.29 (d, 6H, CH(C*H*$_3$)$_2$); ^{13}C NMR ($C_6D_5CD_3$) δ 265.23 (*anti/anti* isomer), 264.87 (*anti* peak of *anti/syn* isomer), 260.47 (*syn* peak of *anti/syn* isomer), 260.05 ppm (*syn/syn* isomer); The following resonances are reported for the major isomer (*anti/anti*) only: δ 155.66, 152.27, 148.17, 147.36, 144.88, 142.04, 140.98, 136.65, 135.27, 132.18, 131.54, 131.14, 131.07, 130.97, 129.27, 128.89, 127.33, 123.23, 89.52, 73.26, 72.87, 69.71, 69.14, 35.86, 35.70, 30.17, 29.92, 24.82, 23.58, 20.84, 20.78, 16.89, 16.84; Anal. Calcd for $C_{82}H_{104}Mo_2N_2O_4Fe$: C, 68.90; H, 7.33; N, 1.96. Found: C, 69.08; H, 7.30; N, 1.88.

Synthesis of [Mo(NAr)(Benz$_2$Bitet)(=CH)]$_2$(1,4-C$_6$H$_4$) (12). H$_2$[**Benz$_2$Bitet**] (86 mg, 0.14 mmol) was added to a stirred solution of **10** (70 mg, 0.069 mmol) in toluene (3 mL). The reaction was stirred at room temperature for three hours, at which time the volatile components were removed *in vacuo*. The resulting dark orange solid was washed with pentane to remove residual H$_2$[**Benz$_2$Bitet**]. The solid was dissolved in ether (2 mL). A powder formed by slowly diffusing pentane into the solution. The powder was isolated by filtration and dried *in vacuo*; yield 50 mg (39%): ^{1}H NMR (C_6D_6) δ 11.24 (s, 1H, MoC*H*R, J_{CH} = 125 Hz), 7.55 (d, 2H, Ar-

C*H*), 7.43 (d, 2H, Ar-C*H*), 7.27 (t, 2H, Ar-C*H*), 7.22 – 6.79 (m, 5H, Ar-C*H*), 6.49 (s, 1H, Ar-C*H*), 5.89 (s, 1H, Ar-C*H*), 3.98 (sept, 2H, C*H*$(CH_3)_2$), 2.55 – 2.11 (br m, 8H, C*H*$_2$-**Bitet**), 1.50 – 1.02 (br m, 8H, C*H*$_2$-**Bitet**), 1.24 (d, 6H, CH(C*H*$_3$)$_2$), 0.92 (d, 6H, CH(C*H*$_3$)$_2$); ^{13}C NMR ($C_6D_5CD_3$) δ 258.38, 154.79, 151.20, 149.08, 145.82, 145.77, 143.95, 143.85, 138.21, 137.55, 136.89, 136.10, 135.72, 135.17, 134.20, 133.77, 133.51, 130.76, 130.34, 130.27, 130.22, 130.16, 129.86, 129.66, 129.32, 129.14, 129.06, 128.91, 128.80, 127.70, 127.04, 126.74, 126.63, 126.55, 126.04, 126.83, 52.22, 50.06, 30.42, 30.27, 29.89, 28.82, 28.45, 24.05, 23.96, 23.63, 23.40, 23.30, 22.94, 21.77.

Synthesis of [Mo(NAr)(MesBitet)(=CH)]$_2$(1,4-C_6H_4) (13). H_2[**MesBitet**] (104 mg, 0.20 mmol) was added to a stirred solution of **10** (100 mg, 0.010 mmol) in toluene (3 mL). The reaction was stirred at room temperature for three hours, at which time the volatile components were removed *in vacuo*. The resulting dark orange solid was washed with pentane to remove residual H_2[**Mes$_2$Bitet**] and then dried *in vacuo*; yield 100 mg (60%): ^{1}H NMR (C_6D_6) δ 11.23 (s, 1H, MoC*H*R, J_{CH} = 125 Hz), 7.20 (s, 1H, Ar-C*H*), 6.97 (s, 1H, Ar-C*H*), 6.92 (s, 1H, Ar-C*H*), 6.88 (m, 3H, Ar-C*H*), 6.64 (s, 1H, Ar-C*H*), 6.08 (s, 2H, Ar-C*H*), 3.23 (br s, 2H, C*H*$(CH_3)_2$), 2.8 – 2.4 (br m, 8H, C*H*$_2$-**Bitet**), 2.57, 2.50, 2.42, 2.26, 2.03, 1.83 (all s, each 3H, C*H*$_3$Mes), 1.7 – 1.4 (br m, 8H, C*H*$_2$-**Bitet**), 0.80 (br s, 12H, CH(C*H*$_3$)$_2$); ^{13}C NMR ($C_6D_5CD_3$) δ 260.50, 154.77, 153.18, 151.90, 145.20, 138.17, 137.76, 137.71, 137.35, 136.79, 136.56, 136.17, 136.08, 136.01, 135.85, 135.83, 135.14, 134.18, 133.8, 132.4, 132.4, 132.42, 129.73, 129.67, 129.56, 128.87, 128.73, 128.63, 128.37, 128.31, 126.81, 126.03, 123.42, 30.51, 30.24, 29.43, 28.84, 24.15, 24.09, 23.99, 23.89, 23.79, 23.56, 23.11, 21.75, 21.67, 21.59, 21.54, 21.41, 21.25; Anal. Calcd for $C_{108}H_{120}Mo_2N_2O_4$: C, 76.21; H: 7.11, N, 1.65. Found: C, 75.88; H, 6.98; N, 1.61.

Observation of reaction between [Mo(NAr)(Pyr)(=CHC$_5$H$_4$)]$_2$Fe•2Li(Pyr) and H$_2$[Benz$_2$Bitet]. H$_2$[**Benz$_2$Bitet**] (2.1 equiv, 113 mg, 0.18 mmol) in toluene (1 mL) was added to a stirred solution of **8** (100 mg, 0.86 mmol) in toluene (3 mL). The solution was stirred at room temperature for three hours, at which time the volatile components were removed *in vacuo*. The solid was dissolved in toluene. The resulting solution was diluted with pentane and placed in a -35 °C freezer. A brown solid formed which was isolated by filtration and dried *in vacuo*: ^{1}H NMR (C_6D_6) (reported for the alkylidene region only) δ 13.9 (7%), 13.37 (86%), 13.3 (7%).

Synthesis of NBDF6. Freshly cracked cyclopentadiene (10.2g, 0.15 mol) and hydroquinone (50 mg) was added to a Fischer-Porter bottle sealed with a Kalrez o-ring. The Fischer-Porter bottle was attached to a vacuum line and a gas cylinder containing hexafluoro-2-butyne (25 g, 0.15 mol). The cyclopentadiene was frozen with liquid nitrogen and the system was placed under static vacuum. The hexafluoro-2-butyne was backtransferred onto the frozen cyclopentadiene. The system was slowly warmed. The system was in a liquid state for approximately one hour before reaching the boiling point of the gas. When this temperature was reached, the reaction exothermed and released the remaining gas. (When repeating this reaction, suggest keeping the system at -30 °C for an extended period of time). A fractional distillation (122 - 126 °C) was completed on the remaining liquid; yield 17.5 g (50%). Residual cyclopentadiene was present so the solution was stored over maleic anhydride for approximately one week and filtered before use. See reference 30 for ^{1}H NMR spectroscopy data.

Example of Polymerization of DCMNBD with Isolated Initiator. DCMNBD (58 mg, 100 equiv, 0.28 mmol) in 2 mL of toluene was added to a stirred solution of **12** (5.2 mg, 0.0028 mmol) in 4 mL toluene. The mixture was stirred for four hours at which time two drops (~20 mg) of benzaldehyde were added. The solution was stirred for an additional hour, at which time

the polymer was precipitated from methanol. The precipitate was collected and dried *in vacuo* before analysis by ^{1}H and ^{13}C NMR; yield 55 mg (98%).

Example of Polymerization of DCMNBD with Initiator Prepared *In Situ*. H_2[**Benz$_2$Bitet**] (12.4 mg, 2.2 equiv, 0.021 mmol) in 1 mL of toluene was added to a stirred solution of **10** (10 mg, 0.0098 mmol) in 4 mL of toluene. The solution was stirred at room temperature for fifteen minutes. At that time, a solution of **DCMNBD** (223 mg, 110 equiv, 0.107 mmol) in 2 mL of toluene was added all at once. The mixture was stirred for four hours at which time two drops (~20 mg) of benzaldehyde were added. The solution was stirred for an additional hour, at which time the polymer was precipitated from pentane. The precipitate was collected and dried *in vacuo* before analysis by ^{1}H and ^{13}C NMR; yield 218 mg (98%).

Polymerization of NBDF6. The procedure for the polymerization of **NBDF6** is analogous to those given for the polymerization of **DCMNBD** except the polymers were precipitated from pentane instead of methanol.

Example of Polymerization of DCMNBD and MTD with Initiator Prepared *In Situ*. H_2[**Benz$_2$Bitet**] (6.8 mg, 2.2 equiv, 0.010 mmol) in 1 mL of toluene was added to a stirred solution of **10** (5 mg, 0.0049 mmol) in 4 mL of toluene. The solution was stirred at room temperature for fifteen minutes. At that time, a solution of **DCMNBD** (58 mg, 56 equiv, 0.28 mmol) in 2 mL of toluene was added all at once. The mixture was stirred for three hours at which time **MTD** (48 mg, 56 equiv, 0.28 mmol) was added. The solution was allowed to stir for another three hours at which time two drops (~20 mg) of benzaldehyde were added. The solution was stirred for an additional hour, at which time the polymer was precipitated from methanol. The precipitate was collected and dried *in vacuo* before analysis by ^{1}H and ^{13}C NMR; yield 100 mg (94%).

4.8 References

(1) Schrock, R. R.; Gabert, A. J.; Singh, R.; Hock, A. S. *Organometallics* **2005**, *24*, 5058.

(2) Gabert, A. J.; Verploegen, E. V.; Hammond, P. T.; Schrock, R. R. *Macromolecules* **2006**, *39*, 3993.

(3) Hamilton, J. G. *Polymer* **1998**, *39*, 1669.

(4) O'Dell, R.; McConville, D. H.; Hofmeister, G. E.; Schrock, R. R. *J. Am. Chem. Soc.* **1994**, *116*, 3414.

(5) Preishuber-Pflugl, P.; Deder, E.; Stelzer, F.; Reisinger, H.; Mulhaupt, R.; Forsyth, J.; Perena, J. M. *Macromol. Chem. Phys.* **2001**, *202*, 1130.

(6) McConville, D. H.; Wolf, J. R.; Schrock, R. R. *J. Am. Chem. Soc.* **1993**, *115*, 4413.

(7) Schrock, R. R.; Lee, J.-K.; O'Dell, R.; Oskam, J. H. *Macromolecules* **1995**, *28*, 5933.

(8) Totland, K. M.; Boyd, T. J.; Lavoie, G. G.; Davis, W. M.; Schrock, R. R. *Macromolecules* **1996**, *29*, 6114.

(9) Hock, A. S.; Schrock, R. R.; Hoveyda, A. H. *J. Am. Chem. Soc.* **2006**, *128*, 16373.

(10) Singh, R.; Czekelius, C.; Schrock, R. R.; Muller, P.; Hoveyda, A. H. *Organometallics* **2007**, 26, 2528.

(11) Kreickmann, T. *Unpublished results.*

(12) Pilyugina, T. S.; Schrock, R. R.; Mueller, P.; Hoveyda, A. H. *Organometallics* **2007**, *26*, 831.

(13) Dolman, S. J.; Hultzsch, K. C.; Pezet, F.; Teng, X.; Hoveyda, A. H.; Schrock, R. R. *J. Am. Chem. Soc.* **2004**, *126*, 10945.

(14) Schrock, R. R.; Jamieson, J. Y.; Araujo, J. P.; Bonitatebus, P. J.; Sinha, A.; Lopez, L. P. H. *J. Organomet. Chem.* **2003**, *684*, 56.

(15) Tsang, W. C. P.; Hultzsch, K. C.; Alexander, J. B.; Bonitatebus, P. J., Jr.; Schrock, R. R.; Hoveyda, A. H. *J. Am. Chem. Soc.* **2003**, *125*, 2652.

(16) Schrock, R. R.; Jamieson, J. Y.; Dolman, S. J.; Miller, S. A.; Bonitatebus, P. J., Jr.; Hoveyda, A. H. *Organometallics* **2002**, *21*, 409.

(17) Alexander, J. B.; Schrock, R. R.; Davis, W. M.; Hultzsch, K. C.; Hoveyda, A. H.; Houser, J. H. *Organometallics* **2000**, *19*, 3700.

(18) Alexander, J. B.; La, D. S.; Cefalo, D. R.; Hoveyda, A. H.; Schrock, R. R. *J. Am. Chem. Soc.* **1998**, *120*, 4041.

(19) La, D. S.; Alexander, J. B.; Cefalo, D. R.; Graf, D. D.; Hoveyda, A. H.; Schrock, R. R. *J. Am. Chem. Soc.* **1998**, *120*, 9720.

(20) Hultzsch, K. C.; Bonitatebus, P. J., Jr.; Jernelius, J.; Schrock, R. R.; Hoveyda, A. H. *Organometallics* **2001**, *20*, 4705.

(21) Tsang, W. C. P.; Jernelius, J. A.; Cortez, G. A.; Weatherhead, G. S.; Schrock, R. R.; Hoveyda, A. H. *J. Am. Chem. Soc.* **2003**, *125*, 2591.

(22) Zhu, S. S.; Cefalo, D. R.; La, D. S.; Jamieson, J. Y.; Davis, W. M.; Hoveyda, A. H.; Schrock, R. R. *J. Am. Chem. Soc.* **1999**, *121*, 8251.

(23) Sinha, A.; Schrock, R. R.; Mueller, P.; Hoveyda, A. H. *Organometallics* **2006**, *25*, 4621.

(24) Tsang, W. C. P.; Schrock, R. R.; Hoveyda, A. H. *Organometallics* **2001**, *20*, 5658.

(25) Dolman, S. J.; Schrock, R. R.; Hoveyda, A. H. *Org. Let.* **2003**, *5*, 4899.

(26) Pilyugina, T. *Molybdenum alkylidene complexes: Syntheses and applications to olefin metathesis reactions* Ph.D. Thesis, Massachusetts Institute of Technology, Cambridge, **2007**.

(27) Bazan, G. C.; Khosravi, E.; Schrock, R. R.; Feast, W. J.; Gibson, V. C.; O'Regan, M. B.; Thomas, J. K.; Davis, W. M. *J. Am. Chem. Soc.* **1990**, *112*, 8378.

(28) Singh, R. *Unpublished results.*

(29) Gribkov, D. V.; Hultzsch, K. C.; Hampel, F. *Chem. Eur. J.* **2003**, *9*, 4797.

(30) Alimuniar, A. b.; Blackmore, P. M.; Edwards, J. H.; Feast, W. J.; Wilson, B. *Polymer* **1986**, *27*, 1281.

Appendix A - Various Monomers for Inner and Outer ROMP Blocks

A.1 Introduction

Chapter 3 discussed the synthesis of ABA triblock copolymers where the inner block was functionalized by the liquid crystal mesogen, **BPP4**, and the outer block was methyltetracyclododecene (**MTD**). Various studies of these systems gave evidence that triblock copolymers synthesized by ring opening metathesis polymerization (ROMP) had the potential to act as thermoplastic liquid crystal elastomers. However, the system must be optimized so the material can exhibit the desired properties discussed in Section 3.1. The glass transition temperature (T_g) of the inner block needs to be lowered to 0 °C or below. A lower T_g of the inner block will enable the system to act as an elastomer at room temperature. The T_g of the outer blocks needs to be between 90 and 150 °C. A lower T_g of the outer blocks will allow the polymer to be more easily processed and will allow the system to achieve long-range ordering, while still providing rigidity as physical crosslinks. This Appendix reports the synthesis and thermal properties of two liquid crystal functionalized inner blocks, either containing a cyclobutene or oxa-norbornene backbone. Also reported is the synthesis and thermal properties of three new outer blocks.

A.2 Liquid Crystal Functionalized Cyclobutene

The monomer shown in Figure A.1, **CBEwBPP4** (4-(1-butoxy-1-oxopropan-2-yloxy)phenyl 4'-(2-(2-(cyclobut-2-enylmethoxy)ethoxy)ethoxy)biphenyl-4-carboxylate), was first synthesized and investigated by Rojendra Singh in our group.[1] Poly(**CBEwBPP4**)$_{100}$ was synthesized by R. Singh on a small scale using the bifunctional initiator, $[Mo(NAr)(OR_{F0})_2(CH)]_2(1,4\text{-}C_6H_4)\bullet 2DME$ (where $OR_{F0} = OCMe_3$; Ar = 2,6-diisopropylphenyl; DME = dimethoxyethane). The polymer was analyzed by differential scanning calorimetry (DSC) and found to have a T_g of -12 °C and a distinct, but broad smectic to isotropic transition

around 100 °C. The synthesis of the monomer needed to be repeated so that triblock copolymers could be synthesized and analyzed. Reported in this Appendix is the revised synthesis of the monomer and additional DSC results.

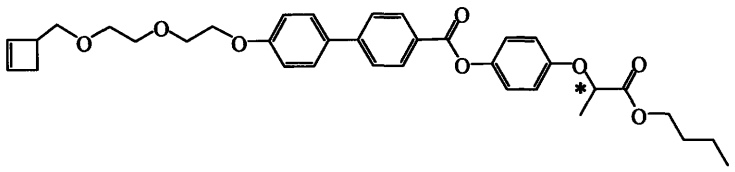

Figure A.1 CBEwBPP4 monomer.

The first step in the synthetic route to **CBEwBPP4** is the synthesis of 4'-(2-(2-hydroxyethoxy)ethoxy)biphenyl-4-carboxylic acid (Scheme A.1). A literature preparation is available for this compound, but the isolation process is difficult. [3] Therefore a modified, simpler preparation was developed. 4'-Hydroxy-biphenyl-4-carboxylic acid is esterified in an acid-catalyzed reaction with MeOH to give the product, methyl 4'-hydroxybiphenyl-4-carboxylate, in virtually quantitative yield.[2] The product was coupled with 2-(2-chloroethoxy)ethanol to yield methyl 4'-(2-(2-hydroxyethoxy)ethoxy)biphenyl-4-carboxylate. The reaction mixture was poured into water and the solid which forms was isolated by filtration and washed. The isolated solid was refluxed in basic solution to saponify the ester. The resulting solution is acidified with HCl and 4'-(2-(2-hydroxyethoxy)ethoxy)biphenyl-4-carboxylic acid was isolated by filtration, washed and dried. All three steps are set up and the product worked up in a matter of minutes; the overall yield is 83%. This yield is similar to the literature preparation which was previously reported for this compound.[3]

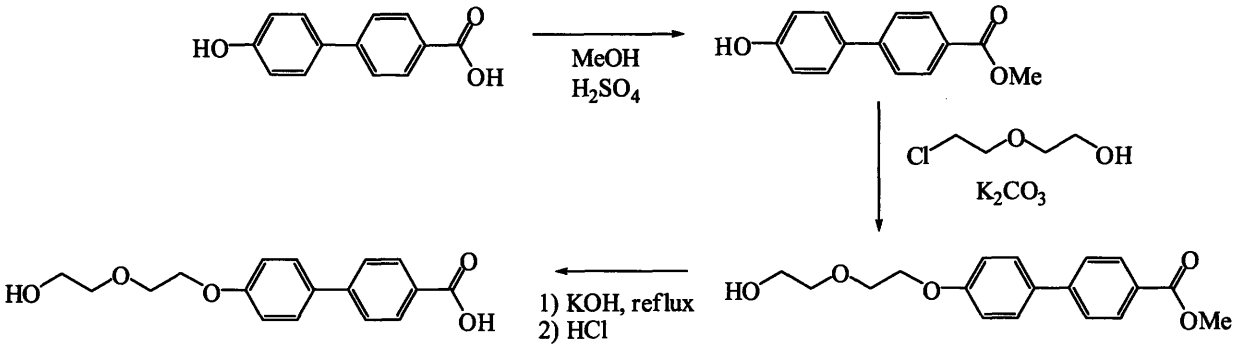

Scheme A.1 Synthesis of 4'-(2-(2-hydroxyethoxy)ethoxy)biphenyl-4-carboxylate.

The syntheses previously reported by Rojendra Singh were modified in order to ease purification and/or to improve yields.[1] The coupling of 4'-(2-(2-hydroxyethoxy)ethoxy)biphenyl-4-carboxylic acid with butyl 2-(4-hydroxyphenoxy)propanoate using DCC/DMAP proceeds readily (Scheme A.2). The column conditions have been optimized in order to allow the products to be separated easily; an improved yield of 85% was obtained versus the previously reported 56%.[1] The tosylation of 4-(1-butoxy-1-oxopropan-2-yloxy)phenyl 4'-(2-(2-hydroxyethoxy)ethoxy)biphenyl-4-carboxylate to afford Tos-**OBPP4** in dimethylformamide gave increased conversion to the product than in dimethylsulfoxide. The column conditions were also optimized. Conversion to Tos-**OBPP4** seems to halt at a particular point despite addition of more tosyl chloride and/or addition of a catalyst such as NaI. Despite less than full conversion, the starting material can be easily isolated from the column and used again in syntheses of Tos-**OBPP4**.

The final synthetic step in the synthesis of **CBEwBPP4** was the coupling of Tos-**OBPP4** with cyclobut-2-enylmethanol (Scheme A.3). The series of reactions to form cyclobut-2-enylmethanol proved to be challenging (Scheme A.4). The intermediates are quite unstable with time at room temperatures, in light, or in harsh medium, so the synthesis must be completed rapidly and efficiently to avoid any extended exposure to such conditions. The first step involves

the chlorination and decarboxylation of cyclobutane-1,1-dicarboxylic acid using sulfuryl chloride and heat.[4] The carboxylic acid moiety was then reduced using borane.[5] The formation of cyclobut-2-enylmethanol proceeded through dehydrohalogenation using potassium *tert*-butoxide.[5]

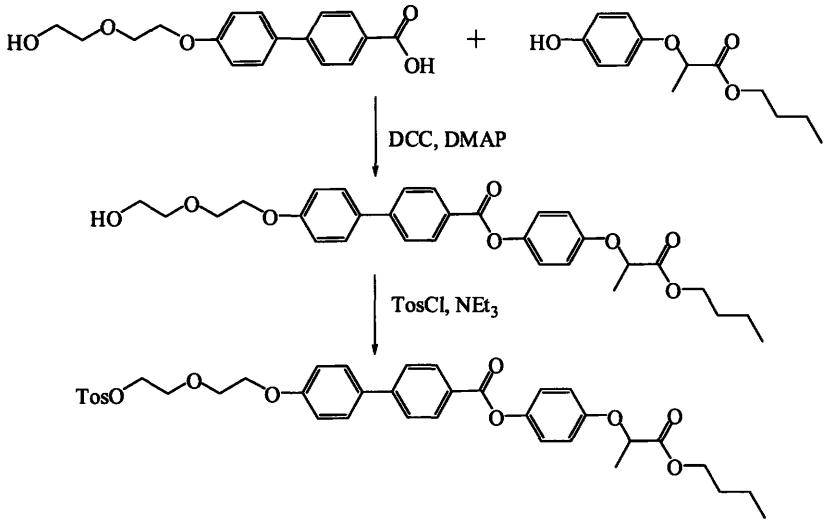

Scheme A.2 Synthesis of Tos-**OBPP4**.

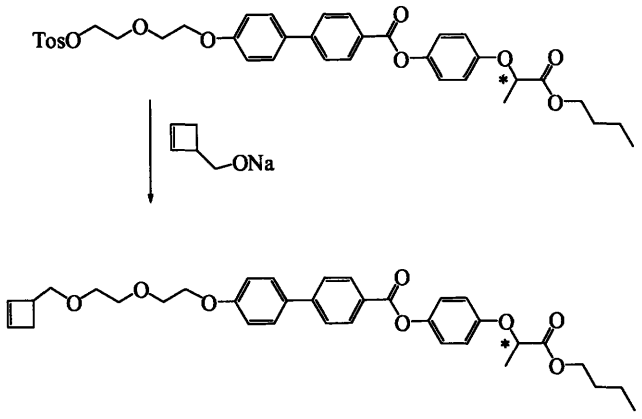

Scheme A.3 Final step in the synthesis of **CBEwBPP4**.

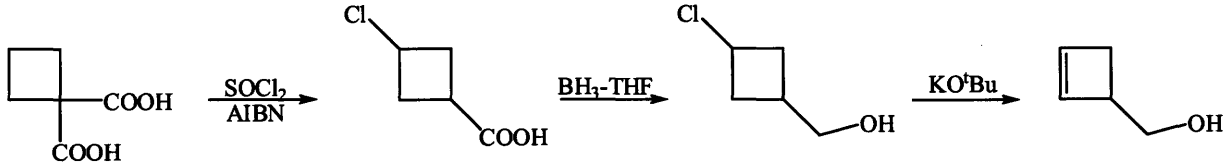

Scheme A.4 Synthesis of cyclobut-2-enylmethanol.

Cyclobut-2-enylmethanol was coupled with the tosylated liquid crystal mesogen to form **CBEwBPP4**. Cyclobut-2-enylmethanol was deprotonated with sodium hydride, and the reaction mixture is added to a solution of Tos-**OBPP4**. This reaction also was challenging as the ester groups in the liquid crystal mesogen often were cleaved by excess sodium hydride and undesired products were isolated (Scheme A.5). The amount of cleaved product decreased when the reaction was performed in dimethylformamide and the deprotonated cyclobutene was filtered before addition to Tos-**OBPP4**.

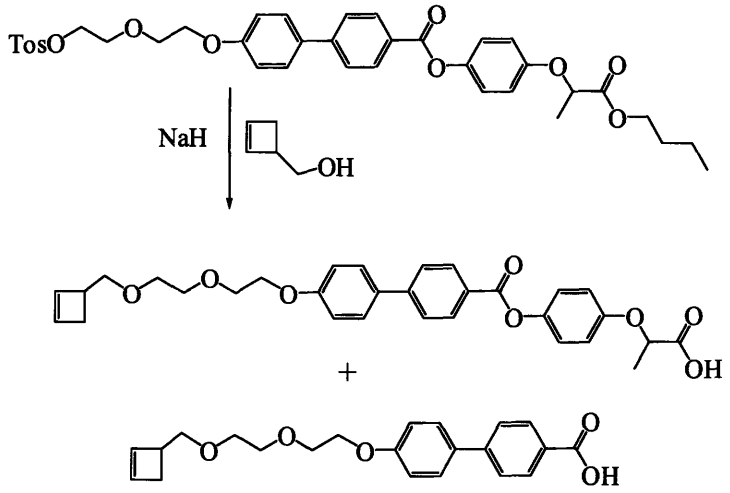

Scheme A.5 Impurities formed in the reaction of Tos-**OBPP4** and cyclobut-2-enylmethanol.

Polymerization of **CBEwBPP4** was completed using $Mo(NAr)(OR_{F6})_2(CHCMe_2Ph)$ (where OR_{F6} = $OCMe(CF_3)_2$ **15**). 100 equivalents of **CBEwBPP4** were added to a stirred solution of the initiator in tetrahydrofuran. The reaction mixture was stirred at room temperature for one hour, and the polymerization was quenched with benzaldehyde. The volume of the solution was reduced to ~1 mL and methanol was added to precipitate the polymer. The gooey polymer clung to the sides of the flask and was dried for further analysis. The ^1H NMR spectrum of the polymer revealed broad resonances. A unimodal peak with a M_n of 13×10^4 and a PDI of 1.91 was observed by gel permeation chromatography (GPC).

The DSC trace revealed a broad T_g around -10 °C, which is similar to that previously reported (-12 °C) (Figure A.2). However, no liquid crystal transition was observed during the scan as opposed to the previously reported liquid crystal transition at ~100 °C.[1] The cause for the lack of transition may be due to the broad PDI of the isolated polymer, because a different initiator was employed for the polymerization, or to an increased scan rate of 10 °C/min as opposed to the reported 5 °C/min. The polymerization was repeated using the bifunctional initiator previously employed. The polymer synthesized with this initiator had a decrease PDI value (~1.5) and the DSC trace was collected at a scan rate of 5 °C/min. However, still no liquid crystal transition was observed. The cause for the discrepancy between the original results (LC transition observed) and the repeated results (no LC transition observed) could be attributed to numerous causes such as (i) an impurity of the monomer being present in the original polymer analyzed or (ii) the ester groups of the LC cleaving during the original polymer work-up which changed the architecture of the LC moiety. Due to the difficulties encountered when synthesizing this monomer and the absence of a liquid crystal transition, further investigations were halted.

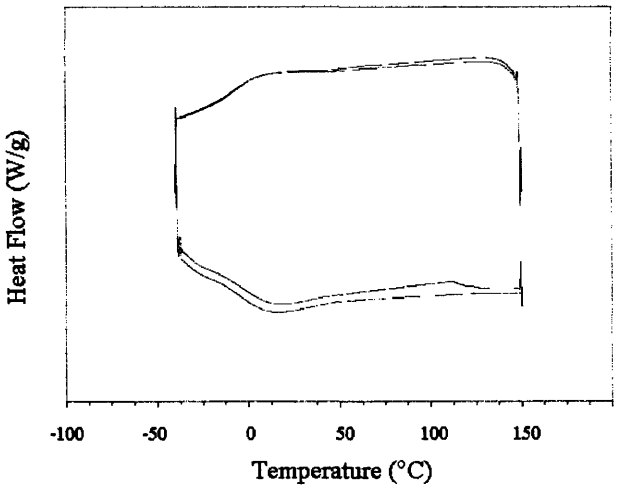

Figure A.2 DSC profile of poly(**CBEwBPP4**)$_{100}$.

A.3 Liquid Crystal Functionalized Oxa-Norbornene

The challenge of finding an appropriate inner block for ROMP is to find a backbone structure that has a low glass transition, preferably below 0 °C. Polymers with a norbornene or norbornadiene backbone, regardless of the spacers to the mesogen, have yet to give rise to an acceptable T_g for our purpose. Changing from a norbornadiene backbone to the corresponding oxa-norbornadiene backbone has been found to lower the T_g of a polymer system. For example, a polymer of dicarbomethoxynorbornadiene has a T_g of 140 °C while a polymer of the oxa-norbornadiene counterpart has a T_g of 107 °C, a decrease of over 30 °C.[6]

A monomer containing an oxa-norbornene backbone and the mesogen **MPOB**-H (4-methoxyphenyl 4-hydroxybenzoate), was synthesized in order to investigate the potential for such backbones to lower the T_g sufficiently (Scheme A.6). The first step in the synthesis of the monomer was the Diels-Alder reaction between furan and methyl acrylate to form methyl 7-oxabicyclo[2.2.1]hept-5-ene-2-carboxylate.[7] The product was reduced to 7-oxabicyclo[2.2.1]hept-5-en-2-ylmethanol, which was coupled with 1,5-dibromopentane to yield 5-(7-oxabicyclo[2.2.1]hept-5-en-2-ylmethoxy)pentan-1-ol. Further reaction with **MPOB**-H yielded the monomer, 4-methoxyphenyl 4-(5-(7-oxabicyclo[2.2.1]hept-5-en-2-ylmethoxy)pentyloxy)benzoate, abbreviated as **ONBwMPOB** (Scheme 6),

ONBwMPOB was polymerized using **15**. The isolated yield of the polymer was 90% and the PDI was 1.46. The DSC analysis of the polymer revealed a T_g of approximately 15 °C and a liquid crystal clearing point of 40 °C. Although changing to an oxa-norbornene backbone from a norbornene backbone lowered the T_g of the resulting polymer (from ~20 °C, when the spacer was nine carbons long),[8] the T_g is still too high for practical purposes.

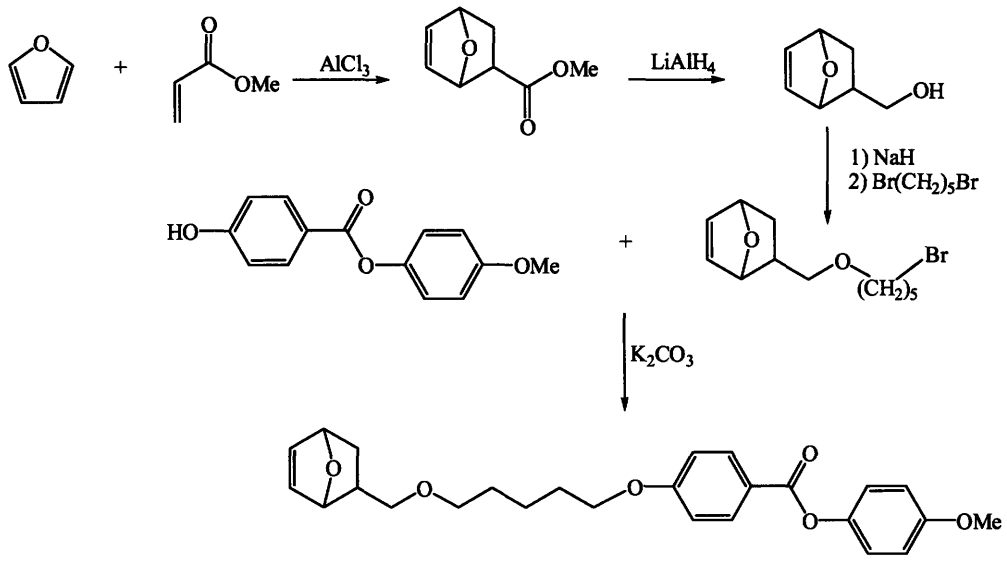

Scheme A.6 Synthesis of **ONBwMPOB**.

A.4 Synthesis of New Outer Blocks

Three desired properties of an outer block for our purpose are that (i) the T_g of the polymer should be between approximately 90 – 150 °C, (ii) the monomer should be preparable in large quantities, and (iii) the monomer should be polymerized in a living fashion by our bifunctional initiators. It is also preferred that the monomer is functionalized by moieties (such as fluorine) that would aid in microphase separation of the triblock copolymer systems. Three outer block monomers were prepared (Figure A.3) according to literature procedures and the synthetic procedures are outlined briefly below. The three monomers are exo-4-cyclohexyl-4-aza-tricyclo[5.2.1.$0^{2,6}$]dec-8-ene-3,5-dione (**NBwNCy**), [3-(4-fluoro-benzoyl)-bicyclo[2.2.1]hept-5-en-2-yl]-(4-fluoro-phenyl)-methanone (**NBwCOPh$_F$**), and bicyclo[2.2.1]hept-5-en-2-yl-phenyl-methanone (**NBwCOPh**). A fourth monomer, 5-pentafluorophenylmethyl-bicyclo[2.2.1]hept-2-ene (**NBwCH$_2$Ph$_{F5}$**), was also targeted and the synthetic results are reported.

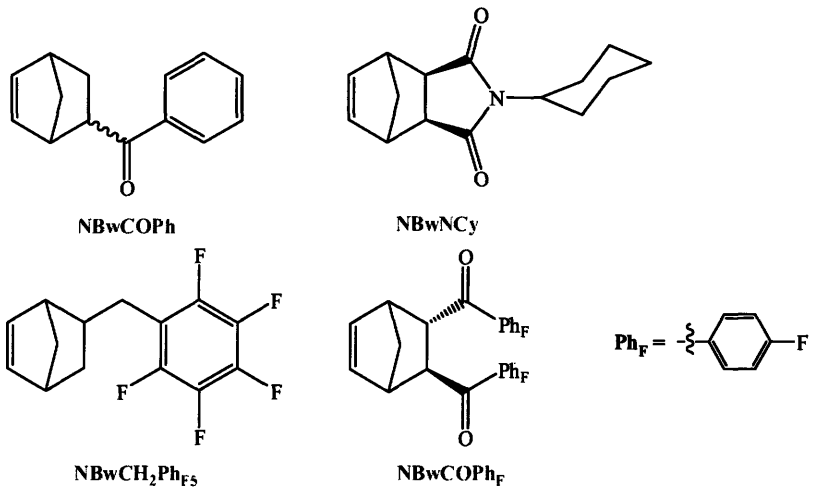

Figure A.3 Outer block monomers investigated.

The monomers were polymerized with **15**, $Mo(NAr)(CHCMe_2Ph)(OR_{F0})_2$ (**16**), and $[Mo(NAr)(OR_{F6})_2(=CHC_5H_4)]_2Fe$ (**6**). The polymerizations were performed by adding the monomer solution (either THF or toluene) to a stirred solution of the initiators, and were quenched with excess benzaldehyde. The polymers were isolated in two ways. First, the reaction solution was concentrated and the polymer was precipitated from methanol. If the resulting polymer was course enough, it was isolated by filtration. If the precipitate was a fine powder, it was isolated by filtration onto a pad of Celite. The polymer was then redissolved in tetrahydrofuran or dichloromethane. The polymers were analyzed by GPC to determine the PDI of the polymer and by DSC to determine the T_g of the polymer. The polymers were analyzed by these techniques to give evidence that the polymerization is living (quantitative yields and low PDI) and to determine whether the T_g is in the desired range.

NBwNCy has been previously polymerized by ROMP using ruthenium catalysts of the type, $[PR_3]_2Cl_2Ru=C=CH(t\text{-Bu}))$, and the T_g of the polymer was recorded at 129 °C.[12] This exact monomer has not been polymerized using any molybdenum initiators. However, similar monomers where the cyclohexyl moiety was replaced with various alkyl or aromatic groups were

polymerized in a living fashion using both **15** and **16**. With the alkyl substituents, the T_g of the polymers ranged from ~50 °C for the *exo* adducts and ~100 °C for the *endo* adducts.[9] For this project, it was decided to synthesize the *exo*-monomer exclusively because in some cases, the *endo* adduct is not polymerized with molybdenum initiators.[10] **NBwNCy** was chosen to be investigated as a new potential outer block because it (i) contains different functional groups which should aid in microphase separation, (ii) is easy to synthesize, (iii) should have a T_g in the desirable range, and (iv) from examples of similar previous work, should be polymerized in a living fashion using molybdenum initiators.

exo-**NBwNCy** (Scheme A.7) was synthesized via the intermediate, 4-oxa-tricyclo[5.2.1.$0^{2,6}$]dec-8-ene-3,5-dione, which was synthesized by the Diels-Alder reaction of maleic anhydride and cyclopentadiene. This intermediate was recrystallized multiple times from chlorobenzene to isolate all *exo* product.[11] Further reaction of the *exo*-intermediate with cyclohexyl amine yielded the monomer, **NBwNCy**.[12]

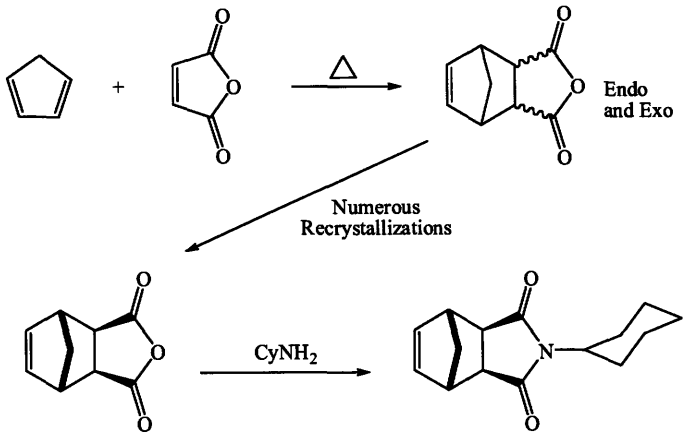

Scheme A.7 Synthesis of *exo*-**NBwNCy**.

Table A.1 shows the results for poly[**NBwNCy**]$_{100}$. The yields were quantitative in all cases, except when using **15** in THF. In most cases, the isolated polymers were insoluble in dichloromethane and THF, so GPC results could not be obtained. The T_g values for the polymers

were higher than what was observed with the ruthenium catalysts (129 °C) and are outside of the desirable range. Therefore, **NBwNCy** is not an ideal monomer for our studies. If the cyclohexyl moiety is changed to another alkyl group, the resulting T_g may be in the desired range.

Initiator	Equiv	Solvent	Yield (%)	Mn (× 1000)	PDI	T_g
15	100	THF	none isolated	-	-	-
	100	toluene	114	not soluble	not soluble	180
16	100	THF	100	52.7	1.03	220
	100	toluene	97	not soluble	not soluble	190
6	100	toluene	96	not soluble	not soluble	170

Table A.1 Polymerization results for **NBwNCy**.

NBwCOPh$_F$ (Scheme A.8) was synthesized by the Diels-Alder reaction of 1,4-bis-(4-fluoro-phenyl)-but-2-ene-1,4-dione and cyclopentadiene.[13] 1,4-Bis-(4-fluoro-phenyl)-but-2-ene-1,4-dione was synthesized via reaction of fluorobenzene with fumaryl chloride.[14] Prior to this study there were no examples of ROMP of **NBwCOPh$_F$** so the T_g was unknown. This monomer was chosen because it could be synthesized readily in large scale, and it contains fluorine atoms which should aid in microphase segregation.

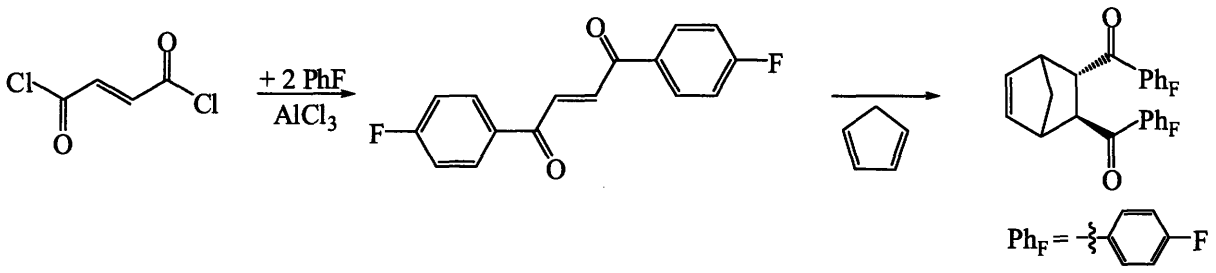

Scheme A.8 Synthesis of **NBwCOPh$_F$**.

The polymerization of **NBwCOPh$_F$** proceeded readily in toluene but was slow in THF. The results are tabulated in Table A.2. The PDI values of all the polymers were low, and the glass transition temperatures were in the appropriate range. Therefore, this monomer is an acceptable candidate for an outer block monomer.

Initiator	Equiv	Solvent	Yield (%)	Mn (× 1000)	PDI	T_g
15	100	THF	68	20.4	1.06	140
	100	toluene	94	26.5	1.09	140
16	100	THF	72	49.9	1.07	140
	100	toluene	93	41.4	1.15	135
6	100	toluene	90	29	1.06	138

Table A.2 Polymerization results for **NBwCOPh$_F$**.

NBwCOPh (Scheme A.9) was synthesized via reaction of bicyclo[2.2.1]hept-5-ene-2-carboxylic acid with phenyl magnesium bromide to yield bicyclo[2.2.1]hept-5-en-2-yl-phenyl-methanol.[15] Oxidation of this intermediate with Jones Reagent yielded the desired compound. This monomer had not been polymerized via ROMP and its properties were unknown. It was chosen to be investigated as a potential new outer block because it was commercially available. After the properties were determined with the commercial source and deemed ideal, it was then synthesized in a large scale for the future synthesis of triblock copolymers. For the polymerization results given in this Appendix, the *endo*:*exo* ratio was 1:2.

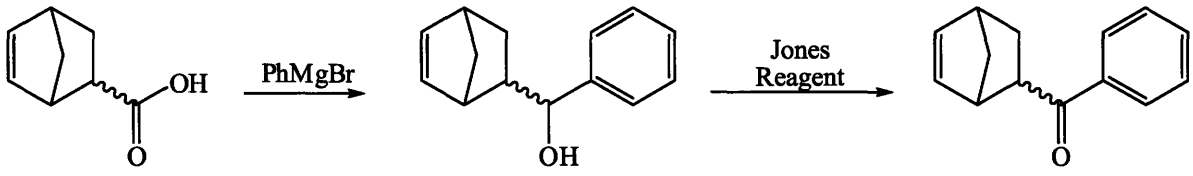

Scheme A.9 Synthesis of **NBwCOPh**.

NBwCOPh was polymerized readily in both THF and toluene (Table A.3). The PDI values remained fairly low, and the glass transition temperatures were within the desired range. Therefore, this monomer is also a suitable candidate for an outer block, although it lacks any fluorine atoms.

Initiator	Equiv	Solvent	Yield (%)	Mn (× 1000)	PDI	T_g
15	100	THF	80	24.1	1.15	-
	100	toluene	98	24.5	1.18	85
16	100	THF	102	20.9	1.33	-
	100	toluene	94	33.4	1.25	100
6	100	toluene	80	22.8	1.15	105

Table A.3 Polymerization results for **NBwCOPh**.

The fourth monomer, **NBwCH$_2$Ph$_{F5}$**, (Scheme A.10) was synthesized by reaction of 1-allyl-2,3,4,5,6-pentafluoro-benzene with cyclopentadiene.[16] However, numerous attempts, either by distillation or column chromatography, to isolate this product cleanly from the starting materials was unsuccessful. This observation suggests of a reverse Diels-Alder process and therefore, this monomer was not used in further studies.

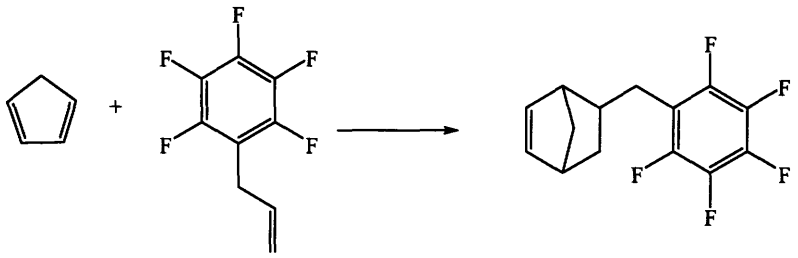

Scheme A.10 Synthesis of **NBwCH$_2$Ph$_{F5}$**.

To conclude this section, three new outer blocks were synthesized, and two have glass transitions temperatures within the desired range, namely, **NBwCOPh$_F$**, and **NBwCOPh**. These monomers can be used in the future synthesis of ABA triblock copolymers prepared for applications towards TPLCEs.

A.5 Conclusions

This Appendix reports the synthesis of various new inner and outer blocks that were prepared with the hope that they could be employed for triblock copolymers synthesized by

ROMP for the application of TPLCEs. The polymers synthesized with both new inner block monomers, **CBEwBPP4** and **ONBwMPOB**, did provide lower T_g values. Unfortunately, both polymers did not provide ideal properties; for poly(**CBEwBPP4**), no liquid crystal transition was observed and for poly(**ONBwMPOB**), the T_g was still above the desired temperature of 0 °C. Three new outer block monomers were also synthesized and two were found to exhibit ideal properties.

A.6 Experimental Procedures

General Procedures. All polymerizations were performed under dinitrogen in a glove-box. Solvents used in the polymerization reactions were purified by passage through an alumina column and stored over 4 Å Linde-type molecular sieves prior to use. Deuterated solvents were degassed and distilled from CaH_2 or sodium benzophenone ketyl. Benzaldehyde was vacuum distilled and stored over molecular sieves. Commercial reagents were used without further purification unless stated otherwise. *exo*-4-Oxa-tricyclo[5.2.1.$0^{2,6}$]dec-8-ene-3,5-dione,[11] *exo*-4-cyclohexyl-4-aza-tricyclo[5.2.1.$0^{2,6}$]dec-8-ene-3,5-dione,[14] 1,4-bis-(4-fluoro-phenyl)-but-2-ene-1,4-dione,[13] [3-(4-fluoro-benzoyl)-bicyclo[2.2.1]hept-5-en-2-yl]-(4-fluoro-phenyl)-methanone,[13] bicyclo[2.2.1]hept-5-en-2-yl-phenyl-methanol,[15] bicyclo[2.2.1]hept-5-en-2-yl-phenyl-methanone,[15] 7-oxa-bicyclo[2.2.1]hept-5-ene-2-carboxylic acid methyl ester,[7] 7-oxabicyclo[2.2.1]hept-5-en-2-ylmethanol,[7] 4'-hydroxy-biphenyl-4-carboxylic acid methyl ester,[2] **6**,[17] **15**,[18] and **16**[18] were prepared according to literature procedures.

NMR spectra were recorded on a Varian INOVA 500 spectrometer. ^1H NMR chemical shifts are given in ppm versus residual protons in the deuterated solvents as follows: δ 7.27 $CDCl_3$, δ 7.16 C_6D_6, δ 2.5 $(CD_3)_2SO$, and δ 2.09 $CD_3C_6D_5$. GPC analyses (solvent = tetrahydrofuran, 1 mL/min) were carried out using a Waters GPC system equipped with 1

Styragel HT3 column (500 - 30,000 MW range), 1 Styragel HT4 column (5,000 - 600,000 MW range), 1 Styragel HT5 column (50,000 - 4×10^6 MW range), a refractive index detector, and a UV detector (254 nm) was used for molecular weight measurement relative to polystyrene standards. A TA Instruments Q1000 was used for Differential Scanning Calorimetry (DSC), the heating and cooling rates were 10 °C min^{-1} in all cases.

Synthesis of 4'-[2-(2-hydroxy-ethoxy)-ethoxy]-biphenyl-4-carboxylic acid methyl ester. 4'-Hydroxy-biphenyl-4-carboxylic acid methyl ester (26.6 g, 0.12 mol), 2-(2-chloroethoxy)ethanol (12.3 mL, 0.12 mol) and K_2CO_3 (48.1 g, 0.36 mol) were dissolved in a small amount of DMF and heated to 90 °C overnight. The solution turned yellow in color and a white precipitate formed. The solution was cooled and poured into a large quantity water. The precipitate was isolated by filtration and washed with a large quantity of water. The isolated white powder was used in the next step without further purification: ^{1}H NMR (DMSO) δ 8.00, 7.78, 7.70, 7.08 (2H each, m, aromatic-C*H*), 4.16 (2H, m, OCH_2), 3.86 (3H, s, CO_2CH_3), 3.76 (2H, m, OCH_2), 3.50 (4H, m, OCH_2); ^{13}C NMR ($CDCl_3$) δ 166.13, 158.93, 144.29, 131.03, 129.82, 128.19, 127.66, 126.24, 115.03, 72.53, 68.91, 67.31, 60.27, 52.10; HRMS (ESI) Calcd for $C_{18}H_{20}O_5$ [M^+]: 316.1305. Found: 316.1309.

Synthesis of 4'-[2-(2-hydroxy-ethoxy)-ethoxy]-biphenyl-4-carboxylic acid. 4'-[2-(2-Hydroxy-ethoxy)-ethoxy]-biphenyl-4-carboxylic acid methyl ester (from previously reported synthesis) was refluxed in a 10% NaOH solution for eight hours during which time the solid dissolved. The solution was cooled to room temperature and poured onto a HCl/ice mixture. The precipitate was collected by filtration, washed with a large quantity water, and dried *in vacuo*. The resulting white powder was pure material; yield 30 g (83% over two steps): ^{1}H NMR (DMSO) δ 12.92 (1H, br s, COO*H*), 7.98, 7.75, 7.68, 7.06 (2H each, m, aromatic-C*H*),

4.66 (1H, br s, CH_2OH), 4.16 (2H, m, OCH_2), 3.86 (3H, s, CO_2CH_3), 3.76 (2H, m, OCH_2), 3.52 (4H, m, OCH_2); This ^1H NMR data match that which was reported previously but was expanded in more detail.[3] ^{13}C NMR (DMSO) δ 167.38, 158.91, 144.02, 131.34, 130.11, 128.95, 128.23, 126.20, 115.09, 72.61, 69.00, 67.39, 60.38; HRMS (ESI) Calcd for $C_{17}H_{18}O_5$ [M^+]: 302.1149. Found: 302.1147.

Additional data for 4'-[2-(2-hydroxy-ethoxy)-ethoxy]-biphenyl-4-carboxylic acid 4-(1-butoxycarbonyl-ethoxy)-phenyl. The compound was prepared according to Reference 1. The compound was purified by column chromatography using ethyl acetate:hexanes (3:2): ^1H NMR (DMSO) δ 8.14, 7.86, 7.74, 7.20, 7.09, 6.95 (2H each, m, aromatic-C*H*), 5.00 (1H, q, CH_3CHO), 4.70, 4.12, 3,77, 3.53, 3.51 (2H each, m, OCH_2), 1.54 (3H, d, CH_3CHO), 1.54 (2H, m, $OCH_2CH_2CH_2CH_3$), 1.28 (2H, m, $OCH_2CH_2CH_2CH_3$), 0.86 (3H, t, $OCH_2CH_2CH_2CH_3$); ^{13}C NMR (DMSO) δ 171.52, 164.66, 159.05, 154.99, 144.91, 144.53, 130.91, 130.43, 128.26, 126.98, 126.34, 122.79, 115.55, 115.06, 72.54, 72.03, 68.91, 67.34, 64.41, 60.28, 30.08, 18.49, 18.31, 13.47; HRMS (ESI) Calcd for $C_{30}H_{34}O_8$ [M^+]: 522.2248. Found: 522.2235.

Synthesis of 4'-{2-[2-(toluene-4-sulfonyloxy)-ethoxy]-ethoxy}-biphenyl-4-carboxylic acid 4-(1-butoxycarbonyl-ethoxy)-phenyl ester (Tos-OBPP4). TosCl (11.4 g, 0.059 mol) was added as a solid to a stirred solution of 4'-[2-(2-hydroxy-ethoxy)-ethoxy]-biphenyl-4-carboxylic acid 4-(1-butoxycarbonyl-ethoxy)-phenyl (20 g, 0.0383 mol) and Et_3N (8.33 mL, 0.059 mol) in DMF, and the reaction mixture was stirred at room temperature overnight. The reaction solution was washed with $NaHCO_3$, water, and the organic layer was dried over Mg_2SO_4. The volatile components were removed from the organic layers *in vacuo* and the residue was purified by column chromatography. Hexanes:ethyl acetate (80:20) was used as the eluent until the TosCl byproduct was eluted. The product was then eluted using 40:60 hexanes:ethyl acetate, followed

by 100% ethyl acetate to flush the starting material from the column. The unreacted starting material can be dried and used again in a future reaction; yield 12.0 g (50%): ^{1}H NMR (DMSO) δ 8.14, 7.87, 7.78, 7.74, 7.44, 7.21, 7.07, 6.97 (2H each, m, aromatic-C*H*), 5.00 (1H, q, CH_3CHO), 4.15, 4.12, 4.10, 3.76, 3.51 (2H each, m, OCH_2), 2.38 (3H, s, CH_3C), 1.53 (3H, d, CH_3CHO and 2H, m, $OCH_2CH_2CH_2CH_3$), 1.28 (2H, m, $OCH_2CH_2CH_2CH_3$), 0.86 (3H, t, $OCH_2CH_2CH_2CH_3$); ^{13}C NMR (DMSO) δ 171.51, 164.66, 158.97, 155.01, 144.91, 144.86, 144.55, 132.42, 130.99, 130.44, 130.08, 128.24, 127.64, 127.00, 126.33, 122.78, 115.56, 115.05, 72.06, 69.96, 68.86, 68.07, 67.15, 64.42, 30.08, 21.05, 18.49, 18.28, 13.45; HRMS (ESI) Calcd for $C_{37}H_{40}O_{10}S$ [M + Na^+]: 699.2234. Found: 699.2231.

Synthesis of 4-(1-butoxy-1-oxopropan-2-yloxy)phenyl 4'-(2-(2-(cyclobut-2-enylmethoxy)ethoxy)ethoxy)biphenyl-4-carboxylate (CBEwBPP4). Under an atmosphere of nitrogen, a solution of cyclobut-2-enylmethanol (0.25 g, 2.0 mmol) in anhydrous dimethylformamide was added to a chilled (0 °C) stirring solution of NaH (60% in oil, 50 mg, 1.2 mmol). The solution was warmed to room temperature over one hour. The solution was filtered through a Schlenk frit and added to a stirred solution of Tos-**OBPP4** (1.4 g, 2.0 mmol). The reaction was stirred at room temperature for 12 hours. Diethyl ether and water was added to the solution, the aqueous layer was washed with water. The organic layers were combined, washed with water, dried over Mg_2SO_4 and the volatile components were removed. Column chromatography on silica gel using ethyl acetate:hexanes (4:6) as the eluent yielded a colorless gel identified as the product; yield 0.4 g (55%): ^{1}H NMR (CD_3Cl) δ 8.08, 7.62, 7.56. 7.03, 6.85, 6,84 (2H each, m, aromatic-C*H*), 6.17 and 6.12 (1H each, m, cyclobutene-CHCH) 4.66 (1H, q, CH_3CHO), 4.41, 4.21, 4.15, 3.96, 3.93 (2H each, m, OCH_2), 3.29, 2.76, 2.34 (1H each, m, cyclobutene-CH), 1.59 (3H, d, CH_3CHO), 1.27 (4H, m, $OCH_2CH_2CH_2CH_3$), 0.89 (3H, t,

$OCH_2CH_2CH_2CH_3$); This ^1H NMR data matches that previously reported but was expanded in more detail;[1] ^{13}C NMR (CD_3Cl) δ 172.74, 166.82, 159.16, 153.69, 152.09, 145.29, 137.61, 137.50, 130.28, 128.49, 126.61, 116.49, 115.77, 115.24, 73.65, 70.22, 70.05, 68.23, 67.81, 67.73, 65.21, 42.55, 34.27, 30.68, 19.12, 18.83, 13.81; HRMS (ESI) Calcd for $C_{35}H_{40}O_8Na$ [M + Na^+]: 611.2615. Found: 611.2623.

Synthesis of 5-(7-oxabicyclo[2.2.1]hept-5-en-2-ylmethoxy)pentan-1-ol. In the glovebox, NaH (0.95 g, 0.040 mol) was added to a stirred solution of (7-oxa-bicyclo[2.2.1]hept-5-en-2-yl)-methanol (4 g, 0.032 mol) in tetrahydrofuran (50 mL) in a Schlenk flask. 1,5-dibromopentane (6.5 mL, 0.047 mol) was added and the solution was removed from the glovebox and placed under a flow of nitrogen. The reaction was stirred under a flow of nitrogen for two hours, at which time it was freezed, pumped, thawed and sealed. The reaction was heated to 70 °C overnight. Water was added to quench the reaction, the THF was removed *in vacuo*, and the aqueous layer was extracted with methylene chloride multiple times. The organic layers were combined, washed with saturated NaCl solution, dried over $MgSO_4$, and the volatile components were removed *in vacuo*. The compound was purified by column chromatography (7:3 hexanes:ethyl acetate); yield 2.0 g (23%): ^1H NMR ($CDCl_3$, major isomer only, *exo*:*endo* 20:80) δ 6.39 and 6.35 (1 H each, m, alkene-C*H*), 5.00 and 4.93 (1H each, m, OC*H*CH), 3.43 (3H, m, $COCH_2$) 3.32 (2H, m, CH_2Br), 2.95 (1H, m, $CHCH_2O$), 2.52 (2H, m, $CHCH_2O$), 2.05, 1.91, 1.60, 1.55 (2H each, m, link-CH_2), 0.71 (1H, m, $CHCH_2CH$); ^{13}C NMR ($CDCl_3$, both *exo* and *endo* peaks are reported) δ 136.29, 135.79, 134.98, 132.38, 79.66, 69.53, 78.27, 77.93, 73.74, 73.39, 70.80, 38.00, 37.86, 33.45, 32.63, 32.58, 28.85, 28.79, 28.57, 28.04, 24.96, 23.92.

Synthesis of 4-methoxyphenyl 4-(5-(7-oxabicyclo[2.2.1]hept-5-en-2-ylmethoxy)pentyloxy)benzoate (ONBwMPOB). 5-(5-Bromo-pentyloxymethyl)-7-oxa-

bicyclo[2.2.1]hept-2-ene (2.0 g, 7.3 mmol), **MPOB**-H (1.78 g, 7.3 mmol), K_2CO_3 (2.01 g, 14.6 mmol), and KI (50 mg) were dissolved in anhydrous DMSO and heated to 90 °C overnight. The reaction was cooled to room temperature and diluted with ethyl acetate. The solution was washed with water, and the organic layers were combined and dried over $MgSO_4$. The volatile components were removed *in vacuo* and the product was precipitated from methanol. The compound was purified by column chromatography; yield 300 mg (10%): ^{1}H NMR ($CDCl_3$) δ 8.15, 7.12, 6.96, 6.94 (2H each, m, aromatic-C*H*), 6.39 and 6.26 (1 H each, m, alkene-C*H*), 5.02 and 4.94 (1H each, OC*H*CH), 4.08 (2H, m, $COCH_2$) 3.83 (3H, s, OCH_3), 3.45 - 2.98 (4H, m, $CH_2O_{link}CH_2$), 2.52 (1H, m, $CHCH_2CH$), 2.03 (1H, m, $CHCH_2CH$), 1.87, 1.65, 1.57 (2H each, m, link-CH_2), 0.71 (1H, m, $CHCH_2CH$); ^{13}C NMR ($CDCl_3$) δ 165.45, 163.49, 157.30, 144.64, 136.44, 132.49, 132.37, 130.70, 122.68, 121.82, 114.59, 114.36, 79.79, 78.41, 73.54, 71.03, 68.22, 55.74, 37.98, 29.49, 29.06, 28.15, 22.89; HRMS (ESI) Calcd for $C_{26}H_{30}O_6$ [M^+]: 438.2042. Found: 438.2139.

Representative polymerization of CBEwBPP4. CBEwBPP4 (100 mg, 0.164 mmol) in THF was added to a stirred solution of **15** (1.25 mg, 0.00164 mmol) in tetrahydrofuran. The solution was stirred at room temperature for one hour, and the polymerization was quenched with benzaldehyde. The solution was concentrated to ~1 mL. Methanol was added to the residue to precipitate the polymer. The gooey polymer clung to the sides of the flask and was dried *in vacuo* for further analysis.

Example of polymerization of outer block monomers. Stock solutions of **15** (34.1 mg in 3 mL, 0.0148 mmol/ml) and **NBwCOPh$_F$** (316 mg in 3.16 mL, 100 mg/mL) in toluene were prepared. The appropriate amount of catalyst stock solution (200 μL, 2.96 μmol) was added to a vial and diluted with 4 mL of toluene. While stirring, the monomer stock solution (1 mL, 0.296

mmol) was added dropwise. The reaction mixture was stirred for two hours, and the polymerization was quenched with benzaldehyde. After thirty minutes had elapsed, the polymer was precipitated from methanol. The solid was isolated on a pad of Celite, washed through with methylene chloride, and the volatile components were removed *in vacuo*: yield 94 mg (94%).

A.7 References

(1) Singh, R. *Unpublished Results.*

(2) Ranganathan, T.; Ramesh, C.; Kumar, A. *Liq. Cryst.* **2005**, *32*, 499.

(3) Hsu, C. S.; Shih, L. J.; Hsiue, G. H. *Macromolecules* **1993**, *26*, 3161.

(4) Lampman, G. M.; Aumiller, J. C. *Org. Syn.* **1971**, *6*, 271.

(5) Maughon, B. R.; Grubbs, R. H. *Macromolecules* **1997**, *30*, 3459.

(6) Bazan, G. C.; Oskam, J. H.; Cho, H.-N.; Park, L. Y.; Schrock, R. R. *J. Am. Chem. Soc.* **1991**, *113*, 6899.

(7) Connon, S. J.; Dunne, A. M.; Blechert, S. *Angew. Chem., Int. Ed.* **2002**, Supporting Information for Z19469.

(8) Singh, R.; Verploegen, E.; Hammond, P. T.; Schrock, R. R. *Macromolecules*, **2006**, *39*, 8241.

(9) Khosravi, E.; Feast, W. J.; Al-Hajaji, A. A.; Leejarkpai, T. *J. Mol. Cat. A* **2000**, *160*, 1.

(10) Bazan, G. C.; Schrock, R. R.; Cho, H.-N.; Gibson, V. C. *Macromolecules* **1991**, *24*, 4495.

(11) To, K. K. W.; Wang, X.; Yu, C. W.; Ho, Y.-P.; Au-Yeung, S. C. F. *Bioorg. Med. Chem.* **2004**, *12*, 4565.

(12) Contreras, A. P.; Cerda, A. M.; Tlenkopatchev, M. A. *Macromol. Chem. Phys.* **2002**, *203*, 1811.

(13) Portevin, B.; Tordjman, C.; Pastoureau, P.; Bonnet, J.; De Nanteuil, G. *J. Med. Chem.* **2000**, *43*, 4582.

(14) Gao, Y.; Jian, X.; Xuan, Y.; Xu, Z.; Lu, Q. *J. Appl. Polym. Sci.* **2002**, *84*, 1866.

(15) Sauers, R. R.; Schinski, W.; Mason, M. M.; O'Hara, E.; Byrne, B. *J. Org. Chem.* **1973**, *38*, 642.

(16) Dario, L.; Piero, P.; Alessandro, Z.; Francesca, P.; Martin, B. *ROMP with Fluorinated Groups* WO2005028402, May 31, **2005**.

(17) Schrock, R. R.; Gabert, A. J.; Singh, R.; Hock, A. S. *Organometallics* **2005**, *24*, 5058.

(18) Schrock, R. R.; Murdzek, J. S.; Bazan, G. C.; Robbins, J.; DiMare, M.; O'Regan, M. *J. Am. Chem. Soc.* **1990**, *112*, 3875.

ACKNOWLEDGEMENTS

This thesis could not have been possible without the support of so many individuals throughout the years. This list can by no means be complete, and I hope that I am able to begin to convey my gratitude to those who have helped me during my five years at MIT, as well as to those who helped me to get here.

First and foremost, I have to thank my advisor, Prof. R. R. Schrock. It has been amazing to work for such a brilliant scientist and a good person. Under his direction, I learn a lot of chemistry and completed some exciting research. He was always willing to provide guidance, but also gave me freedom to discover the science on my own time. It was refreshing to work for someone who was understanding during difficult times (like my "little" explosion) and who understands the importance of having time outside the lab (once in a while!). I enjoyed the hiking trips, ski trips, BBQ's, and Nobel Prize parties as well as getting to know his wonderful wife, Nancy.

Things wouldn't have run quite so smoothly in the Schrock Group without Gretchen! I thank her for the numerous times she has helped me with so many various tasks and for our wonderful discussions about life in general. Best of luck in your new ventures, G! Your presence will surely be missed!

There are so many labmates that I have had the pleasure to cross paths with and although I'd like to list everyone, I will mention those who have had a particular impact on my life and my science. Sharing a lab with Tanya has been a highlight of this journey through graduate school. Having her as a labmate has made these past few years very enjoyable and I treasure the friendship we've formed. I'm so excited that our futures are falling into place in Boston! Zach became my "post-doc" early on when it came to scientific questions. He imparted so much knowledge to me during these past five years and I am thankful that I was able to learn from him. I'm glad that we were able to spend sometime together outside the lab (with Naomi). Jiamin was a great addition to the lab in my third year here and we've had a lot of good times together. She was always willing to lend a hand or talk about one thing or the other. Roje has been a great partner-in-LCs and a good friend too! We had many stimulating (and sometimes hilarious) conversations about chemistry and life.

Jen was my mentor when I first arrived at the "Polymer Palace" and became a "Polymer Princess". I was so sad when she graduated and missed her presence everyday in the lab for at least a month. We had the great time playing softball together and fixing rollerblade wounds (ouch!). Although Sarah and I did not overlap much in the laboratory, I've had the pleasure to continue to stay in touch and to shop with her!

Numerous other labmates have provided many a reagent, answer, or a laugh during happy hour or group meeting. To those in the class above me (Adam, Amrit, Lara, Nathan and Walter), thanks for all the great times, especially the crazy ski trips! To the youngins (Annie, Brian, Keith, Alex, and Maggie), you all added new life to the group when you joined. Best of luck to you in the years to come! Of course, there were many postdocs that I overlapped with too and they are remembered fondly.

I would like to thank Prof. Joseph Sadighi for providing stimulating discussions throughout the years and for serving as my thesis chair. I'm also grateful to Prof. Kit Cummins for serving on my committee and providing useful comments.

Eric Verploegen was an invaluable resource for this research and helped with numerous experiments and answered my endless questions. I'll never forget the Brookhaven trip and how I

lost my keys! I'm appreciative that I had the opportunity to collaborate with Eric and Prof. Paula Hammond.

I also have to thank many of my classmates for fun outside of the laboratory. Venda has been a great friend and TV-buddy over the years. I hope that we will continue to stay in contact in the years to come! Although Chris traumatized me a few times over the years (you know what I'm talking about), he has been a good friend and confident over these years. Amy, Emma, Kevin, Kirsten and Melva also provided much needed fun and support over the years as well.

I'd like to thank my undergraduate advisors, Prof. D. B. Leznoff and Prof. J. A. C. Clyburne for providing me with the laboratory experience and skills that made it possible for me to thrive in the laboratory.

My best friend, Michelle Ma Belle, has been a doll during these years. I'm glad that our friendship continues at full speed ahead (we're at 12 years now)! Your visits here were so much fun! When are we going to go shopping?

I'd like to thank Daryush for being my rock these last 2.5 years. Your love and encouragement were instrumental in my sanity. You are always able to ground me and make me smile. Thank you for being a part of my life.

Lastly, but most importantly, I need to thank my amazing family in Vancouver (Mom, Dad, Kristen and Liana). I wouldn't have survived these years without you all. I'm so lucky that you were able to visit me so many times over the years and that I had your support (even though it was on the phone most of the time)! I'd also like to thank my Grandparents for thinking and praying for me. You are all special people and I'm so thankful that I can call you all family.

Andrea Jennifer Gabert

Education

2002 - 2007 **Massachusetts Institute of Technology,** Cambridge, MA
Ph.D. in Chemistry, Advisor: Prof. R.R. Schrock
Thesis: Synthesis and characterization of bifunctional hafnium and molybdenum initiators for the preparation of ABA triblock copolymers.

1997 - 2002 **Simon Fraser University,** Burnaby, British Columbia, Canada
B.Sc. in Chemistry with Co-operative Education
Honors Thesis (Advisors: Dr. D.B. Leznoff and Dr. J.A.C. Clyburne): Synthesis of neutral amidinate ligands and their transition metal complexes
Undergraduate Thesis (Advisor: Dr. D.B. Leznoff): Synthesis of chelating diamidoether ligands and their transition metal complexes

Relevant Research Experience

Nov. 2002 - May 2007 **Massachusetts Institute of Technology**, Cambridge, MA
Graduate Research Assistant for Prof. R.R. Schrock

- Synthesis of air and moisture sensitive bifunctional molybdenum and hafnium catalysts and the polymerization of various monomers using these catalysts
- Synthesis of ABA triblock copolymers containing side chain liquid crystal mesogens and the thermal and mechanical characterization of the polymer properties in collaboration with Prof. P. T. Hammond at MIT

May 2001 - Apr. 2002 **Simon Fraser University**, Burnaby, British Columbia, Canada
Undergraduate Research Assistant for Dr. D.B. Leznoff and Dr. J. Clyburne

- Development and synthesis of air and moisture sensitive ligands
- Synthesis and characterization of complexes containing the various synthesized ligands

Jan. - Sept. 2000 **BRI Biopharmaceutical Research Inc.**, Burnaby, British Columbia, Canada
Laboratory Technician

- Development and validation of methods suitable for drug analysis, following GLPs and writing SOPs, and operation/maintenance of GC/MS, GC/FID, HPLC and FTIR

Sept. - Dec. 1998 **Canadian Food Inspection Agency**, Burnaby, British Columbia, Canada
Laboratory Technician

- Preparation of samples and chemical analysis for histamine, sulfate, borate, mercury, and moisture content.

Additional Work Experience

2005 - 2006	Co-chair of Women in Chemistry at MIT. Involved in the creation of a mentor/mentee program for incoming graduate women in chemistry and the organization of various professional and social events
2005 - 2006	Member of the MIT Chemistry Graduate Student Council. Involved in the organization of various events for the chemistry department including orientation and visit weekend
2002 - 2003	Teaching assistant for a beginner chemistry lab and an advanced inorganic course at MIT
1998 - 2002	Simon Fraser University Library employee
1998 - 2000	Simon Fraser University Orientation Ambassador
1997 - 2000	Secondary level math and chemistry tutor

Awards and Achievements

Mar. 2005	Cambridge Science Foundation Travel Award
Sept. 2003	Excellence in Teaching Award at MIT
Sept. 2003	Natural Science and Engineering Research Council of Canada (NSERC) Postgraduate Scholarship A
Oct. 2002	Society of Chemical Industry Student Merit Award
Apr. 2002	E.J. Wells Chemistry Book Award
Jan. 2002	Simon Fraser University Open Scholarship
June 2001	NSERC Undergraduate Student Research Award in Universities
2000	NSERC Undergraduate Student Research Award in Industry (twice)

Publications

- Gabert, Andrea J.; Verploegen, Eric; Hammond, Paula T.; Schrock, Richard R. **Synthesis and characterization of ABA triblock copolymers containing smectic C* liquid crystal side chains via ring-opening metathesis polymerization using a bimetallic molybdenum initiator.** Macromolecules (2006), 39(12), 3993-4000.
- Schrock, Richard R.; Gabert, Andrea J.; Singh, Rojendra; Hock, Adam S. **Synthesis of high oxidation state bimetallic alkylidene complexes for controlled ROMP synthesis of triblock copolymers.** Organometallics (2005), 24(21), 5058-5066.
- Leznoff, Daniel B.; Mund, Garry; Jantunen, Kimberly C.; Bhatia, Purvi H.; Gabert, Andrea J.; Batchelor, Raymond J. **Dinuclear iron, cobalt and uranium complexes of new diamidoether ligands.** Journal of Nuclear Science and Technology (2002), (Suppl. 3), 406-409.
- Mund, Garry; Gabert, Andrea J.; Batchelor, Raymond J.; Britten, James F.; Leznoff, Daniel B. **A rare ether-bridged cobalt complex which gives rise to an unusual serpentine metal-ligand binding motif.** Chemical Communications (2002), (24), 2990-2991.

Presentations

- Oral: Gabert, Andrea J.; Verploegen, Eric; Hammond, Paula T.; Schrock, Richard R. **Synthesis and characterization of ABA triblock copolymers with smectic C* liquid crystal side chains via ring opening metathesis polymerization using a bimetallic molybdenum initiator.** Abstracts of Papers, 231st ACS National Meeting, Atlanta, GA, United States, March 26-30, 2006.
- Poster: Gabert, Andrea J.; Schrock, Richard R.; Hock, Adam S. **Synthesis and ring opening metathesis polymerization studies of bimetallic molybdenum catalysts of the type $[Mo(NAr)(OR)_2(=CH\text{-}C_5H_4)]_2Fe$.** Abstracts of Papers, 229th ACS National Meeting, San Diego, CA, United States, March 13-17, 2005.